# Fire Safety Risk Model for a Main Vertical Zone of a Large Passenger Ship

**Alexandros Komianos**

A Thesis submitted in the fulfilment of the requirements for the degree of Doctor of Philosophy

Department of Naval Architecture, Ocean & Marine Engineering

University of Strathclyde

Glasgow, 2023

This thesis is the result of the author's original research. It has been composed by the author and has not been previously submitted for examination that has led to the award of a degree.

The copyright of this thesis belongs to the author under the terms of the United Kingdom Copyright Acts as qualified by the University of Strathclyde Regulation 3.50. Due acknowledgment must always be made of the use of any material contained in, or derived from, this thesis.

Alexandros Komianos

This thesis is entirely dedicated to my late mother, Agapi Tzanidaki, without whom I would not be who I am today.

## Acknowledgements

First and foremost, I would like to wholeheartedly thank my supervisors, Prof. Evangelos Boulougouris and Prof. Dracos Vassalos, for their invaluable support and comments, and time towards the fulfilment of this thesis. Moreover, I would like to thank Prof. Gerasimos Theotokatos for his comments and guidance on the technical aspect of my cases.

Also, I would like to thank my first mentor, Yiannis Romanidis, who introduced me to the notion of a proper marine engineer.

Moreover, I would like to express my gratitude towards my father Antonis Komianos, my brother Nikolaos Komianos as well as Evangelia Galani for their support and encouragement during this long journey.

In addition, I would like to extend my gratitude towards my group of friends, TEG, for their continuous support, especially during the writing up of this thesis.

An honorary mention to Theodoros Chachlakis, Asger Erland Nielsen and Oliver Jores who endured my nagging throughout this journey to enlightenment.

A special mention to Nikolaos Souglakos is absolutely necessary. I would like to express my gratitude towards him and thank him for putting up with my notion of due diligence.

Finally, I would like to thank my partner, literally and in crime, Dr. Beatriz Navas de Maya, for her continuous support and encouragement. I shall remain indebted to her for the rest of my life.

## Table of Contents

## List of Figures

## List of Tables

## Acronyms and Abbreviations

| | |
|---|---|
| AD&A | Alternative Design and Arrangements |
| ASET | Available Time for Safe Egress |
| BBN | Bayesian Belief Networks |
| CAP | Condition Assessment Programme |
| CBM | Condition Based Maintenance |
| COTS | Commercial Off the Shelf |
| DBM | Dynamic Barrier Management |
| DSC | Differential Scanning Calorimetry |
| ECA | Emission Control Area |
| FBD | functional body diagram FBD |
| FLD | Fuel Load Density |
| FEC | Fractional Effective Concentration |
| FED | Fractional Effective Dose |
| FIC | Fractional Irritant Concentration |
| FP | Fire Protection |
| FTP | Fire Test Procedures |
| FMECA | Failure Modes, Effects and Criticality Analysis |
| FR | Flame retardant |
| FX | Fire and Explosion |
| GUI | Graphical user interface |
| HAZOP | Hazard and Operability Study |
| HPRPB | High-Pressure Release Prevention Barrier |
| HoC | Heat of Combustion (kJ/kg) |
| HVAC | Heating Ventilation and Air Conditioning |
| LDS | Leak Detection System |
| LDT | Leak Detection Technique |
| LES | Large eddy simulation |
| LPRPB | Low-Pressure Release Prevention Barrier |
| MADe | Maintenance Aware Design Environment |
| MJ | Mega Joule |
| MSC | Maritime Safety Committee |
| MVZ | Main Vertical Zone |
| NMA | Norwegian Maritime Authority |
| NSRM | Norwegian Ship Risk Model |
| RANS | Reynolds-averaged Navier-Stokes equations (RANS) |
| RSET | Required Time for Safe Egress |
| ppm | Parts per million |
| OD | Optical density |
| SCADA | Supervisory Control and Data Acquisition System |
| SMS | Safety Management System |
| SOLAS | Safety of Life at Sea |
| STPA | Systems Theoretic Process Analysis |
| RoPax | Ro-Ro and Passengers ship |
| Ro-Ro | Ramp on Ramp off ship |

| | |
|---|---|
| RPB | Release Prevention Barrier |
| RPN | Risk Priority Number |
| RUL | Remaining Useful Life |
| RTTM | Real-Time Transient Monitoring |
| PAX | Passenger ship or Passengers (depending on context) |
| POB | People on Board |
| TGA | Thermogravimetric Analysis |
| TTF | Time to Failure |

## Executive Summary

The scope of this thesis is to shed light on the everlasting issue of on-board fires, with a particular focus on large passenger ships, by proposing a fire risk model for a Main Vertical Zone (MVZ). Historically, fire had and always has been a pressing accident type, along with flooding. Despite the regulatory effort, the total loss trend of fire incidents attributes to around 10% of those. Moreover, as per the high-level hazard identification conducted as part of this thesis, it was ascertained that cruise ships dominate the frequency of accidents whereas RoPax dominate the fatalities. The latter could be explained by the fact that numerous RoPax ships operate in less developed countries, where regulation enforcement is questionable and also experience higher transportation work in terms of volume. Conversely with RoPax ships, cruise ships are becoming larger by the day, offering novel designs and pertinent entertainment, which is usually translated into complex designs, in addition to the higher transportation volume in terms of passengers and crew.

Various statistical analyses were scrutinised towards understanding how shipborne fires break out, including the one from research project SafePASS, being the most recent one, and having particular focus on all ships carrying passengers. Amongst all samples the frequency of fire events remained the same, highlighting the issue. Passenger ships, which accommodate large capacities of people experience higher fatality rates, underlining the urgency of improved safety measures. Therefore, for the purpose of this thesis focus was given on large passenger ships. On the other hand, the maritime industry and its stakeholders have always had a rather reactive stance towards safety, with the exception of cruise operators where safety is paramount with respect to their business longevity. The most prevalent example of the aforementioned being the birth of Safety of Life at Sea (SOLAS) after the sinking of the RMS Titanic.

Accordingly with the high-level hazard identification, the engine room appeared to be the most usual culprit for fire and explosion events on board ships, attributing to more than 50% of such events, which is to be expected as ship's engine room acts as a process and propulsion plant with inherent fire risks. The most frequent ignition scenario is the release of flammable oil (fuel or lubricating) which comes into contact with a hot surface, which are abundant in an engine room. Furthermore, the current status of the engine room fire safety has been characterised as sub-optimal as it investigates events only prior or next to ignition and has a particular focus on mitigation through various active and passive means (smoke detectors, deluge systems and fire boundaries respectively). Nevertheless, fire events continue to take place, highlighting the need for further research. Irrespective of the commendable research initiatives, such as project SAFEDOR and FIREPROOF, aimed at introducing the risk assessment and risk-based design respectively, the industry still has a focus on events proximate to ignition.

Additionally, in line with Safety II and resilience engineering, systemic analysis of safety critical equipment and operations is thought to be the way forward towards a fire free system. Safety barriers have been adequately used in other industries, such as aerospace, oil and gas, and navy ships, but their adoption within the maritime industry is lagging behind. Sensory equipment and data analysis have been historically

employed towards inferring safety barrier statuses, particularly that of technical elements. Systemic investigation, on the other hand, necessitates the investigation between the technical system and the asset and the operator, therefore, organisational and operational elements must be taken into account in order to provide a systemic coverage. Consequently, this research proposes a holistic simulation-based Main Vertical Zone (MVZ) fire risk model, specifically designed to demonstrate the efficacy of safety barriers.

The fire risk model of the MVZ was stipulated in the form of a risk contribution tree (bow-tie) having preventive measures on the left-hand side and mitigating on the right. Since engine room fires are historically more prevalent compared to other areas, particular focus was given towards establishing a framework for the systemic derivation of a the so termed Release Prevention Barrier (RPB), aimed at averting engine room flammable oil leaks. Focus on flammable oil leaks was given as the author believes that treating hot surfaces is counter-intuitive as the lagging (if necessary by the provisions) may deteriorate over time and improper fitting could almost be guaranteed through repeated maintenance. The proposed framework offers a systemic structured way of establishing the said barrier, with focus on the placement of sensory equipment, which, as per the literature review, is not straightforward whatsoever. The framework is rather generic in the sense that it can be applied on any flammable oil line of any ship, highlighting its applicability.

On the right-hand side, mitigating measures from SOLAS and the Fire Safety Systems Code (FSS Code) were deemed to be adequate towards that end, mainly due to their historical contribution in mitigating the effects of fire. Moreover, these have been scrutinised adequately within project FIREPROOF. Full-scale 3D Computational Fluid Dynamics (CFD) simulations were utilised towards assessing the risk of fire within the MVZ. Except for the engine room, passenger cabin and large public space decks are also liable to fire events, following the occupancy trends of such ships. Moreover, engine room fires, although statistically prevalent, do not pose as much risk to passengers as the aforementioned decks. To that effect, fire simulations were conducted on all these decks.

To realise the fire simulations and to demonstrate the inherent difficulties posed by the lack of ship-borne fire data, first principle engineering was utilised to the full extent to deterministically assess the risk in way of pyrolysis modelling. For the purpose of the CFD simulations the Fire Dynamic Simulator (FDS) and Pyrosim were utilised, being the industry standard. Thermophysical and chemical data were employed to successfully construct design fires, while the pyrolysis methodology was successfully validated and verified against full-scale experiments, deeming the design fire methodology as suitable for use onboard ships and subsequently assessing the risk within the MVZ. Investigation beyond a MVZ was not sought as it violates the mentality of the MVZ itself, and due to difficulties posed by computational power and respective means necessary to do so. In the case of the engine room fire simulation, a hybrid deterministic approach was stipulated using both first principles and statistical means in way of Monte Carlo simulations. This was performed in an effort to showcase the tremendous difficulties posed by such an endeavour and the reason why deterministic engine room fire simulations are not available.

# 1. Introduction

Historically, fire has always been a prevalent hazard on board all ships, having the potential to affect the ship itself, the crew/passengers, and the environment, posing great risk if left untreated (Eliopoulou Eleftheria, Papanikolaou Apostolos, 2016; Mariska Buitendijk, 2022). More than 90% of the global trade is conducted via shipping (AGCS, 2022), highlighting the importance and necessity for fire safety on board, while the fleet is expanding continuously. On the other hand, the shipping industry and its stakeholders have always held a rather reactive stance against all accident types. This is adequately reflected by the fact that new regulations usually emerge after a major accident/incident has taken place. As such, the most important set of regulations, the International Convention for the Safety of Life at Sea (SOLAS) (IMO, 2020), was devised and consequently adopted after the most recognised ship accident, the sinking of the RMS Titanic.

Stakeholders involved in loss trends such as underwriters, including academic studies, have consistently ranked fire as one of the most important hazards on board. Specifically, as per Allianz's Safety and Shipping Reviews (AGCS, 2022; Allianz, 2020, 2019), although a downtrend was noted in terms of total losses, the fire and explosion events on board ships increased by approximately 10% in the last year. This could be attributed to various factors such as the increased number of ships, amplified technology complexity of the on-board systems - which is tied with the ship type, and the introduction of alternative fuels (IMO, 2023). Additionally, as per these reviews, fire and explosion events consistently rank third with respect to total losses, which puts a spotlight on the accident type. Despite the total losses' trend of fire, from 2002 to 2013, a significant reduction was noted, which could reflect the efforts undertaken by IMO and other stakeholders in averting fires and explosions from happening altogether, or by proper mitigation when a fire breaks out.

General cargo ships were consistently identified as being the usual perpetrator for fire and explosion events, which is well understood as these ships are usually loaded with various cargoes, ranging from wind machine parts to bagged chemicals and grains, which pose great risks in terms of fire (IMO, 2016a, 2016b). Concerning the risk of fire/explosions to the occupants of the ship, the majority of the fatalities, either by direct or indirect (incapacitation-smoke) exposure, were identified to take place in passenger ships, regardless of their nature (purely passenger, cruise). This is well expected as merchant ships operate with the minimum personnel required in order to maximise profit, whilst passenger ships have increased capacity and complexity required to attract customers in terms of being competitive.

Specifically, 64% of the recorded fatalities emanate from ships carrying a vast number of passengers, while the rest are attributed to cargo ships (AGCS, 2022, 2014; Allianz, 2020; Bužančić Primorac and Parunov, 2016). An examination of the fleet revealed that general cargo ships greatly exceed the number of passenger ones. Therefore, although general cargo ships dominate passenger ones in terms of fleet size, fatalities are consistently noted on ships carrying passengers. Frequency-wise, cruise ships dominate other ship types carrying passengers, while RoPax dominate the fatalities (Bužančić Primorac and Parunov, 2016; Eliopoulou Eleftheria, Papanikolaou Apostolos,

2016; Papanikolaou et al., 2015). On the other hand, one must keep in mind that fatality statistics are heavily influenced by major accidents, freak accidents if you will, which tend to skew the potential loss of life. Conversely, the size and complexity of passenger ships are increasing, in an effort to be competitive while also carrying more passengers.

With regards to the origin of fire and explosions onboard ships, the engine room has been consistently identified as the most frequent space of origin (Det Norske Veritas, 2000), which is well expected considering that the engine room houses the majority of the machinery, ranging from main engines to incinerators and boilers, which all require fuel oil to be operated. Pressurised oil is commonly found inside pressure vessels or piping in a ship's engine room, while most combustion machinery operate at high temperatures, which coupled with the presence of oxygen make for a good case for fire. A plethora of regulations are stipulated in SOLAS with respect to the placement of pipes and vessels carrying oil as well as for the appropriate insulation of high temperature, surfaces (IMO, 2020), termed as hot surfaces. In addition to those, regulations also exist for the appropriate placement of detection and mitigation measures (IMO, 2015a). As per the aforementioned, it is more than evident that fires and explosion events on board ships have always posed a prevalent hazard with rather apparent frequency and loss trends.

During the past years, sensory equipment has been extensively utilised across all industries, including household applications, in an effort to obtain data on the operations undertaken. This data could be and is actively utilised in order to infer the status, either by direct flagging or coupled with data analysis (Khaleghi et al., 2013; Mohd Ismail et al., 2019; Rudov-Clark et al., n.d.). Another emerging safety mentality, in line with Safety-II, condition-based monitoring and resilience engineering, is safety barriers. These have been extensively used in the oil and gas and process industries, where the status of technical barrier elements has and is inferred via sensors. Along with the technical element, the operational and organisational ones ensures that the asset is examined in a systemic manner. Unfortunately, the maritime industry has very limited use of such equipment, usually installed to flag the status of a machinery in a "process line" inside the engine room, such as pressure differential sensors in order to understand when a fuel or lubricating oil filter is clogged.

Conversely, the maritime stakeholders have been actively putting effort towards increasing the safety levels of the industry. IMO specifically, through the stipulation of the Formal Safety Assessment on 2002 (DNV, 2002; IMO - Submitted by Denmark, 2008; IMO, 2018a, 2007, n.d.), aimed at informing the stakeholders about the pertinent risks, including fire, while increasing safety and investigating risk control options. Furthermore, through the stipulation of the Goal Based Design (GBS) and the introduction of the risk assessment within the design process, ship designers obtained the freedom of offering increasingly complex, and therefore competitive designs, while proving equivalent safety to a design that adhered to rules/provisions to the letter (IMO, 2016c).

In addition, considerable research efforts have been undertaken by various stakeholders. Prime examples are project SAFEDOR which introduced the concept of

risk analysis and cost-effectiveness in the design process, the fire risk framework from project FIREPROOF, which aimed to treat fire safety in a probabilistic manner in line with the damage stability probabilistic framework. The probabilistic framework for fire risk assessment was furtherly supplemented by the introduction of Probabilistic Fire Simulator from research project SURSHIP. Other stakeholders, such as EMSA, have also coordinated tender research efforts such as tenders Firesafe I and II.

Project SEAMAN, a Joint Industry Project (JIP) aimed at demonstrating methodologies and recommended frameworks towards safety of operations via continuous monitoring and analysis of onboard systems via sensors, with a focus on fire and flooding. Via systems principles such as Systems Theoretic Process Analysis (STPA), safety barriers were sought to be placed in an effort to avert flooding and fire hazards from occurring and/or controlling those once these were realised.

In contrast with the regulatory and research effort conducted through the years, the current status of fire safety could be argued to be sub-optimal, focused on events immediately prior to ignition and with considerable effort put on mitigating the effects of a potential fire (McNay et al., 2019). Passive and active fire-fighting means have been proven to mitigate the fire risk in terms of the potential loss of life (PLL), especially if coupled with the mentality of Main Vertical Zone subdivision, but the frequency of fire remains somewhat constants throughout the past. This thesis aims to tackle the everlasting issue of fire onboard ships, with a specific focus on large passenger ships, mainly due to their increasing size and complexity and the lives carried on board, by proposing a holistic simulation-based Main Vertical Zone fire risk model that amongst other aims to demonstrate the usefulness of safety barriers. A framework for systemic investigation was proposed, while the fire risk within the MVZ was evaluated via full 3D Computational Fluid Dynamics (CFD) simulations taking into account both normal and abnormal situations, in an effort to capture the pertinent risk.

The aforementioned give way to the following questions:

- *How come fires keep taking place on board ships despite all the regulatory effort?*

- *Why are engine room fires ever so prevalent despite their point of origin and ignition pattern is widely known and accepted amongst all stakeholders?*

- How come there is no fire risk model capable of investigating the fire risk on a main vertical zone level?

# 2. Literature review

## 2.1. Statistical overview of onboard fire incidents

The purpose of this chapter is to give an overview of fire and explosion incidents on board so as to provide a basis for this thesis. Various statistical studies of fire and explosion events (FX events) were identified from the available literature whilst the results are collated and discussed hereunder.

The investigation commences with the safety and shipping review of 2022, from Allianz (AGCS) (AGCS, 2022), being an overarching publication/study across all ship types, considering Lloyd's List Intelligence Casualty Statistics. The purpose of the review is to ascertain loss trends, and to derive and highlight risks and challenges relative to the maritime industry. While the report states that 2021 has been a particularly total loss-free year compared to past annual trends, the number of FX incidents on board are have increased by 10%. This could be attributed to a plethora of factors such as the increase in the number of ships, since shipping is responsible for more than 90% of the yearly trade, the introduction of new technologies and particularly new fuels, for example battery-driven vehicles and respective cargoes in bulk. Nevertheless, a single study should not be sufficient to draw any conclusions on the contribution of fires on board ships.

Table 1 presents the total losses for the decade between 2012 and 2022 by vessel type. There is a clear trend, specifically cargo ships (general) present the highest losses followed by fishing vessels and passenger ships. Comparison of the losses between 2012-2022 and 2009-2018 (Allianz, 2019), the timeline that this thesis was compiled, reveals a clear downtrend in the total losses, from 1,036 down to 892, while the top vessel-type contenders are the same.

Further comparison of the aforementioned loss trends against the ones from the period between 2002 to 2013 reveal that the total losses have been significantly reduced, namely from 1,673 (2002-2013) to 892 (2012-2022), presented in Figure 1, which reflect the increased efforts of the industry on safety measures and safety culture.

*Table 1. Total Losses by vessel type (2012-2022). Adapted from:*(AGCS, 2022)

| Ship Type | 2012 | 2013 | 2014 | 2015 | 2016 | 2017 | 2018 | 2019 | 2020 | 2021 | Total |
|---|---|---|---|---|---|---|---|---|---|---|---|
| Cargo | 61 | 40 | 31 | 40 | 35 | 53 | 24 | 21 | 25 | 27 | 357 |
| Fishery | 12 | 13 | 15 | 16 | 10 | 8 | 16 | 14 | 13 | 7 | 124 |
| Passenger | 7 | 8 | 11 | 6 | 11 | 5 | 7 | 5 | 7 | 5 | 72 |
| Bulk | 11 | 15 | 5 | 13 | 5 | 7 | 3 | 3 | 2 | - | 64 |
| Tug | 6 | 7 | 7 | 6 | 7 | 4 | 5 | 4 | 4 | 2 | 52 |
| Chemical/ Product | 8 | 10 | 2 | 3 | 7 | 4 | 3 | 1 | 2 | 2 | 42 |
| Ro-Ro | 6 | 2 | 5 | 6 | 10 | - | 3 | 7 | 1 | 1 | 41 |
| Container | 7 | 4 | 4 | 5 | 5 | 3 | 2 | 1 | 1 | 1 | 33 |
| Supply/ Offshore | 3 | 2 | 3 | 3 | 2 | 2 | 2 | 1 | 1 | 3 | 22 |

| | | | | | | | | | | | |
|---|---|---|---|---|---|---|---|---|---|---|---|
| Barge | - | 3 | 1 | - | 3 | 1 | 2 | 1 | - | 2 | 13 |
| Dredger | 1 | - | 1 | 1 | 1 | 3 | 2 | 1 | 2 | 1 | 13 |
| Tanker | 1 | - | 1 | - | 0 | 2 | 3 | - | 2 | 1 | 10 |
| Unknown | - | 1 | - | 2 | 1 | - | - | 3 | - | - | 7 |
| LPG | 1 | - | - | - | 4 | 1 | - | 2 | - | - | 8 |
| Other | 3 | 6 | 4 | 4 | 1 | 1 | 1 | 7 | 5 | 2 | 34 |
| Total | 127 | 111 | 90 | 105 | 102 | 94 | 73 | 71 | 65 | 54 | 892 |

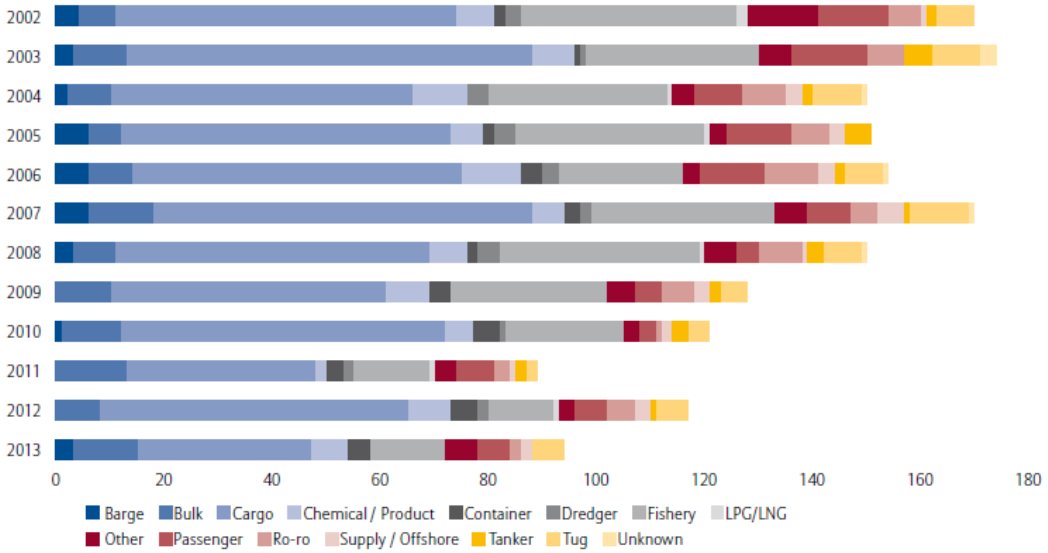


*Figure 1. Total Losses by vessel type (2002-2013).* Continuing with the total losses, Table 2 presents the total losses by accident type for the period between 2012 and 2021. FX events rank third, contributing to 120 losses across the examined vessels. Table 3 presents the total losses by cause for the period between 2002 to 2013 from (AGCS, 2014). As in the previous period, total losses due to fire and/or explosions rank third. It is evident that across all investigated periods total losses due to FX events rank third consistently. Further analysis of the FX events reveals that there is a constant trend of more than 10% regarding total losses.

*Table 2. Total Losses by cause (2012-2021). Adapted from:* (AGCS, 2022)

| Accident Type | 2012 | 2013 | 2014 | 2015 | 2016 | 2017 | 2018 | 2019 | 2020 | 2021 | Total |
|---|---|---|---|---|---|---|---|---|---|---|---|
| Foundered | 53 | 70 | 50 | 66 | 48 | 56 | 33 | 32 | 25 | 32 | 465 |
| Wrecked (grounded) | 29 | 21 | 18 | 19 | 22 | 15 | 18 | 9 | 12 | 1 | 164 |
| Fire/Explosion | 14 | 15 | 7 | 9 | 13 | 8 | 12 | 20 | 14 | 8 | 120 |
| Machinery damage/failure | 15 | 1 | 5 | 2 | 10 | 9 | 3 | 3 | 4 | 6 | 58 |
| Collision (with vessels) | 5 | 2 | 2 | 7 | 2 | 1 | 3 | 3 | 3 | 3 | 31 |
| Hull damage | 7 | 1 | 5 | 2 | 4 | 5 | 2 | 1 | 1 | 1 | 29 |
| Contact | 2 | - | 1 | - | - | - | 2 | 1 | - | - | 6 |
| Missing/overdue | - | - | - | - | 2 | - | - | 1 | - | - | 3 |
| Miscellaneous | 2 | 1 | 2 | - | 1 | - | - | 1 | 6 | 3 | 16 |
| Total | 127 | 111 | 90 | 105 | 102 | 94 | 73 | 71 | 65 | 54 | 892 |

*Table 3. Total Losses by cause (2002-2013). Adapted from:*(AGCS, 2014)

| Accident Type | 2002 | 2003 | 2004 | 2005 | 2006 | 2007 | 2008 | 2009 | 2010 | 2011 | 2012 | 2013 | Total |
|---|---|---|---|---|---|---|---|---|---|---|---|---|---|
| Foundered | 48 | 63 | 75 | 57 | 64 | 70 | 75 | 61 | 65 | 43 | 55 | 69 | 745 |
| Wrecked (grounded) | 22 | 35 | 25 | 24 | 29 | 35 | 34 | 23 | 22 | 27 | 25 | 11 | 312 |
| Fire/Explosion | 35 | 21 | 20 | 16 | 19 | 17 | 16 | 14 | 11 | 7 | 12 | 11 | 199 |
| Machinery damage/failure | 16 | 13 | 9 | 8 | 11 | 14 | 8 | 6 | 4 | 6 | 12 | 2 | 109 |
| Collision (with vessels) | 19 | 20 | 12 | 26 | 23 | 17 | 11 | 13 | 10 | 3 | 5 | 1 | 160 |
| Hull damage | 22 | 12 | 5 | 8 | 4 | 11 | 4 | 7 | 4 | 3 | 5 | - | 85 |
| Contact | 2 | 2 | 3 | 5 | 2 | 2 | 1 | 1 | - | - | 2 | - | 20 |
| Missing/overdue | - | - | 1 | 3 | 1 | 1 | - | - | 1 | - | - | - | 7 |
| Miscellaneous | 9 | 8 | 1 | 3 | 1 | 2 | 1 | 2 | 2 | - | 1 | - | 30 |
| Piracy | - | - | 1 | 1 | - | 1 | - | 1 | 2 | - | - | - | 6 |
| Total | 173 | 174 | 152 | 151 | 154 | 170 | 150 | 128 | 121 | 89 | 117 | 94 | 1673 |

The investigation continues with the examination of FX accidents onboard all ship types. (Papanikolaou et al., 2015) performed a systematic analysis of ship accidents for the period of 1990 to 2012, being an extension/update of a similar endeavour performed by Germanischer Lloyd and DNV, while it was reported in (DNV, 2006), for the period of 1990 to 2003, all conducted under research projects CONTIOPT and SAFEDOR, the latter being paramount towards the developments of fire safety onboard. The analysis included accident occurrence, frequencies, and consequences. Moreover, the accidents were analysed towards to the degree of the severity (accident, incident, etc.), accident category, geographical area, fatalities, and total losses, whilst the casualty data was extracted from IHS Seaweb and only ships built after 1980 were considered.

A plethora of accidents were considered, namely 10,481, whilst the distribution between different serious accident types is presented in Figure 2. By excluding the hull/machinery damage accident type, FX events again rank third, lagging behind collisions and wrecked.

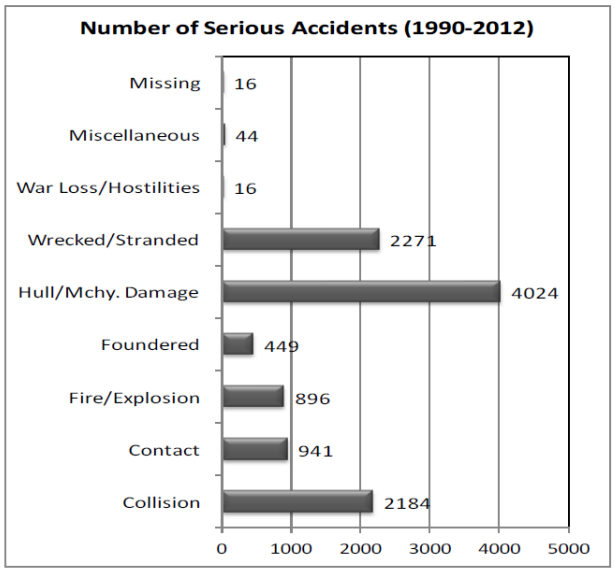


*Figure 2. Distribution of serious accidents between 1990 and 2012. Source:*(Papanikolaou et al., 2015)

Table 4 presents the registered fatalities that have occurred on board the examined ships. In total, 6,569 people have been killed and/or missing. Out of all these fatalities, approximately 64% emanates from ships carrying large number of passengers, namely passenger Ro-Ro and cargo, passenger and cruise ships, whilst the remaining 36% is attributed to cargo ships.

On the other hand, Table 5 presents the operational fleet that was examined, where general cargo ships are heavily dominating over other ship types in terms of shipyears. Conversely to the shipyears, although general cargo ships are more in numbers, the fatalities are dominated solely by ships carrying passengers, namely passenger Ro-Ro, passenger, and cruise ships.

*Table 4. Number of fatalities for the period of 1990-2012. Adapted from:*(Papanikolaou et al., 2015)

| Ship Type | No. of Fatalities |
|---|---|
| Passenger Ro-Ro Cargo | 3,558 |
| General Cargo | 1,434 |
| Passenger | 608 |
| Bulk Carriers | 381 |
| Fishing | 279 |
| Reefer | 71 |
| Cellular Containership | 65 |
| Large Crude Oil | 58 |
| Cruise | 43 |
| Ro-Ro Cargo | 29 |
| LPG | 20 |
| Car Carriers | 17 |
| LNG | 6 |
| **Total** | **6,569** |

*Table 5. Operational fleet of time period 1990-2012. Adapted from:*(Papanikolaou et al., 2015)

| Ship Type | Shipyears |
|---|---|
| General Cargo | 174,544 |
| Bulk Carriers | 88,807 |

| | |
|---|---|
| Large Crude Oil | 34,596 |
| Containership | 55,814 |
| Passenger Ro-Ro Cargo | 28,682 |
| Fishing | 126,128 |
| Passenger | 37,741 |
| Reefer | 17,086 |
| LPG | 14,927 |
| Cruise | 5,699 |
| Car Carriers | 8,476 |
| Ro-Ro Cargo | 7,839 |
| LNG | 2,659 |
| **Total** | **602,998** |

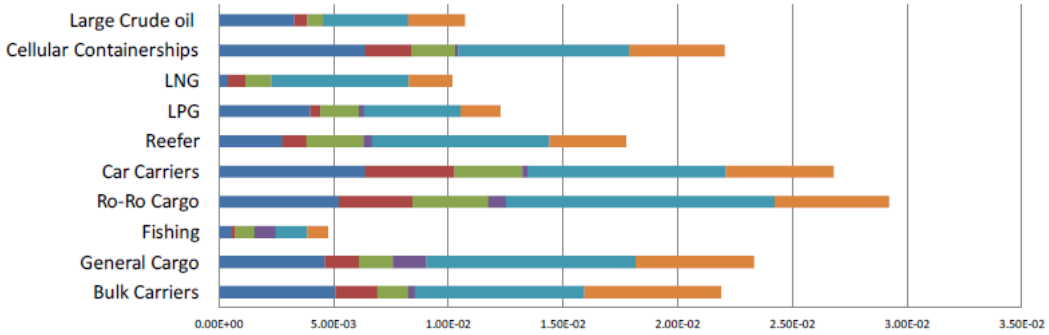


| | Bulk Carriers | General Cargo | Fishing | Ro-Ro Cargo | Car Carriers | Reefer | LPG | LNG | Cellular Containerships | Large Crude oil |
|---|---|---|---|---|---|---|---|---|---|---|
| Collision | 5.07E-03 | 4.62E-03 | 5.15E-04 | 5.23E-03 | 6.37E-03 | 2.75E-03 | 3.95E-03 | 3.76E-04 | 6.38E-03 | 3.27E-03 |
| Contact | 1.81E-03 | 1.46E-03 | 1.90E-04 | 3.19E-03 | 3.89E-03 | 1.05E-03 | 4.69E-04 | 7.52E-04 | 1.99E-03 | 5.78E-04 |
| Fire/Explosion | 1.35E-03 | 1.50E-03 | 8.32E-04 | 3.32E-03 | 2.95E-03 | 2.46E-03 | 1.67E-03 | 1.13E-03 | 1.93E-03 | 6.65E-04 |
| Foundered | 3.04E-04 | 1.46E-03 | 9.20E-04 | 7.65E-04 | 2.36E-04 | 4.10E-04 | 2.01E-04 | 0.00E+00 | 1.07E-04 | 2.89E-05 |
| Hull/Mchy. Damage | 7.38E-03 | 9.13E-03 | 1.40E-03 | 1.17E-02 | 8.61E-03 | 7.73E-03 | 4.22E-03 | 6.02E-03 | 7.47E-03 | 3.70E-03 |
| Wrecked/Stranded | 5.98E-03 | 5.17E-03 | 8.96E-04 | 4.98E-03 | 4.72E-03 | 3.34E-03 | 1.74E-03 | 1.88E-03 | 4.16E-03 | 2.49E-03 |

*Figure 3. Frequency of serious accidents of cargo ships per shipyear for the period of 2000-2012. Source:*(Papanikolaou et al., 2015)

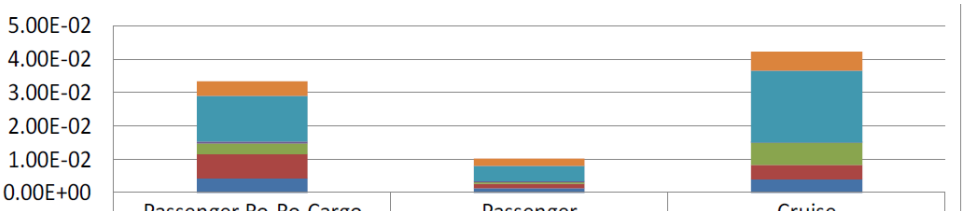


| | Passenger Ro-Ro Cargo | Passenger | Cruise |
|---|---|---|---|
| Wrecked/Stranded | 4.22E-03 | 2.31E-03 | 5.62E-03 |
| Hull/Mchy. Damage | 1.36E-02 | 4.37E-03 | 2.16E-02 |
| Foundered | 4.88E-04 | 3.18E-04 | 1.75E-04 |
| Fire/Explosion | 3.49E-03 | 5.56E-04 | 6.49E-03 |
| Contact | 7.11E-03 | 1.48E-03 | 4.39E-03 |
| Collision | 4.29E-03 | 1.22E-03 | 4.04E-03 |

*Figure 4. Frequency of serious accident occurrence in passenger ships for the period of 1990-2003. Source:* (Papanikolaou et al., 2015)

Figure 3 presents frequencies of serious accidents of cargo ships per shipyear, whereas Figure 4 presents the same but for passenger ships. The frequencies of fire and explosion events are more or less in the same degree on magnitude, but ships carrying passengers. Furthermore, through Figure 4, the seriousness and potential of

fire and explosion events is appreciated, in terms of the human carrying capacity that such vessels offer. Additionally, the highest frequency is noted on cruise ships.

Concerning total losses for the period of 2000-2012, Table 5 presents the frequency of total losses for passenger ships from (Eliopoulou Eleftheria, Papanikolaou Apostolos, 2016), which is practically the exact same analysis as in (Papanikolaou et al., 2015), with the latter being a conference publication.

*Table 6. Frequency of total losses per accident category for Passenger ships for the period of 1990-2012. Adapted from:* (Eliopoulou Eleftheria, Papanikolaou Apostolos, 2016)

| Ship Type | Collision | Contact | Fire/Explosion | Foundered | H&M Dmg | Wrecked |
|---|---|---|---|---|---|---|
| Cruise | 0.00E+00 | 2.38E-04 | 4.77E-04 | 0.00E+00 | 0.00E+00 | 2.38E-04 |
| Passenger | 3.83E-05 | 3.83E-05 | 2.30E-04 | 4.21E-04 | 7.65E-05 | 1.15E-04 |
| Pas. RoRo | 0.00E+00 | 0.00E+00 | 3.96E-04 | 4.45E-04 | 0.00E+00 | 2.47E-04 |

Only pure passenger ships present a noteworthy frequency attributed to collision and hull and machinery damage, whereas other frequencies are relevant.

To furtherly appreciate Table 4, Figure 5 presents the passenger ship fatalities per shipyear by accident category for the period of 1990-2012 in (Eliopoulou Eleftheria, Papanikolaou Apostolos, 2016). It is evident that both grounding and fire and explosion events contribute to the overall fatality rates. As per the study, this can be attributed to ageing fleets and to the fact that a plethora of passenger ships operated in underdeveloped countries where regulations are not properly enforced and safety culture is less robust, for example under-reporting (Psarros et al., 2010). Additionally, one must keep in mind that PLL statistics are heavily influenced by disastrous accidents, for example Costa Concordia's capsizing and Norman Atlantic's fire (IMO - GISIS Report, 2019). These events, although not often, tend to dominate the PLLs.

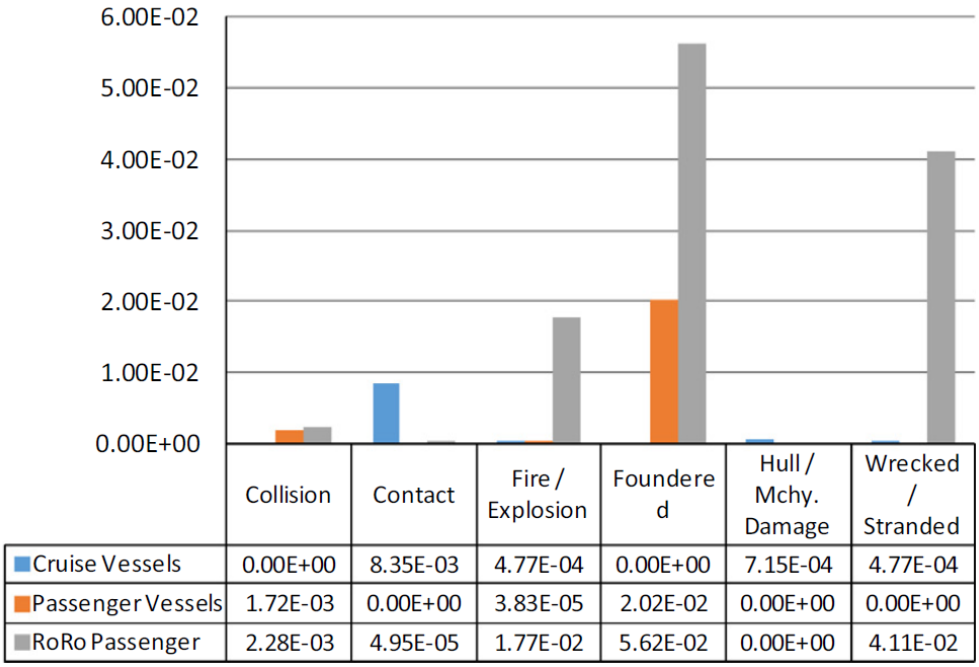


*Figure 5. Passenger ship fatalities per shipyear by accident category for the period of 1990-2012. Source:* (Eliopoulou Eleftheria, Papanikolaou Apostolos, 2016)

To furtherly emphasise the importance of fire and explosion events, another study was identified, namely (Bužančić Primorac and Parunov, 2016), which considered and compared three separate statistical studies in an effort to identify the degree of agreement amongst them. The first one is the ones that have been discussed thus far, namely (Eliopoulou Eleftheria, Papanikolaou Apostolos, 2016; Papanikolaou et al., 2015), the second is the one conducted by AGCS on 2014, namely (AGCS, 2014), whilst the latter is (Butt et al., 2015).

A consideration of the total losses amongst the statistical samples of each reveal a good agreement on the contribution of fire and explosion events towards the total losses, namely around 10%. This is presented in Figure 6. These samples span over 14 years (1990-2013) and although there is a slight degree of overlapping, the frequencies are in good agreement with the earlier cited figures.

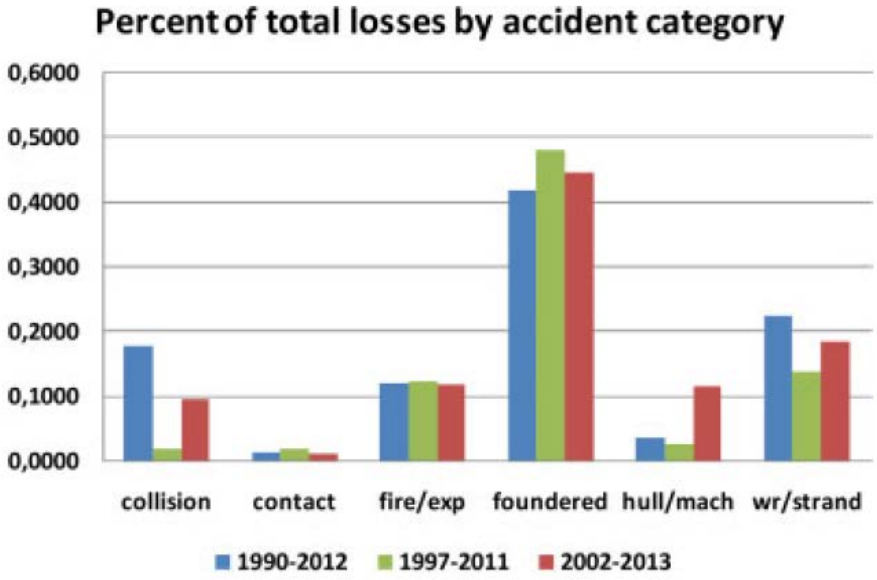


*Figure 6. Total loss percentages by accident category across three statistical samples. Source:* (Bužančić Primorac and Parunov, 2016)

Another statistical study that was utilised in this analysis is that of the research project SafePASS, which stands for 'next generation of life-Saving appliances and systems for saFE and swift evacuation operations on high-capacity PASSenger ships in extreme scenarios and conditions'. This statistical study was chosen since the author of this thesis had direct involvement in its generation as well as the project, and because it was the most recent when this thesis was compiled.

The SafePASS accident database (Stefanidis et al., 2020) was populated by having the safe return to port regulation in mind, meaning that ships having a length overall more than 120 meters or having three or more MVZs were investigated. Furthermore, the database considered only passenger ships, specifically Cruise, RoPax (Ro-Ro and Passengers), RoPax rail and RoPax cargo. The term RoPax in graphs cited hereunder refers to all aforementioned RoPax ships and was kept generic as such. Figure 7 presents the LOAD distribution of all considered ships, highlighting the part of the fleet that was not included.

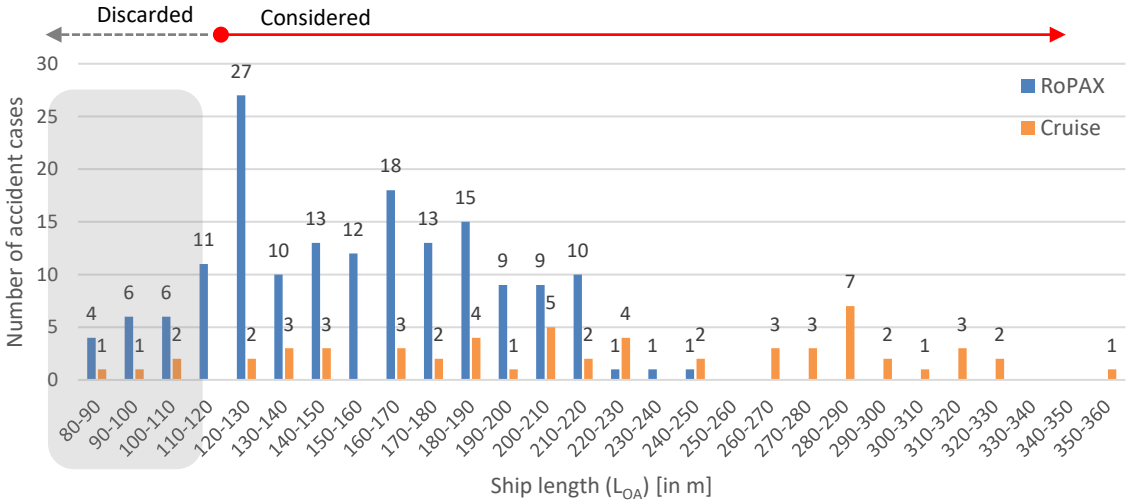


*Figure 7. Distribution of LOA of all ships considered. Source:* (Stefanidis et al., 2020)

The study identified 227 serious accidents, 56 of which contained casualties. Figure 8 presents a breakdown of fire and explosion accidents for the ship distribution that was considered.

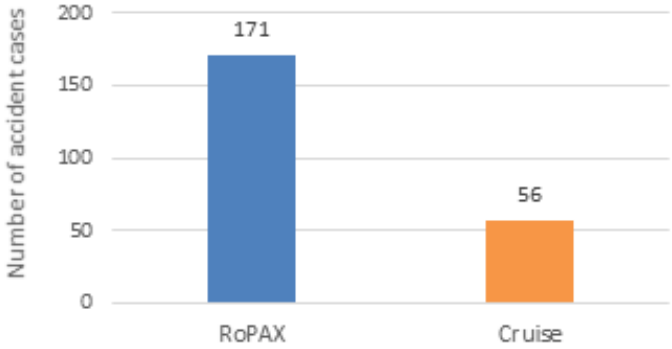


*Figure 8. Breakdown of fire and explosion accidents according to ship type. Source:* (Stefanidis et al., 2020)

Out of all the serious accidents identified in the SafePASS database, it is noteworthy to mention that RoPAX and cruise ships with LOAs greater than 120m are the forerunners, as these were involved in 83.7% and 93.0% for fire and explosion accidents respectively. Figure 9 presents the number of accidents recorded from 1999 to 2020. RoPax ships present high occurrence between 2008 and 2013, with a peak in 2019. The latter also highlights how accident statistics can be influenced, in the sense that some years have demonstrated adequate “safety performance” whilst some others, 2019 particularly, have not. Nevertheless, as mentioned previously, frequencies remain almost constant across all statistical studies.

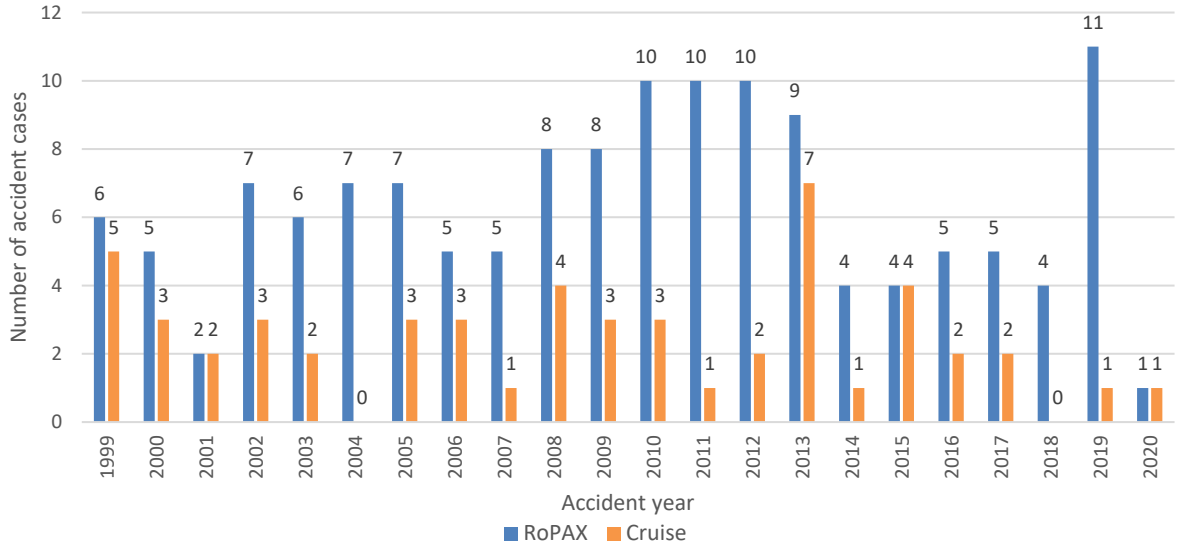


*Figure 9. Fire and explosion accidents per year. Source:*(Stefanidis et al., 2020)


*Figure 10. Global distribution of serious FX accidents. Source:* (Stefanidis et al., 2020)

Figure 10 showcases the global distribution of fire/explosion accidents, with or without fatalities, for the fleet considered. As per the database, the most frequent origin of such accidents is the West Mediterranean Sea, followed by Asia. The former is very well expected as that part of the Mediterranean experiences the heaviest traffic, while there are not many passenger ships doing intercontinental voyages, for example, Europe to the USA.

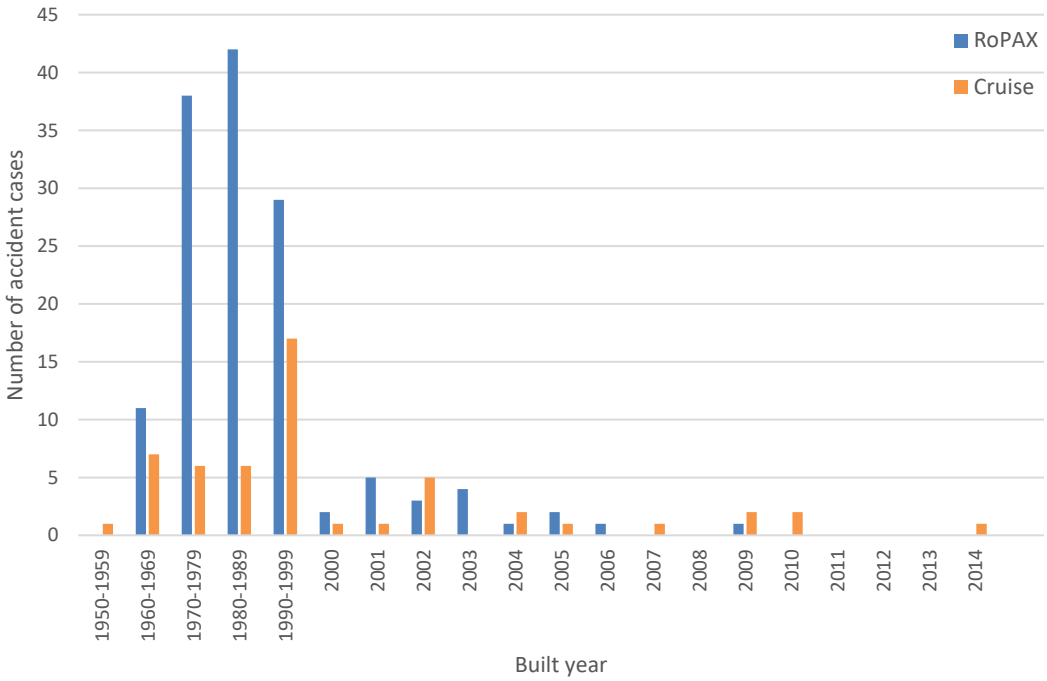


*Figure 11. Distribution of built year of RoPax and cruise ships. Source:* (Stefanidis et al., 2020)

Figure 11 presents the distribution of the year that the considered ships were built. It is very noteworthy to mention that the majority of the accidents were ascertained to be on older ships regardless of their type, which were not built with the same level of safety as newer ones, which is very well expected considering the reactivity of IMO and other regulatory bodies.

Concerning the time of occurrence in terms of daylight and nightlight, Figure 12, presents the relationship between those for the accidents included in the SafePASS database. It is evident that both times have the same occurrences.

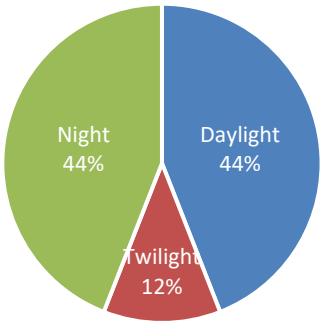


*Figure 12. FX serious accidents in terms of daylight. Source:* (Stefanidis et al., 2020)

In terms of fatalities as derived from the SafePASS accident database for both RoPAX and cruise ships, Figure 13 presents the numbers of fatalities against the people on board (POB). It must be noted that the fatalities presented in the SafePASS database include people that died or were injured or were missing. RoPAX vessels, as defined earlier, tend to dominate the fatalities with 1,734 people lost against 121,256 carried on board, whilst cruise ship accidents contributed to 106 fatalities against 98,175 people carried.

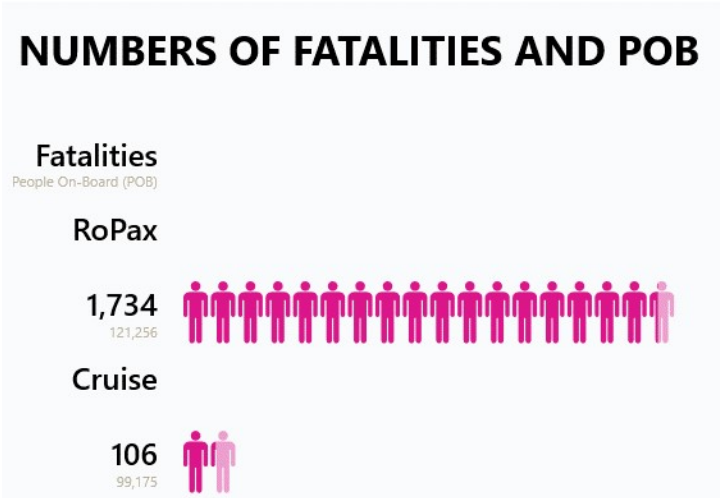


*Figure 13. Number of fatalities and people on board (POB) as per the SafePASS database. Source:*(Stefanidis et al., 2020)

On the other hand, accident/casualty statistics as such, and therefore the potential loss of life (PLL), are easily influenced by individual accidents/occurrences with a high number of fatalities. Such examples are the Al-Salam Boccaccio 98 ("M/V al-Salam Boccaccio 98," 2006) and the Da Shun ("Over 280 dead in Chinese ferry disaster - World Socialist Web Site," n.d.) fires with an excessively high number of fatalities. This can be appreciated through Figure 14 which presents the number of accidents over the fatality ratio, namely fatalities over POB, for both RoPAX and cruise vessels. The proportion of incidents where the fatality ratio lies between 0 and 1% is historically greater than the rest of the classes.

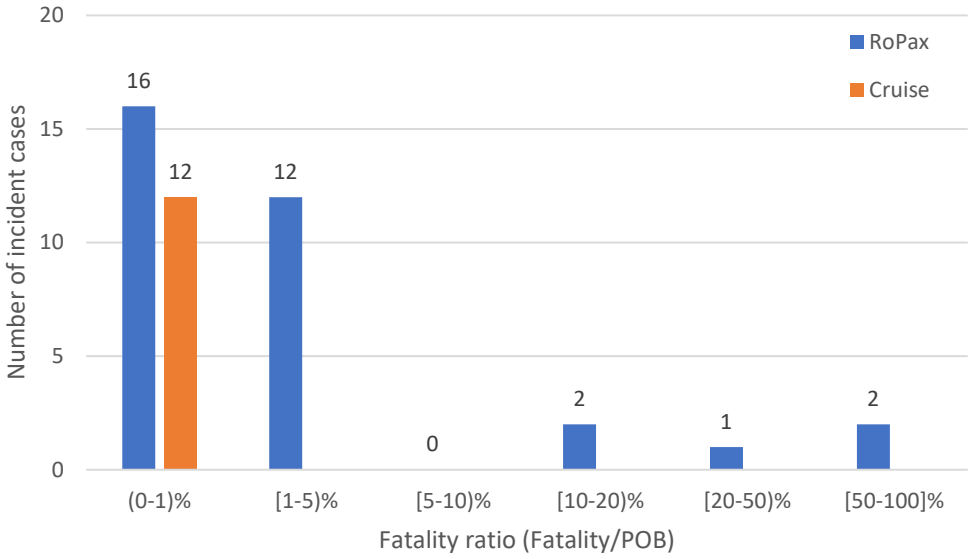


*Figure 14. Incident cases against fatality ratio. Adapted from:* (Stefanidis et al., 2020)

Recapitulating the analysis of the statistical overview of fire/explosion incidents onboard, cruise ships dominate the frequency of accidents whereas RoPax dominate the fatalities. The latter is mainly attributed to the fact that RoPax ships carry vehicles apart from passengers, which poses a greater-additional risk in terms of fire, and the fact that many RoPax ships operate in less developed countries, where regulation

enforcement is questionable, and sustain higher transportation work in terms of volume. On the other hand, passenger ships are becoming increasingly larger, accommodating more passengers than ever, while the designs are increasingly complex with time considering that innovation is paramount το attract passengers and/or customers. Furthermore, despite all the efforts, regulatory or other, to prevent fire from occurring and to mitigate the ensuing effects, the frequency remains constant at the very least whilst the consequences cannot be neglected (Baalisampang et al., 2018). Therefore, for the purpose of this thesis, focus will be given on investigating fires in large passenger ships due to the sheer volume of people on board.

## 2.2. Shipboard Fire Safety

This chapter provides a brief overview of the current status of shipboard fire safety. The purpose is to provide an overview of the current status rather than list all the pertaining regulations.

### 2.2.1. SOLAS

The most prominent set of rules is SOLAS, which was adopted by IMO in 1974 after the sinking of the RMS Titanic (IMO, 2020). The purpose of SOLAS is to set minimum requirements for the safe construction and operation of vessels, whilst the rules are traditionally of prescriptive nature. Following conventions were held, usually due to a major accident taking place, a fact which highlights the reactivity of IMO and, therefore, of the industry.

SOLAS is usually amended via resolutions which are generated by the Maritime Safety Committee (MSC), which has various subcommittees itself, such as the Fire Protection (FP) being directly relevant. If member states are of the opinion that new rules should be issued and/or amended, then the MSC or any other relative committee, call for submissions from the member states. After consideration, these proposals are reviewed by the committee and then circulated to member states. Amendments or new rules require six months before adoption, whilst any member state may object for the following two years. The aforementioned highlight the slothfulness of the procedure and the reactivity of IMO.

Fire safety is governed by Chapter II-2: Construction – Fire protection, fire detection and fire extinction, Ch. II-2 in short. The title itself showcases how this particular set of rules was envisaged along with the respective goals. Chapter II-2 is furtherly subdivided into parts, from A to G. Part A concerns general information such as the objectives and the functional requirements, Part B the prevention of fire and explosion, Part C the suppression of fire, part D the escape, Part E the operational requirements, Part F the Alternative Design and Arrangements (AD&A) and Part G special requirements.

The objectives revolve around the prevention of fire and explosion and the reduction of risk to the asset, cargo, environment and occupants. Furthermore, it provides means of containing, controlling, and suppressing fire and explosion in the compartment of origin (to reduce fire spread), as well as means of escape for both

passengers and crew. In order to achieve the aforementioned objectives functional requirements are incorporated. These are:

- Division of ship into Main Vertical (horizontal) Zones (MVZs) having thermal (and structural) boundaries.
- Separation of accommodation spaces from the remainder of the ship by thermal (and structural) boundaries.
- Restricted use of combustible materials.
- Detection of fire in all MVZs.
- Containment and extinction of any fire in the space of origin.
- Protection of means of escape and access for firefighting.
- Ready availability of fire-extinguishing appliances.
- Minimization of possibility of ignition of flammable cargo vapour.

As per SOLAS, the objectives and, in turn, the functional requirements of Ch. II-2 can be achieved either by ensuring compliance with the prescriptive requirements set in Parts B, C, D, E or G, or by Alternative Design and Arrangements set out in Part F, or a mix of those depending on the design. A prime example of the latter are cruise ships, the revenue of which is highly attributed to the novelty and uniqueness of entertainment on board which, usually, requires designs that fall out of the prescriptive means and require the use of AD&A procedures.

### 2.2.2. Alternative Designs and Arrangements

IMO released the guidelines on alternative design and arrangements for fire safety via Circular 1002 (MSC/Circ. 1002) on its 74$^{th}$ session in 2001, to provide further guidance towards the certification and approval of alternative designs which did not follow the prescriptive rules (IMO, 2001a). These offer a structured engineering analysis methodology to provide technical justification that an alternative design meets the required (or agreed - depending on one's point of view) level of fire safety, including all objectives and functional requirements as stipulated in Ch. II-2. This procedure is commonly termed as performance-based design, similar to the philosophy and principles of risk-based design (Carlos Guedes Soares, Andrzej Jasionowski et al., 2009). Figure 15 presents the AD&A procedure via a flowchart.

In short, the aim of the procedure is to prove that the design offers the same safety performance, or better, as a prescriptive design. In order to demonstrate this, risk-based fire safety engineering is employed. The analysis procedure covers the qualitative identification of sources of ignition and potential growth and smoke and toxicity characteristics of the flammable material present in the (trial) alternative design. This is followed by the setting of performance criteria relevant to Ch. II-2. Amongst other, the qualitative analysis includes:

- Design fire scenarios.
- Assumptions.
- The design fire itself (for example kW and ramp).
- Test data (if necessary).
- Performance criteria.

- Sensitivity analysis.

Then, the safety of the design is evaluated via quantitative analysis, almost always via CFD methods, to demonstrate to the Administration that it meets the stipulated performance criteria, therefore, equivalency has been achieved.

MSC/Circ. 1002 was superseded on 2016 by MSC.1/Circ. 1552, amendments to the guidelines on alternative design and arrangements for fire safety (IMO, 2013). Usually, previous circulars are superseded by newer in the sense that the older is no longer valid or in use. The in-subject circular acts as an annex to the existing ones and provides more specific guidance on the selection of performance criteria for the assessment of survivability of occupants when exposed to fire effluents (heat, smoke, toxicity) and effects (visibility). In addition, these guidelines aim to assist the Administration with respect to the evaluation of the proposed alternative design against the objectives stipulated in Ch. II-2. Furthermore, these guidelines may be utilised to determine minimum safety margins for ASET for non-prescriptive designs.

The most important outcome from this circular is the minimum life safety performance criteria. These concern the maximum air temperature, the maximum radiant heat flux, the minimum visibility and the maximum carbon monoxide concentration. The values are summarised and presented in Table 7.

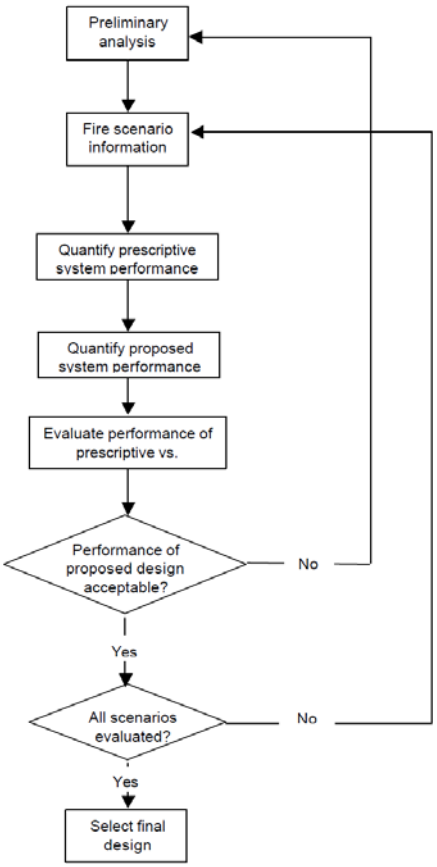


*Figure 15. Process flowchart of alternative design and arrangement procedure. Source:* (IMO, 2001a)

*Table 7. Life Safety Performance Criteria from MSC.1/Circ.1552. Source:*(IMO, 2013)

| **Life Safety Criteria** | **Values** |
|---|---|
| Maximum air temperature | 60ºC |
| Maximum radiant heat flux | 2.5 kW/$m^2$ |
| Minimum Visibility | 5m in spaces ≤ 100$m^2$ |
| Maximum CO concentration | 1,200 ppm (instantaneous exposure)<br>500ppm (for 20 minute cumulative exposure time) |

### 2.2.3. Fire Safety Systems Code

IMO's MSC on its 73rd meeting adopted the International Code for Fire Safety Systems (FSS Code) via Resolution MSC.98(73) (IMO, 2000). The Code's purpose is to provide international standards of specific engineering specifications for fire safety systems on board, as required by Ch.II-2 of SOLAS. The code came into effect on July 2002 and is mandatory and an integral part of Ch.II-2. Since the code itself is sizeable, IMO decided to release it as a separate publication (IMO, 2015b). In 2019 IMO introduced minor amendments to the FSS Code via resolution MSC.457(101) (IMO, 2019a).

The FSS Code concerns international shore connections (flange dimensions), personnel protections such as personal protective equipment, emergency devices, fire extinguishers, fixed gas fire-extinguishing systems, $CO_2$ systems, fixed foam fire-extinguishing systems including both low and high-expansion foam, fixed pressure water spraying and water mist systems, automatic sprinkler systems, fire detection means and respective alarm systems, smoke extraction systems, emergency (fixed) fire pumps, means of escape, inert gas systems and fixed hydrocarbon gas detection systems. Moreover, FSS contains a plethora of relevant standards and guidelines in the form of MSC Resolutions.

### 2.2.4. Fire Test Procedures Code (FTP Code)

IMO in 1996 introduced the fire test procedures via MSC.57(67), adoption of amendments to the international convention for the Safety of Life at Sea (IMO, 1996). The most notable elements of this resolution were the definition of non-combustible materials being determined in accordance with the FTP Code, and the definition of a standard fire test, where specimens are evaluated towards their contribution and behaviour in a fire scenario. Therefore, the FTP Code was adopted via Resolution MSC.61(67) in 1996 (Maritime Organization, 1996). FTP comprises provisions for fire tests which aim to derive flammability, smoke generation and toxicity of materials and items. In light of constant developments of materials used in shipbuilding as well as the enhancement of safety standards, IMO in 2010 revised the FTP Code via Resolution MSC.307(88) (IMO, 2010).

## 2.3. Spatial Origin of Fires on board ships

The purpose of this chapter is to ascertain and evaluate the spatial origin of fire on board ships. Without consulting any literature, a prime candidate concerning the spatial origin of fire on board is the engine room. This is very well envisaged as,

fundamentally, the engine room acts as a propulsion and processing plant where flammable and other volatile materials (toxic, corrosive, etc.) are handled daily. Furthermore, hot surfaces are always present. Hence, there is a constant existence of fuel and ignition sources (hot surfaces from machinery). An examination of the fire triangle, reveals that all elements are constantly present (fuel, heat source and oxygen), awaiting "appropriate" conditions to develop into a fire/explosion.

Further to the aforementioned, according to SOLAS Ch. II-2, Part B, Reg. 4 Para. 2.1.1, no fuel oil with a flashpoint of less than 60ºC can be used on board (IMO, 2020), whereas flashpoint is the temperature at which a substance releases ignitable vapours (Hurley et al., 2016). On the other hand, as per Ch. II-2, Part B, Reg. 4 Para. 2.2.6, surfaces having a temperature of more than 220ºC *shall be insulated properly*. Since the flashpoint of fuels cannot be varied as per one's desire, the hot surfaces rule is rather horrendous, in the sense that if the lagging is non-existent, or damaged (losing its properties) or improperly fit, than a potential release (leak) could develop as a fire.

Concerning potential releases of hydrocarbon fuels, SOLAS in Ch. II-2, Part B, Reg. 4, Para. 2.2.5 provides guidance on the placement of fuel oil piping. In summary, piping *shall not be immediately above or near units of high temperature including boilers, steam pipelines, exhaust manifolds, silencers or other equipment required to be insulated by paragraph 2.2.6*. Therefore, the Administration is aware of the situation, but the rules are clearly inadequate according to the statistics.

Regarding the statistical origin of fire on board, more than half of the fires experienced on board originate in engine rooms (Azzi, 2010; Charchalis and Czyż, 2011; Det Norske Veritas, 2000; Krystosik-Gromadzińska, 2016; Salem, 2006; Stefanidis et al., 2020). Through a statistical study conducted by DNV in (Det Norske Veritas, 2000), 63% of the fires occurred originated in engine rooms, with the remaining percentage split amongst accommodation (10%) and cargo spaces (27%), presented in Figure 16.

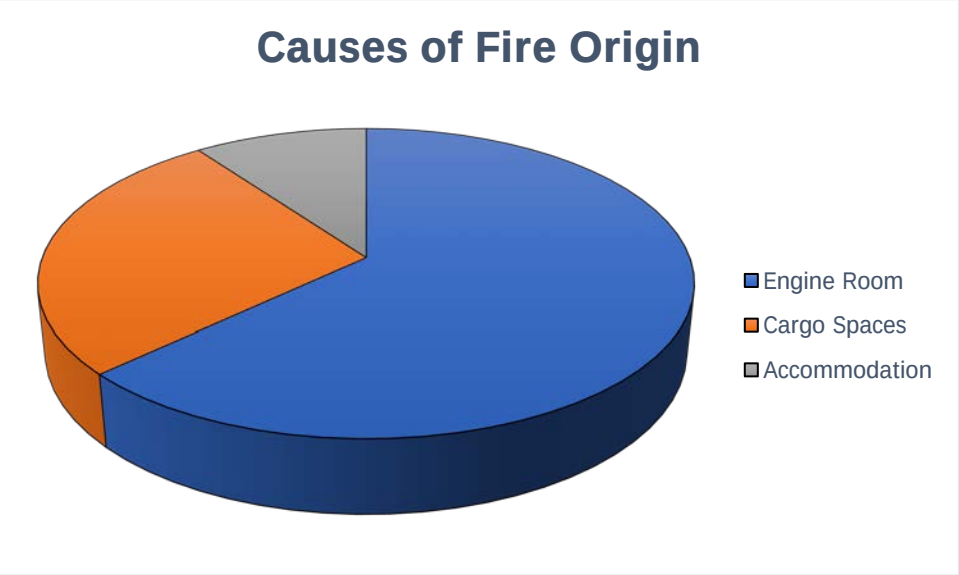


*Figure 16. Causes of fire origin. Adapted from:* (Det Norske Veritas, 2000)

The cargo space fires are very well understood and also supported by the relevant statistics from AGCS in the previous chapters, in the sense that general cargo ships dominate the total losses and, also, because such ships carry volatile cargoes in bulk, which as per the IMDG Code (IMO, 2016b, 2016a), can be of very hazardous nature with respect to fire, such as self-heating cargoes (coal, grains, etc.).

Concerning accommodation spaces, the usual culprits of fire origin are the galley (Souglakos, 2022) and cabins, themselves being either due to electrical faults or human factors in the sense of human (both crew and passengers) negligence. A prime example of the latter is seafarers who fall asleep while smoking in bed (Staffansson, 2010).

Moving on to the SafePASS database for passenger ships, Figure 17 presents the spatial origin of fire/explosion on board, while Figure 18 presents the distribution of fire and explosion in passenger ship engine rooms, providing an overarching and in-depth view. Again and as expected, the majority of fire and explosions are noted in engine rooms, while the remaining are almost harmonically distributed amongst other areas.

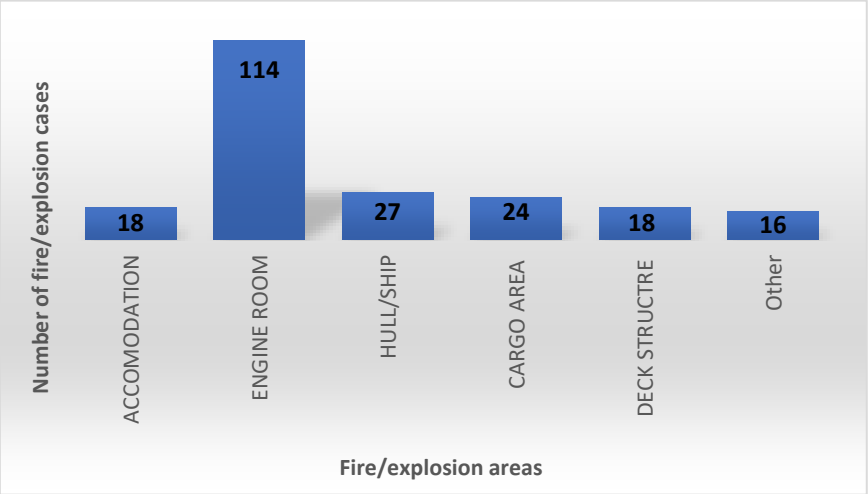


*Figure 17. Spatial origin of fire/explosion on board as per the SafePASS database. Adapted from:* (Stefanidis et al., 2020)

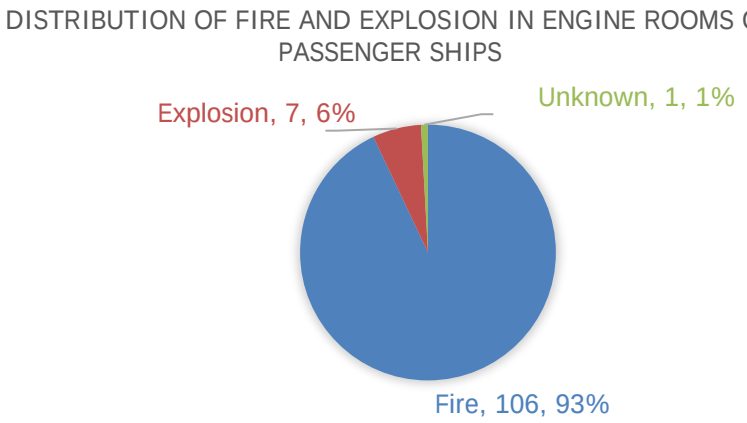


*Figure 18. Distribution of fire and explosion in passenger ship engine rooms as per the SafePASS database. Source:* (Stefanidis et al., 2020)

Engine room incidents are dominated by fire events against very few explosions. Out of the 114 incidents, only 7 are attributed to explosions. Specifically, explosions (deflagrations) are averted via relevant SOLAS rules regarding overpressure, for example in Ch. II-2, Part B, Regulation 4, which prescribe that *provisions shall be made to prevent overpressure in any oil tank or in any part of the oil fuel system, including the filling pipes served by pumps on board* (IMO, 2020). Additionally, there are similar provisions for internal combustion engine crankshafts where an oil mist can be developed and may lead to a crankcase explosion (Liu et al., 2023), specifically Ch. II-2, Part B, Regulation 27. In summary, this regulation prescribes pressure relief means for pressure vessels including internal combustion engines.

Highlighting further the inadequacy of the rules, the Norwegian classification society DNV offers a voluntary Condition Assessment Programme (CAP) where aged ships, mainly tankers, are inspected and their condition is verified towards the hull, and the machinery and cargo systems ("Condition assessment programme (CAP)," n.d.). The objective is to document the quality of aged ships so as to be able to judge based on the condition rather than the age. CAP is offered via two modules: namely, one for the hull and another for the machinery and cargo systems. An integral part of the latter is the so-called hot spot inspection where the society investigates the engine room for potential hotspots, either due to improper application of the lagging or lack thereof. Figure 19 presents a photograph from a hotspot inspection conducted by the crew of an anonymous very large passenger ship, where temperatures in the magnitude of 312$^{o}$C are noted on the exhaust manifold cover, where insulation is not necessary as per the rules.

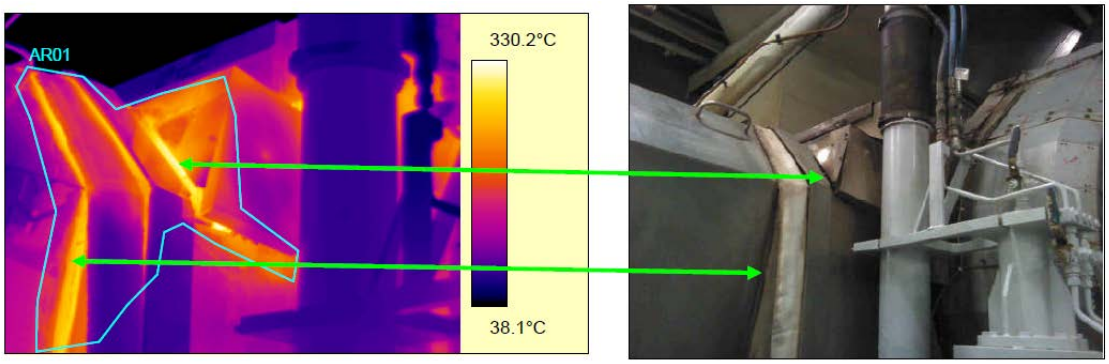


*Figure 19. Hotspot inspection conducted on diesel engine exhaust manifold cover.*

Having ruled out explosions due to the successful regulatory effort, engine room fires are furtherly examined via Figure 20 which presents the distribution of origin for engine room fires (Det Norske Veritas, 2000). More than half of the fires are noted due to the contact of leaked oil with hot surfaces, hence the relevancy of CAP and the inadequacy of the hot surface rule. This is very well expected and supported throughout relevant literature such as (Anantharaman et al., 2015; Azzi, 2010; Baalisampang et al., 2018; Charchalis and Czyż, 2011; Fire and Analysis, 2014; Krystosik-Gromadzińska, 2016; Staffansson, 2010; Troitzsch, 2016).

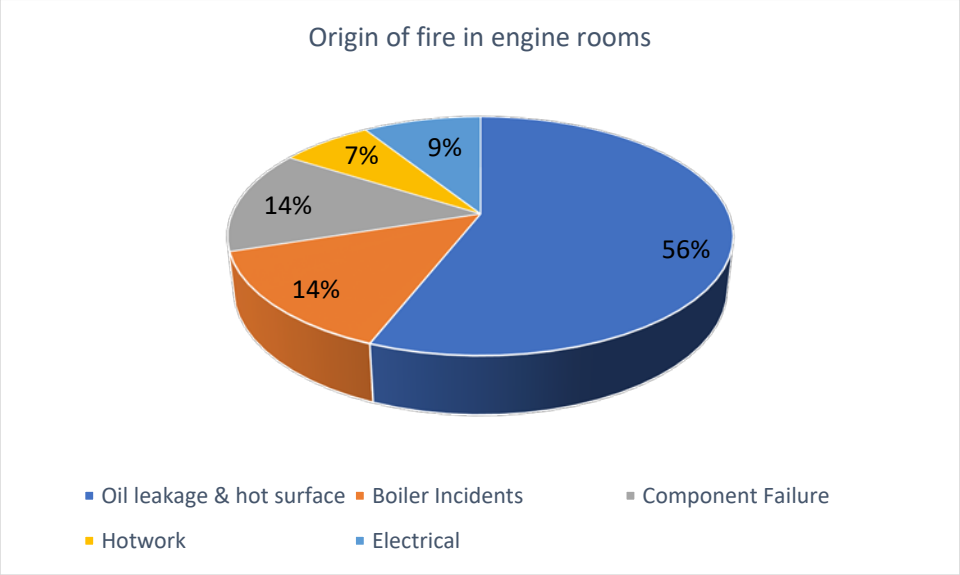


*Figure 20. Origin of fire in engine rooms. Adapted from:* (Det Norske Veritas, 2000)

The oil itself usually leaks from the high-pressure fuel systems on board engines, where flexible pipes are sometimes allowed by the administration. The origin of the leak is, usually, vibrations or material/component failure (Charchalis and Czyż, 2011; Krystosik-Gromadzińska, 2016). The former is very well known and understood by all stakeholders but due to the plethora of the systems in engine rooms, treating those vibrations is a very strenuous task considering the sheer size of passenger ships and their engine rooms.

The leaked fuel fires are seconded by boiler fires, such as (Canedy and Nobles, 2003), and component failures. Hot work incidents can be ruled out provided that a proper risk assessment is conducted prior to those.

## 2.4. Shipboard Fire Safety Research Review

The forefather of shipboard fire safety research was project SAFEDOR which established the concept of risk analysis and cost-effectiveness in the design process (Breinholt et al., 2012; Germanischer Lloyd, 2009). The project's scope was to redefine the approach to safety, meaning that it was not treated as a (design) restraint imposed by the regulatory bodies and flag administrations but as an objective which is investigated in conjunction with the design right from the conceptual stage. In other words, project SAFEDOR's contribution was paramount towards goal-based standards allowing novel, therefore competitive, designs that do not fall under the prescriptive standards, by demonstrating equivalent safety as the prescriptive ones. SAFEDOR investigated both flooding and fire, while the focus in the thesis is fire.

A risk-based design framework using first engineering principles was developed. Furthermore, a risk-based approval process was proposed to IMO but, eventually, it was not adopted. The proposed framework and approval process were adequately demonstrated in various ship types, namely cruise ships, Ro-Ro/RoPax, both gas and oil tankers as well as containerships, through the conduction of FSAs and novel designs

(Nilsen, 2005; Ship Stability Research Centre (SSRC), 2007). A very prominent example was the increase in the size of MVZs and the demonstration of equivalent safety as in a normal one.

Various predictive tools for fire and smoke development and transport were perused, for example in D2.5.5 where ANSYS-CFX, a CFD software, was used to evaluate the behaviour of a fire in a large public space. Additionally, sprinkler interaction was also taken into account for a design that fulfilled SOLAS requirements and for a design that did not as the MVZ was larger (Sinai et al., 2007). The results of these simulations, along with others conducted via zone models, were later used to evaluate the safety of the designs and to propose effective risk control options which were scrutinised against risk evaluation criteria, the latter being an integral part of the project as risk acceptance criteria for safety and the environment were considered in D4.5.2 (Skjong et al., 2005).

Another result of major importance not only to fire safety but safety in general was the publishing of the Risk-Based Ship Design book (Carlos Guedes Soares, Andrzej Jasionowski et al., 2009), which encapsules the risk-based design philosophy. Conversely, a major drawback of SAFEDOR was the lack of a standardised loss-calculation procedure. Great accuracy should not be of high-importance/priority, but the framework shall be able to present mutually acceptable (simulation) results and agreement between stakeholders/analysts responsible for approval.

The research work conducted in SAFEDOR was furtherly expanded in project FIREPROOF (FIREPROOF consortium, 2010). The objective was to develop a universally applicable regulatory framework for fire safety of passenger ships. The outcome of this research endeavour was the proposal to the IMO of a probabilistic fire safety framework similarly with the acclaimed probabilistic damage stability framework/regulation. A probabilistic model was developed for the ignition, and generation of fire scenarios (design fires) as well as numerical models for fire growth and pertinent consequence assessment in the form of potential with great emphasis on incapacitation and/or loss of life for occupants. The FIREPROOF framework was developed in order to be applicable to any space within a MVZ.

Specifically, the mathematical model is able to generate design fire scenarios, fire scenarios, by specifying appropriate probability distributions of the elements governing the fire, such as FLD, growth rate (a), etc. Therefore, for any ship of any design, including novel/non-prescriptive ones, a large amount of design fires could be generated, and their consequences could be collectively assessed which allows for fire risk metrics. By being applicable to any design and by offering risk metrics, the framework was proposed to form statutory regulations for novel designs, but it was not adopted eventually.

Nevertheless, despite the fact that IMO did not implement the FIREPROOF framework, the work conducted in this project was and still is considered as state of the art in terms of design fire generation. (Themelis and Spyrou, 2012, 2010) derived a probabilistic methodology for the generation of design fires. This work investigated the relationship of HRR curves against a plethora of parameters that dictate fire

development, such as the type and amount of fuel (fire load), the growth of the fire etc. Additionally, the geometry could be taken into account in the probabilistic analysis including ventilation characteristics, which heavily influence the development of a fire. The scarce availability and uncertainty of fire-related data, such as the combustible materials, fuel area, onset of decay were overcomed by the specification of probability distributions. This methodology was demonstrated via the generation and input of a design fire into FDS.

However, no suppression systems were taken into account except for the probability of failure of human intervention, the latter being rather pedantic as human intervention in a fire is rather chaotic in the sense that the time and success rate of intervention can only be measured via statistics which do not take into account the actual design of a ship, let alone the situation during a fire. Furthermore, as demonstrated in (Navas de Maya et al., 2022) and (Jeong et al., 2016), human factors are a distinct discipline and should be taken into account as such.

Moreover, the case study heavily relied upon actual experiments/tests in order to justify/validate the selection of HRR curve as thousands were generated via the probabilistic methodology. Specifically, for some parameters, for example the growth rate (α), appropriate distributions have been identified via statistical tests. A fitting example is (Salem, 2016) where the growth behaviour is considered to fit a lognormal distribution, whereas (Themelis and Spyrou, 2012, 2010) consider it as a normal distribution in lieu of data.

Also, in (Salem, 2016) it is argued that the only parameter greatly affecting the ASET, except for the peak HRR obviously, is the growth – this is revisited later on. Another drawback is that it was not tested against other more complex geometries, for example large public spaces/atriums where the fire load is quite different and rather uncertain as spaces as such are the revenue generators of a large passenger ship and are highly novel, therefore, experiments are highly required. In this case, a fire safety engineer should consider the maximum allowable combustible mass as per (IMO, 2001b). Nevertheless, the work conducted under project FIREPROOF and (Themelis and Spyrou, 2012, 2010) allow to investigate many possible designs at the conceptual stage.

Another major research endeavour towards fire safety was project SURSHIP-FIRE, Survivability for Ships in Case of Fire, carried out by the VTT Technical Research Centre of Finland in 2009, which consisted of four sub-projects (Hakkarainen et al., 2009). The first, termed as “Firedata” involved the generation of a free access fire database(RISE Institute, n.d.) of materials/products commonly used in shipbuilding, along with their fire behaviour, for example HRR and growth coefficient. The second, termed as “Hazards” stipulated for the generation of design fire scenarios which was demonstrated on a duty-free shop onboard a passenger ship. The design fire methodology along with VTT’s probabilistic fire simulator (Hostikka et al., 2003) were also demonstrated in (Hostikka et al., n.d., 2003; Hostikka and Keski-Rahkonen, 2003) via cable tunnel simulations. The concept of assessing the hazard probability of critical spaces was created in this sub-project. The third sub-project termed “Structures” investigated fire scenarios under which the structural integrity of the ship is

compromised, whilst the last one, “Evacuation”, demonstrated novel evacuation simulation tools, namely “FDS+Evac”. Here, FDS was used to simulate a scenario generated by the design fire methodology in conjunction with the probabilistic fire tool from VTT and then through Evac an egress simulation on a complex staircase was performed, demonstrating the value of the combined tool.

Via an initiative from EMSA the Firesafe I and II tenders were conducted in 2015 onwards, to investigate, and possibly review and update the fire safety regulations concerning RoRo passenger ships. Workshops with relevant experts were held were on fire hazards on such decks and the studies were commissioned in an overarching manner with respect to the hazards. All stages of fire were evaluated including extinguishment, evacuation and relevant decision making as per the FSA guidelines. That led to the proposal of pertinent RCOs for each aforementioned aspect/stage.

Firesafe I investigated electrical fires only as an ignition risk, a very relevant hazard in RoRo decks, and fire extinguishment failure, including suppression (EMSA, n.d.). Within Firesafe II, the rest of the stages and aspects were investigated, namely detection and decision making, containment and evacuation, and two full-scale tests of alternative detection technologies were undertaken. A fibre optic cable installed on the ceiling of the RoRo deck was tested as well as thermal imaging camers for open deck fires. As part of Firesafe II, a combined cost effectiveness assessment for all RCOs proposed across both studies was performed. Apart from the cost-effectiveness study, Firesafe I and II contributed towards the adoption of MSC.1/Circ.1615: *Interim guidelines for minimizing the incidence and consequences of fires in Ro-Ro spaces and special category spaces of new and existing Ro-Ro passenger ships* (IMO, 2019b).

In 2016 the Norwegian research council commissioned the National Ship Risk Model (NSRM). The objective was to develop risk models tailored for ships navigating in Norwegian waters, and, also, is part of a greater effort regarding risk-informed decision-making (Haugen, Stein; Almklov, Petter Grytten; Nilsen, Marie; Bye, n.d.). To that effect, various risk models were created for different accidents, fire being one of those. The initial focus was given to engine room fires due to their statistical contribution, and models were created for other geometries too, such as galleys, laundry, accommodation (Dokmo Bjørkås, 2016). The risk models are based on Bayesian Belief Networks (BBN) and the Norwegian Maritime Authority (NMA) database was used as a base. The models take into consideration all factors that contribute to a fire, including technical, operational and organisational factors and therefore provide a systemic overview, in line with approaches such as System-Theoretic Process Analysis (STPA).

The drawback of NSRM is the lack of data to populate all the nodes, especially those related to operational, organisational and human factors, which are discussed in (Haugen et al., 2016), where the authors argue that empirical and experimental data were absolutely necessary. Additionally, the influence amongst factors in the BBN model is speculative lacking actual basis/evidence and no distinction amongst ship types was performed, therefore, the models are of general nature which would surely lead to underestimation of hazards especially in the case of large passenger ships with novel designs. On the other hand, the nodes considered in the BBN are pertinent to

reality, which means that the NSRM risk models can be used qualitatively so as to investigate the influence between the factors whilst considering the ship as a system.

Project SEAMAN, Safety Enhancing and Monitoring Applications, established methodologies and recommended frameworks towards the safety of operations via continuous monitoring and analysis of onboard systems, with a focus on fire and flooding. Concerning fire, workshops were held amongst relevant partners and their experts as part of a large passenger ship engine room HAZID and a risk contribution tree models (bow-tie). Accordingly with the ranking, safety barriers were derived, implemented, and monitored via dynamic barrier management. Particularly, the safety barriers were ascertained via STPA and took into consideration all interactions between the systems, the asset, the crew as well as the operator. Onboard sensor data could be used in conjunction with historical data to monitor the technical aspect of the safety barriers, and relevant decision support is offered to the sharp and blunt end, and to assess the. The safety barriers were applied to both sides of the bow-tie, taking into account both preventing and mitigating barriers, enabling a holistic safety approach towards a fire free engine room.

## 2.5. Current Status of Engine Room Fire Safety

Another highly significant contribution on the subject of engine room fire safety is (McNay et al., 2019). The aim of the study was to examine and determine the state and focus of engine room fire safety via scrutinization and identification of biases and ranking of all constituents involved. The constituents that were examined are regulatory and classification society requirements, FSA as a rule-making tool, accident investigations, for both prevention and mitigation. The objective of the endeavour was to establish the effectiveness, including cost-effectiveness, of the aforementioned facets governing fire in engine rooms.

It is rightfully argued that a system's behaviour cannot be changed merely by observing/monitoring or reacting to its events, or by over-analysation of components in isolation (Besnard and Hollnagel, 2014). In other words, increasing the layer of protection does not make the system safe, since the system itself (engine room) is a sociotechnical one, including the machinery (technical aspect), people (operational aspect) and the organisational aspect. Furthermore, the author discusses that the reason behind engine room fires is attributed to inadequate design, failing to examine the engine room as system. To that end, the author introduces the concept of safety barriers to tackle engine room fire safety, highlighting their contribution to system safety.

The study commences by stating the obvious, the usual perpetrator is the release/leak of oil coming into contact with a hot surface, whilst the contribution of engine room fires remains unchanged despite all efforts. Furthermore, the author laid out a hypothesis; the current approach towards fires in engine rooms/machinery spaces is rather reactive in nature and focuses on the detection of hazards that have already occurred, for example stopping the supply of fuel after a release has taken place. In order to test the hypothesis, the so-called biases were determined by ranking the safety strategies within its aforementioned constituent of safety. Prevention was

subdivided into four sub-categories; eliminating a hazard, preventing systemic, contributing, and direct causal factors, presented in Table 8. Concerning the effectiveness level, a linear scale was used allowing for explicit use, instead of a tactical one, such that the mitigating aspect of loss prevention is ranked as the worst.

*Table 8. Strategies for loss prevention. Adapted from:* (McNay et al., 2019)

| Focus | Strategy Category | Safety Function | Example Barrier System | Effectiveness Level (priority scale) E |
|---|---|---|---|---|
| Prevention | 1 | Eliminate hazard | Decisions at concept and detailed design stages (based on risk assessment, tests, and other studies): substitution, simplification, decoupling, replacement, etc. | 6 |
| | 2 | Prevent systemic factors of incident | Strong safety culture, effective inter-organisational links, industrial best practices, robust safety assessment methodology, flawless standards and practices and regulatory oversight | 5 |
| | 3 | Prevent contributing factors of incident | Safety management system (SMS), clear communication and responsibilities and roles, crew training and supervision, adequate manning, fire drills | 4 |
| | 4 | Prevent direct factors of incident | Passive and active safety systems (thermal insulation, leak prevention, condition monitoring, etc.), and their inspection and maintenance actions | 3 |
| Mitigation | 5 | Control accident (stopping from propagating to loss) | Management decisions (training, staffing, preventive maintenance etc.), automatic detection and suppression systems, emergency shutdown, ventilation control system etc. | 2 |
| | 6 | Reduce damage (loss) | Management decisions (training, staffing etc.), containment (structural fire protection, fire doors etc.), automatic and manual firefighting equipment and preparedness, evacuation equipment and preparedness | 1 |

The loss prevention strategies were considered on a risk contribution tree (bow-tie), as presented in Figure 21. Under the review, it was ascertained that the focus of fire safety lies on proximate events immediately prior to ignition taking place and/or mitigation, whilst the former is situated just left of the (fire) event itself. The way forward, as per the research conducted, is via a systematic approach, with focus on the left of the bow-tie, such that systemic and contributing factors are accounted for, apart from the direct which are somewhat looked after.

Therefore, this research endeavour is of paramount importance as it sheds light on the everlasting paradigm of engine room fires, while the proposal of systemic

examination is in line with approaches from other safety-intense industries, such as oil and gas (Aina Eltervåg, Tommy B. Hansen, Elisabeth Lootz, Else Rasmussen, Eigil Sørensen, Bård Johnsen, Jon Erling Heggland, Øyvind Lauridsen, 2017) which is known for measuring safety, aerospace (Rising and Leveson, 2018), nuclear (Kecklund et al., 1996) and process (Yuan et al., 2022). Furthermore, the author proposes dynamic barrier management (DBM) in order to strengthen the existing barriers in place, specifically in relation to the events around the centre of the bow-tie (Figure 21).

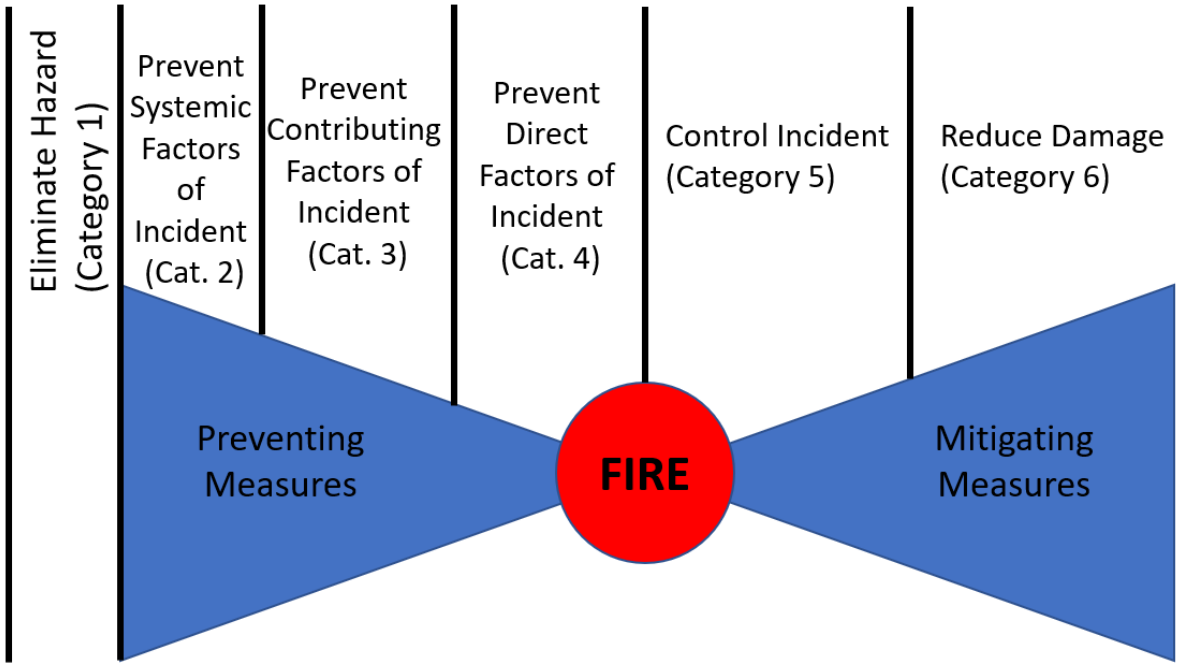


*Figure 21. Bow-tie showcasing the loss prevention strategies. Adapted from:* (McNay et al., 2019)

Via continuous analysis of the "health" of the relevant barriers and, by extension, the overall risk of the system, DBM would allow to measure performance on the sharp end of category 4 to the very least. With respect to bias, the current focus on elimination of direct factors is attributed to the wide use of linear, event-based models for accident analysis, such as Reason's Swiss cheese model (Reason, 2000), presented in Figure 22, or the Domino effect (Heinrich, 1941), where a system is merely the sum of some components. Indeed, such models have had and still have great impact on how we examine safety but with the ever-increasing complexity of systems such approaches may fall short, therefore, a systems approach is crucial.

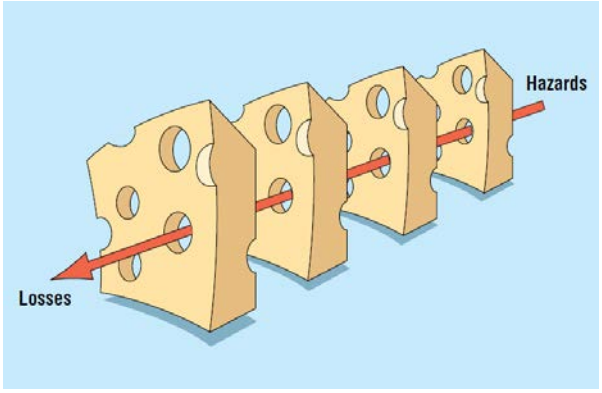


*Figure 22. Reason's Swiss cheese accident model, showing different layers of protection. Source:* (Reason, 2000)

## 2.6. Leak Detection Systems

Since the 1970s, the issue of leak detection in pipelines has remained a significant concern, regardless of the type of commodity being transported, such as water or petroleum products (Henrie et al., 2016). It might be anticipated that over the span of fifty years, the pipeline industries, including the oil and gas sector, would have made significant progress in addressing this urgent matter. However, this assumption is not entirely accurate. During this period, numerous methods and techniques for leak detection utilizing diverse approaches, whether physical or otherwise, have been suggested.

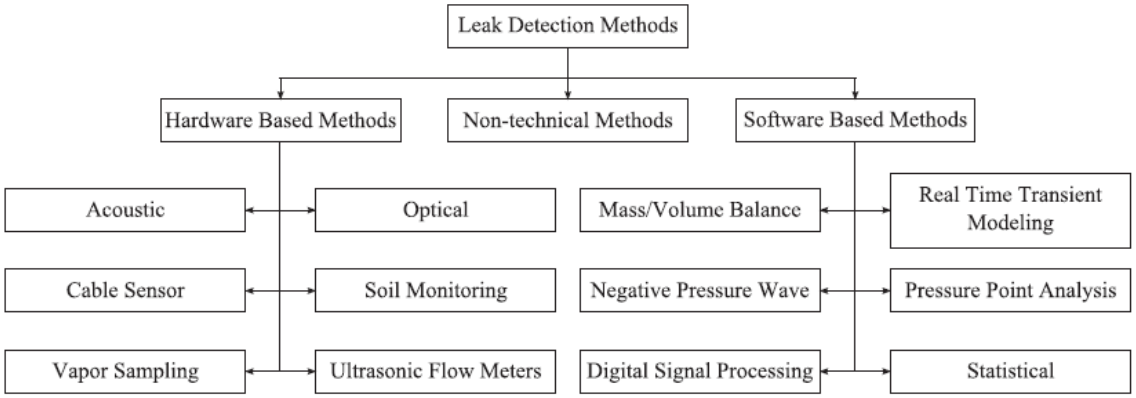


*Figure 23. Classification of lead detection approaches based on technical nature. Source:* (Murvay and Silea, 2012)

To that effect, relevant literature was identified and perused accordingly in order to identify possible technologies and/or techniques for leak detection. Figure 23 presents a high-level classification of available leak detection approaches as summarised in (Murvay and Silea, 2012). As per Figure 23, the leak detection methods were broken down into groups which depend entirely on the technical nature and operation of the leak detection techniques (LDT). Therefore, LDTs were broken into three groups; namely, hardware-based methods, non-technical methods, and software methods.

Other classifications, such as the one from (Adegboye et al., 2019), presented in Figure 24, have grouped LDTs into exterior methods, visual/biological methods, and Interior/Computational methods.

A cross-examination between Figure 23 and Figure 24 reveals that these two classifications are entirely the same but with different nomenclature. As implied by the classification, non-technical/visual/biological methods involve human involvement as a fundamental component, relying on the senses of vision, hearing, and osphresis for detection. In certain cases, trained sensory dogs are employed to detect and identify the presence of the commodity (Geiger, 2006). For clarity, these methods were referred to as non-technical methods.

Moving on, both hardware/exterior and software/interior approaches utilise sensors for leak detection. The distinction lies in whether the sensor itself is capable of directly sensing the leak. In other words, hardware/exterior methods rely on sensors that do not require extensive software or pre-processing of signals to detect leaks. These

sensors are capable of identifying "abnormalities" in the pipeline as indicators of a leak. Additionally, most of these methods require physical contact between the sensor and the pipe. For instance, a fibre optic sensor consists of a fibre cable installed along the bottom of the pipe, which can detect contact with foreign substances such as oil. In this case, there is no background software involved; the sensor alone provides the leak alarm.

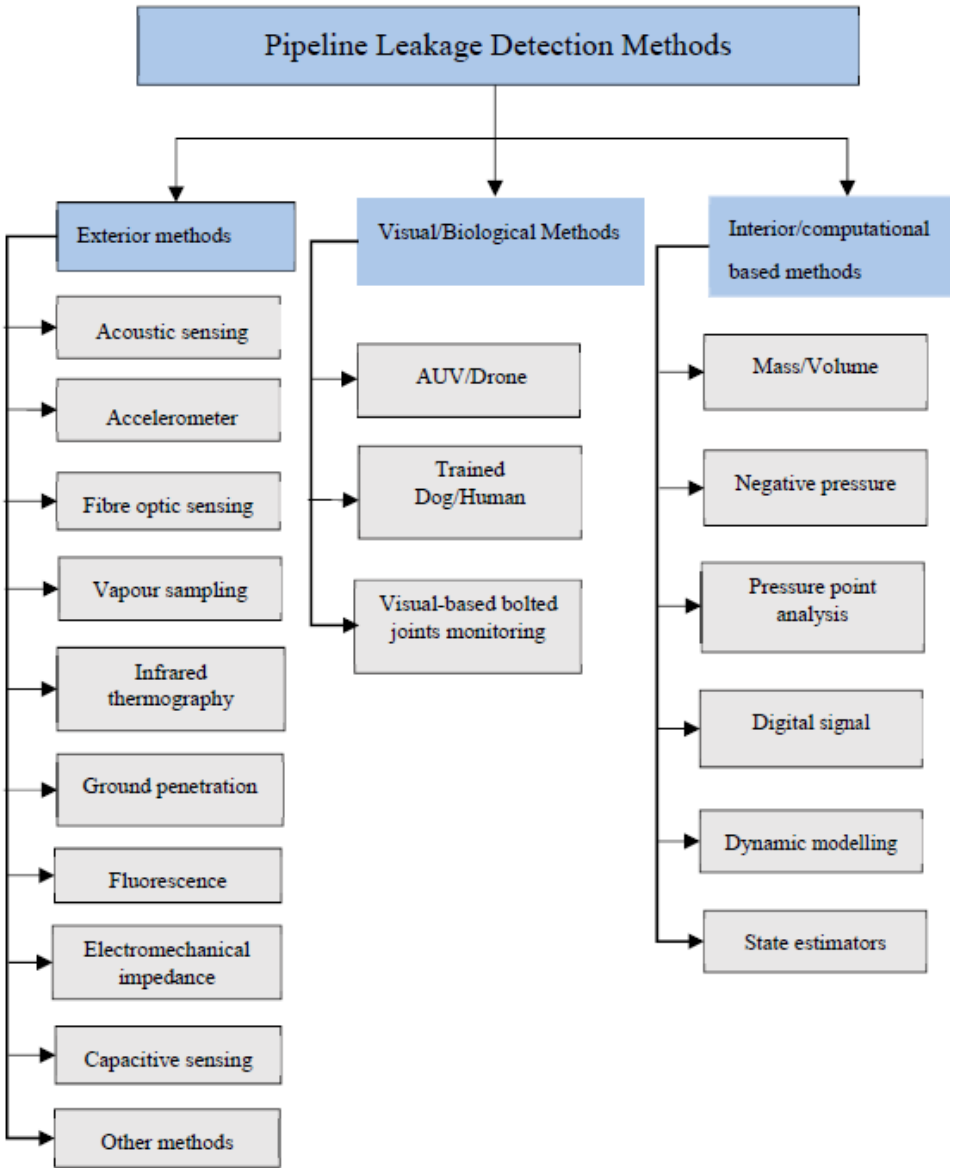


*Figure 24. Alternative classification of leak detection approaches. Source:* (Adegboye et al., 2019)

Software/internal methods heavily rely on computational algorithms and receive data from sensors. The sensors, in collaboration with the software, continuously monitor various oil parameters within the pipe, such as temperature, pressure, flow rate, and more. By utilising sensor fusion, leak inference can be achieved.

Moving forward, the terms "hardware" and "software-based" detection will be used, following the classification presented in Figure 23.

It is important to note that the variations in the classifications are primarily at the top-level nomenclature, while the techniques themselves remain the same. Additionally, it should be acknowledged that these classifications originate from the pipeline industry, which transports a wide range of commodities (e.g., petroleum products) through various modes (on land, buried, subsea, etc.). Therefore, certain solutions and techniques may not be applicable in the context and geometry of a ship or an engine room, respectively.

In the following section, both hardware and software leak detection techniques are furtherly discussed in terms of their applicability in ship engine rooms.

### 2.6.1. Hardware-based Leak Detection Methods

Table 9 presents a summary of available hardware-based leak detection Table 9. Hardware based leak detection methods. Source:(Adegboye et al., 2019)methods, along with principle of operation, and strengths and weaknesses of each. With respect to the applicability of those in ship engine rooms, it became immediately clear that the ground penetration radar is not suitable for the environment of operation, as well as the vapour sampling since it is applicable only to gaseous commodities.

The potential use of acoustic sensors was considered as a means to address the issue at hand. These sensors are capable of quickly detecting the occurrence of a rupture (indicating a possible loss of containment) through acoustic sensing and are relatively easy to install. However, it was found that these sensors are highly susceptible to environmental and background noise (Martins and Seleghim, 2010), which can lead to Type I and II errors, namely false positives, and false negatives, respectively. Considering the noise levels typically present in an engine room and the fact that leaks may not always originate from ruptures, it was concluded that such sensors are not suitable for this application.

Another potential solution that appeared promising was capacitive sensing. However, during the review process, it was observed that these sensors are primarily used in subsea pipelines. Additionally, the sensor must come into direct contact with the leaking oil to trigger an alarm. In the case of a jet leak, this sensor was found to be inadequate and therefore disregarded. Based on this evaluation, it was concluded that hardware-based detection methods are not applicable for the scope of this particular case study.

*Table 9. Hardware based leak detection methods. Source:*(Adegboye et al., 2019)

| Methods | Principle of Operation | Strengths | Weaknesses |
|---|---|---|---|
| Acoustic Emission | Detect leaks by picking up intrinsic signals escaping from a perforated pipeline. | Easy to install and suitable for early detection, portable and cost-effective. | Sensitive to random and environmental noise, prone to false alarms and not suitable for small leaks. |
| Fibre Optics Sensing | Detect leaks through the identification of temperature changes in the optical property of the cable induced by the presence of leakage. | Insensitive to electromagnetic noise and the optical fibre can act both as sensor and data transmission medium. | The cost of implementation is high, not durable and not applicable for pipelines protected by cathodic protection systems. |
| Vapour Sampling | Utilise hydrocarbon vapour diffused into the sensor tube to detect trace concentrations of specific hydrocarbon compounds. | Suitable for detecting small concentrations of diffused gas. | Time taken to detect a leak is long, not really effective for subsea pipelines. |
| Infrared Thermography | Detect leaks using infrared image techniques for detecting temperature variations in the pipeline environment. | Highly efficient power for transforming detected objects into visual images, easy to use and fast response time. | Quantifying leak orifices smaller than 1.0 mm using IRT-based systems is difficult. |
| Ground Penetration Radar | Utilise electromagnetic waves transmitted into the monitoring object by means of moving an antenna along a surface. | Timely detection of leakage in underground pipelines, reliable and leak information is comprehensive. | GPR signals can easily be distorted in a clay soil environment, costly and require highly skilled operator. |
| Fluorescence | Proportionality between the amount of fluid discharged and rate of light emitted at a different wavelength. | High spatial coverage, quick and easy scanning for leaks. | Medium to be detected must be naturally fluorescent. |
| Electromechanical Impedance | Utilise mechanical impedance changes deduced by the incident of pipeline defect. | A single piezoelectric transducer can serve as both sensor and actuator. | It is only applicable for metal pipelines, operational limitations in high temperature environments. |
| Capacitive Sensing | Measuring changes in the dielectric constant of the medium surrounding the sensor. | It can be employed for detection in non-metallic targets. | Requires direct contact with the leaking medium. |
| Spectral Scanners | Comparing spectral signature against normal background. | Capable of identification of oil type (light/crude) and thickness of the oil slick. | The amount of data generated by a spectral scanner is large which limited its ability to operate in nearly real-time. |
| Lidar Systems | Employed pulsed laser as the illumination source for methane detection. | Able to detect leaks in the absence of temperature variation between the gas and the surroundings. | High cost of execution and false alarm rate. |
| Electromagnetic Reflection | Measure emitted energy at different wavelengths. | It can indicate leak location | It can be affected by severe weather. |

### 2.6.2. Software-based Leak Detection Methods

The operational principle, strengths, and weaknesses of each method are summarized in Table 10, along with pertinent studies. Upon the conduction of a brief review of these methods, it became apparent that this particular method class holds significant promise, especially when compared to hardware-based approaches. In the previous section, namely the hardware-based approaches, the suitability of sensors was carefully examined based on specific abilities and characteristics such as detection speed and accuracy. In other words, instinctively, functional requirements against which the leak detection system (LDS) is evaluated were stipulated, which, in turn, lead to the instinctive formation of primary and secondary functional requirements as per (DNV-GL, 2019).

These functional requirements are imperative, as per the literature, when selecting a LDS for an application. In the context of a ship engine room, the primary functional requirement of a hypothetical LDS would be to be capable of detecting a loss of containment. The secondary requirements would be the estimation of leak rate and leak localisation.

*Table 10. Software-based leak detection methods including relevant material/studies. Adapted from:* (Adegboye et al., 2019).

| Methods | Principle of Operation | Strength | Weakness | Relevant Material |
|---|---|---|---|---|
| Mass-volume Balance | Utilises discrepancy between upstream and downstream fluid mass-volume for determining leakage | Low cost, portable, straightforward, and insensitive to noise interference. | Leak size dependent, not applicable for leak localisation | (Henrie et al., 2016; KROHNE Group, n.d.; OptaSense, n.d.; Pipe, n.d.) |
| Negative Pressure Wave | Utilises negative pressure waves propagated due to pressure drops as a result of a leakage | Fast response time and suitable for leak localisation | Only effective for large instantaneous leaks | (Adegboye et al., 2019; Ostapkowicz, 2016) |
| Pressure Point Analysis | Monitor pressure variation at difference points within the pipeline system | Appropriate for underwater environments, cold climates and adequately functioning under diverse flow conditions | Leak detection is challenging in batch processes where valves are opened and closed simultaneously. | (Akib et al., 2011; Golmohamadi, 2015) |
| Digital Signal Processing | Utilises extracted signal features such as amplitude, frequency wavelet transform coefficients, etc., from acquired data | Good performance, suitable for detecting and locating leak positions | Easily prone to false alarms, and cab be masked by signal noise. | N/A |
| Dynamic Modelling / Real Time Transient Monitoring | Detects leaks using the discrepancy between measured and simulated data based on conservation equations and the equation of the state of the fluid. | Applicable for leak detection and localisation, fast and a large amount of data possible to be handled. | High computational complexity, expensive and labour intensive | (Adegboye et al., 2019; Henrie et al., 2016; Isermann, 2012; Whaley et al., 1992) |
| State Estimation | Estimates the missing variables using a set of algebraic equations that relates a set of input, output and state variables | Suitable for reconstruction of the state vector and estimating the missing variable. | The limitations vary based on estimator classes such as poor convergence factors, computational complexity, discarding of uncertainties during simulation, etc. | N/A |

Conversely, the functional requirements themselves are situational to the environment of application, commodity, piping system design, regulatory requirements. For example, the requirements pertinent to an underground pipeline would be quite different from those of a sub-sea one (Shama et al., 2018).

Subsequently, other functional requirements could be stipulated, such as additional/complementary data (trends, tables, etc.) that aid a potential analyst in diagnosing the system, or calculation of a pipe rupture probability (Henrie et al., 2016).

Mass/volume balance leak detection systems have served as a foundational method in the field, being one of the earliest solutions available and still widely utilized by various leak detection system vendors (Henrie et al., 2016; KROHNE Group, n.d.; Network, n.d.; OptaSense, n.d.; Pipe, n.d.). These sensors operate as flowmeters, relying on the principle of mass conservation; if the mass of a material entering the pipeline does not match the mass exiting the pipeline, it indicates the presence of a leak. In practice, the conservation of standard volume is often substituted for mass conservation.

In an ideal system, the mass/volume balance approach appears flawless. However, in reality, where transient flow states occur, this is not the case. Specifically, the instantaneous amount/volume of fluid in the pipeline must be considered. Understanding the impact of transient states requires acknowledging the paradigm that when pressure at the inlet is increased, more fuel enters the pipeline than exits, resulting in a phenomenon known as line pack or packing rate. Line pack introduces the largest source of uncertainty in these leak detection systems. Other sources of uncertainty include instrument uncertainty (typically ±5%) (Network, n.d.) and input data uncertainty, such as noise.

Consequently, the main drawback of this method lies in its assumption of steady-state conditions, which affects the time required to detect a leak. As a result, while relatively small leak rates can be detected, the detection time needs to be extended to minimize false alarms. Additionally, due to the nature of this leak detection system, it is unable to pinpoint the exact position or location of the leak. This limitation can be overcome by employing "smart sensor placement," which involves increasing the number of sensors in the pipeline, albeit at the expense of cost-effectiveness. It is evident that mass/volume balance leak detection methods are accompanied by significant uncertainty. Therefore, in real-world applications, these methods need to be supplemented with additional approaches to enhance their effectiveness.

The principle of operation for Negative Pressure Wave leak detection is based on the assumption that when a leak occurs, there is a sudden pressure drop and a decrease in the instantaneous flow rate. This pressure drop, propagates in both upstream and downstream directions along the pipeline, generating a negative pressure wave on the upstream side. By installing two pressure sensors, one before and one after the suspected leak location, the negative pressure wave can be detected (Adegboye et al., 2019; Ostapkowicz, 2016). This technique allows for leak localization, but it is most effective in detecting large, instantaneous leaks such as pipe ruptures, and it is unable to capture progressive leaks that develop gradually over time. This limitation serves

as a compelling reason for rejecting this particular leak detection system in the context of an engine room.

At the core of Pressure Point Analysis leak detection system lies statistical analysis. It involves comparing readings from various pressure sensors against measured or even simulated data to identify statistical trends (Adegboye et al., 2019; Akib et al., 2011; Golmohamadi, 2015). If the incoming (measured) pressure significantly deviates from the measured/historical pressure, it indicates the occurrence of a leak. In an ideal scenario, slow-developing or small leaks can be detected through this statistical analysis, but pinpointing the exact location of the leak is challenging. Moreover, false alarms can be triggered by valve openings/closures and transient events, which are common in fuel oil systems of ships. Consequently, this type of LDS would not provide accurate system state estimation, leading to a potential increase in likelihood of false alarms.

As the term suggests, Real-Time Transient Monitoring (RTTM) relies on a real-time transient model of the pipeline, characterised by a plethora of equations of conservation (Adegboye et al., 2019; Henrie et al., 2016; Isermann, 2012, 2011; Whaley et al., 1992), and lies very close to the principle of dynamic modelling and digital twins, as suggested by Table 10.

- Continuity (conservation of mass),
- Momentum (Newton's 2$^{nd}$ law),
- Energy (conservation of energy, including the thermal modelling - optional),
- Pipe wall expansion,
- (equations of) State (relationship between P, T, ρ),
- Viscosity,
- Darcy-Weisbach Friction Factor (f), and
- Machinery (pumps, filters, etc.).

Since the operating pressure of a pipeline is usually transient (Henrie et al., 2016), the physical flow parameters present a similar behaviour. Steady-state conditions are usually scarce as the flow characteristics vary with time. Hence, RTTM proposes that a model created via the aforementioned equations would enable for the calculation of the instantaneous transient flow parameters.

A real-time transient model (RTTM) approach represents the pipeline assuming no leakage. The continuity equations ensure that mass is conserved within the pipeline or the examined control volume, for smaller sections. Any violation of this conservation indicates the presence of a leak. Therefore, the disparity between the measured values from sensors and the estimated values is utilised to infer a leak. Leak inference can be derived from a transient perspective, a statistical perspective, or a combination of both, as presented in Figure 25.

Incorporating statistical methods/models into the RTTM is a common practice to enhance the transient model. Some vendors may market this as Extended-RTTM, but it is merely a marketing strategy as the inclusion of statistical methods is inevitable.

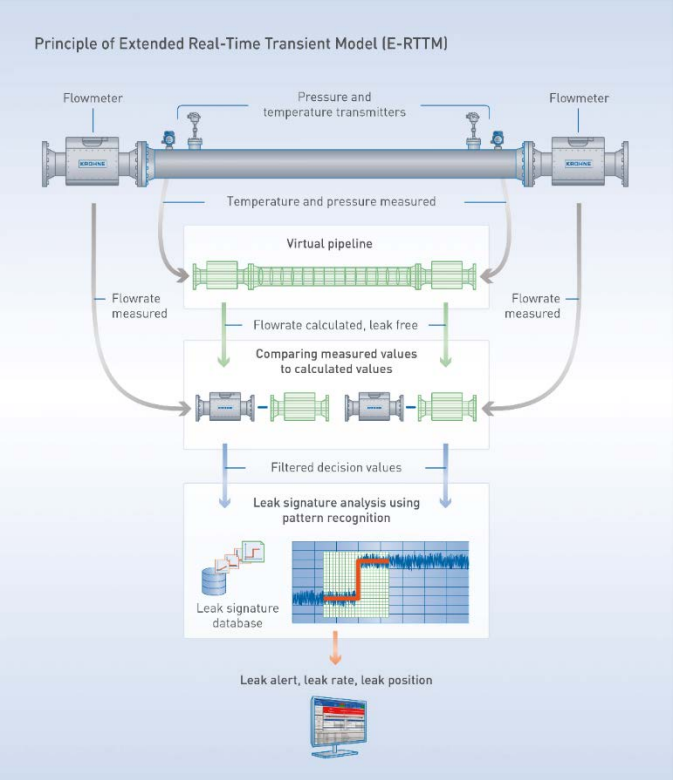


*Figure 25. Principle of operation of a commercial RTTM leak detection system. Source:* (KROHNE Group, n.d.)

While RTTM relies on computational modelling for leak inference, it necessitates input data. This underscores the importance of sensory equipment such as flowmeters (mass/volume balance sensors), pressure sensors, and temperature sensors. These instruments provide the necessary data as input to the equations and serve as a reference for leak inference. Consequently, RTTM represents a significant improvement over mass/volume balance leak detection techniques.

Furthermore, RTTM-based leak detection systems are implemented in two main approaches. Namely, either by computing the line packing rate exclusively, thereby enhancing the speed and reliability of mass/volume balance leak detection, or by calculating all of the equations mentioned previously.

One computational challenge in RTTM is that some of the equations are partial differential equations with independent variables like time and position, which cannot be solved analytically. Different discretization techniques (e.g., finite difference methods) and numerical techniques (e.g., explicit, and implicit integration) are available (Geiger, 2006). Each discretization and numerical approach have their own advantages and disadvantages, impacting the fidelity of the solution, response time, and accuracy of leak detection.

Lastly, there are a few techniques that were not explicitly discussed or reviewed above. These are not considered to be left out or neglected as their usage has been implied quite a few times thus far. For examples, digital signal processing is required whenever there is a sensor or a complex system, as sensor data is noisy, outliers require rejection, missing data imputation and filtering amongst others. Hence, these were considered as auxiliary techniques/tools to other leak detection technologies.

## 2.7. Research Gap

From the review presented in the previous sections, it is more than evident that the current status of fire safety onboard is not effective in preventing them. This is heavily supported by the statistical review presented and discussed in this chapter. In summary, despite the plethora of provisions in the regulations, fire events have a very clear trend in terms of total losses, consistently ranking third across various studies with or without overlapping years (samples) of examination. Moreover, cruise ships tend to dominate the frequency, whereas RoPax ships dominate the fatalities, where the potential loss of life can be heavily influenced by a single freak accident, for example the fire onboard the RoPax Norman Atlantic.

Engine room fires have been ascertained, and verified through the literature review, to statistically occur in the engine room via the release of flammable oil which comes into contact with hot surfaces. Additionally, the current status of fire safety, as per (McNay et al., 2019), has been identified as reactive in its nature, meaning that there is only focus on hazards that have already been materialised. Furthermore, great emphasis has been given on mitigation strategies and technologies, such as water mist deluge systems, passive fire protection, etc., in an effort to avert the consequences.

What SOLAS, or the regulatory provisions in general, have not considered yet is to examine the engine room or any other fire-prone deck/enclosure as a system, having technical, organisational and operational aspects/elements. Other safety intense industries, such as the oil and gas, and process, have a proven record of using systemic approaches (Aina Eltervåg, Tommy B. Hansen, Elisabeth Lootz, Else Rasmussen, Eigil Sørensen, Bård Johnsen, Jon Erling Heggland, Øyvind Lauridsen, 2017; Astrup et al., 2016; Fornes, 2016; Heinrich, 1941; Kecklund et al., 1996; Kujath et al., 2010; Lauridsen et al., 2016; Rathnayaka et al., 2011a, 2011b; Sobral and Guedes Soares, 2019; Sondre Øle, Anne Wahlstrøm, Helle Fløtaker, 2016; Yuan et al., 2022), which presents a research gap in terms of the maritime industry as no such approaches had been identified upon completion of this thesis.

One may argue that the available leak detection technologies could be utilised towards averting the release of flammable oils, but as per the literature review conducted on the available solutions, a straightforward approach is impossible due to the limitations discussed. Furthermore, treating only the technical aspect of the leak issue is not sufficient and a systemic approach is paramount, otherwise barrier degradation and consequent failure are ensured (Sklet, 2006; Sondre Øle, Anne Wahlstrøm, Helle Fløtaker, 2016). Therefore, a systemic approach in way of safety barriers and dynamic barrier management have been identified as a gap in the literature.

Additionally, large passenger vessels are of outmost interest due to the amount of people onboard, while these are segregated into MVZ in terms of fire safety. Thus far, no research has been conducted having the MVZ in mind. No risk models had been identified during the literature review, except for the NSRM one, (Azizpour, 2016; Haugen et al., 2016; Haugen, Stein; Almklov, Petter Grytten; Nilsen, Marie; Bye, n.d.), a Bayesian Belief Network risk model, which is trivial due to the lack of data required

to populate the nodes in the network. Specifically, there is lack of fire risk models irrespective of the possible approaches that are available, examining a MVZ in a large passenger ship. This is another research gap identified in the literature. Regardless of the approach adopted, except for the engine room, the MVZ risk model should also capture the risk emanating from other areas/decks within the MVZ, such as large public spaces and passenger cabins. The latter would offer completeness in terms of fire risk.

Therefore, as per the aforementioned, this thesis aims to fulfil two different research gaps in way of fire safety. Namely:

- Lack of systemic approaches, such as safety barriers and dynamic barrier management, monitor the release of flammable oil in large passenger ship engine rooms.

- Lack of a fire safety risk model in way of a main vertical zone of a large passenger ship.

# 3. Research Questions, Aims and Objectives

## 3.1. Research Questions

As per the literature review conducted, the majority of the fires experienced on board ships statistically occur in engine rooms, while the most predominant ignition being due to leaked/released oil coming into contact with hot surfaces. Moreover, regardless of the considerable regulatory and research efforts concerning the elimination of fires on board, the frequency remains constant while the size of passenger ships is only increasing with time. Leak detection methods are not straightforward and are very dependent on the applicable situation, amongst other factors. For example, sensors able to detect leaks exist and are installed in ships, but those operate after the leak has taken place.

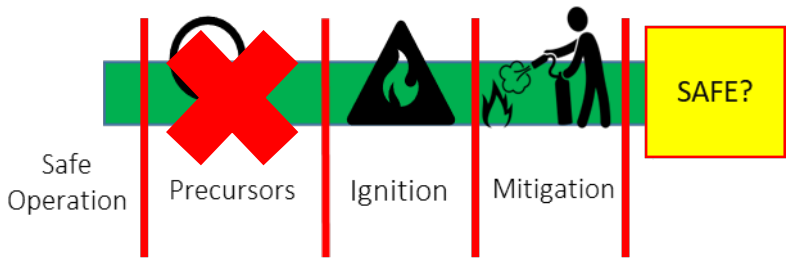


*Figure 26. Fire development timeline*

On the other hand, a research gap was noted since the current state of engine room fire safety focus, summarised in Figure 26, lies on detection of proximate technical events, not precursors, prior to and post-ignition, eliminating direct factors, i.e. flammable oil supply, and providing damage control/mitigation, i.e. fire dampers, deluge systems, etc.

The state of fire safety can be considered trivial as it does not investigate and identify latent causal factors, and to consider the engine room, if not the whole main vertical zone, as a system having a plethora of components with various interactions amongst technical, operational, and organisational elements.

Therefore, the following research questions emanate:

- Which areas of a large passenger ship should be monitored for their fire risks?
- Could safety barriers aid in averting fires from taking place?
- How can safety barriers be implemented in the context of a large passenger ship engine room?
- How can we provide sensor-based early detection of technical fire precursors in large passenger ship engine rooms?
- Is it feasible to implement a dynamic barrier management scheme?

- In the uneventful case of fire breaking out, how can a risk model predict and quantify the effects from the engine room to other decks?

- How could a risk model of a MVZ be augmented and optimised so as to capture the impact of fire risk?

These research questions and the precursor approach are presented in Figure 27.

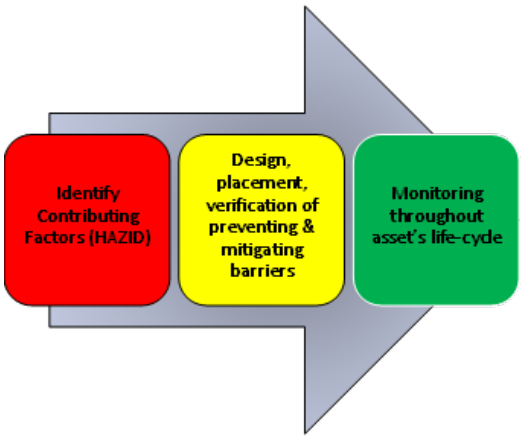


*Figure 27. Precursor approach to fire safety*

## 3.2. Aims and Objectives

The aim of the thesis is to establish a holistic risk-based fire safety model for a main vertical zone of a large passenger ship, able to predict and quantify the consequences of fire from the engine room to other decks, via the implementation and dynamic management of safety barriers concerning the prevention and fire simulations for the mitigation.

Investigation on a MVZ level was considered as such since the corresponding fire scenarios would increase exponentially with the inclusion of each additional zone. This would surely lead to a chaotic fire risk model and, also, violates the rationale of the MVZ itself. On an investigation level, considerations beyond one MVZ could be paramount but not in the case of a fire risk model, where adherence and compliance to the rules and provisions is presupposed.

In order to achieve the aforementioned aim, the following objectives must be achieved:

- Identify and analyse critical ship areas with respect to fire safety with particular focus on the engine room and its machinery, in order to develop appropriate safety barriers as necessary. These barriers shall prevent an event from occurring and protect against its consequences.

- Derivation of dynamic safety barrier management framework for the identified areas and machinery that are contained within. The dynamic barrier management will offer diagnostics with respect to a decision support system.

- Development of a risk contribution tree (bow-tie) model that is able to capture and quantify the fire effects in the case that a fire originates in the engine room but breaks out of it. Furthermore, the risk model shall take into account the fire risk of all critical ship areas.

### 3.3. Contributions to the field

The **developed risk model** addresses the research gaps identified and provides answers to the stated research questions. It provides a significant contribution to the area of fires onboard ships, with emphasis on **large passenger ships**. It goes beyond the state-of-the-art as it provides a **holistic simulation-based** approach that **captures the impact of dynamic barriers**.

The final output of this research is a fire safety risk model in way of a risk contribution tree having both a preventative and mitigating aspect. For the former, a framework able to derive and monitor safety barriers for the prevention of flammable oil releases/leaks was proposed. For the latter, the mitigating provisions of the regulations were taken into account in order to quantitatively assess the risk. 3D Computational Fluid Dynamic (CFD) simulations were conducted, involving the engine room as well as passenger cabin and large public space decks, in order to demonstrate the MVZ fire risk model.

The research work conducted in this thesis offers an original viewpoint on the significance of fire safety of large passenger ships. The necessity for the investigation on a MVZ level originated from the design philosophy of the MVZ itself and the existing legal framework (i.e. SOLAS). Due to their large size, passenger ships are divided as such, and so did the risk model that was proposed. According to the literature review, no other similar fire risk model has been presented.

Another contribution was the update of the fire accident statistics and the analysis of accident investigation reports on large passenger ships. This has been used and validated with industry experts in the EU H2020 project SafePASS and in the Joint Industry Project (JIP) SEAMAN. This work is original and was used in order to identify the critical ship areas and scenarios for the simulations.

Additionally, the framework proposed in order to avert, and potentially monitor for, flammable oil releases in engine rooms of large passenger ships was another contribution of this thesis. The framework takes into account traditional risk modelling approaches, such as failure trees, failure modes, effects, and criticality analysis along with the concept of safety barriers in order to derive technical barrier elements for flammable oil systems found in engine rooms. Furthermore, operation towards dynamic barrier management were also undertaken, in way of sensory equipment necessary to monitor the status of the safety barriers. The framework was demonstrated for the fuel oil line of a large passenger ship engine room within a main vertical zone, with the use of traditional risk methods and a commercial-off-the-shelf application.

Finally, the simulation-based methodologies that were employed for all critical fire scenarios were also another contribution of this thesis in terms of ship fire safety. The ultimate outcomes, concerning the incapacitation of occupants in the simulations, provided a realistic depiction based on the numerical results obtained from the quantification methods used to construct the design fires. Furthermore, the approach adopted from the evaluation of the fire risk on the cabin and large public space deck case studies were also novel in way of the maritime industry, which lacks available fire safety data as such.

# 4. Methodology

## 4.1. Risk Contribution Tree

In order to fulfil the first research question, a high-level HAZID was conducted through the literature review, where it was ascertained that, statistically, the majority of fires break out in the engine room, an area of any ship where flammable liquids (fuel oil, lubricating oil, etc.) and hot surfaces are abundant. Historically, engine room fires break out due to the uneventful release of flammable liquids which come into contact with said hot surfaces and contribute as such to more than 50% of fires.

Contrastingly with the frequencies in the literature, the engine room fires do not necessarily dominate the fatalities as these do not pose the highest consequences all the time, mainly due to passive firefighting means, safety barriers if you may, redundant/multiple suppression deluge systems, relevant alarms, and, depending on the size of the ship, dedicated qualified trained crew which supervise those (Azzi, 2010). Prime examples of such scenarios are cabin fires (Esther Marshall, 2023) and large public spaces. Additionally, these two areas are where the occupancy lies during night-time and daytime respectively, as per the SafePASS statistical analysis. Thus, a fire risk investigation in way of the risk contribution tree on these would full proof the validity and usefulness of a MVZ risk model.

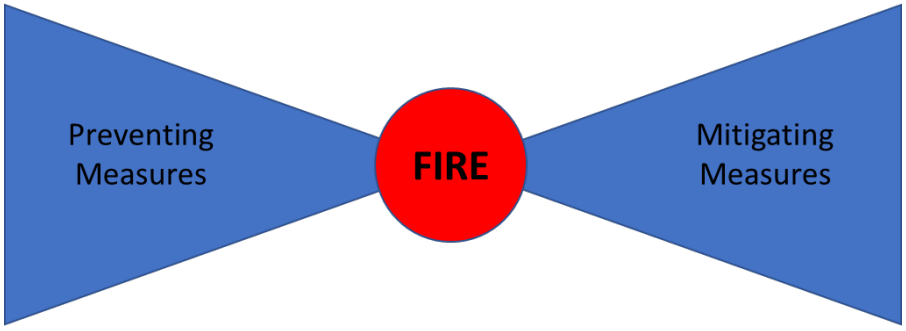


*Figure 28. Fire Bow-tie Model*

A generic bow-tie model is presented in Figure 28. On the left-hand side, preventative measures are taken into account in an effort to avert the unwanted event from occurring. In the case of this thesis, the unwanted event is a fire. Mitigating measures are usually included on the left-hand side of the bow-tie, in an effort to mitigate or eliminate the event after taking place.

In order to fulfil the second to fourth research questions, safety barriers and dynamic barrier management were considered to be the way towards a fire free large passenger ship. As per the literature review conducted on safety barriers, placing them arbitrarily, without proper structure, would prove to be detrimental since the ship, and therefore the system, would not be treated systemically. Accordingly with (Aina Eltervåg, Tommy B. Hansen, Elisabeth Lootz, Else Rasmussen, Eigil Sørensen, Bård Johnsen, Jon Erling Heggland, Øyvind Lauridsen, 2017; Astrup et al., 2016; Fornes, 2016; Kecklund et al., 1996; Kim, n.d.; Kujath et al., 2010; Lauridsen et al., 2016; Pitblado et al., 2016; Sobral and Guedes Soares, 2019; Sondre Øle, Anne Wahlstrøm, Helle Fløtaker, 2016; Yuan et al., 2022), in order to stipulate barrier functions,

prevalent hazards/situations must be identified accordingly. Therefore, a framework for the derivation, placement and monitoring of safety barriers for the identified hazards is imperative and absolutely necessary for the realisation of the aforementioned research questions and respective objectives.

Regarding the necessity for mitigating barriers, the right-hand side of the bow-tie, as rationalised in (McNay et al., 2019), the current focus of engine room fire safety lies upon mitigating measures in way of passive and active fire-fighting systems. Namely, the MVZ itself and the fire boundaries are classed as passive ones, while detectors and deluge systems as passive ones. Moreover, through project FIREPROOF, a plethora of fire risk analyses, including sensitivity, have been conducted on those (FIREPROOF consortium, 2010; George et al., 2012; Themelis et al., 2011; Themelis and Spyrou, 2012, 2010). Therefore, it was determined that there is no necessity to assess any mitigating measures as part of this risk contribution tree.

Conventionally, risk models are accompanied with Failure Tree Analysis (FTA) as well as Event Tree Analysis (ETA) (IMO - Submitted by Denmark, 2008; IMO, 2016c; Nilsen, 2005). Concerning the former, various operations are proposed later on within this chapter, to infer the status of the engine room safety barrier, including FTA per component, diagnostic system behaviour qualitative simulations, and FMECA. It is therefore considered that the preventative aspect of the bow-tie model has been treated.

In terms of using an event tree in the case of engine room fire, it is believed that the geometric complexity of a large passenger ship engine room renders the fire propagation a very intricate issue. Traditional event tree analysis models could be an extremely copious task. In the case of cabin deck fire scenarios for example, event trees can be considered as a straightforward approach as presented in Figure 29. Therefore, mapping a potential fire in the engine room via ETA was considered as very restrictive.

As a result, fire simulations were considered as a promising way in order to quantify the effects of fire risk emanating from engine rooms fires.

In order to assess the fire risk emanating, with respect to the sixth research question, fire simulations were utilised. Specifically, computational field model full 3D fire simulation codes were preferred as these provide the most tangible results, compared against zone models and their simplifications considering uniform layer distributions which surely provide fast, preliminary/indicative, results but lack the appropriate level of fidelity with respect to the heavily time-dependent and exceedingly tied interactions of the overabundance of the physical and chemical phenomena that take place during a fire. Consequently, FDS and Pyrosim were employed for this purpose.

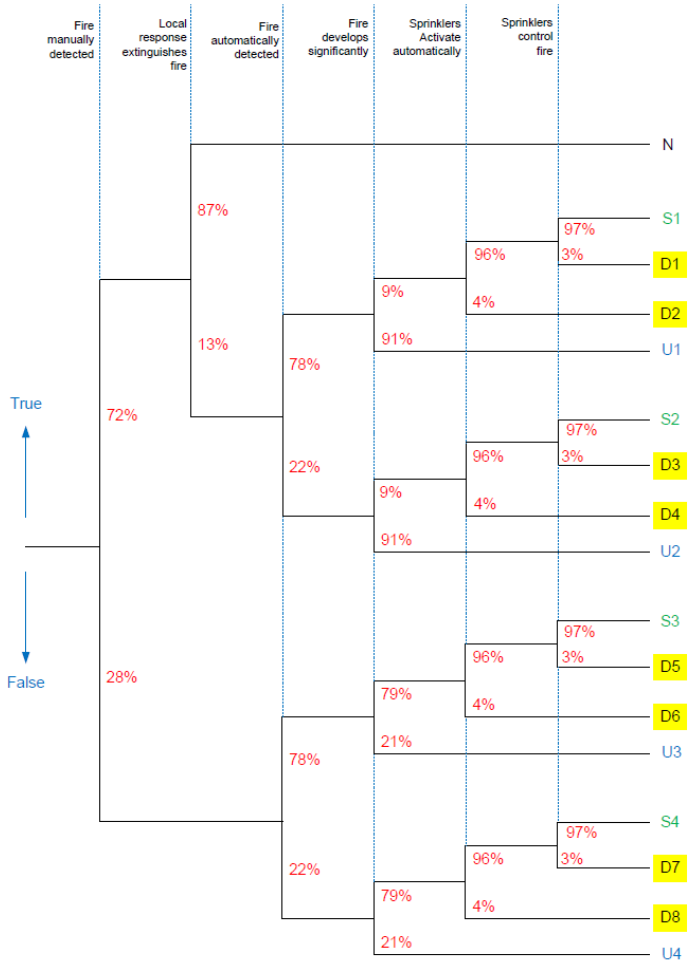


*Figure 29. Stateroom fire event tree from project FIREPROOF. Source:* (FIREPROOF consortium, 2010)

Concerning the fire simulation scenarios, the engine room is the prime candidate as per the research gap and respective research question. In theory, it would be possible to simulate a fire over the whole MVZ of a ship but that would require huge models which would surely be rather complex in terms of both the required computational power and time needed to complete such a simulation. Furthermore, it would be more optimal to stipulate risk models for each MVZ of a passenger ship, liable to the general arrangement of a ship and as per the mentality of the MVZ itself (in SOLAS).

Due to the statistical contribution of engine room fires, the investigation naturally commenced on the engine room, with particular focus given to it. The high-level procedure followed to derive a risk model for a main vertical zone of a large passenger ship is summarised in a flowchart format in Figure 30. The investigation begins through a high-level HAZID in way of how engine room fires occur, was conducted through literature pertaining to both qualitative and quantitative aspects. The former refers to prevalent fire hazards and respective scenarios in engine rooms while the latter refers to the statistical contribution of those.

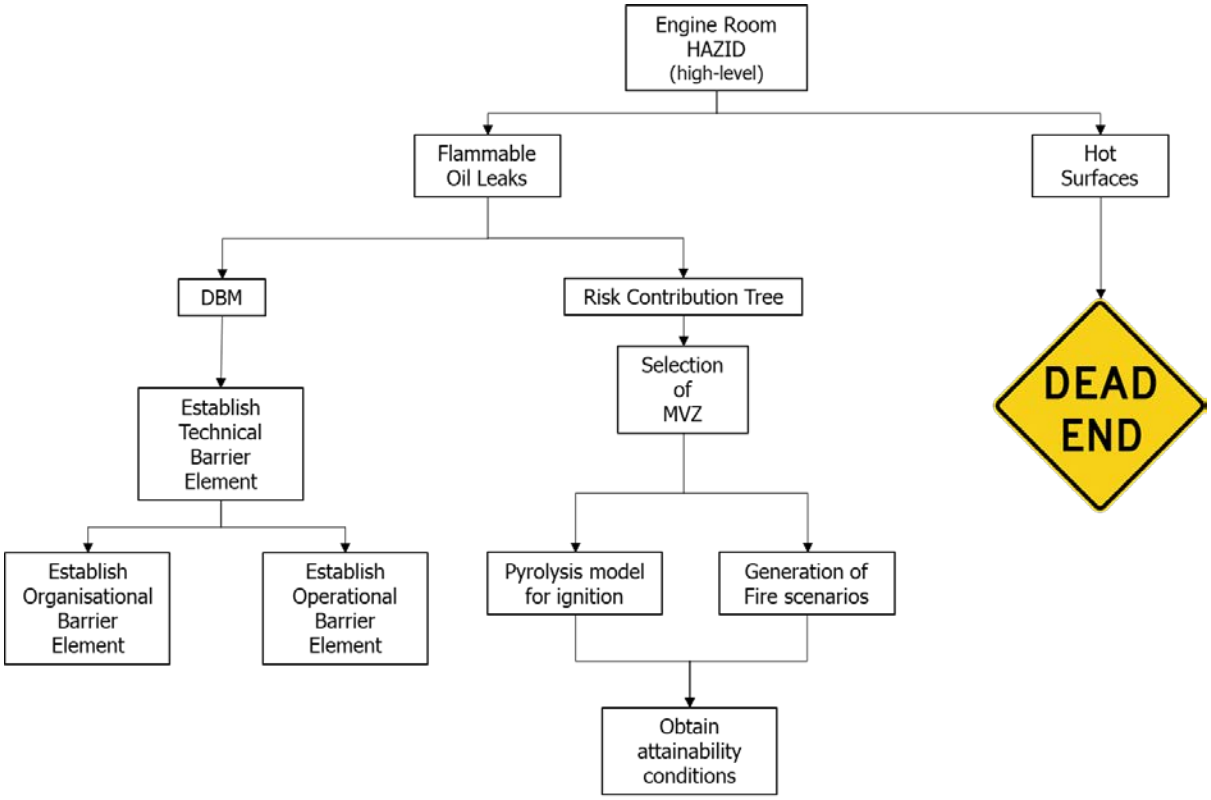


*Figure 30. Approach adopted to create a fire risk model for a MVZ of a large passenger ship.*

### 4.1.1. High-level Hazard Identification

The statistical analysis, the quantitative aspect of the HAZID, revealed that cruise ships are more frequently involved in fire incidents, while RoPax ships have a higher fatality rate. This is mainly because RoPax vessels not only carry passengers but also vehicles, which intrinsically increases the risk of fires. Additionally, many RoPax ships operate in less developed countries with questionable enforcement of regulations and handle a greater volume of transportation work. On the other hand, passenger ships are continuously growing in size to accommodate more passengers, and their designs are becoming increasingly complex to prioritise innovation and attract customers. Despite efforts, whether regulatory or otherwise, to prevent and mitigate the effects of fires, the frequency of such incidents remains consistently at least, with the consequences being too significant to overlook, in terms of the passengers, environment and safety. Hence, this risk model was emphasised on fires specifically in large passenger ships due to the significant number of people on board.

Concerning the qualitative HAZID in terms of the most frequent type of fire experienced across all engine rooms, the release of flammable oil coming into contact with a hot surface was ascertained across all examined literature, with the vast majority of incidents happening due to this. Additionally, as per the investigation on applicable regulatory rules, it was noted that surfaces having temperatures below 220$^{o}$C do not require insulation and fuel oil with flashpoints above 60$^{o}$C can be used on board.

Therefore, as per the high-level hazard identification, the risk model was focused towards averting fires emanating from the release of flammable oil coming into contact with hot surfaces (uninsulated or otherwise).

In terms of the first research question, there are two possible pathways, namely eliminating flammable oil leaks, and/or removing hot surfaces.

### 4.1.2. Hot Surfaces

One of the risks identified via the high-level HAZID was the presence of hot surfaces, usually on engines or other relevant equipment, presented in Figure 18, which as per SOLAS must always be kept under 220ºC. These hot surfaces are an integral part on how engine room fires happen, as these provide the heat source necessary to ignite flammable oil.

On the other hand, as per the discussion in Chapter 2.3, the aforementioned rule currently imposed by SOLAS, has been regarded as inadequate mainly due to two reasons. The former is the flashpoint of fuel oils, being more than 60ºC while a hot surface is 220ºC, which is why such incidents are still prevalent. If leaked pressurised flammable oil comes into contact with such surfaces, ignition is usually guaranteed as part of the oil will evaporate instantaneously and, subsequently, the vapours may ignite due to the existing presence of the hot surface. The latter is the insulation/lagging itself, in the sense that the insulation may be compromised due to maintenance, irrespective of the urgency for maintenance/repairs, and due to the age of the ship. This is why the CAP surveys were discussed earlier in the literature review.

Therefore, monitoring hot surfaces could not be very fruitful unless the respective SOLAS rules changes. Furthermore, lagging degrades via time and/or improper fitting, which is another item that would need further inspection. Additionally, monitoring hot spots would require some sort of imaging, either with thermal cameras or other means, whereas these hotspots, as per Figure 19, are usually situated in nooks and crannies which poses further difficulties. Due to the above, treating hot surfaces was not regarded as the way towards a fire free engine room, hence focus was given on flammable oil leaks.

In order to full-proof this decision and, consequently, the methodology towards the risk contribution tree, and as part of Project SEAMAN, a HAZID a workshop was held in Oslo, Norway on April 2018, where relevant partners/stakeholders, gathered to identify and evaluate, via expert input and ranking, the engine room fire hazards. The workshop was conducted prior to COVID-19; therefore, fourteen (14) experts gathered in person to discuss and rank the identified hazards. The board of experts consisted of stakeholders' representatives from multiple streams of the maritime industry, including shipowners/operators, experts from the classification society DNV, and technology manufacturers, including both engineering and data related equipment manufacturers (including sensory equipment for both the maritime and the oil and gas industries).

Additionally, the HAZID was conducted on a semi-qualitative basis, meaning that expert input and their respective knowledge played a crucial role on both the identification and the ranking of the engine room hazards. The consortium focused the HAZID on two elements of the fire triangle, namely flammable material (fuel) and ignition sources. As per the findings of the workshop, the release of flammable oil (both fuel and lubricating) ranked the highest, with hot surfaces following. Therefore, the results of the HAZID conducted for the purpose of this thesis were validated through the workshop.

## 4.2. Flammable Oil Leaks

Having ruled out the possibility and usefulness of treating hot surfaces, flammable oil leaks were chosen for further investigation via the risk contribution tree. The flammable oil contained and utilised within an engine room are fuel oil (HFO, LSHFO, MDO, etc.) and lubricating oils. Statistically, hydrocarbon leaks are more prevalent, therefore, pertinent focus was given on fuel oil leaks.

## 4.3. Framework for the Systemic Derivation of the Release Prevention Barrier

Due to the ruling out of hot surface monitoring and its pertinent usefulness, the derivation of safety barriers, as part of the preventative aspect of the risk model and thesis, was focused on averting flammable oil leaks, while the barrier would prevent the realisation of those into the engine room. Furthermore, the in-subject barrier is of an active nature, meaning that it continuously monitors the pertinent systems, along with the operational and organisational elements, whilst sensors are envisaged to be utilised to infer its status.

Since the barrier would protect against a potential flammable oil release, the barrier was termed as Release Prevention Barrier (RPB). The investigation of the RPB commences with the technical element of the RPB, being the backbone, and then towards the other elements, namely operational and organisational, providing a systemic coverage. Additionally, performance requirements and performance influencing factors for each element are absolutely necessary in order to aid with inferring status and, therefore, maintaining the barrier. Without this, diagnosis, and prognosis, dynamic barrier management in other words, cannot be obtained.

Having conducted a literature review on safety barriers and DBM, leak detection techniques were investigated towards their suitability for the RPB. Despite having identified methods that may prove fruitful towards the endeavour, DBM stipulates that the prevalent failure must be investigated thoroughly, therefore, sensors must be placed strategically. In order to do so, a breach of containment, i.e. a leak, must somehow be constituted as well as the behaviour of the RPB under both normal and abnormal conditions such as a leak.

The diagnostics focus on the detection of faulty barrier statuses or states that would eventually lead to degradation of the barrier, a fact which also supports the necessity of an appropriate decision support scheme/system. The latter stems from the principles of condition-based monitoring (CBM) (Knutsen et al., 2014). Conversely,

prognostics would enable to broaden the sensor data into future knowledge, explicit or informed estimations, of the barrier state, while the ultimate goal would be to predict the Remaining Useful Life (RUL) or Time to Failure (TTF) (Aizpurua and Catterson, n.d.; Moir et al., n.d.; Niculita et al., 2012; Rudov-Clark et al., 2009, n.d.; Zhang et al., 2018).

In order to achieve this, a constructive systematic analysis was conducted employing various operations/aspects of both safety and marine engineering

Naturally, the following queries must be answered:

- What constitutes a breach of containment (i.e. flammable oil leak)?
- How does the technical barrier element behave under normal operating conditions?
- How does the technical barrier element behave under abnormal conditions (leak)?

In order to shed light on the aforementioned questions, several approaches were researched and, consequently, identified whilst their contribution/usefulness was heavily scrutinised towards the questions at hand. These were Failure Modes, Effects and Criticality Analysis (FMECA), Hazard and Operability (HAZOP) and Systems Theoretic Process Analysis (STPA) (Dawson et al., 2015).

Via comparison of the nature, qualities, and outcomes of each, it was established that FMECA is the most suitable technique towards understanding how the technical element of RPB could fail. This is because FMECA mainly investigates on the component level (Aina Eltervåg, Tommy B. Hansen, Elisabeth Lootz, Else Rasmussen, Eigil Sørensen, Bård Johnsen, Jon Erling Heggland, Øyvind Lauridsen, 2017; Bolbot et al., 2019; Jonassen and Sjølie, 2016; Kritonas Dionysiou, 2019). Furthermore, the philosophy of component-level analysis follows the reasoning of obtaining barrier functional requirements. Conversely with FMECA, STPA considers the interactions between the system and the controller, aims at identifying causal factors of the identified hazards. FMECA on the other hand, analyses on component level, takes the system architecture into account and through case studies it has been evidenced to be more than capable of identifying additional hazards (Bolbot et al., 2019; Isermann, 2012, 2011; Sulaman et al., 2019). With respect to the RPB, since the system has already been built and is well into operation, the FMECA was conducted on a bottom-up approach, such that each component was examined to the lowest level of indenture (Marvin Rausand, 2004).

Concerning the behaviour of the RPB under both normal and abnormal operations a reliability, prognostics, and health management suite was employed, namely Maintenance Aware Design Environment (MADe) (MADe, 2019; MADe-PHM Technology, 2018a, 2018b; Siemens, 2017). MADe is a commercial off the shelf (COTS) application widely utilised for safety investigations as well as for prognostics and health management of engineering systems. Incentive for doing so was drawn from (Konstantinos Milioulis, 2019; Kritonas Dionysiou, 2019; Moir et al., n.d.; Niculita et al., 2017, 2012). First and foremost, MADe allows the user to create a functional

body diagram (FBD) of the system that requires investigation, including existing sensor means. Furthermore, the suite allows for diagnostic, What-If, analysis, several safety operations including FMECA, and sensor set analysis.

What-if analysis allows for injection of the identified, via the FMECA, faults on the FBD of the RPB, and offers great insight on how a system fails, including any failure propagation. For the purposes of this thesis, it was utilised to establish the notion of a flammable oil leak in the RPB. Through the conduction of the FMECA, components that are able to leak can be identified and subsequently these could be tested towards the system (RPB) behaviour. Finally, the sensor set analysis could prove to be very useful towards the placement of sensors, as the application offers an extensive library of real sensors used amongst industries. Nevertheless, in case the sensor set analysis is not useful towards the derivation of the RPB, an extensive literature review had already been conducted on leak detection techniques and respective technologies.

The various procedures investigated and discussed towards the development of a framework for the derivation of the technical element of the RPB presented in Figure 31.

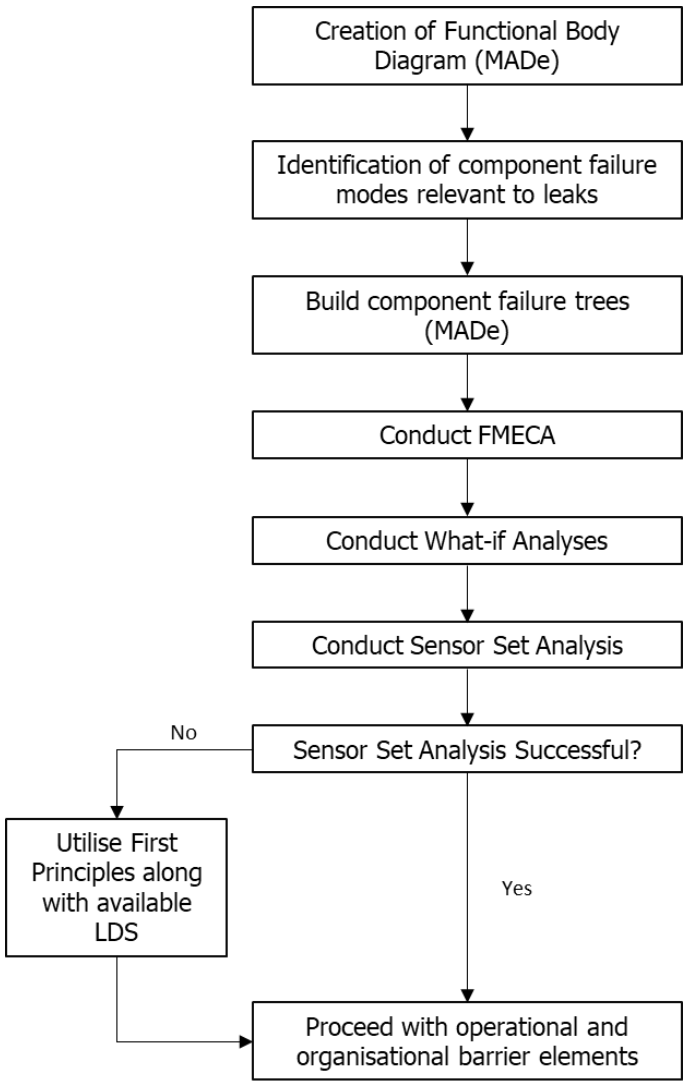


*Figure 31. Framework for the development of the technical RPB element.*

## 4.4. Fire Risk Modelling

The next step towards the realisation of the risk contribution tree is to account for cases when the RPB might fail as well as for other decks that present inherent fire risks. In other words, it is imperative that the risk model takes into account and quantifies the consequences of a fire that escapes the engine room but is stemming directly from it. Additionally, the engine room is not the only fire prone space within a MVZ of a large passenger ship, therefore, cabin and large public space decks were also included in the assessment of fire risk.

Each of these spaces (engine room, cabins/staterooms, and large public space) was regarded as a separate case study investigated in its own chapter. Furthermore, for both daytime and night-time occupancy scenarios, large public spaces and cabins respectively, simulations were performed considering normal conditions, where deluge systems are working as intended, and abnormal ones were deluge systems do not work, offering a complete picture of the risk that might be experienced.

A deterministic approach was employed for the case studies of the cabin and large public space decks, in way of modelling the pyrolysis phenomenon. Pyrolysis modelling involves the thermal decomposition of a material and the generation of flammable vapours which in turn may ignite coming into contact with a heat source. Such an approach is data intensive, in terms of the plethora of physical and thermal (fire-related) parameters that must be defined for each material and item present in the simulation geometry. It is heavily dependent on available thermal property data and the appropriateness of the pyrolysis model via the input of suitable values. Furthermore, such an approach could be applied to other decks, irrespectively of the geometry (ship or not), as first principle engineering has been utilised to its fullest extent. Such an approach, therefore, can be applied to a very wide range of applications and was employed to successfully assess the fire risk of the aforementioned geometries.

The methodology employed for the fire risk assessment of the cabin and large public space decks is presented in **Error! Reference source not found.**. The design fire methodology incorporated a first principles approach utilising material thermal properties that are discussed later on, in order to deterministically assess the fire risk. Conventional design fire approaches usually summarise the fire emanating from all the materials present in a space via a single burner, with a predetermined heat release rate and effluents, either via historical fire databases (RISE Institute, n.d.) and/or other approaches such as the probabilistic ones cited in project FIREPROOF and project SURSHIP (FIREPROOF consortium, 2010; George et al., 2012; Hakkarainen et al., 2009; Themelis et al., 2011; Themelis and Spyrou, 2012, 2010). Such approaches are remarkably effective, and their usefulness has been highlighted adequately within the literature review of this thesis. Furthermore, such approaches, especially the probabilistic ones, highlight the tremendous complexity and data required, with the accompanying uncertainty, of fire phenomena and the simulation itself.

On the other hand, deterministic approaches as the one proposed within this section, require explicit knowledge not only of the materials present in a geometry and their

chemical properties, but of specific thermal behaviour data, the so-termed “pyrolysis data”, which is the novelty of this approach and the case for first principle deterministic approaches in large passenger ships.

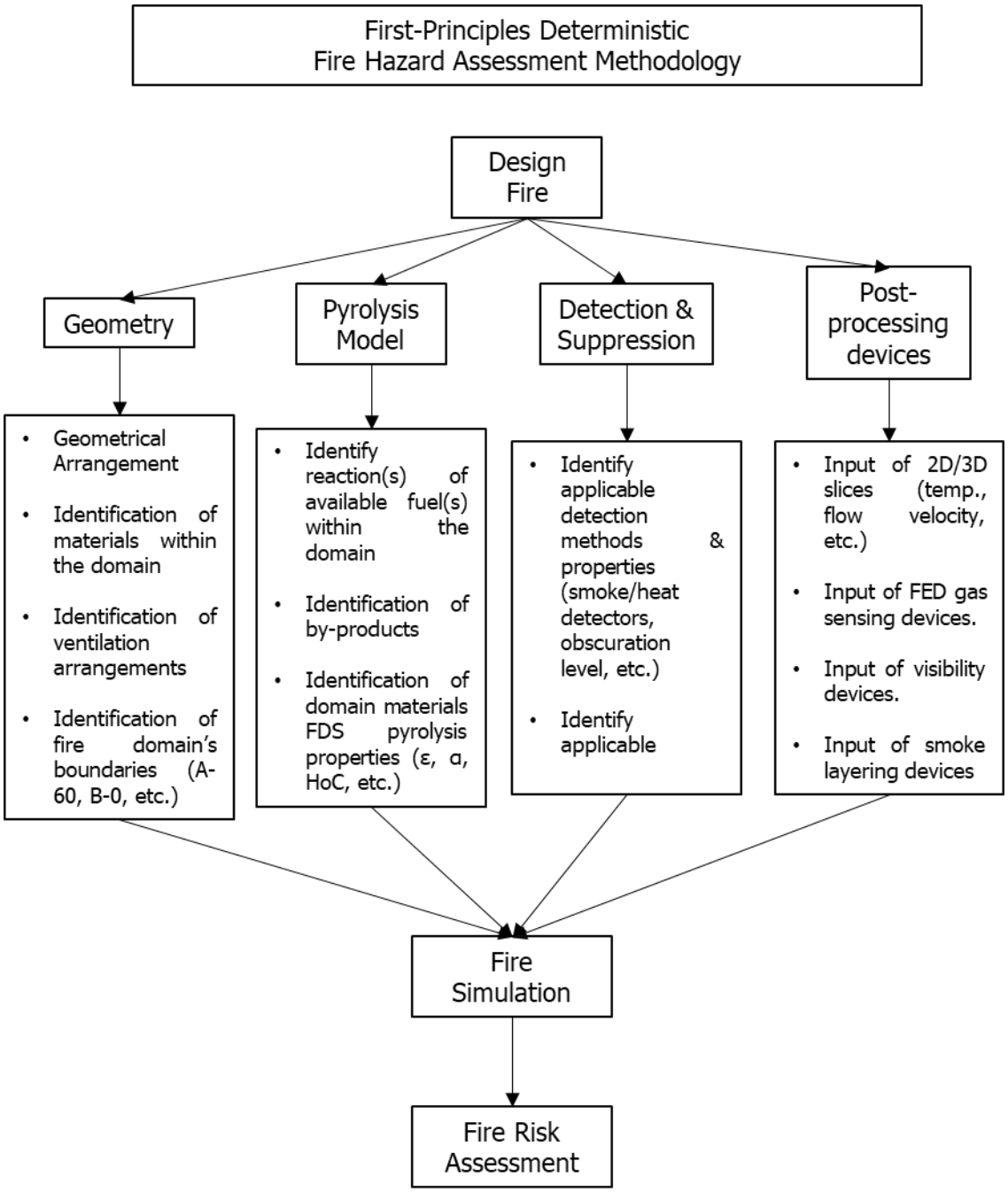


*Figure 32. First Principles Deterministic Fire Risk Assessment Methodology*

The design fire approach initiates with the identification and investigation of the geometry, in terms of its arrangement and available ignition sources. The latter is imperative as it acts as basis for the simulation and is usually a qualitative assessment. At this stage, available materials and ventilation requirements are identified. Additionally, fire boundaries of both the extremities and the available rooms/spaces are also investigated.

The pyrolysis model incorporates the modelling of the thermal decomposition of a material and the subsequent generation of flammable gases, which, in turn, may ignite in the presence of a heat source. Such an approach is rather data intensive, in terms of the plethora of physical and fire-related parameters that need to be defined for each one of the materials present in the space as well as the availability of those, the latter is discussed furtherly below. Approaches as such are entirely dependent on the availability of material thermal properties as well as the appropriateness of the pyrolysis model via the input of suitable values.
Thermal physical parameters of materials are of outmost importance in such an approach as the growth of the fire is very sensitive to the thermal properties of those. These parameters are:

1. density (ρ),
2. specific heat ($c_p$),
3. (thermal) conductivity,
4. emissivity (ε), and
5. absorption coefficient (α).

The nature/purpose of the majority of the parameters above are widely available (for most materials) except for the emissivity and absorptivity. Emissivity is the ratio of the actual amount of radiation emitted by a surface to the one emitted by the surface of a black body. The absorption coefficient (α) quantifies the amount of radiation absorbed by the surface of material to the maximum possible amount of a blackbody.

In terms of the pyrolysis, FDS allows for several approaches for describing the burning of solids and liquids. The approaches are relative to the availability of materials properties and the properties dictate how rapidly the materials heat up and how these burn. The pyrolysis values are not merely physical thermal parameters and are obtained only by specific laboratory tests, such as Thermogravimetric Analysis (TGA) and Differential Scanning Calorimetry (DSC).

The former, TGA, employs an analytical technique to determine the thermal stability of a material and its fraction of volatile components by monitoring weight changes for samples heated at predefined and constant rates. The latter, DSC, is a technique in which the difference in the heat required to increase the (internal) temperature of a material is measured as a function of temperature.

If a material is to be modelled for pyrolysis than such aforementioned values are necessary (McGrattan et al., 2004). Furthermore, unless the in-capture material has been subjected to TGA/DSC tests than any value input would be very questionable and such an approach should be avoided.

The pyrolysis related parameters are:

1. Heat of Combustion (HoC),
2. Reference Temperature,
3. Heating Rate, and
4. Pyrolysis range.

The HoC (kJ/kg) dictates the energy released per kilogram of a material burned, measured in combustion bomb calorimeters. Reference temperature (°C) is the temperature at which the mass fraction of material/sample decreases at the maximum rate, under a TGA experiment and should not be confused with the ignition temperature. The heating rate (K/min) is the rate at which the temperature of a TGA/DSC setup apparatus was increased/incremented, whereas the pyrolysis range (°C) is the range of temperature that the material pyrolyzes, usually 80 °C in absence of laboratory test data.

The HoC and reference temperature are the bare minimum required to model the pyrolysis phenomenon. The last two are optional as FDS is able to compensate in lieu of such data (McGrattan et al., 2022a). Nevertheless, for some material these were identified, whereas for others some typical values, as per the literature and FDS manual, were inputted.

The pyrolysis approach was, therefore, employed as both the cabin and large public space materials are commonly found in household situations or other industries (i.e. aviation), where considerable effort has already been invested over the past decades (Zalok et al., 2009).

The last element of the fire modelling, irrespective of whether a pyrolysis approach has been utilised, is the input of chemical reaction(s) that take place during a fire, in terms of the reaction between the fuel vapours and the oxygen present. FDS offers two approaches, the simple and the complex, whilst, in reality, there can be multiple solid/liquid combustibles in a fire. The “simple chemistry” combustion approach assumes that there is a single fuel composed primarily from atoms of Carbon (C), Hydrogen (H), Oxygen (O), and Nitrogen (N) that reacts with oxygen in the compartment to form water (H2O), carbon dioxide (CO2), carbon monoxide (CO) and soot. Essentially, the fire engineer is responsible for defining both the C, H, O and N values and the post-combustion yields of CO and soot.

Conversely, complex stoichiometry requires the user to define all reactions in greater detail, meaning that the gas species, or mixtures of those, must be explicitly defined along with the stoichiometry of reaction. Clearly, the latter is suitable for real-life applications but explicit knowledge on every fuel and its relevant chemical properties might not be always feasible. Furthermore, the complex stoichiometry approach is very costly computationally, hence, the simple approach was created by the developers of FDS.

Moving on, the fire detection and suppression measures must be ascertained. To that end, SOLAS and the FSS Code provide the type and specification of those.

In accordance with the FSS Code, Chapter 9, paragraphs 2.3.1.2, 2.3.1.3, and 2.4.2.2, the specifications for smoke detectors were established. These specifications include the required number of detectors, their spacing, and the specific conditions that trigger their activation based on smoke density. The smoke detectors were designed to operate when the smoke density reaches a level of up to 12.5% obscuration per meter,

with a minimum threshold of 2% obscuration per meter. These criteria ensure that the smoke detectors are responsive to smoke presence within the designated area.

Regarding means of fire suppression, only automatic suppression can be modelled, namely conventional sprinklers or mist systems such as high-pressure water fog ones. Due to the complex and rather laborious modelling required (McGrattan et al., 2022c, 2022b), the utilization of mist systems like high-pressure water fog systems in FDS would necessitate extensive effort, therefore, sprinklers were selected. Further to the hi-fog modelling necessities, the purpose of this chapter is to elaborate on the case study conducted in order to demonstrate the usefulness of a main vertical zone fire risk model. If required in the feature, more complex suppression systems could be modelled, such as hi-fog ones.

The sprinkler activation conditions along with spacing requirements were identified in FSS Code, Chapter 8, paragraphs 2.3.1.1 and 2.5.2.3. According to those, the sprinklers shall be designed to activate within a temperature range of 68-79°C, and the minimum required flow rate is 5 $L/m^2/min$ over the area covered by the sprinklers. For the purpose of the cabin and large public space deck simulations, the nominal activation temperature was set at 68°C, having a conservative approach.

To assess the effects of fire in a FDS simulation, relevant post-processing tools are imperative. These provide post-processing data in terms of the physical parameters required to assess the risk in the domain. Therefore, post-processing devices must be places strategically throughout it. These are 2D/3D “slices, which monitor quantities such as temperature, flow velocities of the gasses present, the visibility level, smoke layer height devices, which affect the visibility and consequently the evacuation, aspirator devices such as FED detectors, aiding in assessing the fire hazards, heat and toxic effluent effects, on human occupants.

The data potentially obtained from the FED and smoke layer heigh devices, are ultimately used to assess the tenability status of the domain, in accordance with the life safety performance criteria cited in (IMO, 2016c) and presented in Table 7 in the literature review.

Recapitulating, the first principles methodology described above was utilised to assess the fire risk of both the cabin and large public space deck. These are cited on separate sections, whilst the cabin deck is described first as it was successfully validated and verified, the latter especially being of outmost importance as it highlights the usefulness of a first principles deterministic approach which lies entirely on thermophysical data of the materials present in any geometry.

# 5. Release Prevention Barrier Case Study

## 5.1. Background

The scope of this chapter is to delve on the operations, methods and procedures employed in order to derive the in-subject safety barrier and to allow for diagnosis and prognosis, hence, to allow for dynamic barrier management, as per the framework laid out in Figure 31. The in-capture safety barrier incorporates technical, organisational and operation elements. To allow for the inference of the technical barrier element, an active technical element, sensors are utilised, which would provide real or next to real-time monitoring of the barrier status.

For the purpose of this case study, an existing/real very large passenger ship was selected, in an effort to examine the aforementioned including existing sensor equipment that might be already installed on board, in an effort to make this case study widely applicable and, ultimately, would make the case for the framework for placing such barriers. The details of the ship are confidential, and throughout this chapter it shall be referred to as the case study vessel. All drawings presented within this chapter and relevant information stemming from those have been adapted from the original ones.

The flammable oil discussed within this case study pertains only to conventional fuel oil (HFO, LSHFO), lubricating oil is not considered, but the framework can be easily extended as the machinery and engineering philosophy between the two systems are of the same nature. Furthermore, the potential of the machinery to create an electrical fire is also excluded from the scope of this case study.

This case study presented and discussed in this chapter was also an integral part of project SEAMAN, which sought to establish methodologies or frameworks, and recommended practices through the establishment of safety barriers and continuous monitoring and analysis of safety critical systems onboard, with focus on fire and flooding. The author of this thesis was an integral part of the fire stream of the project while all operations cited hereunder are entirely theirs. The project was led by the classification society DNV, while the results cited hereunder have been scrutinised by both the Norwegian Research Council, funding the project, and DNV.

## 5.2. Boundaries and Limitations of the Release Prevention Barrier

Before delving into any detail, the boundaries of the system investigated in this case study are stipulated hereunder. The case study vessel has two identical engine rooms, each of which having three 4-stroke engines (V-type) that drive electric generators, which feed electricity to the azipods and other requirements of the vessel. These engines are of the same maker while the sole difference being the amount of cylinders per engine.

Figure 33 presents a schematic depiction of the fuel oil delivery systems of one of the two engine rooms, with all relevant machinery and existing sensory equipment. The system presented spans from the service tank(s) which contain HFO, LSHFO and MDO

up to the engines. The first two fuels are utilised on a daily basis, for navigation through international and emission control areas (ECAs), whilst the last for maintenance purposes only.

Fuel passes from the service tanks towards various machinery (i.e. pumps, filters, heaters, etc.) that condition its properties into appropriate ones for combustion in the engines. The pressure of the fuel before being pumped into the engine for combustion was quite low, namely 7-9 bar, compared against the pressure of the fuel before injection in the cylinders, which is way above 1,000 bar as per the engines' project guides. To that effect, due to the great variation in the pressure magnitudes, the fuel oil delivery system was segregated into two, the low-pressure and the high-pressure system. Consequently, investigation of the RPB also followed the same philosophy, it was broken down to the low-pressure and the high-pressure RPB, LPRPB and HPRPB respectively, a distinction which is clearly depicted in Figure 33.

Hereunder, the boundaries and operation philosophy of each system are cited.

### 5.2.1. Low-Pressure RPB boundaries

Owing to the complexity and abundance of machinery within the low-pressure system, it was furtherly segregated into smaller sub-systems and components, by investigating the functions of those, as presented in Figure 33.

A sub-system is a group of components that operate together to realise a function. As an example, the feed sub-system is responsible for pumping the fuel furtherly into the fuel system, while its components comprise of identical screw pumps, for redundancy purposes, manual fuel strainers and respective valve assemblies.

Additionally, sensors were also identified, the purpose of which is to monitor the pressure before and after the aforementioned machinery. Specifically, differential pressure sensors are installed before and after the strainer, and a pressure control level sensor after the screw pump. By interviewing the crew of the case study vessel, it was ascertained that function of both sensors is to troubleshoot the respective machinery. Namely, the differential sensors monitor whether the strainer is blocked, whilst the pressure control one after the pump is monitoring for any pressure changes that may indicate a leak, but this is dependent on the behaviour of the system and was thought to be one of the operations required in order to understand the behaviour of the system and, therefore, the behaviour of the low-pressure RPB.

The discovery of existing sensory equipment is paramount mainly due to two reasons. Firstly, it blatantly showcases the current state of engine room fire safety, confirming the findings of (McNay et al., 2019), which stipulate that no precursors are investigated, and the crew might be notified of a potential leak after it has taken place, which justify the necessity of placing safety barriers that take into account latent causal factors. Secondly, it highlights the potential of the framework that was developed as part of this case, which is cited and discussed further onwards.

The low-pressure sub-system was segregated into the following:

a. Feed Sub-system,
b. Filtering Sub-system,
c. Flowmeter Sub-system,
d. De-aeration Tank (component)
e. Venting Valve (component)
f. Booster Sub-system, and
g. Duplex Filter.

A comprehensive list of all identified sub-systems of the technical elements of the LPRPB along with the respective components, as identified for the purposes of this case study are cited in the appendix, specifically Appendix A.

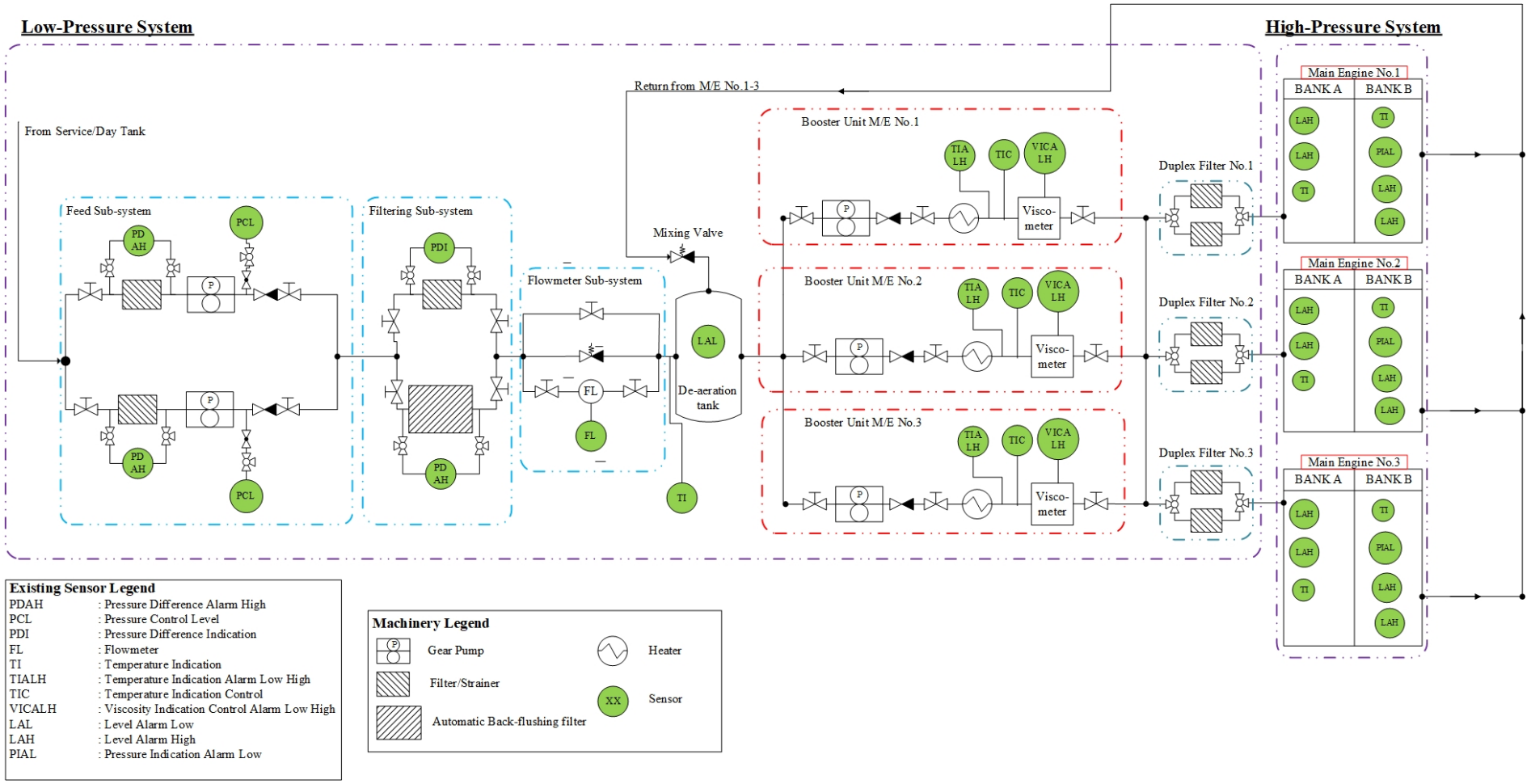


*Figure 33. Schematic depiction of the fuel oil delivery system of one engine room of the case study vessel, adapted from original ones.*

Fuel from the service tanks enters the system and is directed to feed sub-system, which is responsible for filtering and pumping the fuel further on. Also, the feed sub-system was duplicated for redundancy and maintenance purposes. Afterwards, fuel is directed into the filtering sub-system which furtherly refines the fuel to remove potential impurities present. The filtering sub-system comprises of an automatic back-flushing filter and a manual one in case the automatic is offline for maintenance or other reasons. Then, the fuel passes into the flowmeter sub-system, where a flowmeter monitors the quantities, and then the de-aeration tank where spilled (not utilised) fuel oil returns from the engines. Thus far, the feeder, filtering, and flow-meter sub-systems along with the de-aeration tank and valve are common for all three engines contained in the same engine room.

Continuing, the fuel is directed into the booster system, which is per engine. Within the booster sub-system the fuel pressure is furtherly increased via a screw pump and then passes through a heater which is controlled via a viscometer, both of which make sure that the fuel viscosity is optimal for proper combustion. Although the booster sub-systems are not duplicated, via investigation it was ascertained that their flowrate capabilities allow for one booster sub-system to service more than one engine. Finally, before being fed into the main engine, fuel is passed through duplex filters (for redundancy).

### 5.2.2. High-Pressure RPB Boundaries

The high-pressure fuel system and, therefore, of the high-pressure RPB (HPRPB), commences at the end of the low-pressure one, in other words, at the engine manifold. The engines within the case study engine room are of the V-type and are equipped with common rail technology as per their project guide. A description of the operation of the high-pressure system is cited hereunder.

From the low-pressure side of the system, the fuel makes its way into the engine manifold. From there, it passes through a flow control valve and gets pumped to high pressure by reciprocating pumps of the piston type. Such pumps are operated by the engine camshafts as per the project guide. As a result of the design of the high-pressure pumps, a small amount of oil is intentionally released back into the system. This “controlled leakage”, known as the "clean leak fuel oil drain" or pump slippage, does not indicate a real failure, or a leak, of the HPRPB. Moving on, the fuel is directed to an accumulator, often referred to as the common rail, where it is stored under high pressure (>1,000bar). For engines arranged in a V-type configuration, there is one pump and corresponding accumulator for every two engine cylinders in each engine bank. Each accumulator serves two injection valves, one for each cylinder. These injection valves themselves have a design that allows some fuel oil to leak. This slipped fuel is directed to the fuel oil return and then sent to the de-aeration tank for recirculation. Again, this leaked fuel does not constitute a failure mode, or a leak of the, the HPRPB. Irrespective of the number of cylinders, all accumulators are interconnected to ensure pressure equalization throughout the system. In case of overpressure, there is a start and safety valve located at one accumulator that relieves the system by diverting excess fuel into the fuel oil return line. To protect the system from pressure pulsations, a pressure damper is installed after the start and safety

valve. There's also a three-way valve after the damper, which provides the option to channel all fuel into the clean leak FO drain if necessary.

Since the system of the HPRPB is less complex than the LPRPB, segregation into sub-systems was not necessary while the boundaries of the HPRPB are clearly presented in Figure 33.

A comprehensive description of all components contained within the technical element of the HPRPB as identified for the purposes of this case study are cited in the Appendix, specifically A.

## 5.3. Systemic Analysis of the Release Prevention Barrier

The purpose of this section is to lay out the procedures undertaken in order to investigate the fuel oil system and to develop the release prevention barrier. As stated previously, the RPB comprises of a technical, organisational, and operational barrier elements. In order to infer the status of the technical element, sensory equipment was employed.

Despite that case study vessel has existing sensory equipment on the fuel oil line, as well as reportedly some sort of barrier, which, in theory, monitors the pressure of the low-pressure one, no data was available nor any documentation relative to that. Therefore, the existing sensor coverage was regarded as highly questionable. To that end, the investigation commences with the examination of the queries stipulated in the methodology chapter, with the inclusion of an additional one owing to the existing sensory equipment discovery. Namely:

- Is the existing sensory equipment adequate to infer the status of the barrier?

The investigation commences with the technical elements of the low-pressure and high-pressure RPB.

### 5.3.1. Technical Element of LPRPB

The functional body diagram of the LPRPB is presented in Figure 34. The colour of each line represents a different flow within the system. Namely, green lines represent materials, red lines represent energy and blue lines information. The subdivision of the LPRPB in sub-systems, in light blue, is clearly depicted, whereas other blocks are merely components.

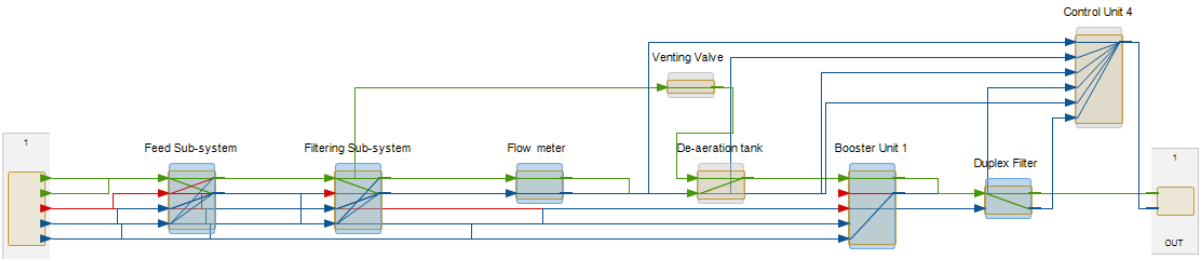


*Figure 34. Functional Body Diagram of LPRPB in MADe.*

It comprises of a duplicated feed sub-system and a single booster unit, whilst the control unit is fictitious but is absolutely necessary for input and output signals to/from machinery, including sensors. The decision to model the system for only one engine was taken in favour of simplifying the model. Further results could be easily extrapolated to the rest of the booster assemblies for each engine. The inputs to the system represented by the FBD are unfiltered fuel oil, and the output is treated, in terms of purity and viscosity, fuel oil that is directly fed to the engine manifold.

In theory, the engine could also be added as a component in Figure 34 which would allow the returned fuel oil from the engine into the de-aeration tank to be modelled. Initially, this was the choice, in order for the model to be realistic and robust. Upon

the conduction of the diagnostic, what-if, analysis it was ascertained that adding the engine component in the FBD resulted in a feedback loop to the system in way of the re-circulated oil, which, in turn, resulted in an abnormal/unexpected behaviour. Having consulted with the developers of the software, and via circulating both Figure 33 and the model file, it was jointly ascertained that the engine was indeed posing a feedback loop in the system and was consequently removed. Furthermore, via the aforementioned the functional body diagram model was considered validated (Hillston, 2003; Martis, 2006; Sargent, 2010; Vrijdag et al., 2009).

In order to declutter this section, the design philosophy of MADe along with the operations undertaken to build components and, consequently, the FBD presented in Figure 34, are included in the Appendix, namely Appendix A3 and Appendix A4.

#### 5.3.1.1. LPRPB Component Failure Modes

All components were considered for their failure roots and causes, except for piping. To that end, relevant literature was identified and perused accordingly. Specifically, the Handbook of Reliability Prediction Procedures for Mechanical Equipment, Offshore and Onshore Reliability Data Handbook, and others were employed (Anantharaman et al., 2015; Cicek et al., 2010; Goble and Siebert, 2008; Khattak et al., 2016; Logistics Technology Support Group and (CDNSWC), 2010; OREDA, 2009; Panchangam and Naikan, 2013; Prasad et al., 2010; SINTEF, 2002; SINTEF Technology, 2009).

Table 11 summarises the component failure modes for all components in the LPRPB system. A comprehensive table containing all sub-systems and respective failure modes can be found in the Appendix, specifically Appendix A5.

*Table 11. Summary of LPRB component failure modes.*

| Sub-System | Component | Failure Mode |
|---|---|---|
| Feed & Booster Unit | Motor | Open Circuit |
| | | Electrical Potential Decreased |
| | | Fractured |
| | | Property Mismatch |
| | Pump | Fractured |
| | | Abraded |
| Feed & Filtering | Suction Strainer / Filter | Blocked |
| | | Loose |
| All sub-systems | Sensors | Open Circuit |
| | | Electrical Potential Decreased |
| | | Dielectric Strength Decreased |
| | | Property Mismatch |
| | Valves | Abraded |
| | | Cracked |
| | Control Units | Open Circuit |
| | | Short Circuit |
| Filtering | Auto back-flushing Filter | Blocked |
| | | Open Circuit |
| | | Electrical Potential Decreased |

| | | |
|---|---|---|
| N/A | De-aeration Tank | Corroded |
| | | Perforated |
| Booster Unit | Heater | Oxidized |
| | | Perforated |
| | | Blocked |

#### 5.3.1.2. LPRPB Component Failure Trees

The failure modes identified in the previous section and are presented in Table 11 were fed into each component in MADe. For example, Figure 35 presents the failure tree of a suction strainer contained within the feeder sub-system. The failure modes of interest are blockage and loose fit. Since the latter is able to contribute to a potential fuel oil leak, since the filter is becoming loose, the brown hexagon represents a leakage, whilst the black one a symptom – loss of pressure. Such failures are of particular importance towards the function of the technical barrier element of the LPRPB as it represents a loss of containment, which may instigate a degradation, or even a complete failure, of the element.

Additionally, the loss of pressure is part of the system behaviour and acts as input for the What-if diagnostic simulations that are cited on the next section, as well as in the sensor set analysis as it indicates to the application possible spots for sensors. Lastly, the loss of pressure is the definition of loss of containment and, therefore, a fuel oil leak. In other words, **a leak is expressed as a loss of pressure** (Thames Water, n.d.).

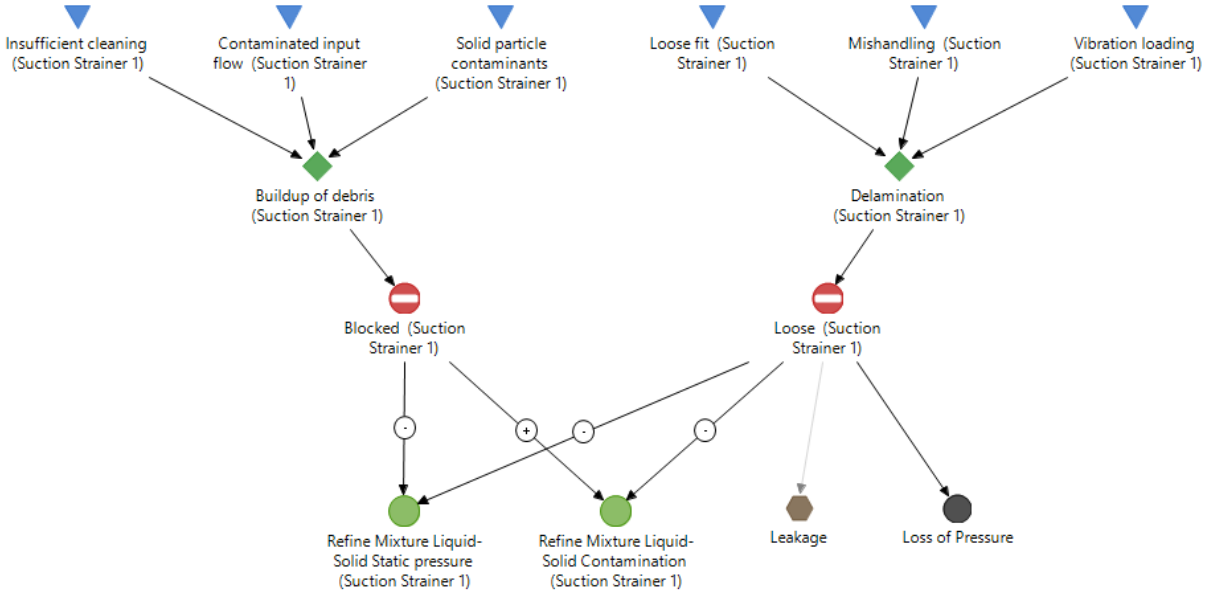


*Figure 35. Failure Tree of suction strainer component.*

#### 5.3.1.3. LPRPB Diagnostic Analysis (What-if Simulations)

The purpose of ascertaining the failure modes of each component compiled with the knowledge of those that may cause a loss of containment/leak, was to derive which ones require simulation along with the respective failure injection, i.e. loss of pressure. All components flagged were subsequently simulated. MADe utilises the nature of the

flow along with functional connections between components and sub-systems using Fuzzy Cognitive Maps (FCM). Particularly, MADe creates a matrix with all causal connections between in and our-flow properties per component, which is then utilised in the diagnostic simulations, termed as propagation table. Therefore, the diagnostic analysis is of the qualitative type and aids in understanding the barrier element behaviour under the faults that it should protect against.

These failures are injected manually by the user, which is later evaluated through the response table, a tabular representation of the response of each component per each time unit. As an example, Figure 36 presents the results of a what-if simulation, with a failure injection on valve “Valve_1_FD_upper”. The green number “1” in Figure 36 represents the failure injection on the component, while the downwards arrow represents the flow response, which is negative due to loss of containment on that component.

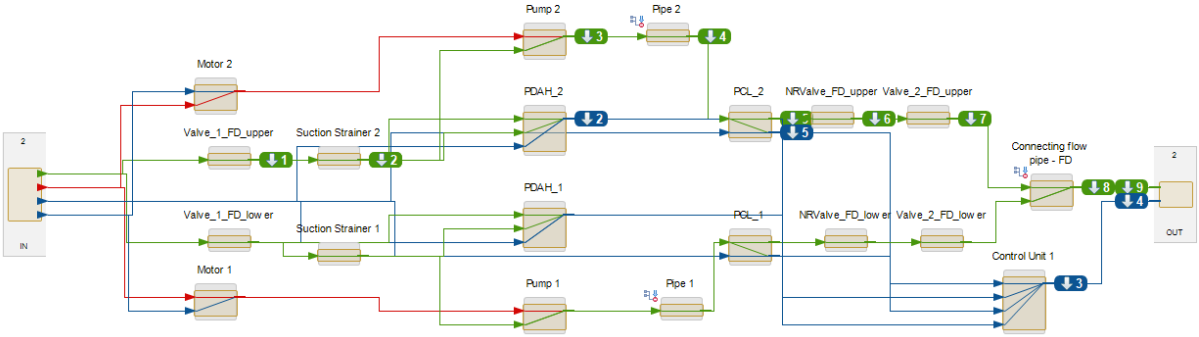


*Figure 36. Low pressure failure injection simulation on Valve_1_FD_upper – effect on feed sub-system.*

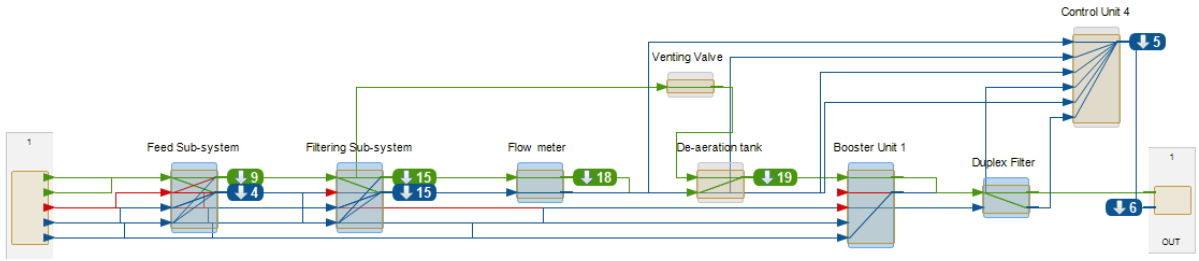


*Figure 37. Low pressure failure injection on Valve_1_FD_upper - effect on the whole system.*

Figure 37 presents the effect of the leak throughout the whole LPRPB, where the pressure seems to drop throughout the system uniformly. By conducting what-if simulations as such for each component able to contribute to a loss of containment in the LPRPB, the behaviour of technical barrier element was understood. Moreover, as propagation tables are quite lengthy, the propagation for the presented failure injection is presented in full in the Appendix, specifically Appendix A6.

Through the identified failure modes, it was noted that overpressure may occur in the system, mainly due to blockages and clogged components. Furthermore, pumping pulses may also be developed. Failure injection relative to the aforementioned were also conducted, where it was noted that the pressure rises in the system uniformly. With respect the LPRPB technical element in this particular case study, overpressure shall be averted via mechanical relief means as in SOLAS Ch. II-2, Reg. 4, Par. 2.2.4

"Prevention of overpressure" (IMO, 2020). As a note, no such means were noted in the drawings for the case study vessel.

#### 5.3.1.4. Failure Mode, Effects and Criticality Analysis of the LPRPB

After the completion of the diagnostic analyses, a Failure Modes, Effects and Criticality Analysis was conducted on the LPRPB in an effort to rank the risk of the components liable to producing a loss of containment. For the purpose of this particular framework, the Risk Priority Number (RPN) method was employed as it was favoured over the availability method. For each component of interest, the Occurrence (O), Severity (S) and Difficulty of Detection (D) were calculated (Defense, 1998; US Department of Defence, 1980), (DNV, 2001). Furthermore, it is imperative to mention that only the components liable to produce a leak were considered in the FMECA.

Due to the lack of knowledge regarding the existing safety barrier and relevant sensors on the case study vessel, resulted in the conservative population of many detection and severity fields. The RPN is calculated as $RPN = O \times S \times D$, therefore, it logically results that some components score quite high.

The only assumption taken in terms of the components, was to neglect some valves noted on the return line of the fuel oil. In particular, these are situated at the return line between the venting valve and the de-aeration tank and have no major task in the operation of the LPRPB. Besides, literature supports this assumption (Anantharaman et al., 2015; Niculita et al., 2017; Wärtsilä, 2007).

Assumptions were made during the Failure Mode, Effect and Criticality Analysis in order to derive the failure rates (λ values) of a few components. Although extensive efforts were put into ascertaining the actual failure rates, it was impossible to do for all components. Namely:

- the automatic back-flushing filter was deemed as one fit for lubricating oil,
- the flow-meter sensor was considered as a pressure sensor, and
- the viscosity sensor was considered as a temperature sensor.

Figure 38 summarise the RPNs of the components, while an exhaustive table containing all Occurrence, Severity and Detection fields can be found in the Appendix, specifically Appendix A7.

According to (DNV, 2001) and (Institution, 2018) the table of the FMECA does not have strict standards and can be manipulated as per the scope of the analysis. The highest scoring components (RPN >100) were:

- Temperature and Viscosity Sensors,
- Suction Strainers/Filters, and
- Valves (irrespective of type).

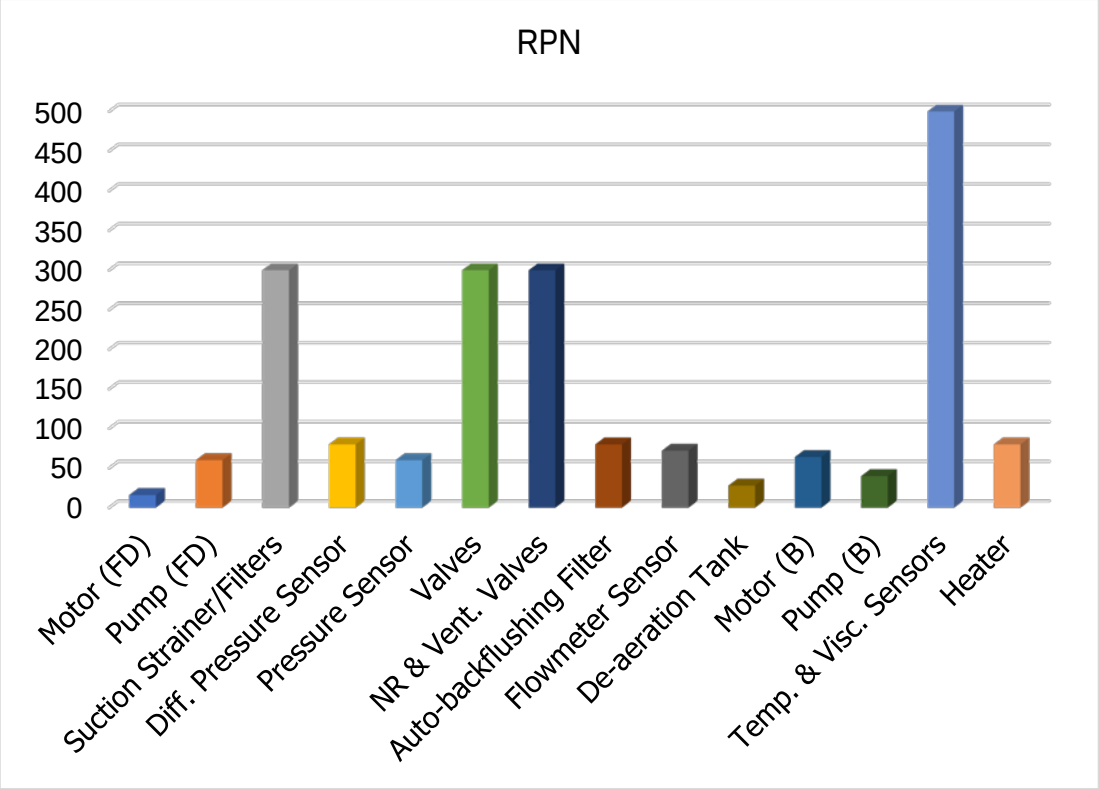


*Figure 38. Risk Priority Numbers for LPRPB components that may lead to a loss of containment.*

The sensors were scored rather conservatively, hence these score highest, since no prior knowledge on their nature and operation was available. This led to their severity and occurrence being ranked at 10, the highest (worst) score. This implies that their failure is hazardous and without warning, whilst there is no chance that the control system will detect the failure. Provided that such sensors were of the self-diagnosing type, both severity and detection would have scored much lower. Their severity was also ranked high as these two sensors control the steam heater in the booster sub-system, which could potentially leave the fuel untreated and at suboptimal conditions. Viscous oil may not be able to be furtherly pumped into the engine which, in turn, could pose further damage to other components (Ford, 2012).

Suction strainers, filters, and valves were kept in mind for further treatment in the sensor set analysis that follows this section. It must be noted that under normal circumstances such analyses and relevant investigations would be accompanied with proposing system changes to increase safety or the reliability, but this is not the purpose of this particular analysis, as its goal was to discover components/machinery that contribute to loss of containment within the technical element of the LPRPB in a constructive manner, which, in turn, will be utilised in the sensor set analysis that follows.

#### 5.3.1.5. Sensor Set Analysis

Existing sensory means had already been included in the FBD during its creation. All sensors were modelled but were not “activated”. An activated sensor, specifically the flowmeter sensor (not the flowmeter component) is presented in Figure 39, where the symbol underneath denotes the activation of the sensor.

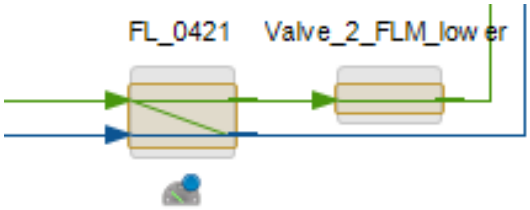


*Figure 39. Activation of flowmeter sensor (FL_0421) in MADe.*

In terms of the sensor set analysis, MADe considers the existing sensory means along with the critical components that were established via the FMECA and the failure trees. That is, components that were able to cause a loss of containment on the LPRPB were selected for the sensor set analysis. Such components are visually flagged by two concentric hollow circles.

Concerning the available sensor library offered by MADe, and specifically for the failure mode of interest, a wide range of sensors was noted. Upon examination of those, it was immediately revealed that the sensors were not able to be fitted on the flagged components regardless of the fact that these monitor leaks. A prime example of such was an optical leak detector, which essentially is an optical fibre cable that senses leaks via direct contact with the leaked medium (OptaSense, n.d.). A table listing the available sensors included in the MADe library can be found in the Appendix, namely Appendix A8.

Despite that the sensors were not fit for the purpose of inferring the status of the low-pressure technical element of the RPB, an investigation on the components that were flagged for sensor placement was conducted. Initially, it was ascertained that MADe proposed sensor placement for all components in the FMECA, including ones that scored low on their RPN due to their low historical contribution, such as pumps in the feeder sub-system. Needless to say that these were neglected from the analysis. For clarity purposes, Figure 40 presents the locations where MADe proposed to place sensors specifically for the feed sub-system. Furthermore, visual bugs were noted in way of missing sensor placement (concentric circles) at two valves, namely “NRVALVE_FD_upper & lower”. These two no-return valves should have been flagged as per their RPN.

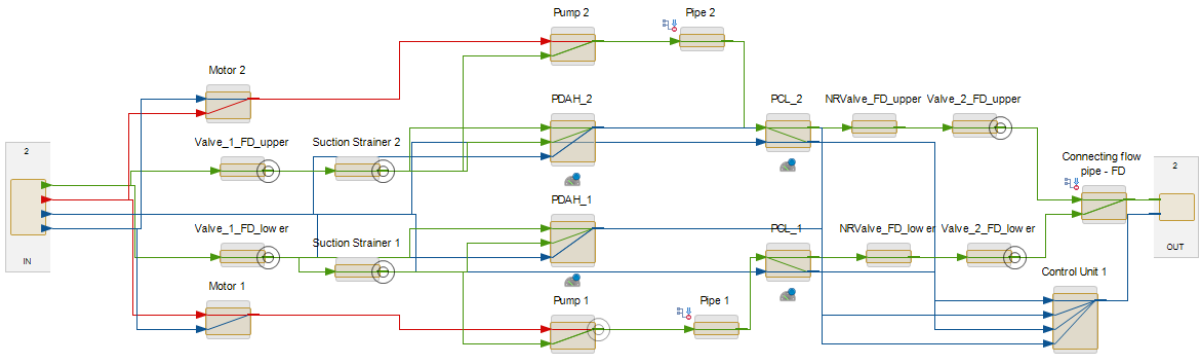


*Figure 40. Locations for sensor allocation in feed sub-system of the technical barrier element of the LPRPB, as shown in MADe.*

As per Figure 40, the following components in the feed sub-system of the technical barrier element of the release prevention barrier were flagged for sensor placement:

1. Valves:
    1.1. Valve_1_FD_upper & lower,
    1.2. Valve_2_FD_upper & lower, and
    1.3. NRVALVE_FD_upper & lower.
2. Suction Strainers 1 and 2.

The sensor set solutions for the remaining sub-systems and/or components is presented per sub-system in the Appendix, specifically Appendix A9.

To recapitulate the sensors set analysis, it was concluded that although the appropriate components were flagged, in terms of those that are able to create a loss of containment, the available sensors in the MADe library were not fit for the purpose. Consequently, as per the framework proposed in **Error! Reference source not found.** for the development of the technical RPB element, focus was shifted towards first principle engineering and the literature review on available leak detection systems and respective techniques conducted in Chapter 2.6.

#### 5.3.1.6. Real-Time Transient Monitoring Leak Detection System to Enable Diagnostics

Since the sensor set analysis in MADe was not productive, solely due to the limitations imposed by the sensor library, focus was diverted towards first principles engineering thinking. Moreover, even if any of the available sensors could be fitted in all components, none of those would be able to detect a loss of containment in the LPRPB, let alone any latent causal factors, since all fall under the hardware-based leak detection methods (Chapter 2.6.1).

As per the literature review conducted in Chapter 2.6.2, leak detection techniques and relevant systems are quite particular to the application and the functional requirements necessary. Nevertheless, the review of software-based solutions in 2.6.2 clearly highlights Real-Time Transient Monitoring and Dynamic Modelling as prime candidates to establish diagnostics on the technical element of the RPB. Additionally, these are used quite extensively as shown by the presented commercialised solution in Figure 25. Principle of operation of a commercial RTTM leak detection system. Source: (KROHNE Group, n.d.). For the scope of the technical element of the RPB, RTTM was considered to be the most fruitful.

Amongst other factors, the performance of a real-time transient model (RTTM) is influenced by several key aspects, including:

- Data fidelity (accuracy, availability, sampling interval) and placement of flowmeter sensors,
- Data concerning the temperature, pressure, and flowrate of material (inputs/outputs) for all branches of the system,
- Real time information on the properties of the fuel (density, viscosity, etc.), and
- System Architecture.

From the aforementioned it is evident that the success of such a system relies on the accuracy, reliability, and availability of real-time data throughout the whole system, as well as to a finely tuned supervisory control and data acquisition system (SCADA), tailored to the nature of the LPRPB (DNV-GL, 2019; Golmohamadi, 2015; Henrie et al., 2016; KROHNE Group, n.d.). Additionally, the literature also suggests the necessity of trained personnel monitoring the system (Adegboye et al., 2019).

As a rule, the shorter the sampling intervals the greater the accuracy achieved (Henrie et al., 2016), but this is translated into additional sensory equipment and increased costs. Therefore, a structured way of placing these sensors could be a digital twin model of the technical element of the LPRPB in addition to the RTTM system. Figure 41 presents an example of a poorly instrumented network of pipes and machinery, while Figure 42 a well instrumented one (Henrie et al., 2016). On the other hand, Figure 118 presents a very small segment of the LPRPB between the feed and filtering sub-systems.

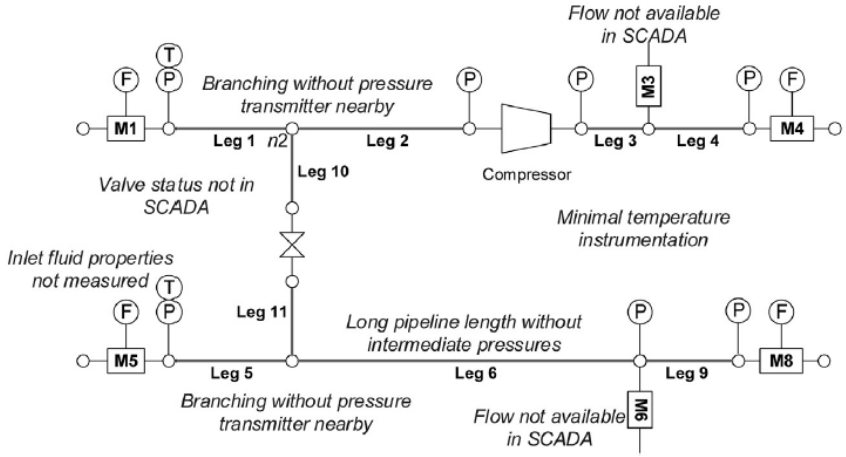


*Figure 41: Poorly instrumented pipeline. Source:*(Henrie et al., 2016)

Based on visual evaluation, it was determined that the current sensors in the LPRPB are insufficient to support an effective real-time transient model leak detection system. Specifically, there is a lack of information regarding sensor functionality, such as obtaining inlet pressure readings from existing pressure difference sensors, absence of existing sensory data (or simulated), and a lack of tools to model the fuel oil system and assess its leak detection performance with the current sensor capabilities.

*Figure 42: Well instrumented pipeline, Source:* (Henrie et al., 2016)

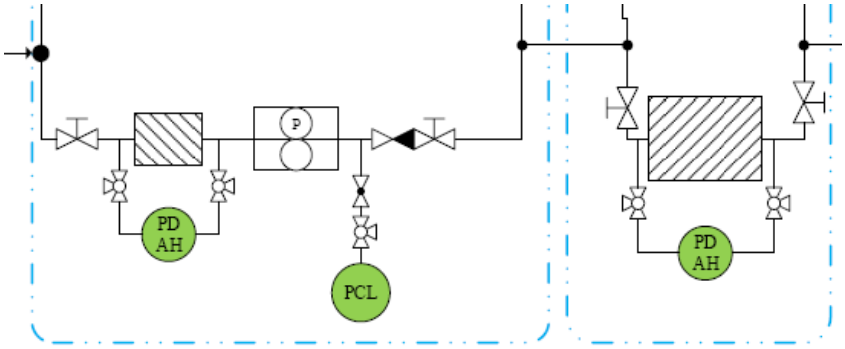


*Figure 43: Segment of technical element of the LPRPB between the feed and filtering sub-systems.*

Following the placement philosophy in Figure 117, Figure 119 presents the same segment as Figure 118 where pressure, temperature and flowmeter sensors have been placed at every branch, and before and after each component. Components that flagged low in the FMECA could be neglected but these were kept in order to highlight that this placement philosophy is exhaustive and would surely lead to increased costs for its intended purpose.

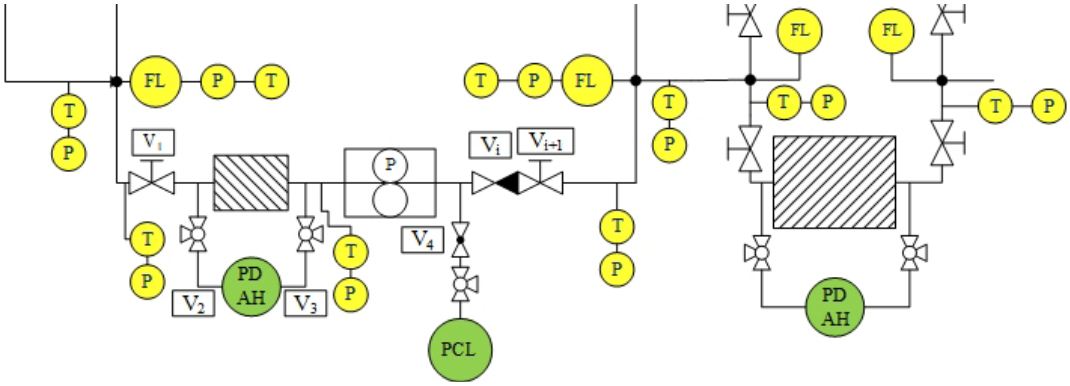


*Figure 44: Example of additional sensor coverage on LPRPB*

Conversely, the exhaustive placement would, in theory, enable for the following to be accomplished:

- In-Outflow are measured, enabling volume flow balance calculations.
- Flow balance calculations on smaller segments, for example between the inlet and outlet of a sub-system would enable not only high accuracy but leak localisation.
- All necessary valves, which were flagged high on the FMECA, are accounted for.

#### 5.3.1.7. Towards Enabling Diagnostics for the Technical Element of the RPB

Deploying an extensive sensor placement strategy could potentially yield high accuracy, but it would come at a significant cost. Furthermore, the computational time required for processing the data, using the conservation equations, may exceed the available time to detect a leak before it escalates into a fire, rendering the technical elements of the RPB ineffective. Moreover, the cost associated with the arbitrary

addition of sensors, along with the required processing infrastructure, would be substantial.

To implement a diagnostics for the LPRPB, it is necessary to create a computer-based model of the system using relevant equations, essentially building a virtual fuel oil system or a digital twin. Unfortunately, in this case study, the essential tools, such as suitable software, and detailed information including a diagrammatic representation of the network with all the necessary specifics, were unavailable. Consequently, the development of an effective real-time transient model (RTTM) was not feasible. Additionally, once the system is modelled, it becomes crucial to perform sensitivity analyses to determine the appropriate sensory equipment along with appropriate functional requirement (for example, detection of 1% leak). Ideally, this analysis would be accompanied by a cost-effectiveness assessment, revealing the true expenses associated with implementing such a leak detection solution.

Once the model of the fuel oil system is constructed, its accuracy and reliability can be assessed through a verification and validation process. This involves comparing the outputs of the model with real-time flow and pressure measurements obtained from the actual system (Hillston, 2003; Sargent, 2010). The model may require further refinement and tuning to ensure its alignment with the observed data. It is imperative to mention that the mathematical techniques employed for modelling the system's digital twin and addressing sources of uncertainty, such as noise, are highly dependent on the specific circumstances. Citing specific mathematical techniques in this context may lead to inaccuracies, as the appropriate techniques would vary from case to case.

Lastly, concerning prognostics, as the technical element of the LPRPB is quite complex, and no data of any form is available, it was highly uncertain as to which techniques are applicable or even if these applicable forthrightly.

### 5.3.2. Technical Element of HPRPB

The purpose of this section is to elaborate on the operations conducted to enable diagnostics for the high-pressure technical barrier element of the release prevention barrier. The same questions as in the low-pressure element were investigated. The high-pressure element spans right after the low-pressure one and is limited only to the engine, as presented in Figure 33.

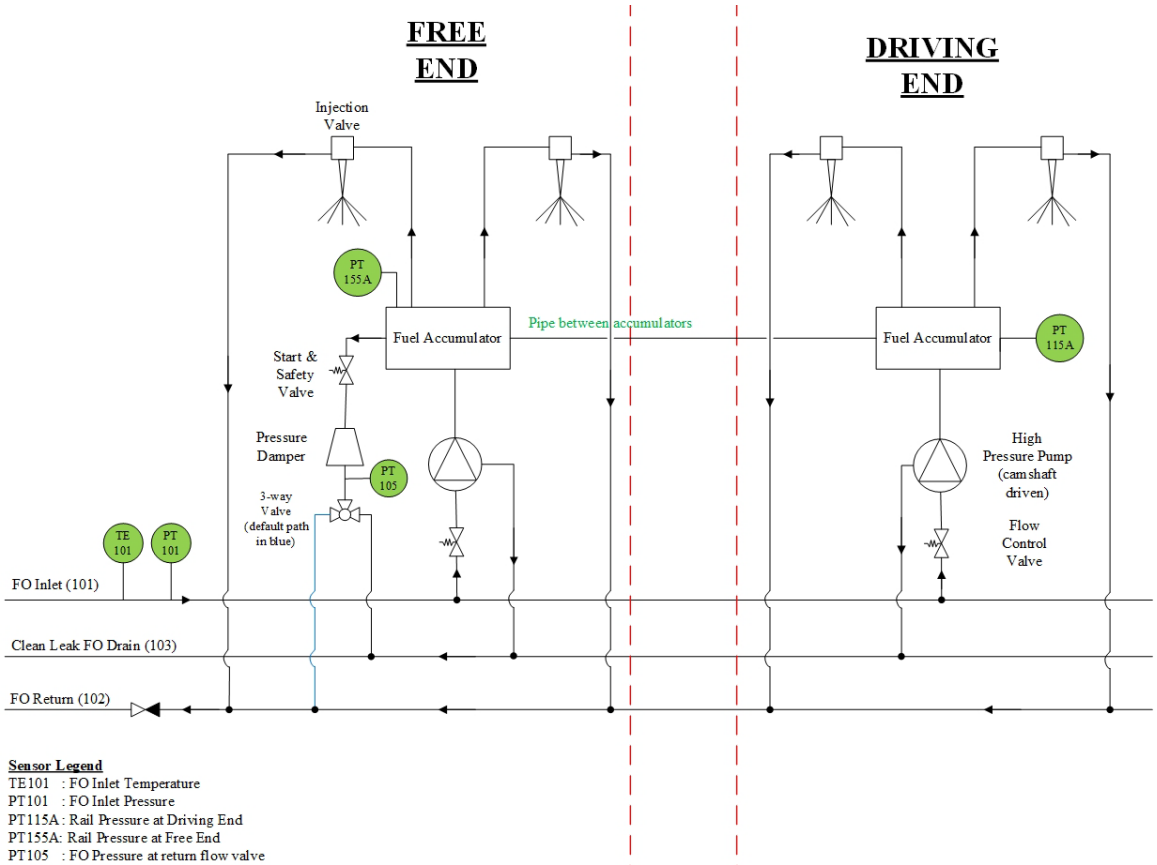


*Figure 45: Internal combustion engine's fuel delivery system, depicting two accumulators (4 cyl. in total). Adapted from:* (Wärtsilä, 2007)

Figure 45 presents the fuel oil delivery system of one of the case study vessel's 4-stroke engines, specifically depicting two accumulators (common rails) which are interconnected. Upon first examination, it is apparent that the engine is equipped with quite a few sensors, but as in the case of the LPRPB, no information was available on the purpose of the monitored parameters apart from basic functions which are to be expected. As an example, the sensor PT155A denotes a rail pressure sensor at either the driving or free end of the engine. The reason why the name is the same is due to accumulators being interconnected in order to equalise the pressure. Furthermore, in the case of over-pressure, which is well expected due to the nature of the piston pumps, the start and safety valve is automatic, therefore, the sensor could only provide an indication in the engine control unit and control room.

The next sections investigate the HPRPB technical element by performing the same operations as in the LPRPB. Figure 46 presents the functional body diagram of the technical element of the high-pressure release prevention barrier.

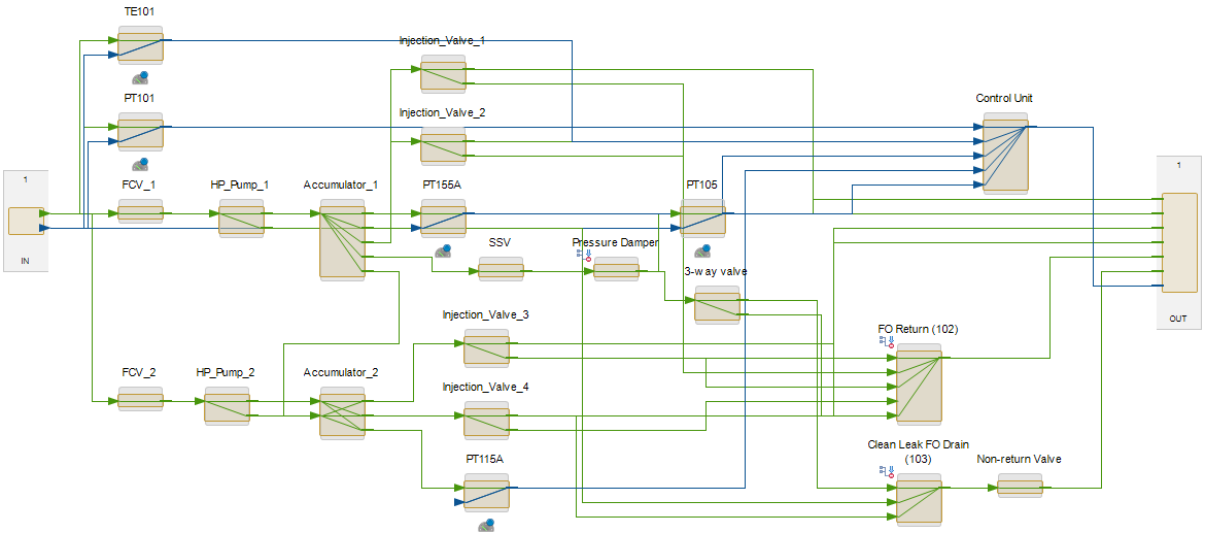


*Figure 46: Functional Body Diagram of HPRPB in MADe.*

As in Figure 45, two accumulators were designed, while the FBD represents the fuel oil delivery system with respective injection system for four cylinders in total. The results of any of the following operations that were conducted could be easily extrapolated to the whole engine, irrespectively of the cylinder arrangement.

It is quite imperative to mention that all operations cited hereunder with regards to both modelling the FBD and the conduction of the diagnostic analysis were initially performed on an FBD containing only one accumulator with two cylinders in order to rule out possible errors and feedback loops, as in the case of the LPRPB, aiding in the validation of the functional body diagram model of the high-pressure barrier element.

#### 5.3.2.1. HPRPB Component Failure Modes

The failure roots and mode for all the components within the high-pressure element were identified except for the case of piping. Table 12 presents a synopsis of the possible failure modes as identified through pertinent literature. An exhaustive table containing all failure modes can be found in the Appendix, namely Appendix A10**Error! Reference source not found.**. As the components of the high-pressure system are quite similar to those in the low-pressure, no prominent failure modes were noted.

*Table 12: Summary of high-pressure FO component failure modes*

| **Component** | **Failure Mode** | **Failure End Effect** |
|---|---|---|
| Control Valve(s) | Abraded | Fuel Oil Leak |
| | Cracked | |
| High Pressure Pump (reciprocating) | Fractured | Fuel Oil Leak |
| | Abraded | |
| Accumulator | Perforated/Cracked | Fuel Oil Leak |
| | Corroded | |
| Injection Valve(s) | Clogged Atomizer | Improper injection & consequently combustion |
| | Early/Late Opening | |
| | Ball seat erosion | Leaking injection valve, leads to improper combustion |

| | | |
|---|---|---|
| Pressure (Pulsation) Damper | Inoperable bladder (if bladder type) | Pulsation from accumulator will not be dampened, pipes might rupture, i.e. FO Leak |
| Sensors (Pressure, Temperature) | Open Circuit | Faulty or no measurements at ECU |
| | Electrical Potential Decreased | |
| | Dielectric Strength Decreased | |
| | Property Mismatch | |
| | Dielectric Strength Decreased | |

#### 5.3.2.2. HPRPB Component Failure Trees

As per the framework in Figure 31, the following step was to input the identified failure roots and modes into MADe, in order to ascertain the symptoms of the technical barrier element components. Figure 116 presents the failure tree of accumulator located on the free end of the engine which also houses the start and safety valve which is of outmost importance in terms of engine room safety and engine operation. The failure modes are perforated and corroded which is attributed, as per the literature, on corrosive contaminants which damage the surface coatings, or surface, of the valve itself. Either one of the two failure modes may lead to a loss of containment and pressure would drop across the accumulator. The plethora of outputs of the failure tree is due to the multiple tasks of the accumulator, providing fuel to the injection valves, fuel to adjacent accumulators and excessive fuel to the safety valve.

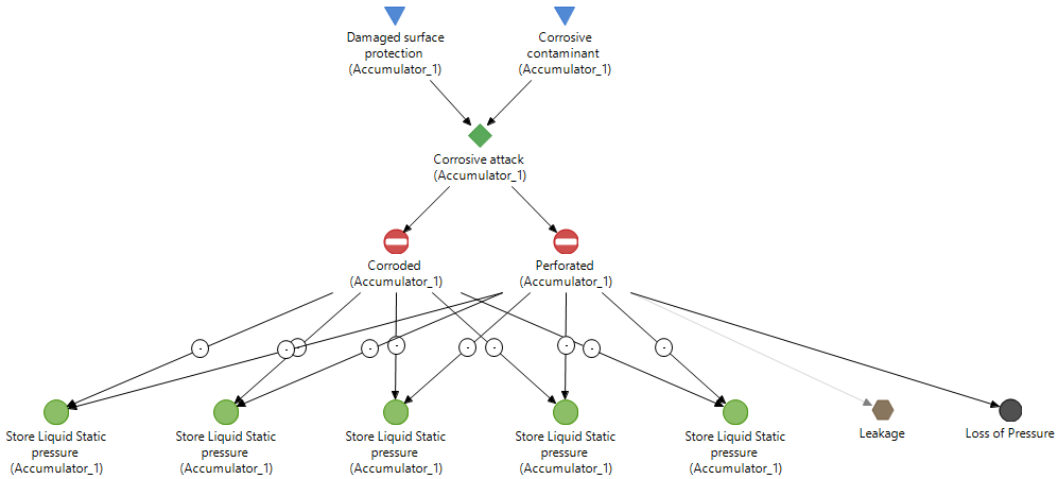


*Figure 47: Failure Tree of an accumulator (at the free end of the engine)*

#### 5.3.2.3. HPRPB Diagnostic Analysis

What-if diagnostic simulations were conducted specifically on the components that have the potential to develop leaks, characterised by their leak failure modes in the previous section. Among these components, Figure 48 illustrates the impact of a leaking flow control valve (FCV_1), showcasing the resulting pressure drop throughout the system. The analysis encompassed all relevant components susceptible to leakage. For a comprehensive breakdown of this simulation, including step-by-step details and the response table refer to Table 25 in Appendix, specifically Appendix A11.

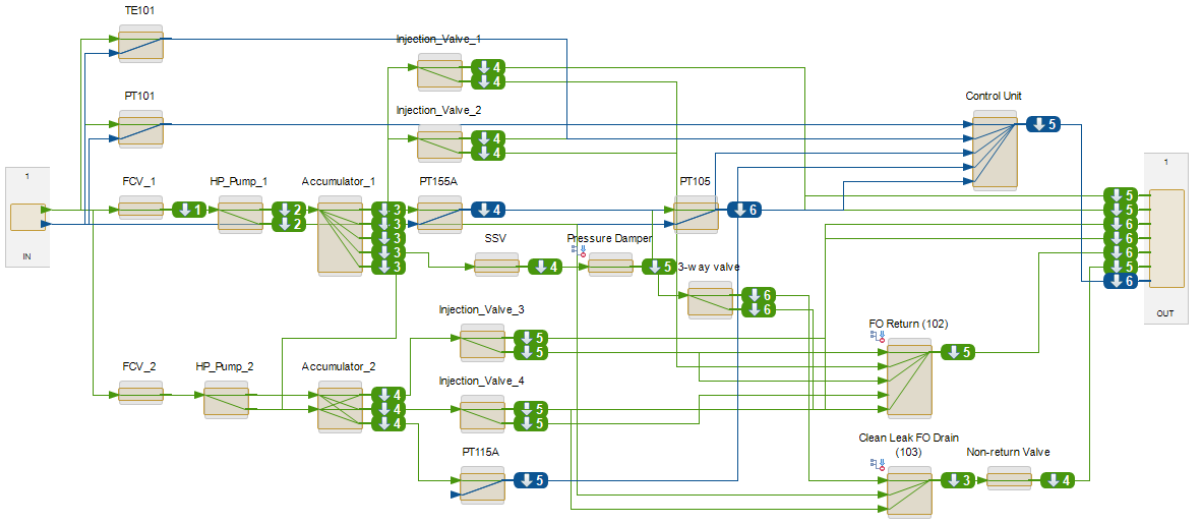


*Figure 48: High-pressure failure injection on FCV_1 - effect on the whole system*

Overpressure and respective pressure pulsations are high expected within the whole system, and this is why the return line is equipped with a pressure damper in order to equalise it. These overpressures are to be expected and are attributed to the operating principles of the reciprocating pumps which are designed to slip fuel. Furthermore, as these pumps are driven by the engine's camshaft and in the case of overpressure the safety valve operates.

#### 5.3.2.4. Failure Modes, Effects and Criticality Analysis of the HPRPB

Similarly with the low-pressure element, the risk priority method was also employed for the high-pressure system, while focus was given solely on components that could cause a loss of containment. Figure 49 summarises the RPN scores as calculated by the identified Occurrence rates. An exhaustive table containing all values for O, S and D can be found in Table 26 in the Appendix, specifically A12.

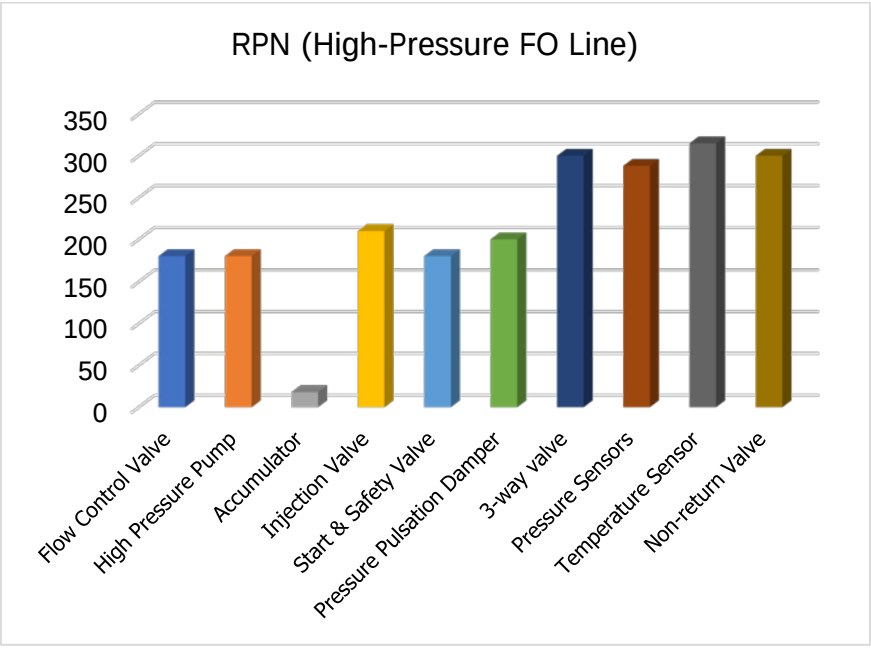


*Figure 49: High-Pressure RPB RPN Scores*

Assumptions were taken towards the completion of the failure mode, effects and criticality analysis presented in this section, to derive that failure rates (λ rates) of a few components. Despite extensive efforts in way of finding those, it was impossible to conduct for all components. To that effect, the following assumptions were taken:

- The flow control valve was considered as a process valve,
- the start and safety valve were also considered as process valves,
- the in-engine temperature sensors were considered as resistance temperature detectors, and
- the no-return valve was considered as a generic valve.

The majority of the components scored high RPNs, more than 100, except for the accumulator. Sensory equipment was treated quite convectively regarding their Occurrence and Severity due to no prior knowledge on those. Additionally, other components scored quite high since their impact with respect to a loss of containment is rather impactful. This is attributed to the great magnitude of pressure within the accumulator and pumping part of the system coupled with immediate proximity to hot surfaces as shown in Figure 19, therefore the maximum fire safety risk. Contrastingly with the aforementioned, the low-pressure side of the system can be deemed as rather safer due to the low-pressure operation coupled with respective SOLAS provisions cited in the literature review concerning the proximity of piping carrying flammable oil to heat sources.

The components that were flagged through the FMECA were:

1. All valves (flow control, start and safety and, 3-way)
2. high-pressure pump, and
3. pressure damper.

From the investigation and respective findings of the low-pressure barrier element coupled with the review on leak detection technologies, a RTTM system with mass/volume balance sensors could be possibly installed, but great attentions must be paid to the magnitude and behaviour of the pressure owing to the overpressure potential. Since the sensor set analysis offered by MADe was not fruitful there was no necessity to present the sensor set solutions for those, as the components that may create a loss of containment within the technical element of the HPRPB have already been ascertained through the FMECA.

### 5.3.3. Operational and Organisational Elements of the Release Prevention Barrier

In this previous sections, a thorough investigation was conducted on the technical barrier elements (HP and LP) at the lowest level of indenture, and suitable locations for sensors were determined. Subsequently, the sensors capable of leak detection and their respective techniques were extensively scrutinized in the context of implementing a dynamic barrier management system in a very large passenger ship's engine room. However, since this research endeavour follows a systemic approach, it is essential to also consider the operational and organizational barrier elements of the RPB. Therefore, this section elaborates on these aspects.

Figure 50 illustrates the interplay between technical, organizational, and operational barrier elements to ensure the effectiveness of the barrier function (Aina Eltervåg, Tommy B. Hansen, Elisabeth Lootz, Else Rasmussen, Eigil Sørensen, Bård Johnsen, Jon Erling Heggland, Øyvind Lauridsen, 2017). It could be argued that the technical elements, specifically the LDS, would form the backbone of the barrier. As discussed earlier, a combined RTTM and Mass/Volume Balance LDS is a complex system that would require trained personnel to monitor and interpret the system inputs and outputs. This highlights the crucial importance of operational and organizational elements. Only when these elements are properly implemented can the barrier guarantee safety throughout the system.

The organizational and operational elements interact with the technical element to varying degrees. A key question that simplifies their necessity is: "*Who does what with which equipment in failure, hazard, and accident situations?*"(Aina Eltervåg, Tommy B. Hansen, Elisabeth Lootz, Else Rasmussen, Eigil Sørensen, Bård Johnsen, Jon Erling Heggland, Øyvind Lauridsen, 2017). In the context of this barrier, the technical element is responsible for hardware and component monitoring, the operational element involves personnel monitoring the system (if deemed necessary), and the organizational element encompasses the functions and specific competencies required by the personnel.

Since the technical barrier element is currently incomplete, it is not logical to derive the performance influencing factors and functional requirements at this stage. Past experiences, industry knowledge, and relevant literature on barrier systems, including those in the oil and gas sector, indicate that system states can be underestimated, rendering the barrier elements ineffective. Therefore, explicit operational and organizational elements should be cited at this point.

Once the technical barrier elements are finalized, attention must be focused on determining the performance influencing factors for the personnel. This will allow for the specification of performance requirements, such as manning levels and competency training, as well as subsequent certification. These performance requirements may encompass aspects such as functionality, integrity, and robustness/survivability (Aina Eltervåg, Tommy B. Hansen, Elisabeth Lootz, Else Rasmussen, Eigil Sørensen, Bård Johnsen, Jon Erling Heggland, Øyvind Lauridsen, 2017). Examples of training and procedures may include operating the LDS system,

interpreting system outputs (e.g., using a traffic light system to monitor status) (Fornes, 2016), and visual leak detection during engine room rounds.

Regarding the organizational barrier element, it is crucial to document personnel with defined roles and/or functions, along with the required competencies, to ensure the realization of the barrier function. Performance shaping factors for the personnel, such as fatigue management, are of utmost importance. All procedures necessary for maintaining and operating the other barrier elements must be documented and readily available for both the sharp end (frontline personnel) and the blunt end (management and support functions). These procedures should be incorporated into the operator's Safety Management System (SMS) (IMO, 2018b).

Paragraph 1.2.2 in Part A of the International Safety Management (ISM) Code emphasizes the objective of the SMS, which is to continuously improve safety management skills of personnel both ashore and onboard, including adequate preparation for emergencies . The identified risks to the ship, personnel, and the environment must be assessed, and corresponding safeguards must be developed. Additionally, functional requirements for the SMS are also necessary.


*Figure 50: Interaction between technical, organisational, and operational barrier elements, showing performance requirements and influencing factors. Source:* (Aina Eltervåg, Tommy B. Hansen, Elisabeth Lootz, Else Rasmussen, Eigil Sørensen, Bård Johnsen, Jon Erling Heggland, Øyvind Lauridsen, 2017)

# 6. Risk Contribution Tree

## 6.1. Background

The purpose of this chapter is to lay out and elaborate on the procedures and methods utilised in order to resolve the fifth research question towards the realisation of a fire risk model for a large passenger ship, in terms of a fire risk contribution tree, a bow-tie model, that would be able to predict and quantify the effects of an engine room fire in case it breaks out of it. In case the release prevention barrier fails, and a fire is realised, the effects and consequences on the occupants must be evaluated.

For this case study specifically and in order to demonstrate the risk contribution tree, the unwanted event is a fuel oil leak fire. On the right-hand side, mitigating measures are placed traditionally. In the context of fire safety and as per applicable rules such as SOLAS, FSS Code, etc., there are a plethora of mitigation measures of both active and passive nature, if one is considering the mitigating measures as safety barriers. Active measures include smoke/flame detectors, deluge systems, etc., while fire subdivisions are passive measures.

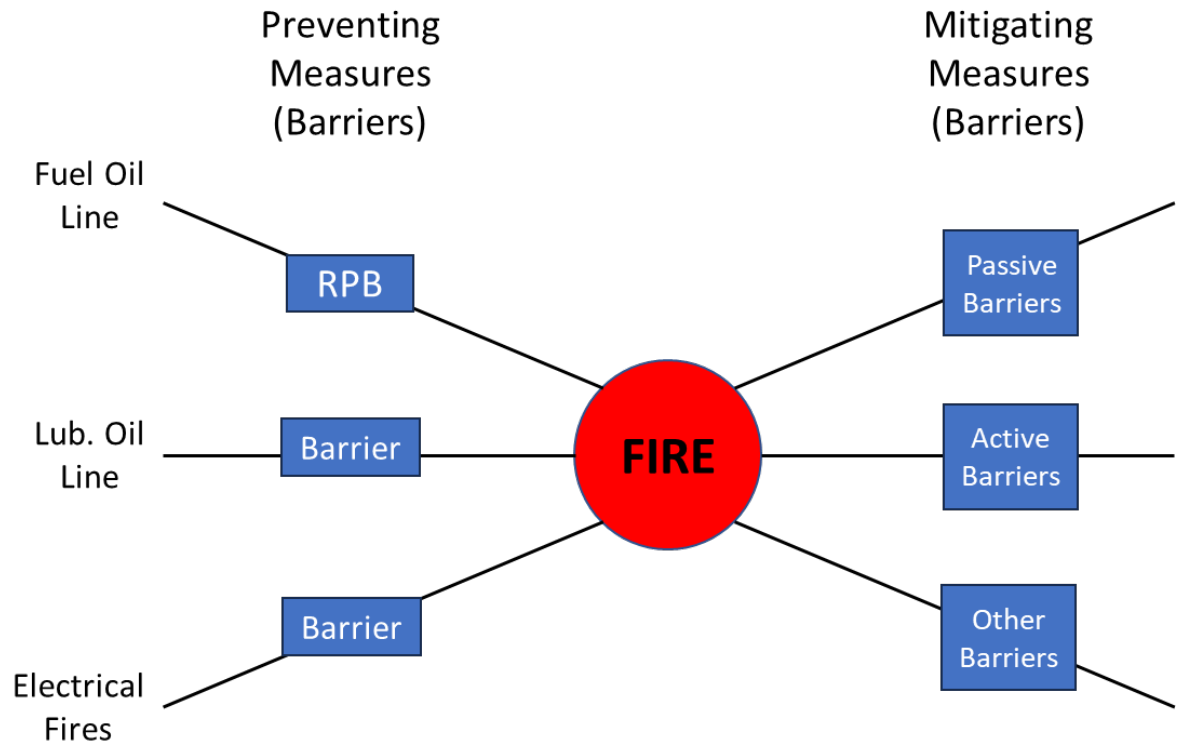


*Figure 51. Risk Contribution Tree of MVZ.*

The rationale pertaining to the risk contribution tree is presented in Figure 51. The RPB lies on the left-hand side of the bow-tie, acting as a preventative barrier, hence the name. Concerning mitigating barriers, SOLAS and the FSS Code provide existing ones. Namely, fire boundaries/subdivisions, deluge systems, HVAC systems (dampers) and $CO_2$.

Further to the above, part of the case study presented in this chapter was an integral part of a European Union Horizon 2020 funded research project SafePASS, which had as a primary objective to redefine the evacuation procedures and respective systems (procedures, life-saving appliances) including regulatory efforts, for large passenger ships (SafePASS Consortium, 2022). Within the efforts of the research project, a risk modelling tool was developed, required to demonstrate a decision support system relevant to emergency response and evacuation. The risk model itself intended to capture the real-time risk of flooding and fire, in relation to the decision support, within very large passenger ships, having a dynamic nature. A database consisting of applicable numerical simulations for flooding and fire scenarios was imperative towards the realisation of that risk model. Therefore, the stateroom and large public space decks that are elaborated in the following chapters were a direct and original contribution of the author of this thesis as part of the SafePASS Project. Additionally, these two scenarios have been considered as validated though the research projects, both towards the inputs and the outputs of the relevant simulations.

## 6.2. Main Vertical Zone of Case Study Ship

Large passenger ship engine rooms may span over multiple main vertical (fire) zones, and as a result the risk contribution tree was focused on only one MVZ for the purpose of this case study and thesis. A different large passenger ship was selected for this case study, the one used for the purposes of project SafePASS, presented in Figure 52, while the owner/manager is anonymous.

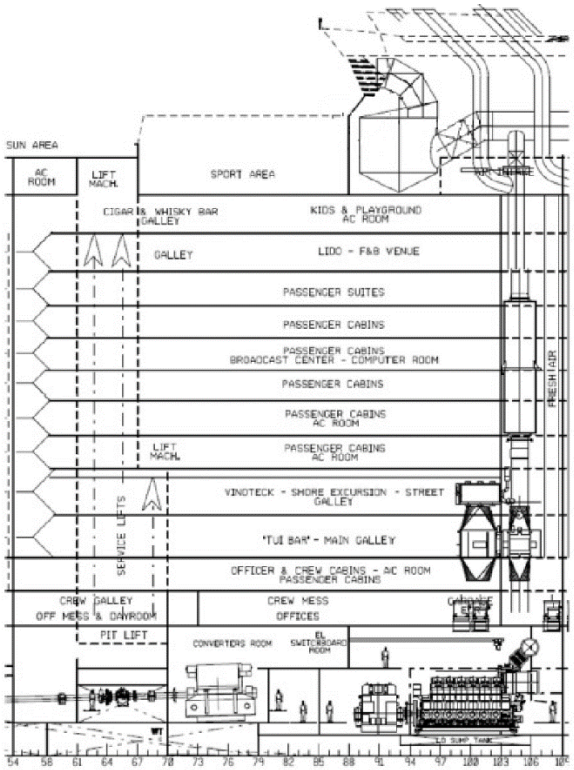


*Figure 52. Main vertical zone of investigation for the fire simulations. Source:* (Stefanidis et al., 2020)

The MVZ presented in Figure 52 has, apart from portion of the engine room, a plethora of decks with staterooms/cabins, both standard and luxury ones, galleys, and large

public spaces. The engine room itself contains two main four-stroke engines that drive alternators (generator sets), incinerators, both of which present inherent fire risks as per the literature review, as well as propulsion motors. Consequently, via qualitative evaluation, it was chosen for the purpose of this case study due to the inherent fire risks posed. Furthermore, for this case study, a standard cabin deck was chosen opposed to a luxury one as these are found in multiple decks, contrastingly to the luxury ones.

# 7. Cabin Deck Fire Simulation Case Study

In this chapter, the design fire methodology that was devised in the methodology chapter, and consequently employed to conduct the fire simulations of the cabin and large public space deck via FDS/Pyrosim is described. The ultimate purpose of those was to evaluate the fire risk emanating in order to be able to assess it in terms of visibility, heat, and exposure to heat and relevant toxic effluents.

## 7.1 Geometry

This section described the fire simulations conducted for the passenger cabin deck scenario, considering a night-time scenario where guests are asleep in their rooms. As mentioned previously, one of the standard cabin decks was considered for this simulation as these span over multiple decks of the ship. Figure 53 presents the arrangement of a standard passenger cabin deck within the main vertical zone of investigation, namely on the seventh deck.

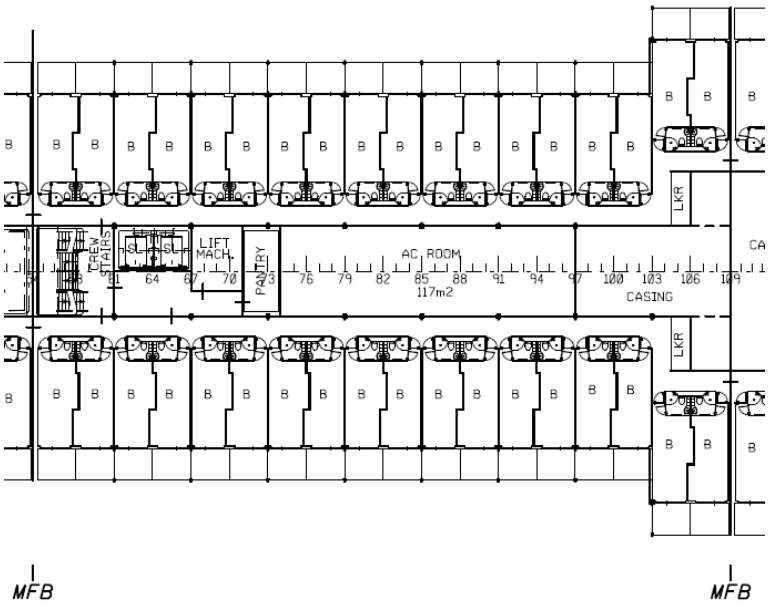


*Figure 53. Standard stateroom deck*

Passenger cabins are located on both port and starboard side of the deck, while along the centreline there are various spaces and crew-only stairwells, while passenger stairwells and elevators are located on each adjacent side of the deck forward and aft.

In terms of importing the geometry of Figure 53 in Pyrosim, the GUI companion application of FDS, geometrical simplifications are imperative as convex shapes cannot be modelled. Additionally, the CFD domain is subdivided into rectangles representing control volumes were the equations are solved. Therefore, complex shapes were avoided.

There were no drawings or inventory for the items included in each cabin of the deck, nor for the air conditioning room contained along the centreline. Consequently, the air conditioning room was neglected from the simulation as it is a service space requiring A-60 insulation. The items within each cabin were kept to a minimum in terms of its functionality as these simulations intended to showcase the capabilities of the fire risk model in this thesis. Additionally, the cabin bathrooms were also neglected. Any additional item could potentially be added to represent a more accurate fire load.

To that effect, the items included in each cabin are as follows:

1. Bed, consisting of:
1.1. Wooden frame,
1.2. Foam mattress,
1.3. Bedsheet.
2. Carpet.
3. Bulkheads (A and B type), consisting of:
3.1. Steel sheet,
3.2. Rockwool insulation,
3.3. PVC veneer.

Furthermore, the cabins have carpets, windows, and the bulkheads along with their respective materials (insulation, PVC veneers, etc.). In order to realise the coordinates and particulars for the geometry creation in Pyrosim, SOLAS was advised for the necessary types of boundaries between respective spaces. For example, the bulkheads between MVZs shall be of A-60 type, the ones between staterooms to be of B-15 type (IMO, 2014). Every component of the geometry has been modelled on a 1:1 basis to allow for fidelity and result appropriateness.

The passenger cabin deck as modelled in Pyrosim is presented in Figure 54.

## 7.2. Fire Simulation Scenario and Ignition Source

The ignition source was considered to be a lit cigarette depicted as a red dot on the carpet, starboard side in Figure 54, which an occupant dropped. The choice of ignition was as such since cigarettes are the most common point of fire origin in residential situations, whereas the cabin was selected arbitrarily (Nilsen, 2005). In terms of the pyrolysis modelling, the dropped cigarette, being the heat source in the simulation, would heat up and pyrolyze the carpet, which would generate flammable vapours, which, in turn, would ignite by the cigarette.

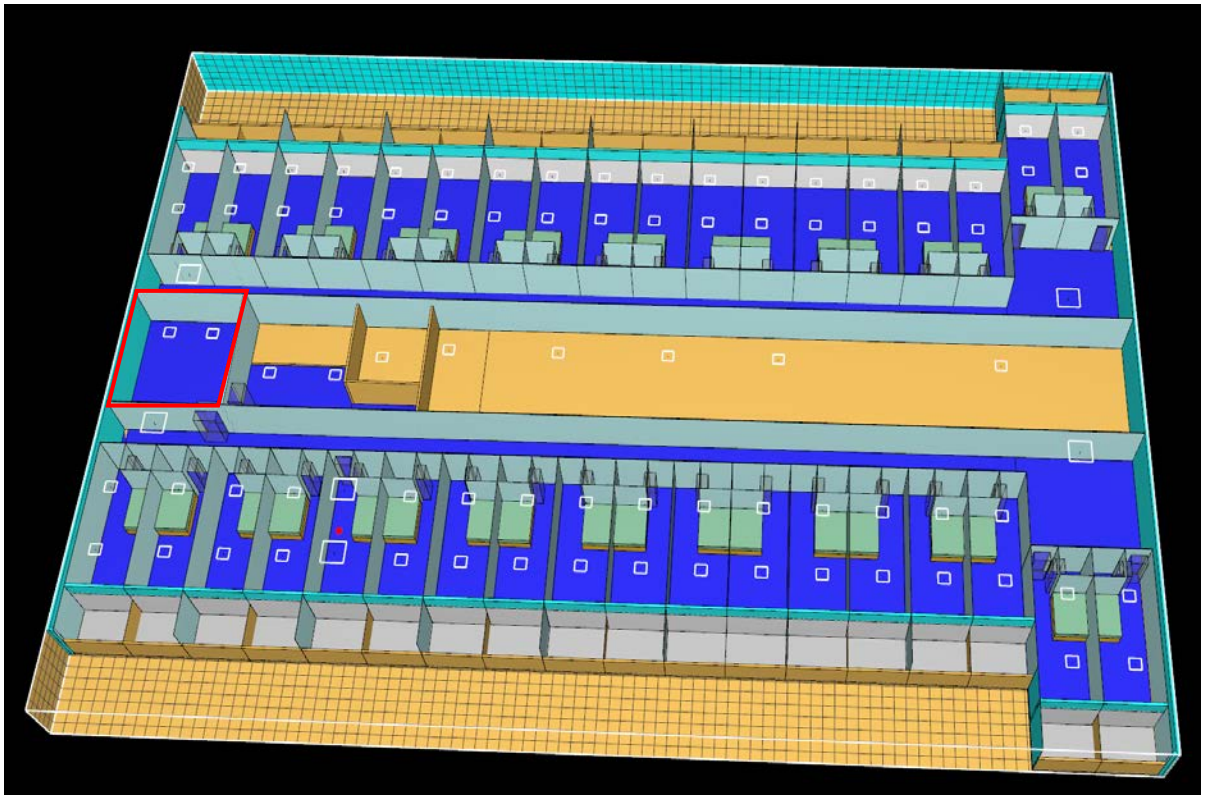

*Figure 54. Passenger Cabin Deck modelled in Pyrosim.*

The access to forward and aft main vertical zones was deliberately blocked to enable for the generation of smoke and toxic effluents and consequent assessment of human occupants within. The only exception was the crew stairwell, marked with a red parallelogram in Figure 54. Additionally, the only door that was left open during the simulation was the one where the fire emanates, and it was done purposedly to account for the worst-case scenario where the cabin occupants flee but the self-closing mechanism of the door fails to operate.

## 7.3. Ventilation Characteristics

The ventilation characteristics for the cabins, stairwell and corridors were identified from SOLAS. Specifically, air charges per hour were identified and pertinent inlet and outlet ventilation outlets were modelled in Pyrosim. As an example, each cabin required 6 air changes per hour, hence a cabin inlet provided 0.081$m^3$/sec flow rate of air.

It is imperative to mention that FDS offers a comprehensive HVAC module with a dedicated solver, conducting the calculations for the ventilation system completely independent of the “fire” ones. Moreover, smoke control devices such as dampers can also be modelled, but these are not used in a cabin deck. Further to the aforementioned, the HVAC plans and smoke extraction strategy of the deck were not available, therefore, a simpler inlet/outlet vent approach was favoured.

## 7.4. Pyrolysis Model

### 7.4.1. Materials

A complete list of the materials included in the simulation is cited:

The thermal parameters of the materials included in the geometry are presented in Table 13.

*Table 13. Material Thermal Properties.*

| Material | Density ($kg/m^3$) | Specific Heat $c_p$ (kJ/kgK) | Thermal Conductivity λ (W/mK) | Emissivity (ε) | Absorptivity (A) |
|---|---|---|---|---|---|
| Carpet | 157 | 1.36 | 0.04 | 0.9 | N/A |
| Fabric | 140 | 1.4 | 0.03 | 0.7 | N/A |
| Foam | 28 | 1.7 | 0.05 | 0.9 | N/A |
| PVC | 1,380 | 1.5 | 0.14 | 0.95 | 0.885 |
| A-60 type Rockwool | 80 | 0.7 | 0.04 | 0.94 | N/A |
| Plywood (FR) | 545 | 1.215 | 0.12 | 0.86 | N/A |
| Galvanized Steel | 7,850 | 0.483 | 51.9 | 0.75-0.85 | 0.36 |
| B-type Rockwool | 80 | 0.75 | 0.041 | 0.94 | N/A |
| Glass Pane | 2455 | 0.84 | 3.46 | 0.8-0.9 | N/A |

All the materials presented in Table 13 represent an item in the simulation domains. As an example fire-retardant plywood was utilised to construct a bed frame, while foam was utilised for a mattress. Generic engineering databases such as the ones offered in SFPE Handbook of Fire Protection Engineering and the website engineering toolbox (DiNenno et al., 2002; Engineering Toolbox, n.d.; Hurley et al., 2016; omega.co.uk, n.d.). Other sources were (DRShip Europe, n.d.; Ioannou, 2019; ISOVER, n.d.; Morgan Advanced Materials, n.d.; SeaRox - Marine & Offshore Insulation, n.d.; Thomas and Heselden, 1972; Xiang et al., 2013). Furthermore, where possible, vendors having Classification Society approvals were also pursued.

Material CO, CO2 and soot yields were also identified through the aforementioned references, shown in Table 14, excluding the ones for the rockwool, steel and the glass pane. These were neglected as they do not contribute to the fire.

*Table 14. Material Yields*

| Material | Yield CO (g/g) | Yield CO2 (g/g) | Soot Yield (g/g) |
|---|---|---|---|
| Carpet | 0.0588 | 1.748 | 0.0214 |
| Fabric | 0.08 | 1.56 | 0.089 |
| Foam | 0.042 | 1.57 | 0.227 |
| PVC | 0.9 | 1.42 | 0.39 |
| Plywood (FR) | 0.06 | 1.4 | 0.017 |

Table 15 presents the HoC and reference temperatures for the pyrolyzing materials in the cabin. These were laboriously identified from (Janssens, 2005; Zhang et al., 2014a).(Grønli et al., 2002; Janssens, 2005; Livkiss et al., 2018; Mikulčić et al., 2019; Moltó et al., 2006; Sun et al., 2007; Xiang et al., 2013; Zhang et al., 2014b).

*Table 15. Material Pyrolysis Parameters*

| Material | Heat of Combustion (MJ/kg) | Reference Temperature (oC) |
|---|---|---|
| Carpet | 24.8 | 150 |
| Fabric | 32.5 | 320-380 |
| Foam | 34 | 320-340 |
| PVC | 20 | 400 |
| A-60 type Rockwool | 4.48 | 200 |
| Plywood (FR) | 4.48 | 280 |
| Galvanized Steel | 17 | N/A |
| B-type Rockwool | 7.5 | 200 |

### 7.4.2. Ignition Initiation

The carpet was of special interest as the fire was expected to start there. An option with respect to modelling the ignition is to input a heat source of appropriate intensity (Watt) and dictate to FDS that this will interact with the carpet to provide vapours, which may or may not ignite.

Since fire initiation from cigarettes is widely known and very well expected in all scenarios, cigarettes nowadays are made out of low propensity paper, which means that a dropped cigarette will not always start a fire (Baker^, et al., 2016). It will pyrolyze the carpet, it is common to see some black smoke emitted, but it is uncertain whether enough vapours will be generated and/or if these will be ignited from the heat provided by the cigarette.

The heat emitted (not heat flux) from a cigarette is on the magnitude of 5W, around 950$^{o}$C, while the heat flux is 35-42 kW/m$^2$ (Krasny et al., 2007). Solids may ignite when exposed to a heat flux in the magnitude of 10-20 kW/m$^2$ (Hurley et al., 2016). In order to test the pyrolysis procedure, small-scale trial simulations were performed with only the carpet and the cigarette, and it was noted that not always the vapours were enough to start a fire. To overcome the fact that low propensity cigarette designers successfully did their task, another approach was adopted for the fire initiation.

A common option to setting a fire is to specify the Heat Release Rate (HRR) of a burning material, usually expressed per unit area of the material, termed as Heat Release Rate per Unit Area (HRRPUA) (Hurley et al., 2016). Provided that the fire

safety engineer identifies a TGA/DSC laboratory test for a fire-retardant carpet exposed to the same heat emitted by a cigarette, then the pyrolysis approach for the carpet specifically is not required, and ignition initiation is guaranteed (McGrattan et al., 2022a).

To that effect, a TGA study for a flame-retardant aviation carpet was identified, (Feng et al., 2016), which was furtherly supplemented by a study from National Institute of Standards and Technology (NIST), where the carpet was exposed to various heat fluxes to study the ignition characteristics (Walton and Twilley, 1984). One of the heat fluxes employed closely matches the one of a cigarette, namely 50kW/m$^2$. Therefore, it was decided that only the carpet will have a specified burning, via the input of an HRRPUA and a respective fire ramp emanating for the experiment. The peak HRRPUA that the selected carpet emits is 300kW presented in Figure 55, whilst the ramp (fraction of HRR per time) along with the corresponding HRRPUA per time in Table 16. Negative ramps, to model extinguishing/starvation, cannot be used in FDS.

*Table 16. Carpet HRRPUA and ramp against time. Source* (Walton and Twilley, 1984)

| Time (sec) | Ramp (fraction) | HRRPUA (kW) |
|---|---|---|
| 0 | 0 | 0 |
| 17.3 | 0.132 | 50 |
| 18.2 | 0.263 | 100 |
| 31.3 | 0.395 | 150 |
| 38.3 | 0.526 | 200 |
| 46.3 | 0.658 | 250 |
| 55.6 | 0.789 | 300 |
| 65.0 | 1.000 | 380 |
| 83.3 | 0.789 | 300 |

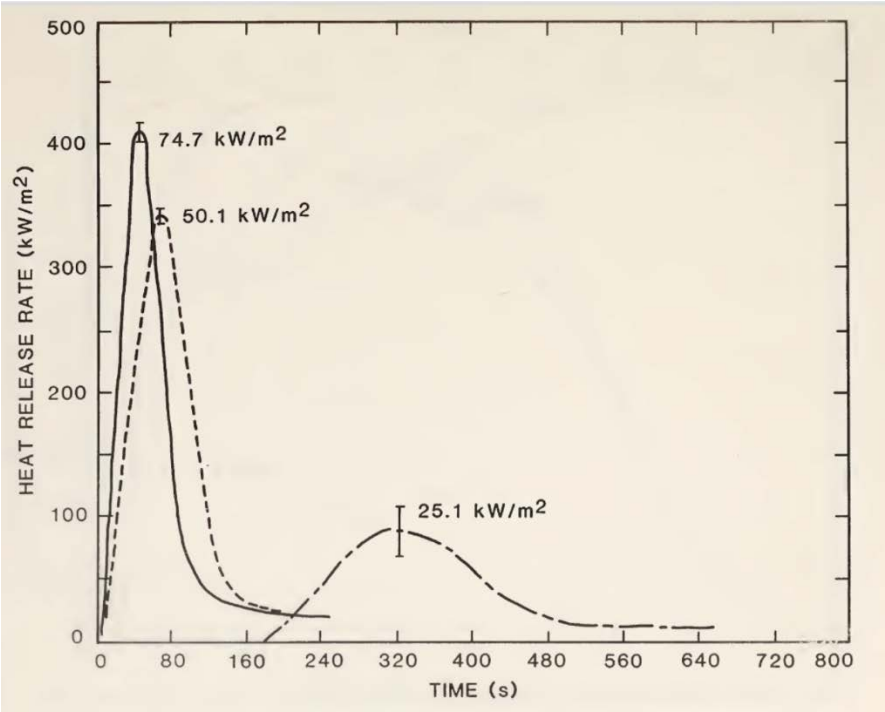


*Figure 55. HRRPUA of carpet. Source:*(Walton and Twilley, 1984)

### 7.4.3. Single Cabin Trial Simulation – Model Verrification

The fire modelling approach cited thus far was undertaken for a single cabin test. This was conducted as per traditional fire safety engineering due diligence. The deck spans over 40m along the centreline, has 38 staterooms with many surfaces each. This surfeit of surfaces invites potential errors, which is very common with CFD, therefore the approach was tested on a single cabin to rule out potential errors. Figure 56 presents a two-cabin (side by side) arrangement, where tests were conducted on the left one only. No fire detection and fire-fighting means were used in the test case.

In this particular test, the aforementioned carpet HRRPUA was not employed, as the fire resulting from the interaction between the cigarette and the carpet is specified via the input of HRR. Instead, flammable simulation materials were set in such a way that the pyrolysis by-products will be the fuel. Instead of letting the fire develop with time, this resulted in an instantaneous combustion of all combustible items and the total HRR could be evaluated for its appropriateness.

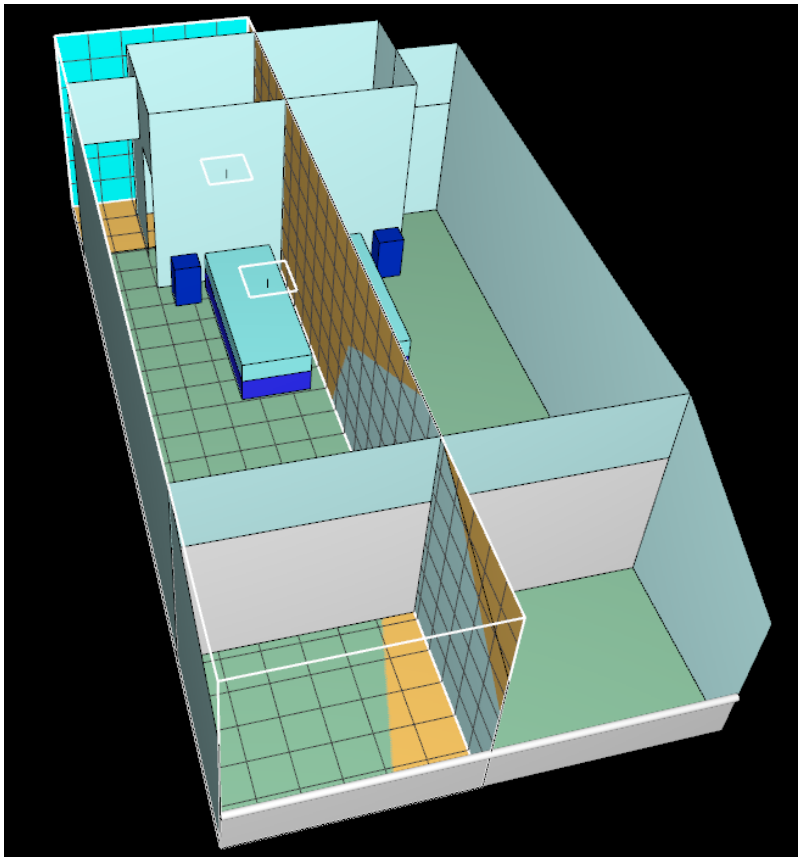

*Figure 56. Single Cabin in Pyrosim*

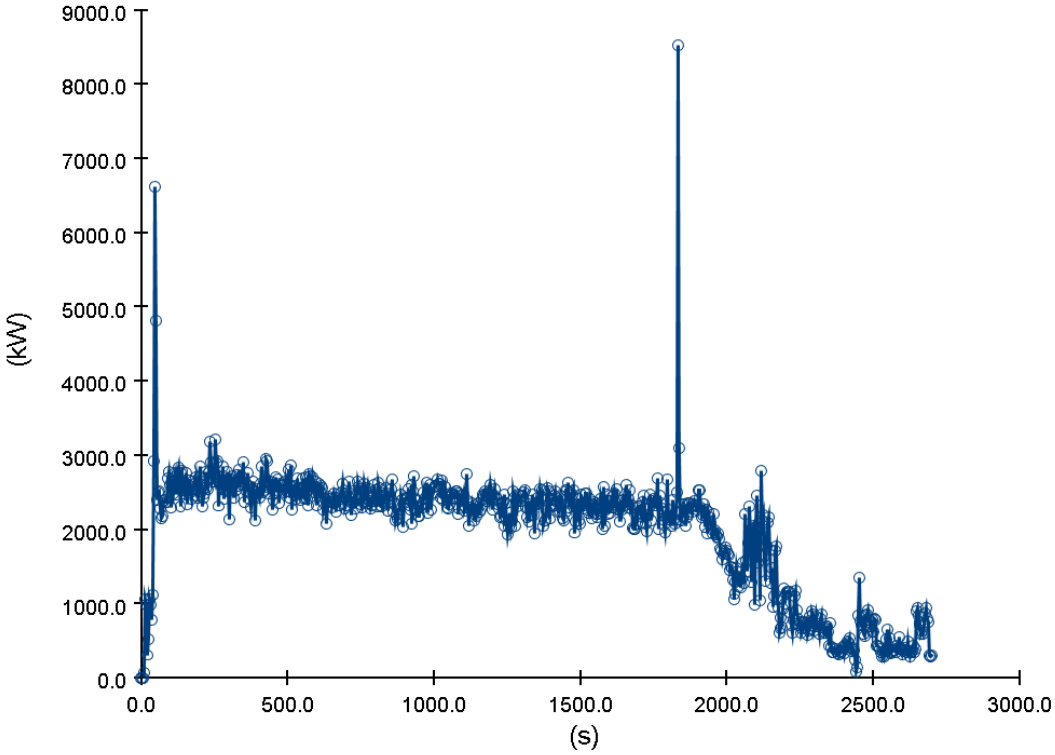


*Figure 57. HRR of cabin fire simulation test*

Figure 57 presents the resulting HRR curve of the cabin fire test. In the first couple of seconds, the HRR develops gradually when it abruptly peaks due to the instantaneous combustion of all items (flashover). Then it "stabilises" around 2-3MW until it decays a little bit before the 2,000second time.

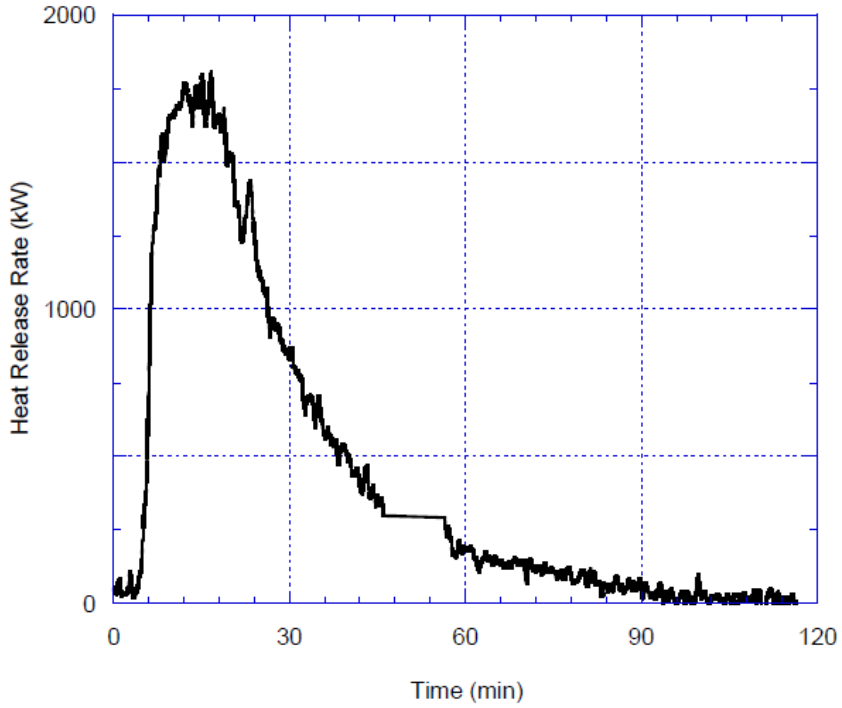


*Figure 58. HRR of a cabin under full-scale fire tests. Source:* (Arvidson et al., n.d.)

Figure 58 presents the HRR of a full-scale cabin fire test conducted by the Research Institutes of Sweden (RI.SE), where the cabin was made out of realistic materials. The peak HRR from the graph is a little less than 2MW, whereas in the relevant report it is explicitly mentioned that the generated hot gasses were so high that part of the smoke plume was leaking out of the test geometry, resulting in an underestimation of the fire (Arvidson et al., n.d.). Furthermore, the approach employed for this trial simulation overestimated the fire since all materials pyrolyzed instantaneously and became fuel, which is not as per how the phenomenon works, as no real combustion is purely efficient and there's always volatiles generated from the pyrolysis phenomenon (DiNenno et al., 2002; Drysdale, 2011; Hurley et al., 2016). Therefore, the trial simulation was in good agreement with a real full-scale test and was, therefore considered verified. With respect to validation, this was performed according to the fidelity and appropriateness of the input variables for the creation of the items (Hillston, 2003; Martis, 2006; Sargent, 2010).

### 7.4.4. Detection and Firefighting/Suppression Systems

The appropriate amount and spacing of smoke detectors were identified for all relevant room types in the cabin deck geometry. Furthermore, sprinklers were also installed per cabin and as required by the applicable codes mentioned earlier.

### 7.4.5. Post-processing devices

Strategic placement of appropriate post-processing tools/devices was implemented within the defined boundaries of the simulation domain. These included 2D and 3D slices that monitored parameters such as temperature, visibility, and gas velocity. Additionally, devices were employed to monitor the smoke layer height, which directly impacts visibility, as well as the heat and toxic effluents emitted by the fire, affecting the occupants' ability to escape. The slices were positioned along the length of both corridors (port/starboard), while devices were also placed in the fire cabin and along the entire corridor. These devices, including those measuring visibility and assessing the hazards posed by heat and toxic effluents, played a crucial role in evaluating the fire risks faced by occupants. The assessment of fire hazards to occupants often involved quantifying the Fractional Effective Dose. Specifically for the FED devices, the activity level of the sensing device was set to "at rest" in order to reflect the night-time scenario. Additionally, it is worthy to be mentioned that the in-capture FED device, inputted via Pyrosim, is able to calculate incapacitation via both exposure to toxic effluent and/or heat.

The domain prior to the initiation of any simulations, including ventilation inlets and outlets, 2D slices, sprinklers, and gas sensing devices is presented in Figure 59.

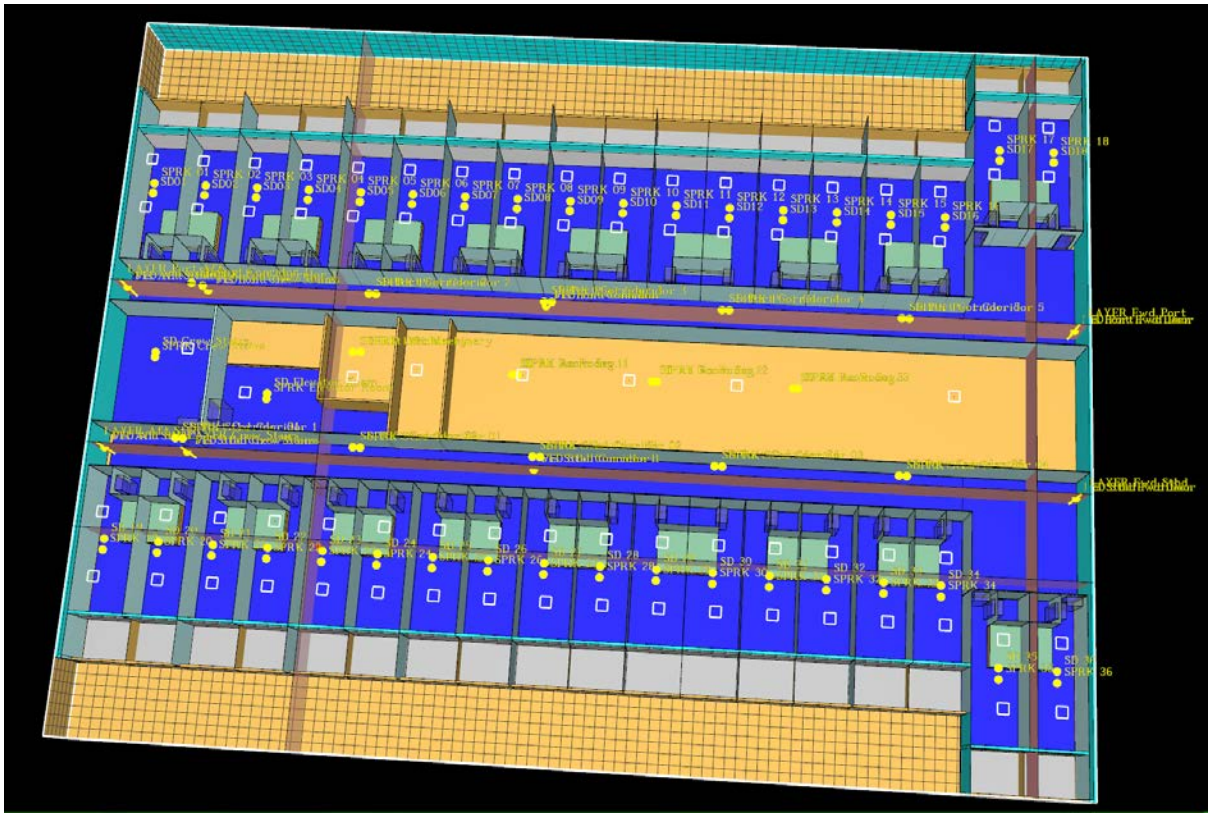

*Figure 59. Passenger cabin deck in Pyrosim presenting ventilation inlets/outlets, sprinklers and post-processing devices.*

### 7.4.6. Simulations

Although not absolutely necessary, the simulation time was set to one hour. Safe return to port regulations may provide a very good justification to do so, but, nevertheless, it was elected to simulate for longer time intervals. Needless to say that the purpose of the simulations were to evaluate the fire risk on occupants, and not to test the validity of the fire boundaries prescribed by SOLAS.

A computational grid, or mesh, with a spacing of 0.5m was chosen for the simulation. This spacing was selected as a reasonable compromise between calculation accuracy and computational time, considering the physical extents of the deck.

Two scenarios were considered, that is with and without fire-fighting, considering a "normal" and worst-case scenario cases, each of which are cited separately.

#### 7.4.6.1. Passenger Cabin Fire Simulation without Active Firefighting

The heat release rate of the fire is presented in Figure 60. It is apparent that the HRR gradually increased with time, which was directly attributed to the pyrolysis that was taking place via the contact of the cigarette with the carpet, creating pyrolyzate. After approximately 1,000 seconds, the heat release rate starts to increase gradually, reaching a magnitude of around 1.5-2 MW. This increase in HRR caused other combustible materials in the cabin to ignite, leading to a further escalation of the fire energy, as illustrated by the curve.

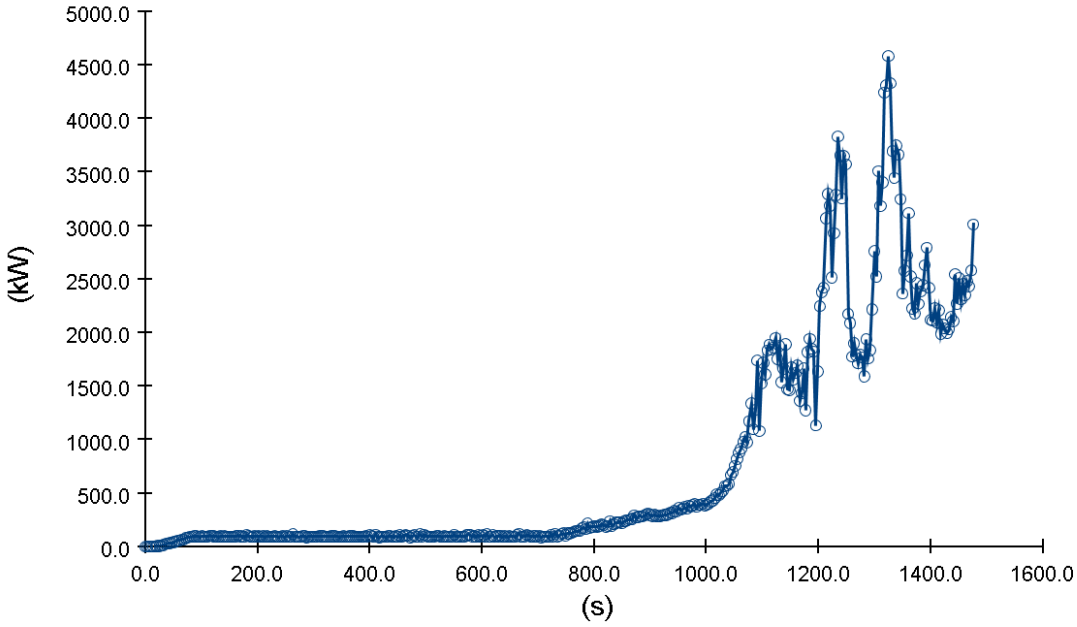


*Figure 60. Passenger cabin deck HRR (no sprinklers).*

At around 1,500 seconds the simulation crashed due to pressure instabilities caused by the generation of flammable gasses. The fact that the deck was practically isolated from the environment outside, except for ventilation inlets and outlets did not provide any aid towards the aforementioned. Nevertheless, adequate occupancy data were obtained.

The development of smoke at 600 seconds is presented in Figure 61. Some smoke has already been generated which is mainly spread inside the cabin of fire origination and some right outside of it. This smoke was generated due to the smouldering fashion of the combustion at that time instance. Furthermore, the smouldering combustion is furtherly confirmed by the absence of flames.

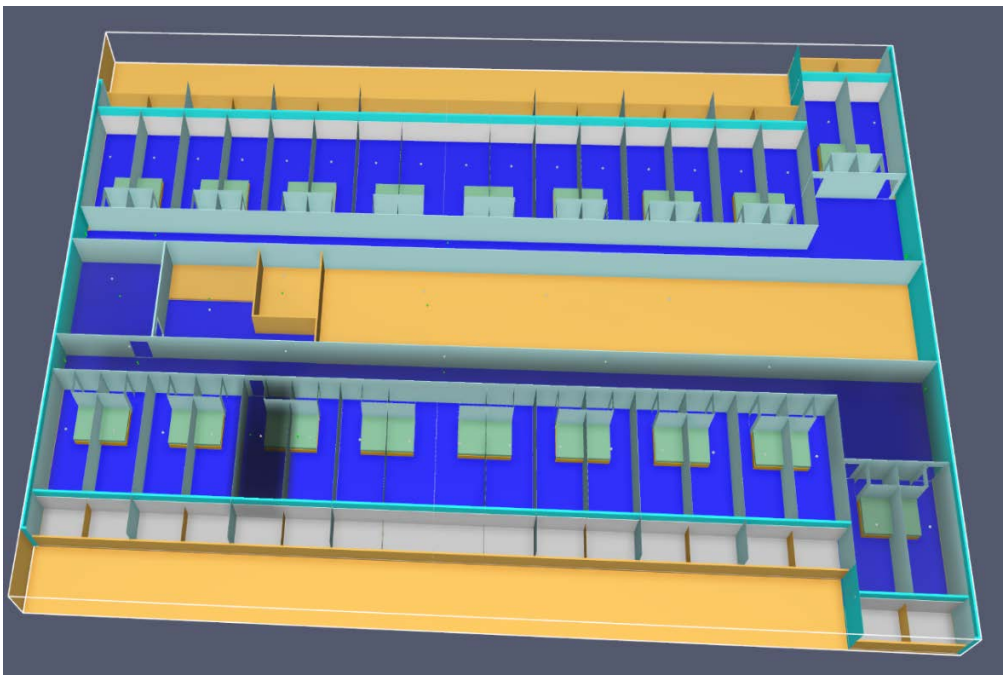

*Figure 61. Smoke development at 600 seconds*

Further smoke development along is presented in Figure 62. This is the same time instance where the HRR increases in Figure 60. The difference in smoke filling can be readily noted. Furthermore, the smoke had started filling the stairwell compartment on the aft centreline part of the deck.

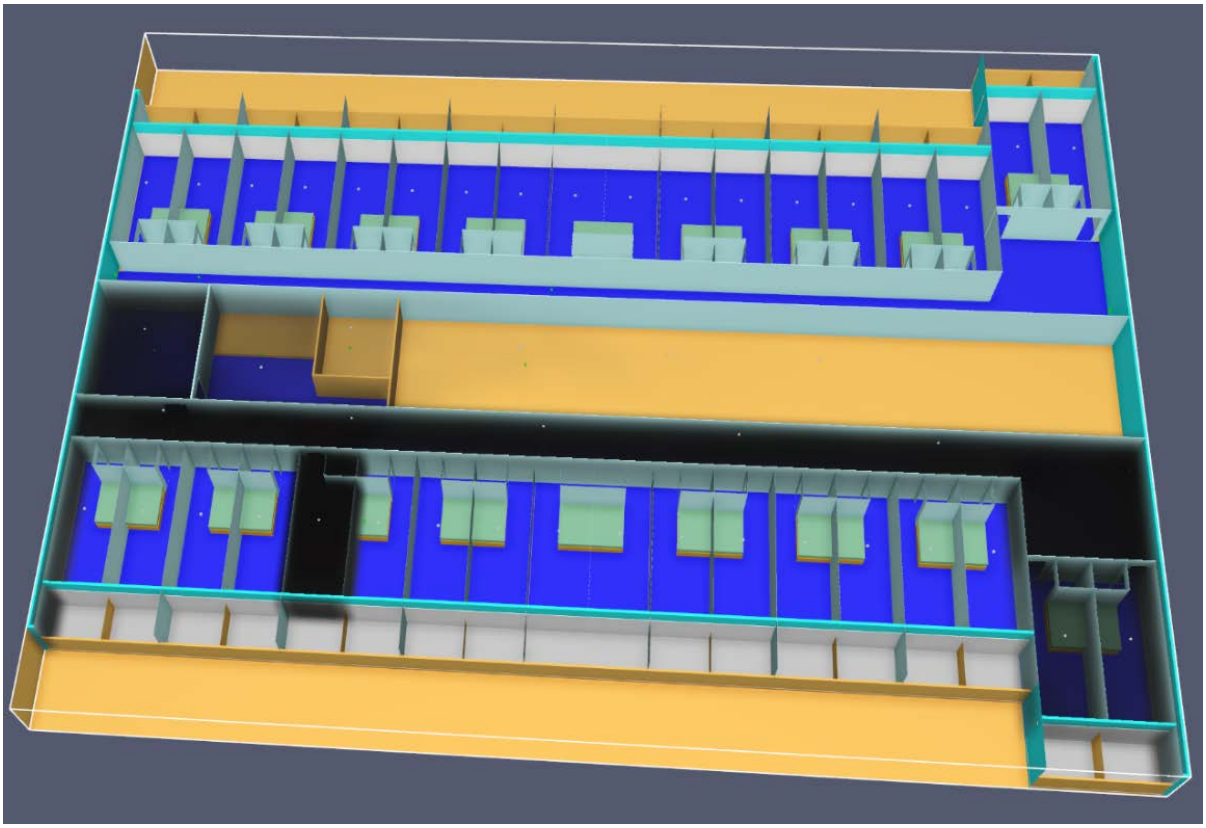

*Figure 62. Smoke development at 1,200 seconds.*

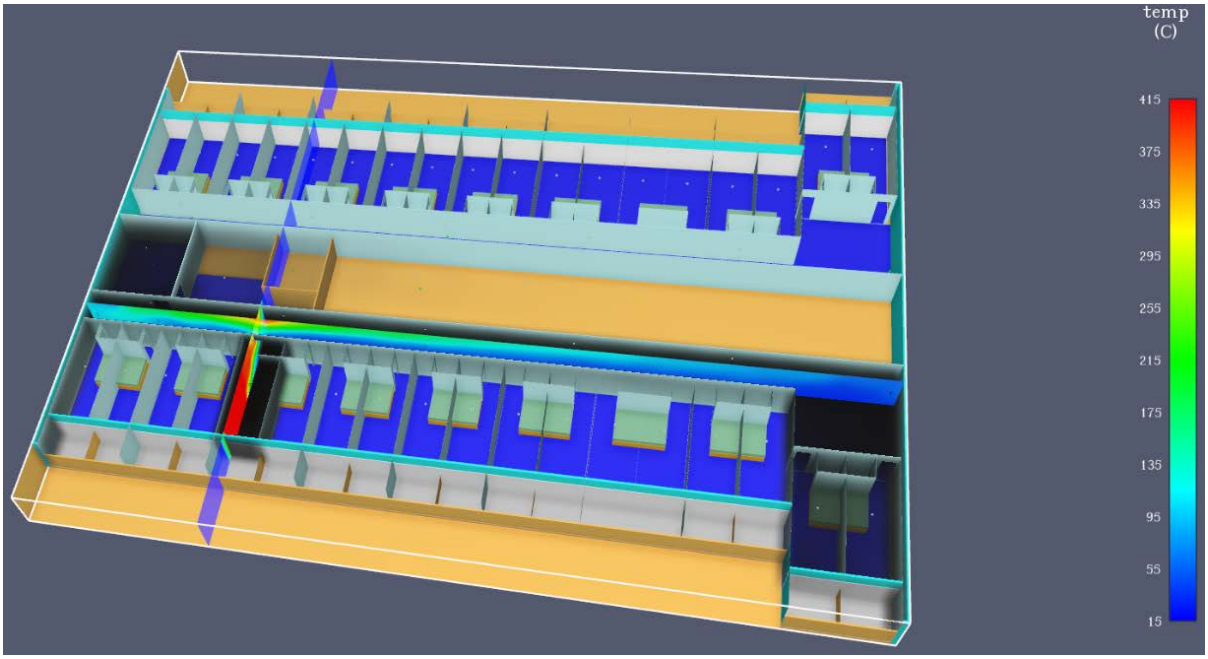


*Figure 63. Smoke and temperature development at 1,200 seconds.*

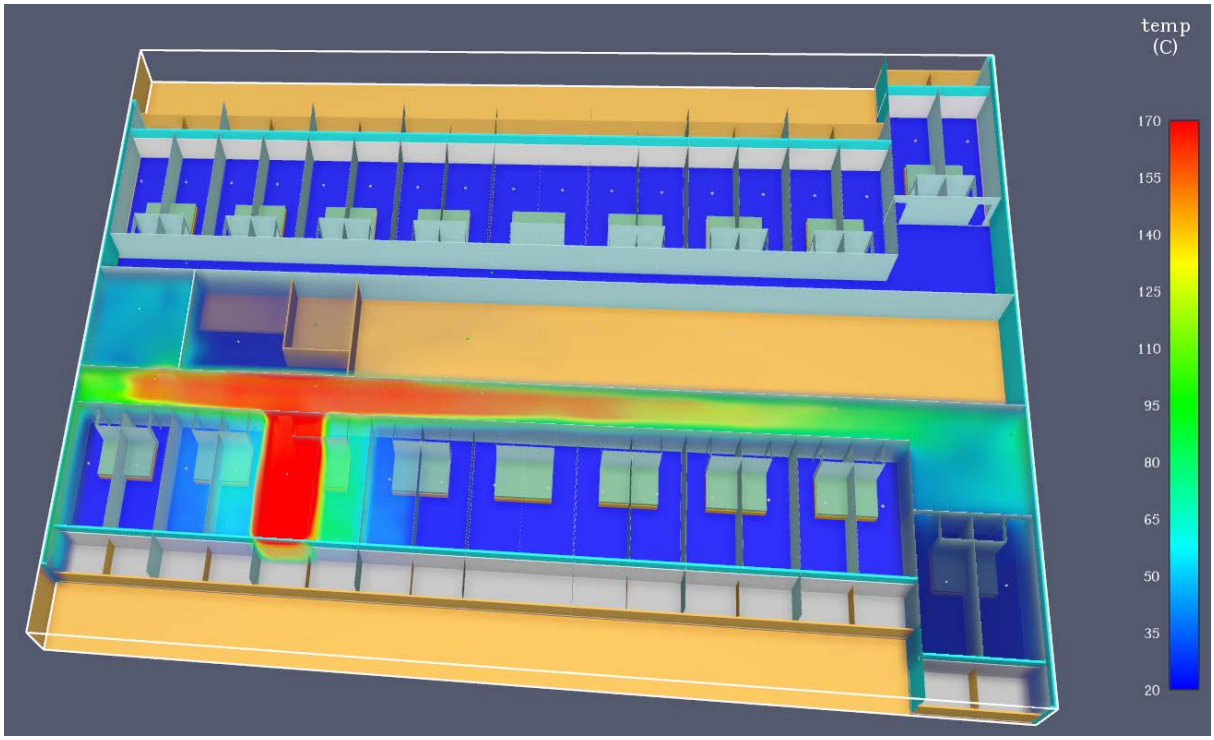


*Figure 64. 3D evolution of temperature at 1,200 seconds.*

Figure 63 presents the same time instance as Figure 62 but with two 2D temperature slice on x and y-axis activated. The one on the y-axis presents the magnitude of the temperature inside the room of origin, which is well above 400ºC, whereas the other one on the corridor, where much lower temperatures were noted. Furthermore, since the x-axis 2D slice runs along the corridor, a visual representation of the smoke layer height can be seen, effectively showing the spread of heat both in term of vertical distribution but also distance from the cabin of origin. In addition to the 2D temperature slices in Figure 63, Figure 64 presents a 3D slice of the temperature aiding in the visualisation of the aforementioned.

In terms of visibility, Figure 65 and Figure 66 present the 3D evolution of visibility at 600 and 1,200 seconds respectively. Note that the colour scale of the visibility is somewhat backwards as read denotes good visibility. At 600 seconds there is no visibility in the cabin of origin, whereas the corridor is noticeably in a better state. On the other hand, at 1,200 there is absolutely no visibility and any potential occupants within should be considered as a fatality.

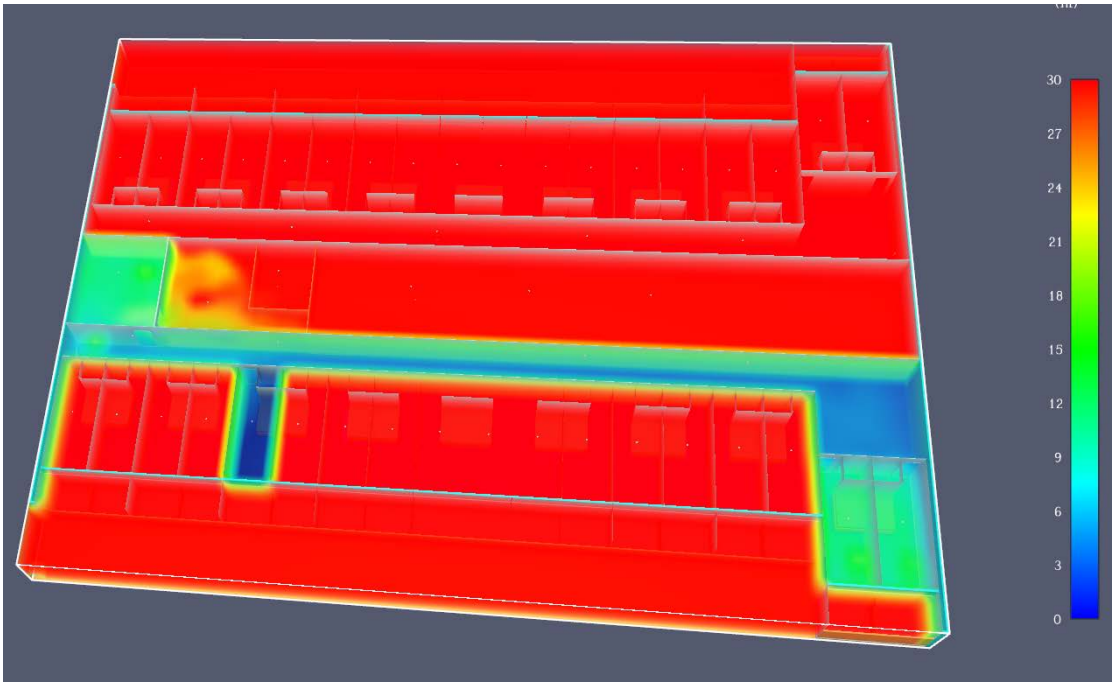


*Figure 65. 3D evolution of visibility at 600 seconds*

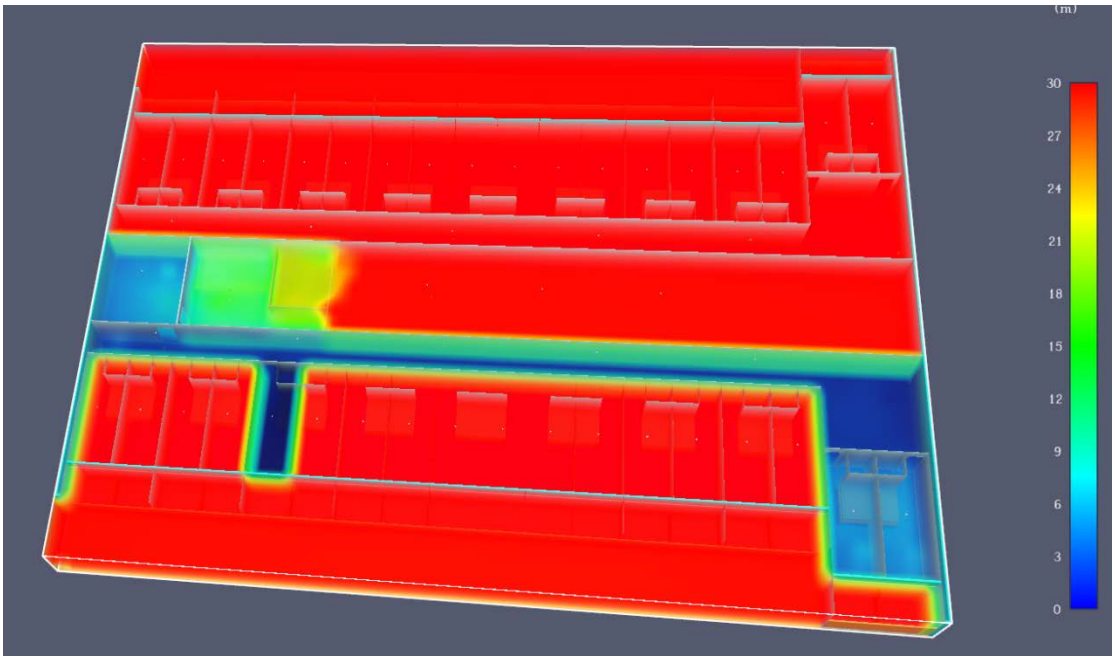


*Figure 66. 3D evolution of visibility at 1,200 seconds*

To assess the impact of the fire and the extent of smoke accumulation, devices to measure smoke layer height and visibility were strategically positioned within the cabin and at various points along the corridor. These can be found in the appendix, namely Appendix B1.

Concerning incapacitation of occupants, Figure 67 presents the fractional effective dose at the aft starboard corridor. FED is a dimensionless measure that quantifies the impact of airborne irritants, fire effluents, and heat on individuals. In real-life scenarios, FED values can be influenced by inhalation of primary fire effluents, inhalation of secondary fire effluents (which requires knowledge of specific chemical

compounds present), and exposure to heat. FED values greater than 1 indicate a potential for incapacitation.

In the simulations conducted, a FED device was used to measure the combined effect of fire effluents and heat on occupants, presented in Figure 67. Based on the output of the simulation model, it was observed that occupants could experience the effects of incapacitation around 900 seconds after the fire initiation, primarily due to exposure to toxic fire gases. This observation aligns with the principles of physics, as smouldering combustion tends to produce more harmful toxic effluents (Karlsson and Quintiere, 2000).

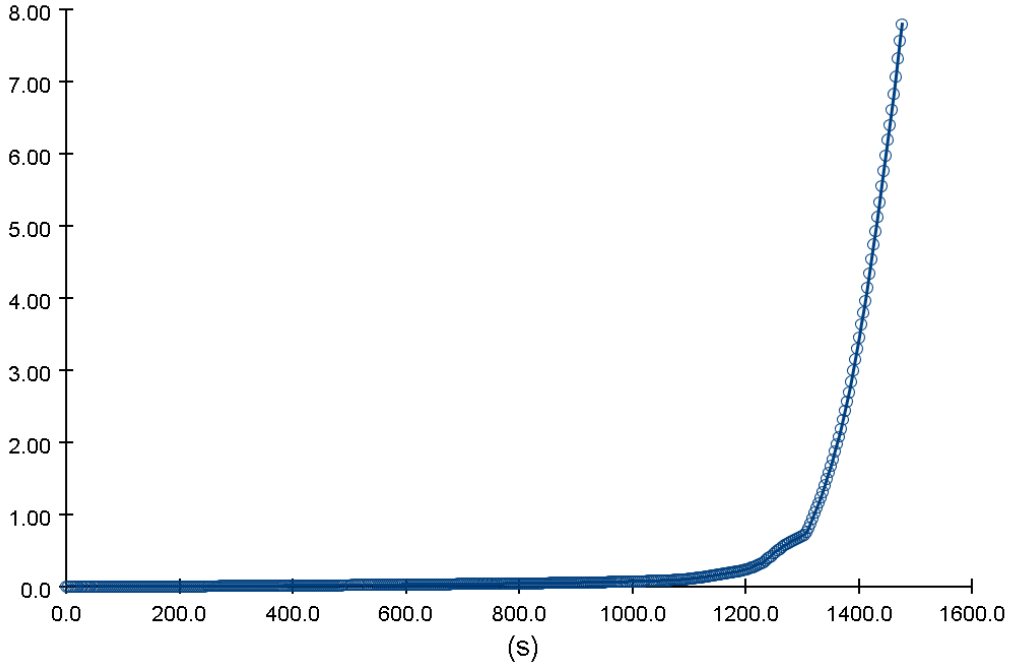


*Figure 67. Fractional Effect Dose at aft starboard corridor.*

### 7.4.6.2. Passenger Cabin Fire Simulation with Active Firefighting

The simulation parameters remained the same, except for the activation of the sprinklers. The sprinklers themselves were set to activate at 68$^{o}$C. This time, the whole one hour was successfully simulated. Figure 68 presents the HRR of the simulation with sprinklers activated. Contrastingly with the simulation were no active firefighting measures are present, the HRR grows slightly over time, with a magnitude of around 100kW, which is considerably less than the one presented in Figure 60. Then, its behaviour stabilises for the remaining time of the simulation. This was attributed directly to the effect of the sprinklers in controlling the HRR of the fire, and therefore, facilitating better conditions in terms of heat. Mover, this is well expected as the main contribution of sprinklers, apart from the self-explanatory of extinguishing the fire, is to control the HRR of the fire, and to avert it from reaching a flashover.

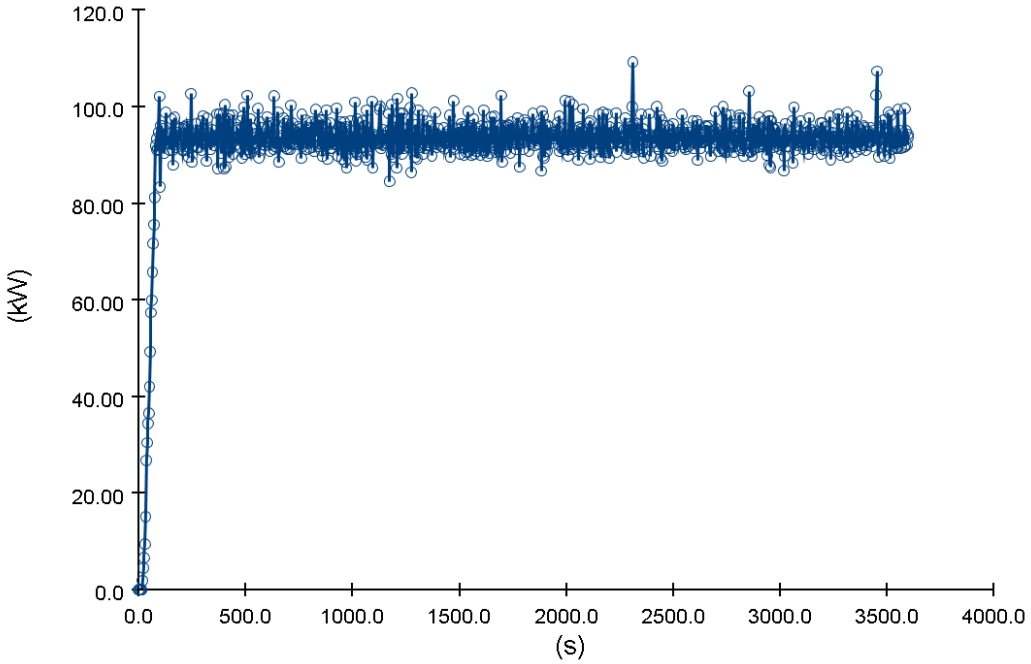


*Figure 68. Passenger cabin deck HRR with sprinklers.*

Figure 69 presents the smoke development at 60 seconds, along with a 2D temperature slice on y-axis to demonstrate the temperature inside the cabin of origin. The temperature in the 2D slice is quite low, around 40-50$^{o}$C, while after examination of the temperature post-processing devices, the maximum temperature experienced was 70$^{o}$C. Furthermore, the sprinklers activated a little before the time instance presented.

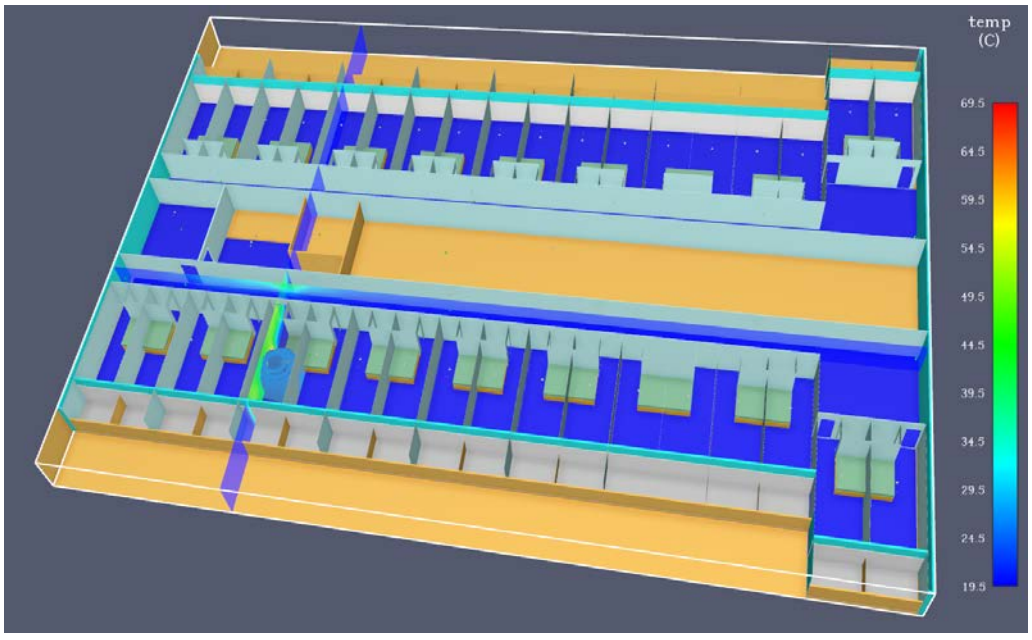


*Figure 69. Smoke development and sprinkler activation at 60 seconds*

Figure 70 presents the smoke and temperature development at 2,500 seconds, well into the simulation. The same magnitudes as before are noted, no change in temperature at all, therefore, the sprinklers were rather successful in averting the fire from growing and spreading to other items within the room of origin.

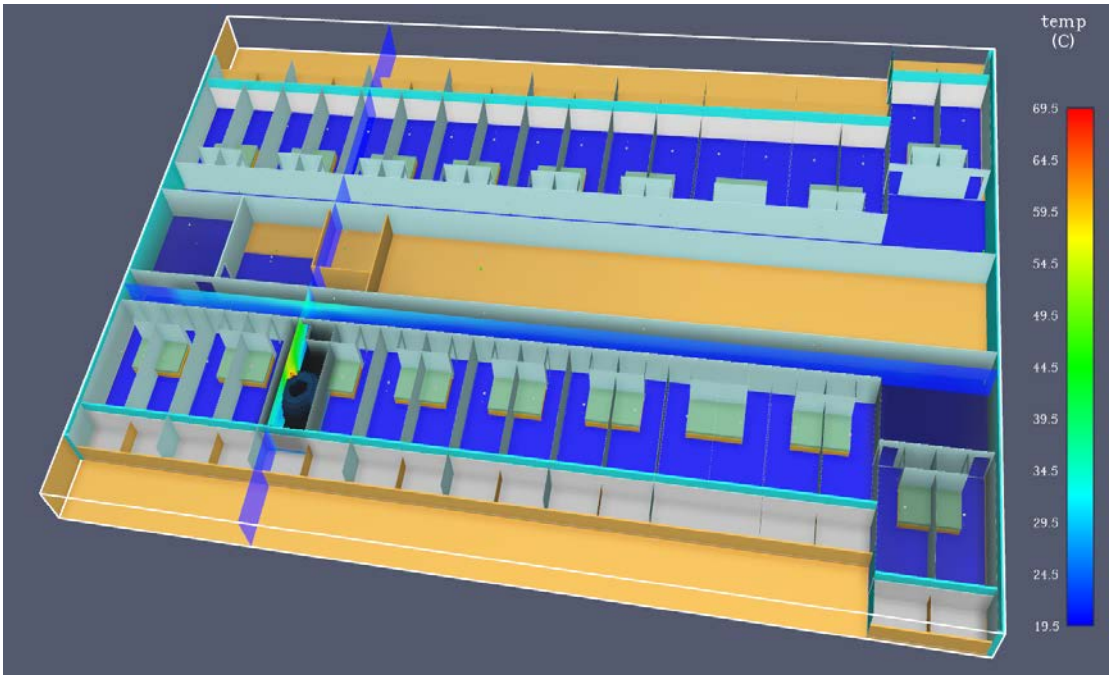


*Figure 70. Smoke and temperature development at 2,500 seconds*

In addition, only the cabin sprinkler was activated while the room appears to be riddled with smoke. Regarding the visibility of the scenario, Figure 116 presents a 3D visibility slice, where the room of fire origin is indeed filled with smoke while the corridor has more than adequate visibility.

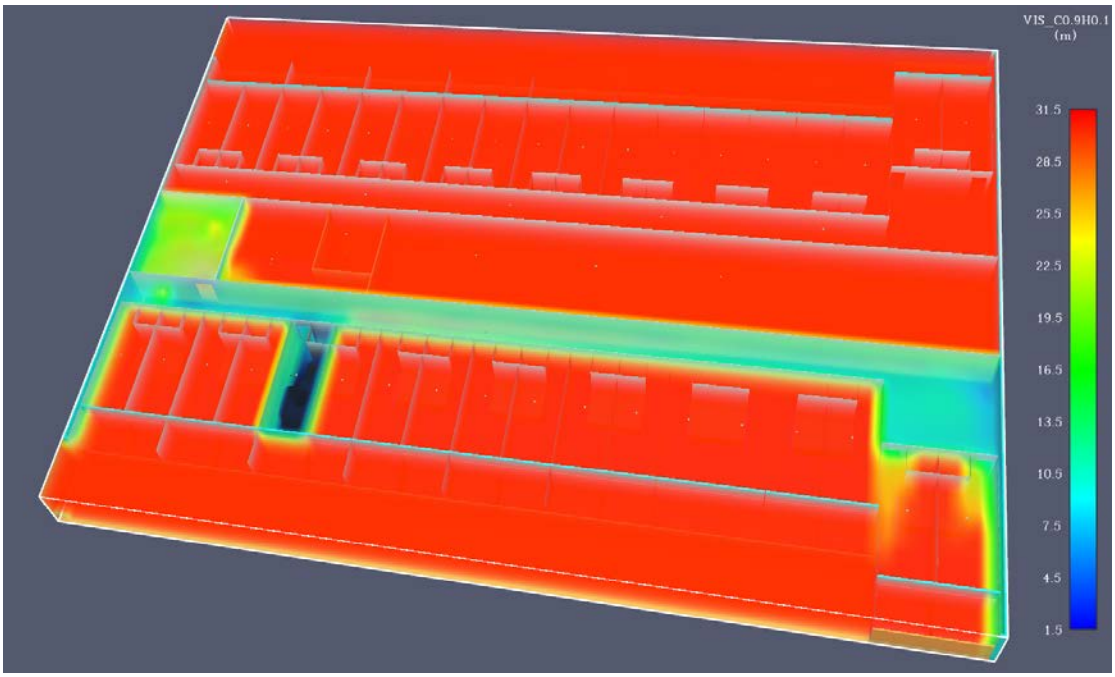


*Figure 71. 3D visibility slice at 60 seconds*

To assess the impact of the fire and the extent of smoke accumulation, devices to measure smoke layer height and visibility were strategically positioned within the cabin and at various points along the corridor. These can be found in the appendix, namely Appendix B.

The plot of the FED of the aft-most starboard corridor device is plotted in Figure 72. The FED experienced by a potential occupant is will below 1, therefore no incapacitation is expected, except for possible occupants inside the cabin of origin.

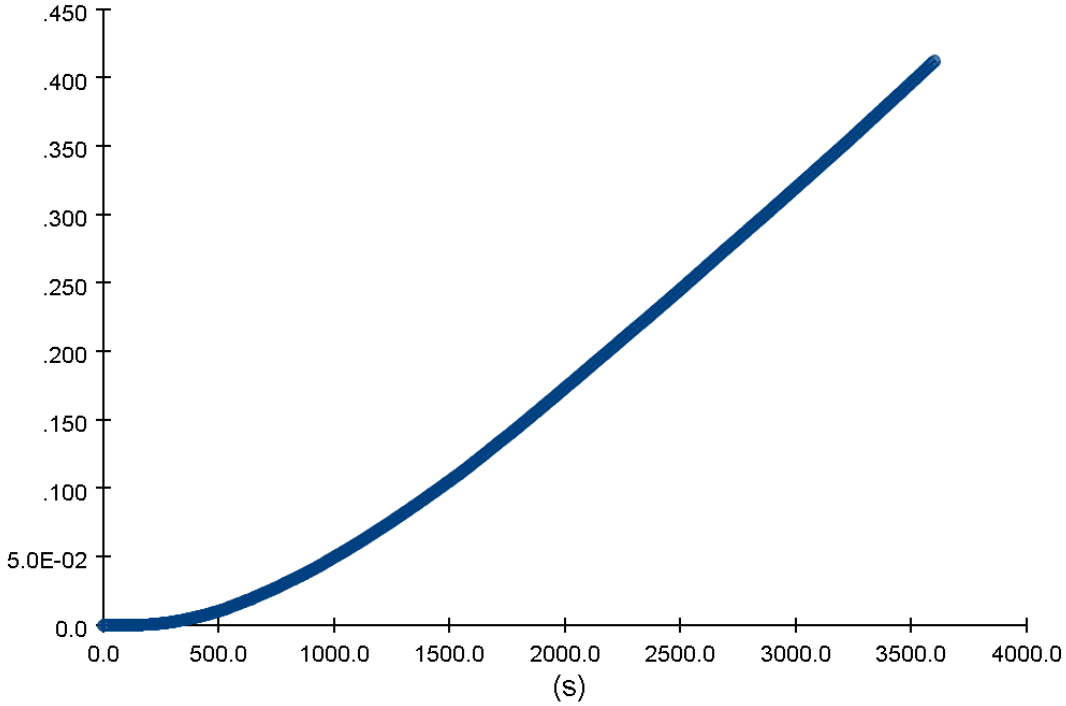


*Figure 72. Fractional Effect Dose at aft starboard corridor (with sprinklers)*

## 8. Large Public Space Fire Simulation Case Study

This section describes the fire simulations conducted for the large public deck in Figure 52. This scenario considered the occupancy of the large passenger ship during daytime, where passengers are expected to be anywhere but their cabins, hence the relevance of the scenario. Figure 73 presents the arrangement of the large public space deck within the main vertical of investigation, namely on the fourteenth deck.

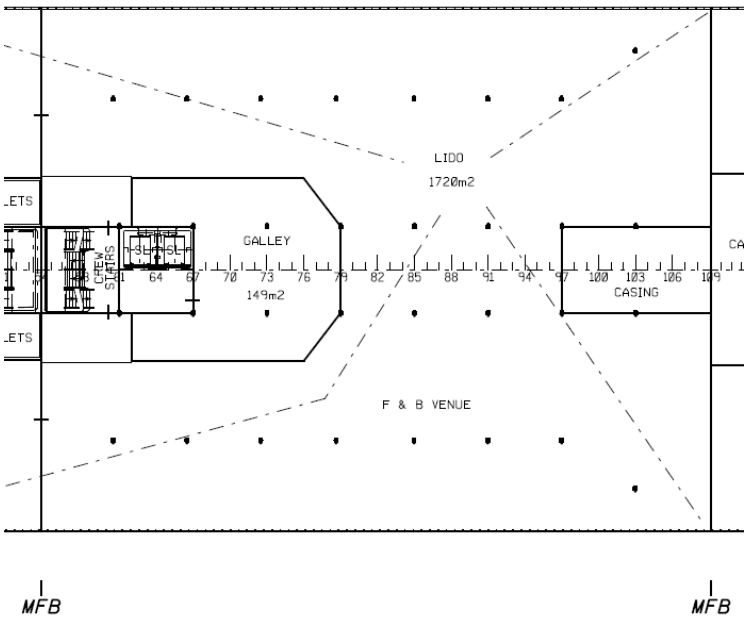


*Figure 73. Large public space deck.*

Unlike the passenger cabin deck, the large public space was entirely barren, being a massive empty space. Owing to the simplicity of the deck, no simplification were required towards importing/designing in Pyrosim. The deck appears to have a small galley, smaller than the one located on deck 7, crew stairwells – which is to be expected as these usually span for the whole vertical extent of the ship and a lift-pit.

Since the large public deck has no specified function/purpose, no furniture/equipment were available for any part of it. Therefore, in order to demonstrate the functionality of the main vertical zone fire risk model, this deck was considered as a restaurant, with seating arrangements for the passengers. Furthermore, the galley was completely neglected as it requires A-60 insulation. The same was applied for the engine casing located forward.

Appropriate seating with relevant spatial distribution were allocated on the deck, including social distancing measures since the simulation was performed on the peak of COVID-19. Figure 74 presents the large public space as it was created in Pyrosim.

The items included in the simulation domain were as follows:

1. Chairs, consisting of:
1.1. Wooden frame,

1.2. Foam cushion,
1.3. Fabric cover.
2. Tables (made out of wood).
3. Carpet.
4. Bulkheads (A and B type), consisting of:
4.1. Steel sheet,
4.2. Rockwool insulation,
4.3. PVC veneer.

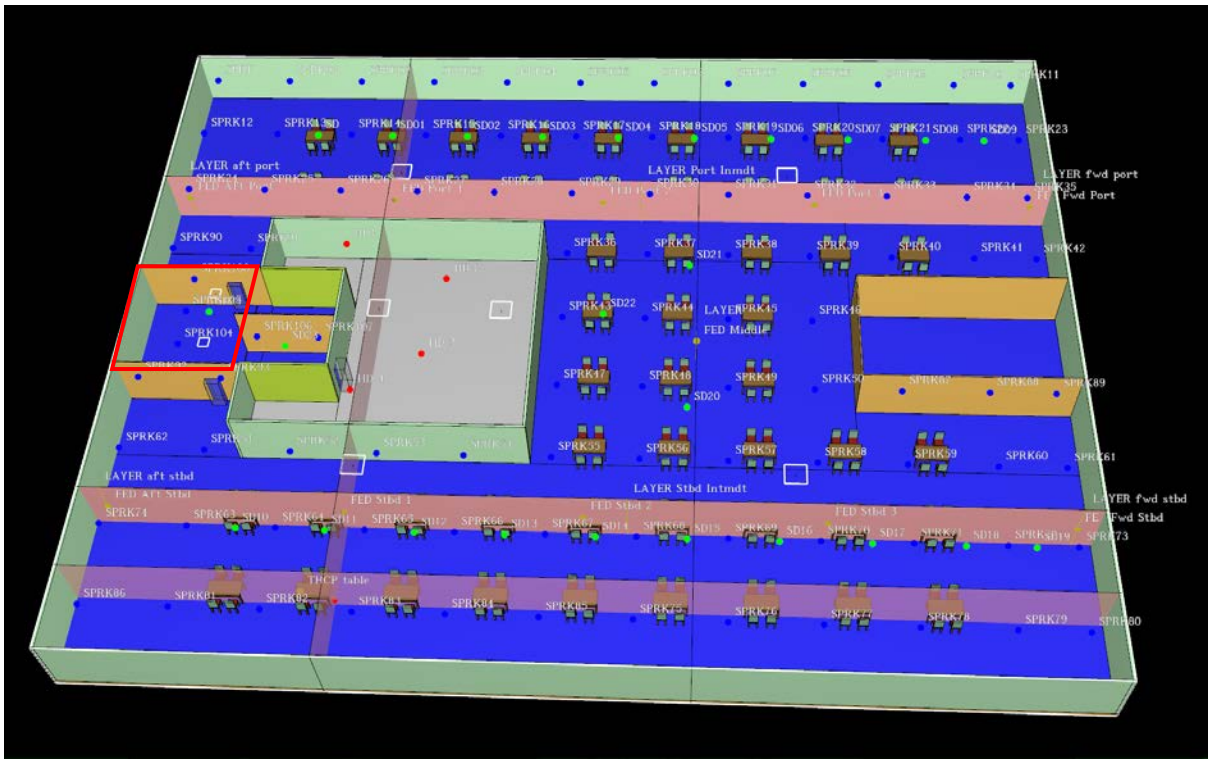


*Figure 74. Large public space deck imported into Pyrosim, including all relevant detection, suppression, and sensing devices.*

## 8.1. Fire Simulation Scenario and Ignition Source

As in the cabin deck, the ignition source was considered to be a lit cigarette dropped by a rather negligent occupant. The location of the cigarette was chosen randomly, while it is represented by a red dot in Figure 74, located on the aft starboard side of the deck.

Access to other main vertical zones was blocked, in order to account for the accumulation of smoke and harmful fire effluents. The crew stairwell, marked with a red parallelogram in Figure 74, was left with its doors open, which, apparently also provide access to the galley. Despite that the galley was not taken into account into the simulation in terms of available fuels/flammable material, its door was left open in order to account for the smoke filling (visibility) of that compartment.

### 8.1.1. Ventilation Characteristics

The ventilation characteristics for the large public space portion, stairwell and galley were identified from SOLAS. Specifically, air charges per hour were identified and pertinent inlet and outlet ventilation outlets were modelled in Pyrosim in way of inlet/outlet vents. The HVAC module was not employed as the HVAC plans for the decks, including smoke extraction strategy, were not available.

The volume flow for the restaurant space is 1.43 $m^3$/sec, whereas for the galley 5.9 $m^3$/sec. Although the galley's contribution to the fire in terms of available fuel(s) was not modelled, its ventilation characteristics were utilised. This decision was taken as the ventilation characteristics heavily affect the fire in terms of available oxygen for combustion, which may result in a ventilation-controlled fire instead of a fuel-surface controlled one, as well as the smoke filling and transport characteristics.

### 8.1.2. Pyrolysis Model

Similarly with the cabin deck fire simulation scenarios, a deterministic approach was employed in terms of pyrolysis modelling.

### 8.1.3. Materials available in the large public space deck

The tables consisted of fire retardant (FR) plywood, following SOLAS rules (IMO, 2020). The seating, consisted of FR plywood, foam, and fabric. Due to the data requirements implied by the first principles deterministic approach that was employed, the materials present in the large public space where the same as in the passenger cabin deck scenario.

Therefore, the materials along with relevant thermal and pyrolysis parameters are presented in Table 13, Table 14 and Table 15

### 8.1.4. Ignition Initiation

The ignition approach is assumed to be a dropped cigarette on the carpet which will pyrolyze and create a smouldering combustion fire which may spread over other objects and respective materials in the large public space deck.

Moreover, since the materials and the fire modelling approach were heavily scrutinised for the purpose of the passenger cabin deck simulations, there was no requirement to run mock/trial simulations in smaller parts of the large public space as the approach had already been put to test.

### 8.1.5. Detection and Firefighting/Suppression Systems

The appropriate quantity and spacing of smoke detectors were identified for the seating and galleys areas in the large public deck geometry. Furthermore, sprinklers were also installed as required by the applicable codes.

### 8.1.6. Post-processing devices

Adequate, as per the requirements of SOLAS and FSS Code (IMO, 2020, 2015b), post-processing tools/devices were allocated within the boundaries of the large public space deck. These were 2D/3D slices monitoring temperature, flow velocities and visibility. Smoke layer height devices were also placed within the domain, specifically at both extremities and intermediate parts of the deck, in order to make sure that the smoke layer height is properly identified due to the large size of the deck. In fact, since there are practically no boundaries except for those of the main vertical zone, additional 2D slices were incorporated if one compares these with the passenger cabin deck simulation. Also, FED devices were placed at regular intervals in order to evaluate it properly and avoiding having the FED readings skewed due to their spatial distribution. For this scenario, the activity level prescribed to the FED sensing devices was set to day-time activity, which implies a smaller dose/value of toxic effluents, heat and/or visibility required for occupant incapacitation.

## 8.2. Simulations

As in the passenger cabin deck, the simulation time was set to one hour, although not necessary as discussed previously. A computational mesh with a spacing of 0.5m was chosen for the simulation, considered to be a reasonable compromise between calculation accuracy and computational time, considering the physical extents of the deck.

Two scenarios were considered. One without active fire-fighting, being the worst-case scenario, and one with sprinklers. Hi fog deluge systems were not employed due to inherent modelling difficulties which would potentially induce additional errors.

Since the first principles deterministic approach had been validated and verified via the passenger cabin deck, and due to the materials being kept the same, there was no necessity for mock/trial simulations, or any operations towards validation/verification of the model.

### 8.2.1. Large Public Space Fire Simulation without Active Firefighting

The heat release rate of the simulation is presented in Figure 75. As in the cabin scenario, the HRR gradually rises over time, with low magnitudes, when at around 400seconds, the HRR slope begins to increase. The low heat release rate behaviour was attributed to the cigarette pyrolyzing the carpet.

At around 1,000 seconds, the HRR slope increases almost on an exponential behaviour. This could be attributed to successful fuel packages, objects that is, catching fire.

In order to test the aforementioned hypothesis of successive fuel package ignition, a thermocouple was placed on the table adjacent to the dropped cigarette. On the other hand, the autoignition temperature of the FR plywood is around 600$^{o}$C. Figure 76 presents the temperature plot of the thermocouple.

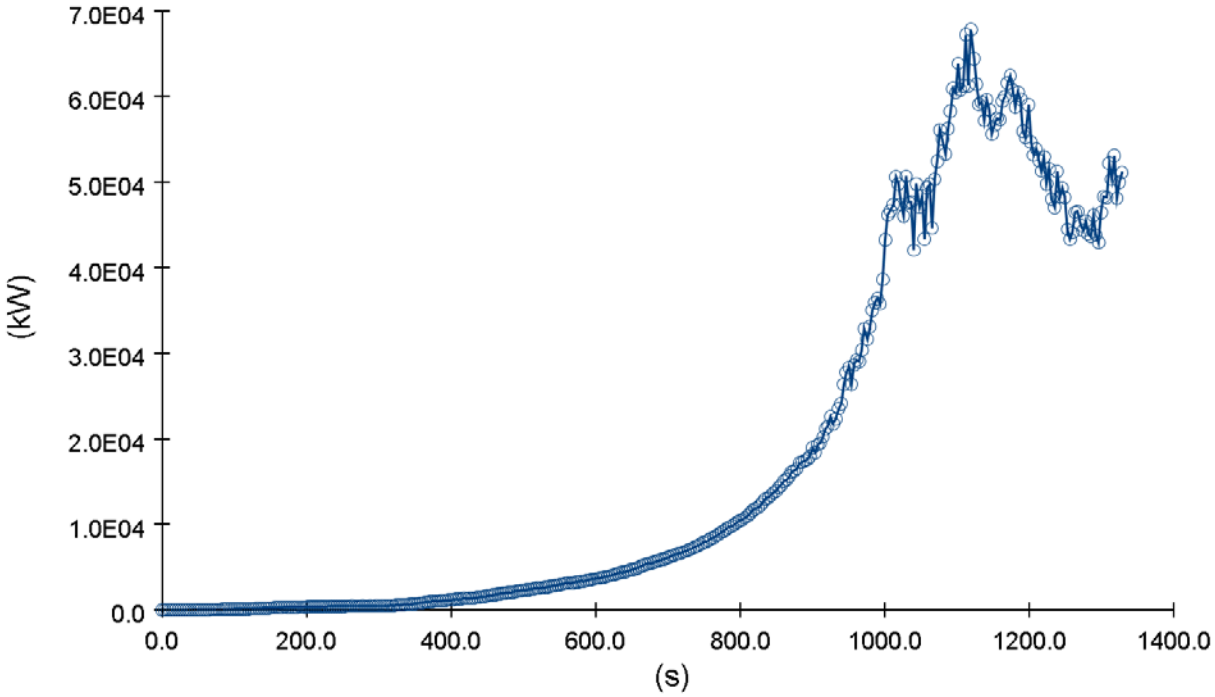


*Figure 75. Heat release rate of large public space with no active firefighting.*

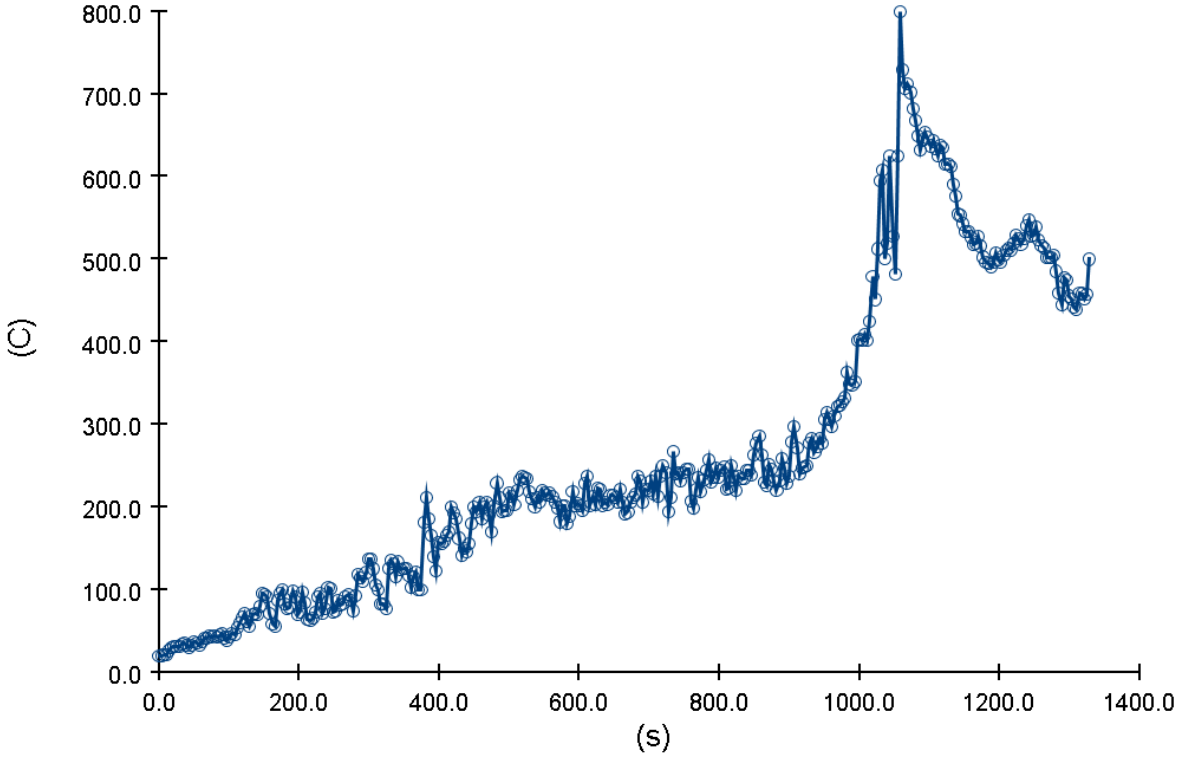


*Figure 76. Temperature plot of thermocouple placed on the table adjacent to the fire initiation.*

It was noted that at approximately 1,000 seconds the temperature of the environment close to the table is around 600ºC, which denoted that the table ignited at that time instance, which contributes to a sharp increase of the HRR in Figure 75.

The simulation crashed after 1,400 seconds due to pressure numerical instabilities, but adequate fire safety results were obtained, nevertheless.

Figure 77 presents the fire and smoke development in the deck enclosure. The majority of the smoke was noted around the fire origin point, namely starboard aft side, while smoke is starting to slowly spread over the rest of the enclosure. No visible flames were noted that the time instance of 600 seconds, mainly due to the smouldering combustion fashion of the carpet and adjacent to the point of origin items.

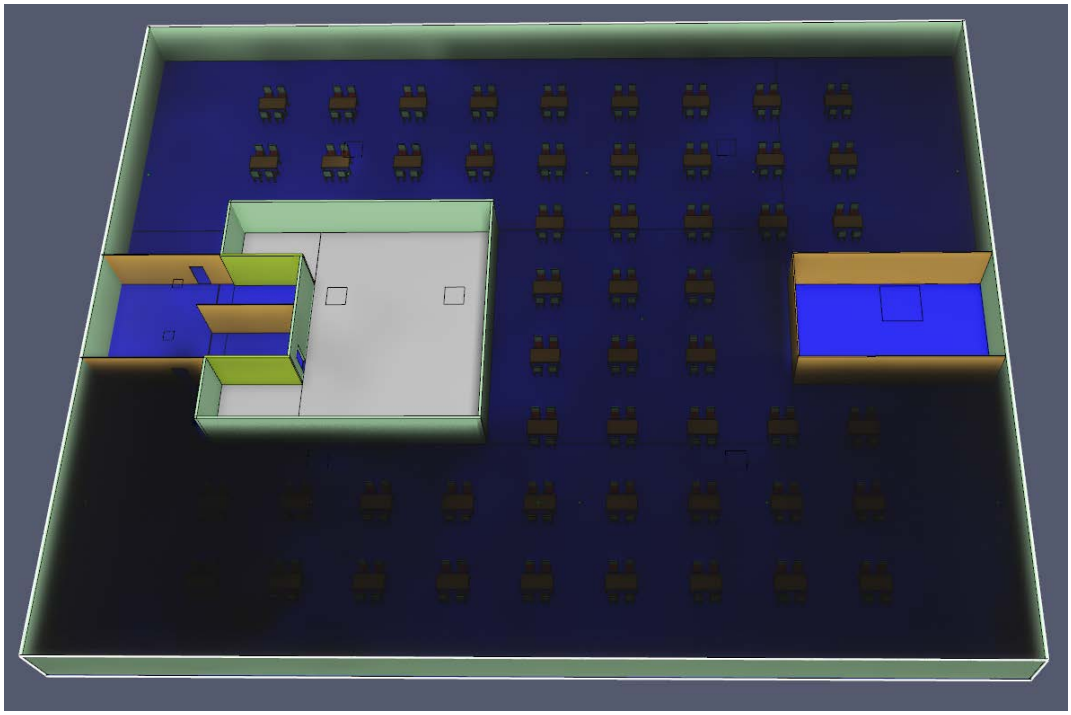

*Figure 77. Smoke and fire development in the large public space at 600seconds.*

Figure 78 presents the magnitude of temperatures experienced on the deck via a plethora of 2D slices. At 600 seconds, the area around the fire origin experiences temperatures of approximately 500ºC which span on almost the entire vertical length at that point.

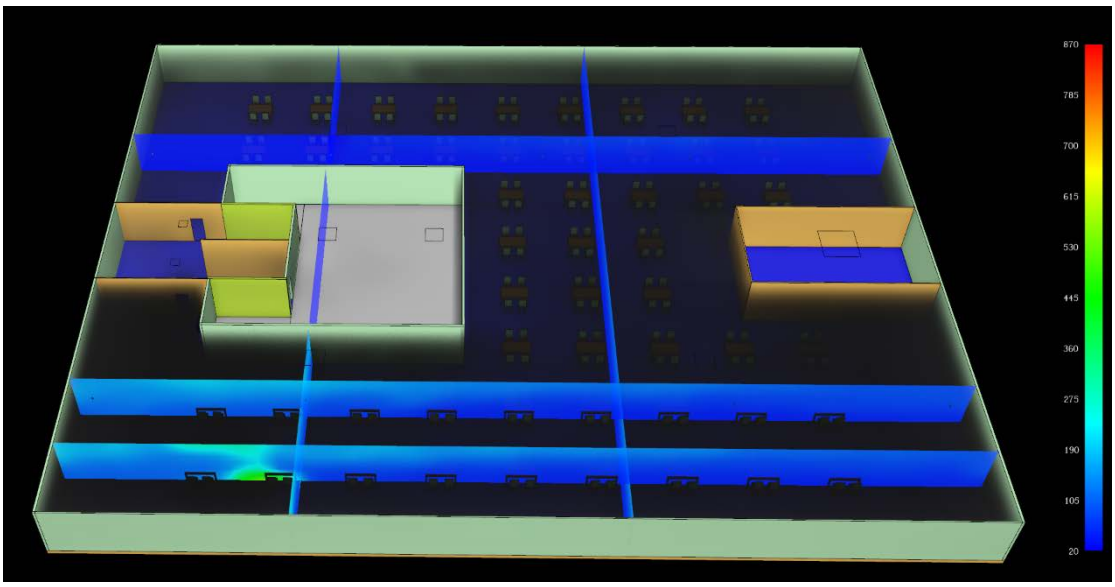


*Figure 78. Temperature development at 600 seconds via 2D temperature slices.*

Moving towards the forward end of the large public space deck, at the same time instance, the temperature magnitudes are considerably lower than that of the fire origin point, which is well expected considering that the deck spans over an entire main vertical zone. This indicates that for the time instance of 600 seconds, the smoke development poses greater risk to occupants than the fire itself.

Figure 79 presents a 3D slice of the temperature along the span of the entire length of the deck. Temperatures in the magnitude of 400ºC were noted close to the fire origin, whereas considerably lower, namely around 200ºC as one moves further away from the fire.

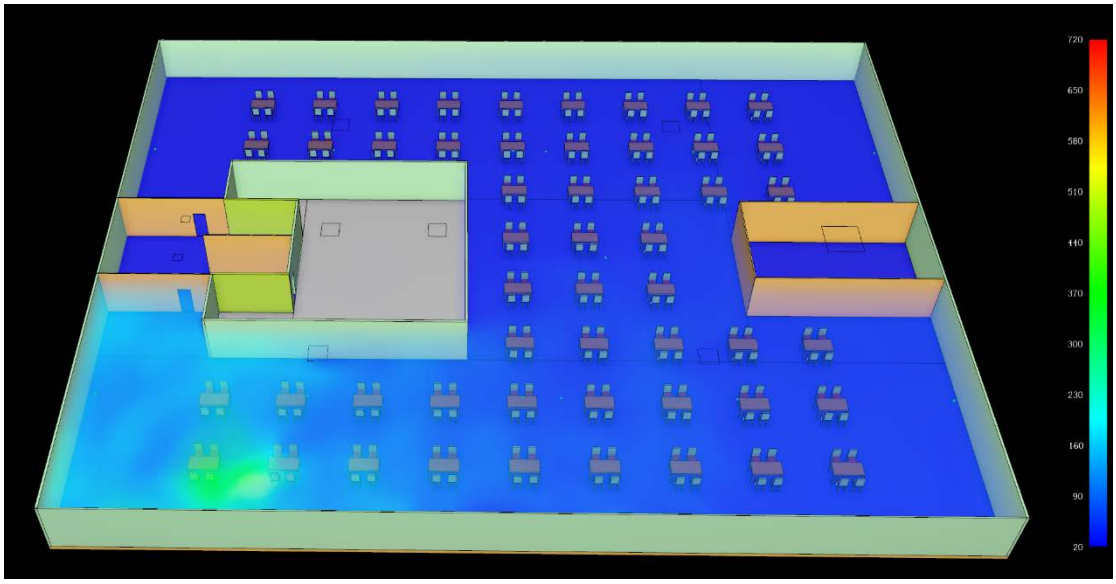


*Figure 79. 3D evolution of heat at 600 seconds.*

Figure 80 presents the evolution of visibility over the entire deck via a 3D slice device. Keep in mind that the colour scheme is red for good visibility and blue for no visibility. Very low visibility was noted around the fire origin, whereas visibility increases as one

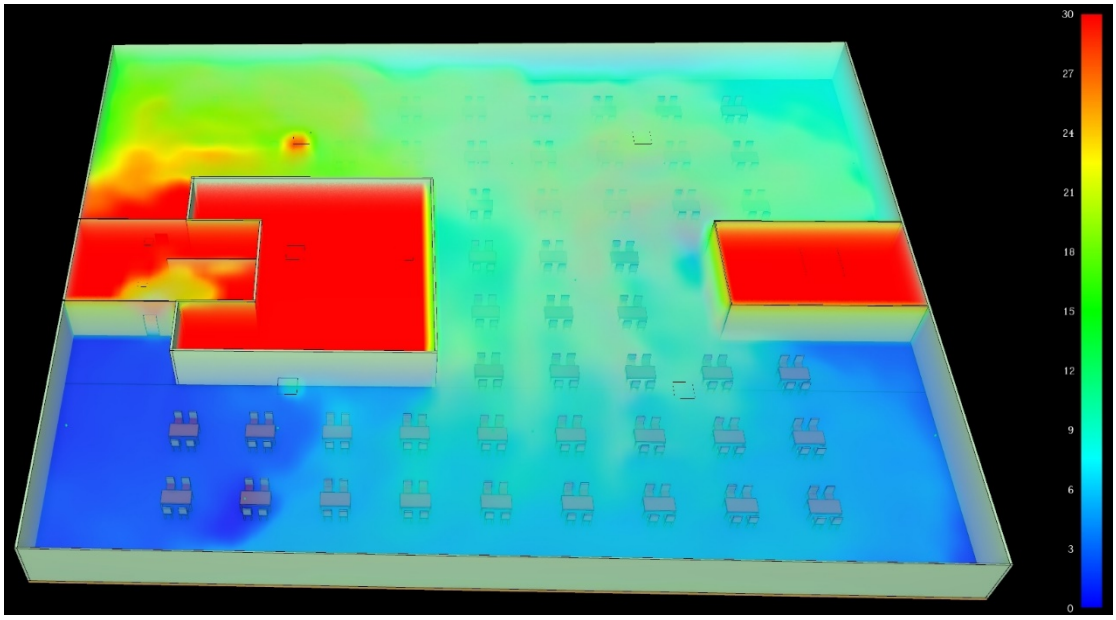


*Figure 80. 3D evolution of visibility at 600 seconds.*

moves further away from the fire. Direct comparison of the temperature and visibility 3D slices at 600seconds presented in Figure 79 and Figure 80 is made against Figure 82 and Figure 83, which present the fire development, 2D evolution of heat via numerous respective slices, and smoke development at 1,000 seconds respectively.

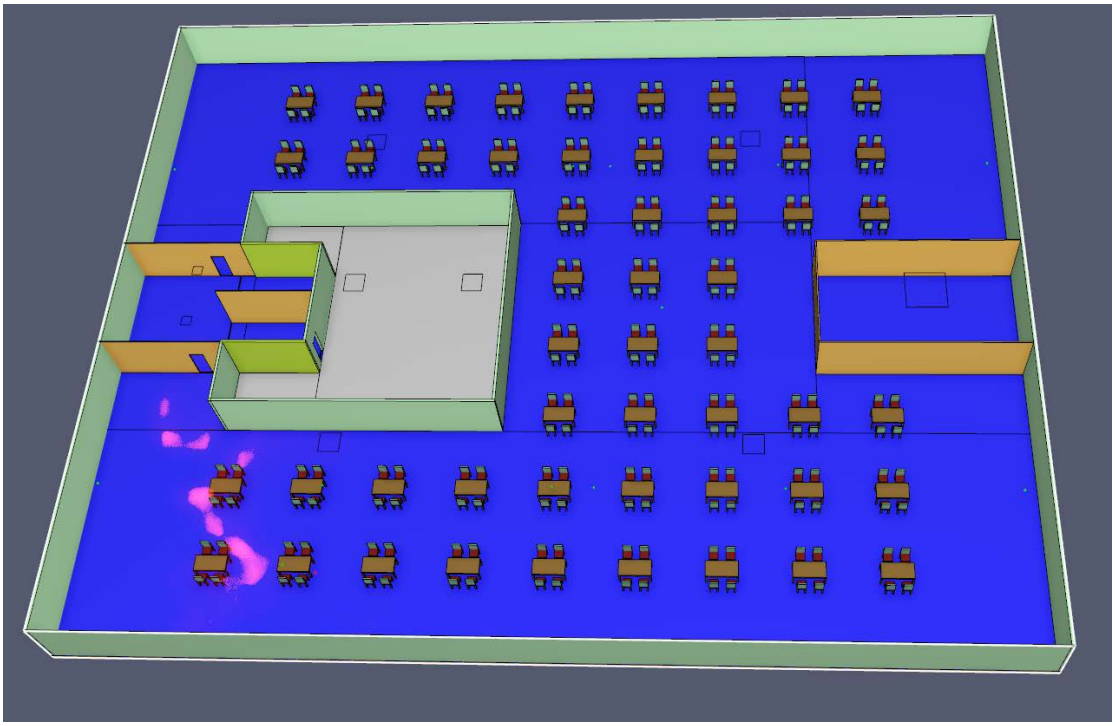

*Figure 81. Fire development at 1,000 seconds.*

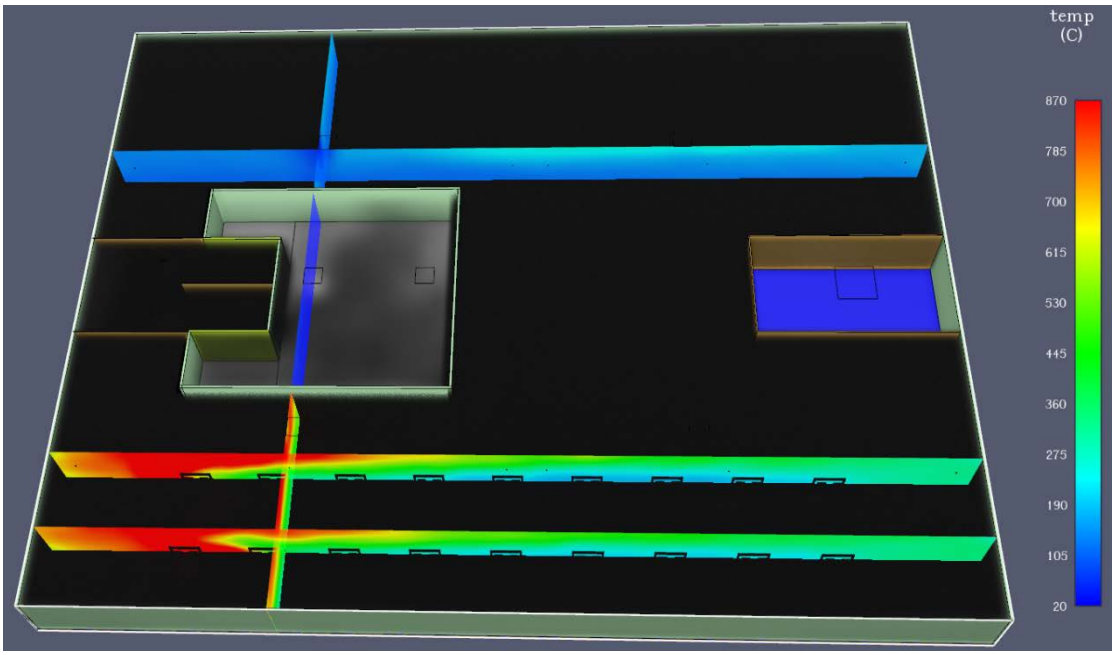


*Figure 82. 2D evolution of heat at 1,000 seconds.*

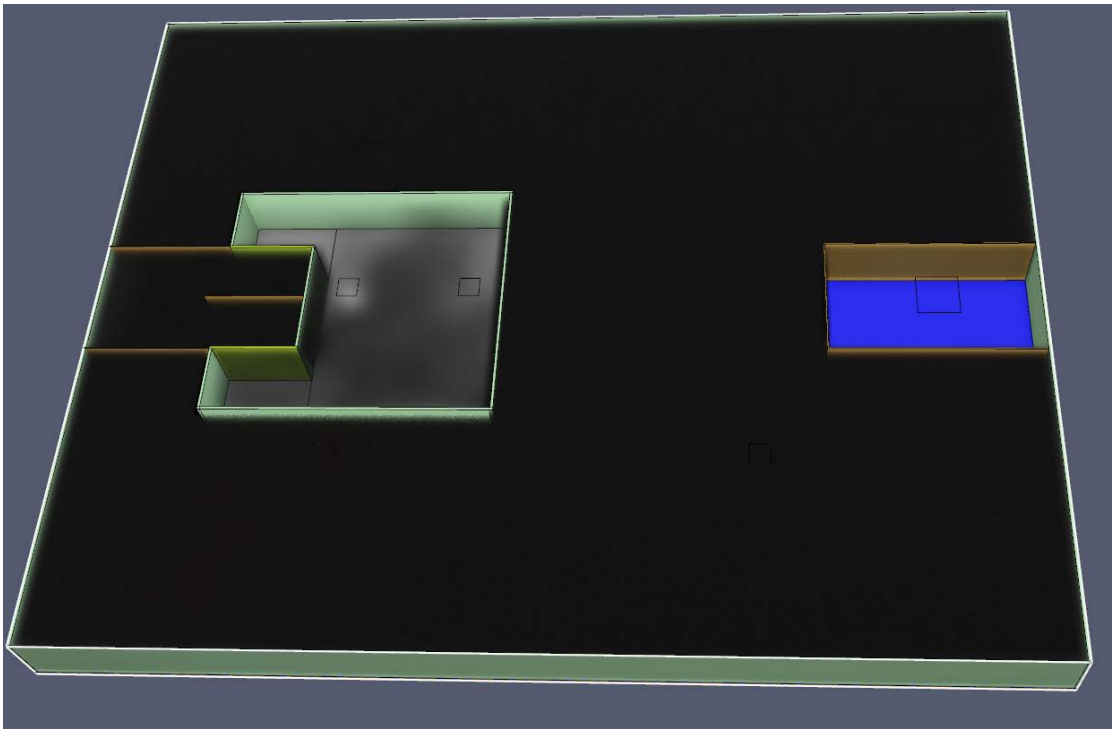

*Figure 83. Smoke development at 1,000 seconds.*

The flames have engulfed the whole aft starboard side of the geometry, when the HRR peaks in Figure 75 while the majority of the compartment is riddled with smoke. Figure 82 in particular presents the magnitudes of temperatures in various locations in the geometry at 1,000seconds. No heat “leak” was noted from the burning part of the geometry to the galley area, furtherly verifying the modelling aspect of the boundaries. The area around the fire experiences great temperatures, approximately 800$^{o}$C, which spans over the whole height of the enclosure, specifically on the aft starboard. As one moves towards the forward of the geometry the temperatures get lower, especially on the port of side of the geometry.

In other words, due to the size of the deck greater temperatures are noted around the fire as expected whereas smoke presents itself as the prime candidate for harming the occupants. This is furtherly substantiated through the examination 3D slices, presented in Figure 84 and Figure 85. Keep in mind that the colour scale of the 3D slides for the temperature is blue for low temperatures and red for high. In hindsight, the carpet should not have been modelled in blue colour. At 150 seconds there is no temperature increase which is attributed to the smouldering combustion of the carpet, whereas at 1,500 seconds high temperatures are developing and spreading considerably.

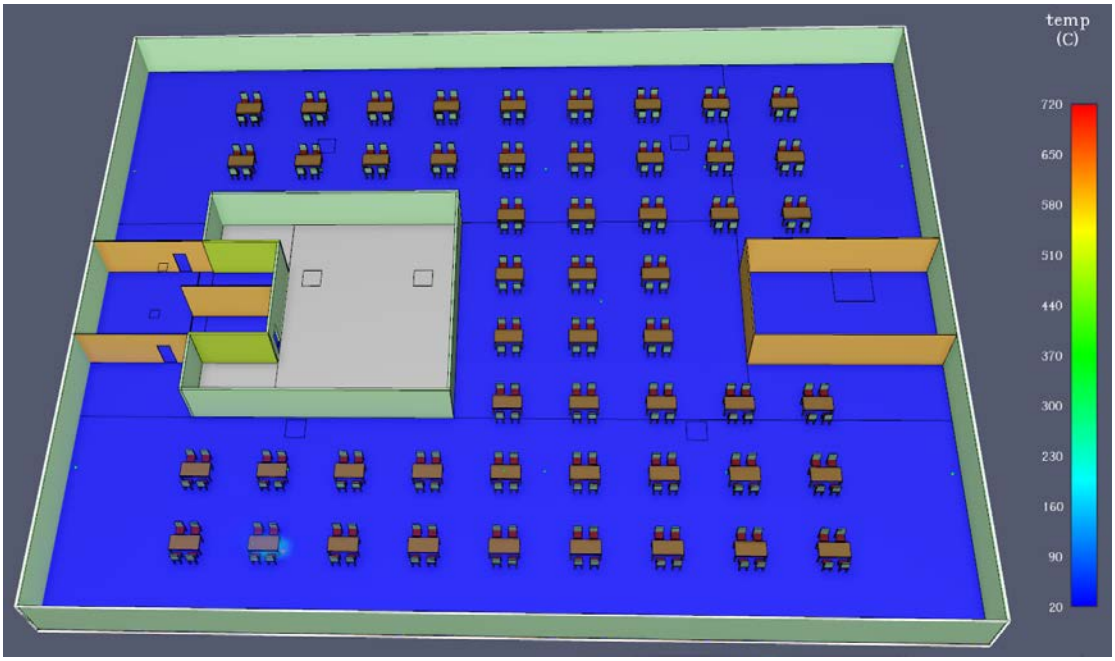


*Figure 84. 3D slice of temperature distribution at 150 seconds*

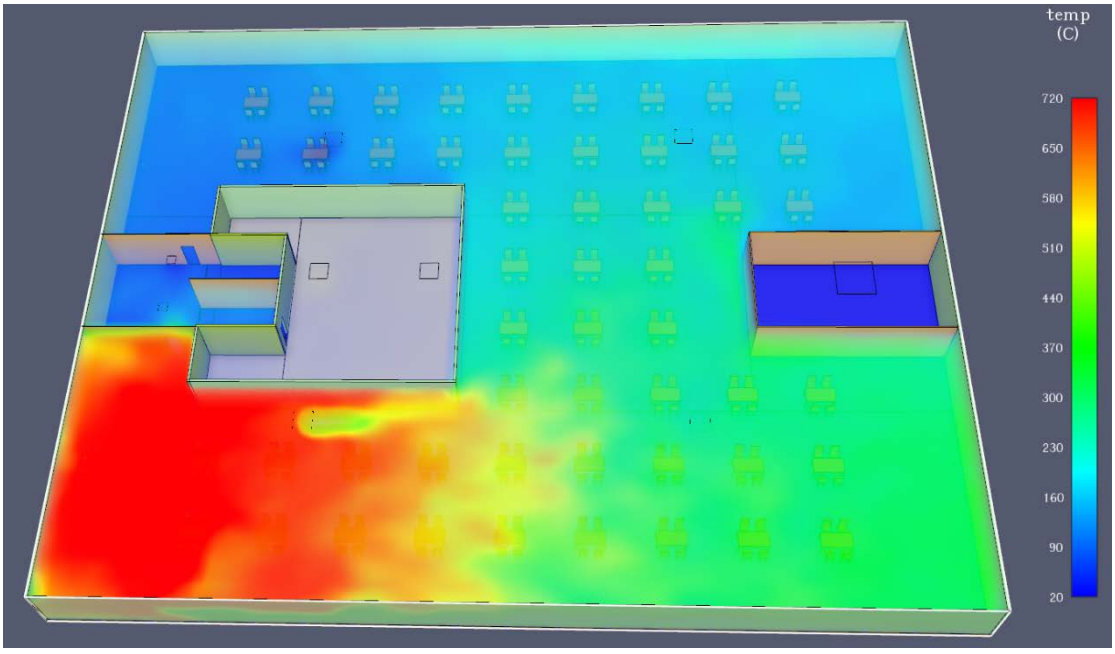


*Figure 85. 3D slice of temperature distribution at 1,000seconds*

The situation is furtherly appreciated through 3D visibility slices presented in Figure 86 and Figure 87. At 150 seconds the visibility around the fire ignition point is considerably hindered but well over 10 meters, whereas at 1,500 there is no visibility.

To assess the impact of the fire and the extent of smoke accumulation, devices to measure smoke layer height and visibility were strategically positioned within the cabin and at various points along the corridor. These can be found in the appendix, namely Appendix B3.

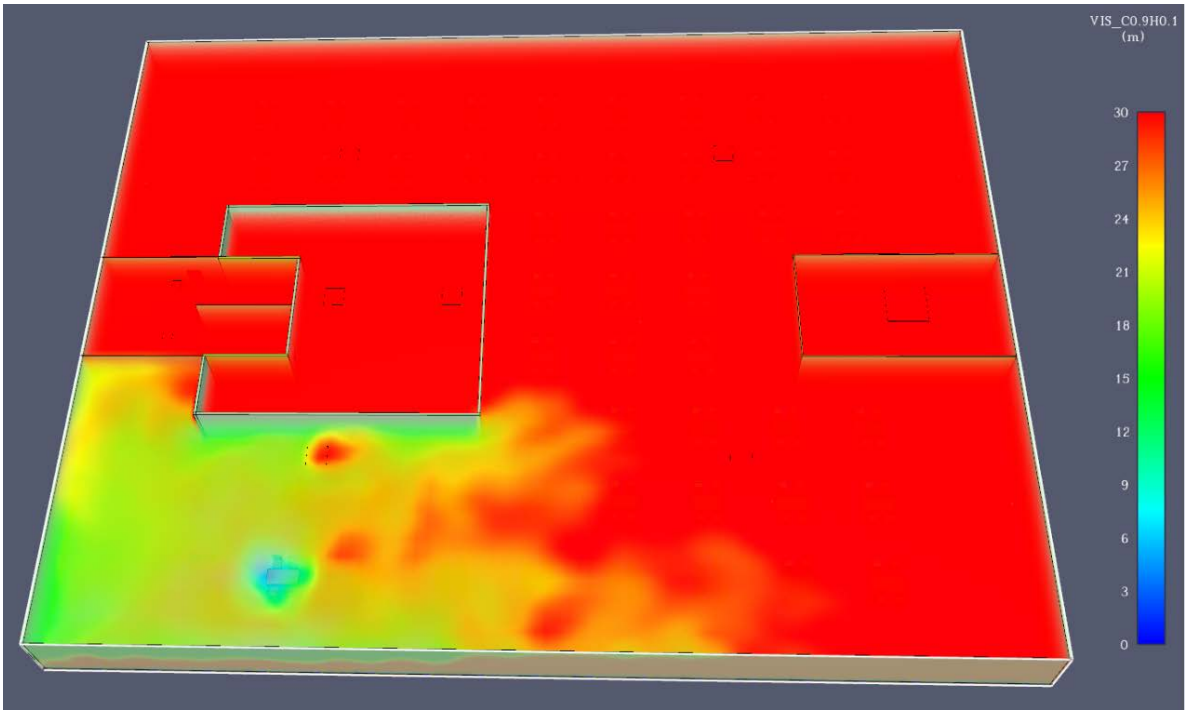


*Figure 86. 3D slice of visibility at 150 seconds*

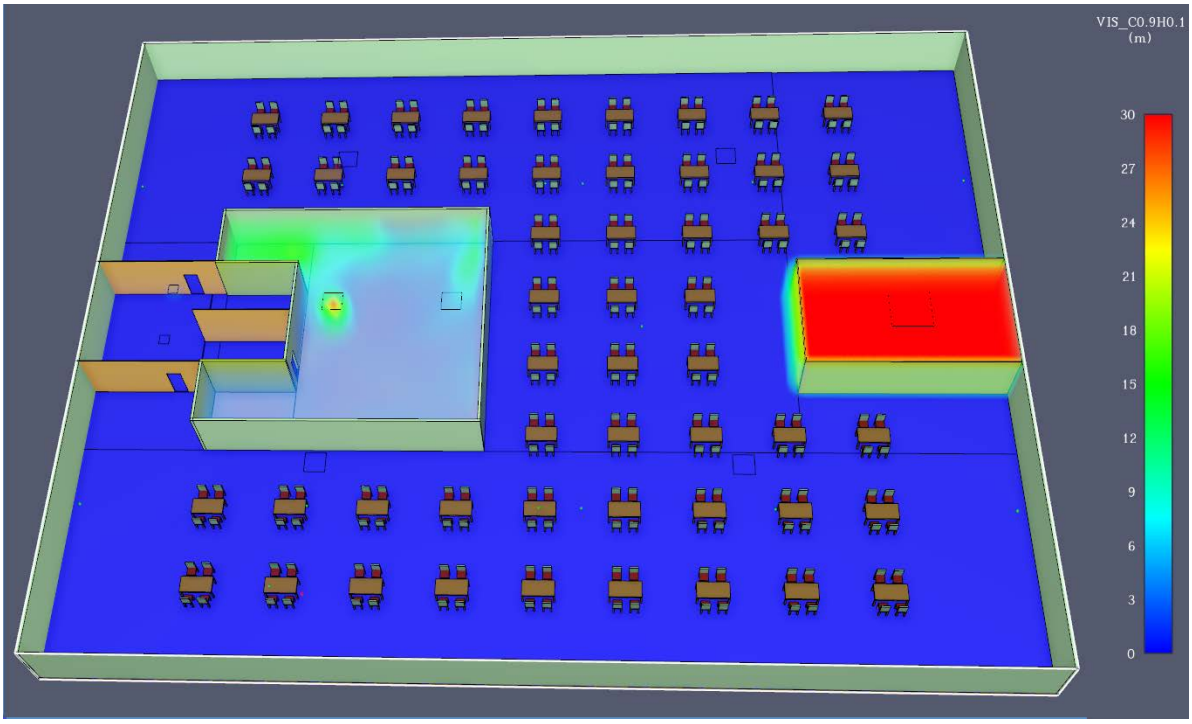


*Figure 87. 3D slice of visibility at 1,500 seconds*

Figure 88 presents the evolution of FED on the aft starboard side of the deck enclosure. It was evaluated through the device that at around 1,013 seconds, the hazards from the fire will surely incapacitate occupants, either by exposure to heat or smoke.

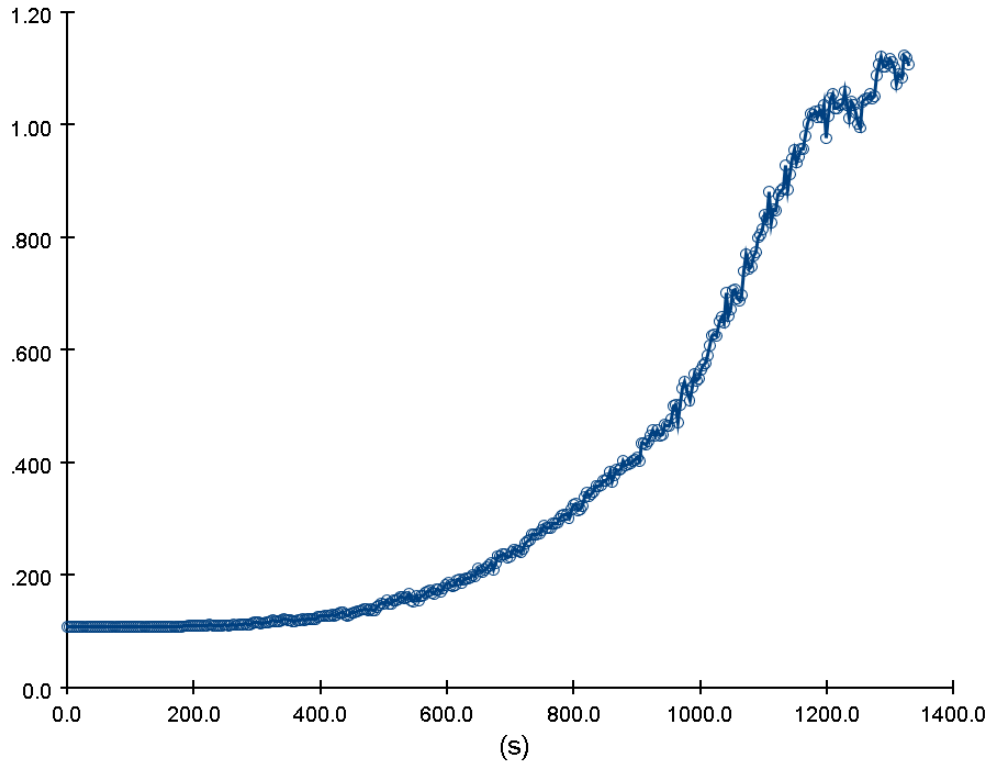


*Figure 88. FED of the large public space fire simulation without active fire-fighting.*

### 8.2.2. Large Public Space Fire Simulation with Active Firefighting

The simulation parameters remained the same, except for the activation of the sprinklers, which were set to activate at 68°C. The whole one hour was successfully simulated. Figure 89 presents the HRR of the simulation with sprinklers activated. Compared against the case with no active fire-fighting measures, the magnitude of the achieved HRR is considerably lower.

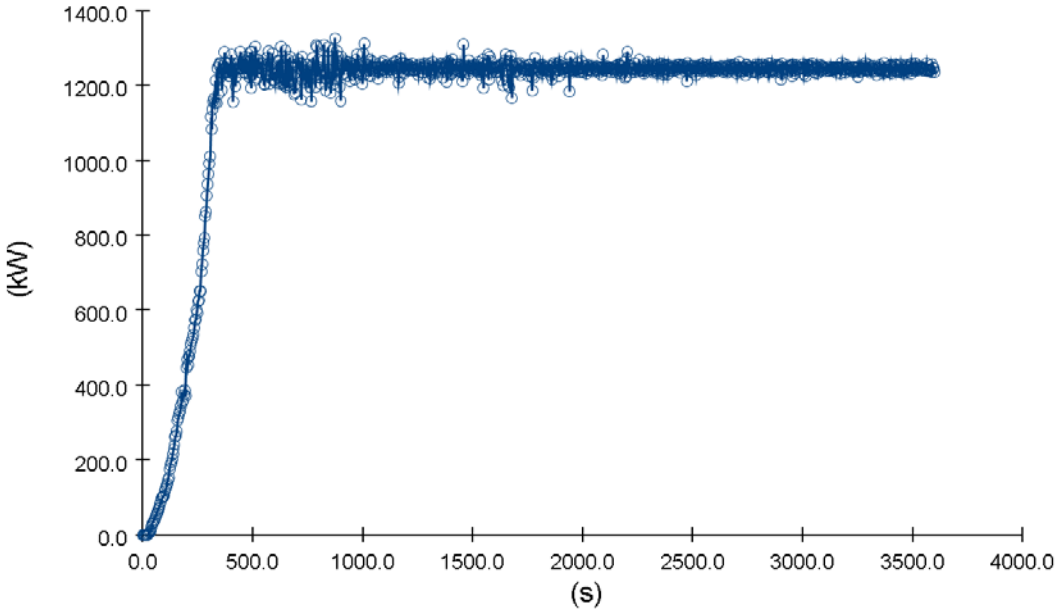


*Figure 89. Heat release rate of large public space with active firefighting.*

Specifically, the HRR reached in this simulation was around 1.3MW whereas in the case with no active firefighting measures, the magnitude reached rates of 6-7MW under a “fully developed” stage. The reduction in HRR was entirely attributed to the effect of sprinkler activation.

Figure 90 presents the smoke filling degree along with 2D temperature slices along the entire length of the starboard side. The specific time instance of presentation was due to the activation of the first sprinkler, which is clearly shown in Figure 90. Furthermore, the sprinklers were not grouped towards their activation. Therefore, these activated as dictated by the behaviour of the fire. The temperature around the fire origin noted on the activation instance was 170$^{o}$C, as per the thermocouple placed on the table adjacent to the point of origin. Considerably lower temperatures were noted further away from the fire.

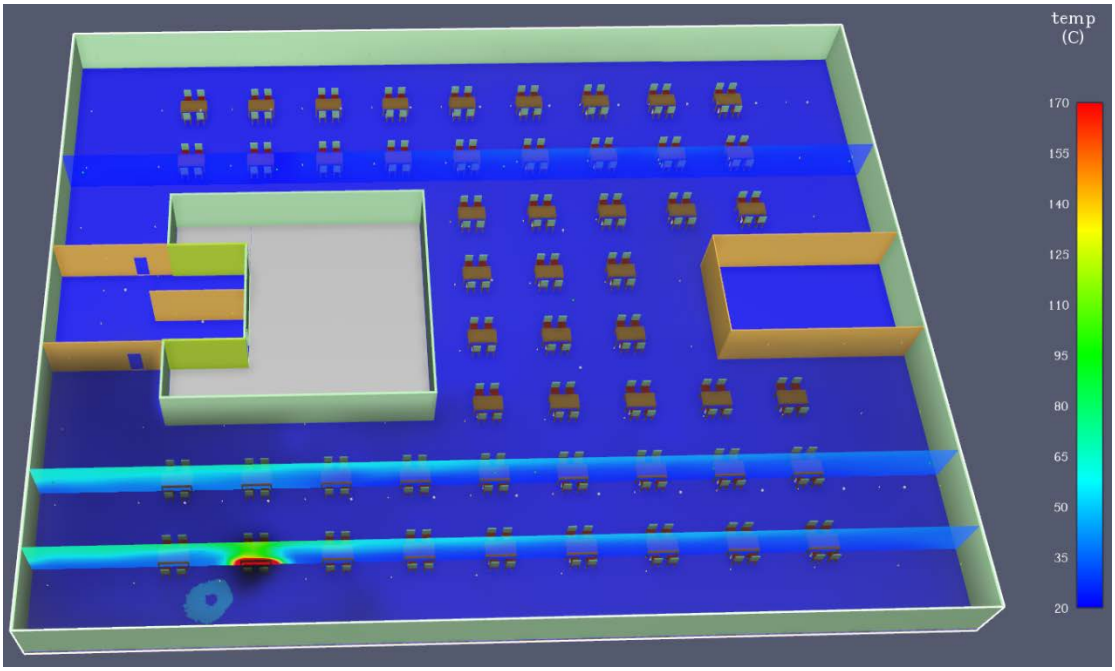


*Figure 90. Smoke filling along with 2D temperature slices on starboard side at 275 seconds.*

Figure 91 presents the smoke filling and various 2D temperature slices at the time instance of 600 seconds. Considerable amounts of smoke were generated at that time, that propagated to other parts of the geometry. Despite the smoke filling, the temperatures around the starboard side of the enclosure remain practically the same as those in Figure 90. Furthermore, additional sprinklers have automatically been activated which aid in keeping the temperatures as low as mentioned previously.

In terms of visibility, Figure 92 and Figure 93 present the visibility via a 3D slice spanning over the entire deck at 275 and 600 seconds respectively. At 275 seconds, the visibility around the point of fire origin is minimal whereas it is acceptable at other parts of the enclosure. In contrast to the aforementioned, at 600 seconds the aft and forward starboard sides are riddle with smoke with very low visibility whereas the port side seemed to be in a much better state visibility-wise.

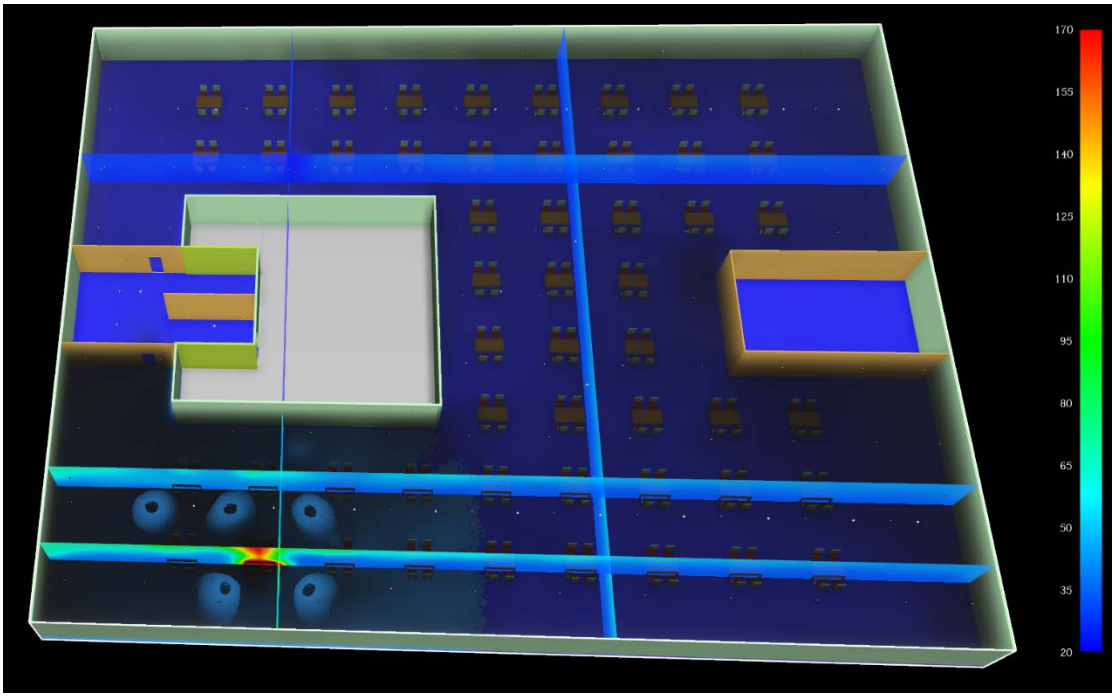


*Figure 91. Smoke filling and temperature 2D slices at 600 seconds.*

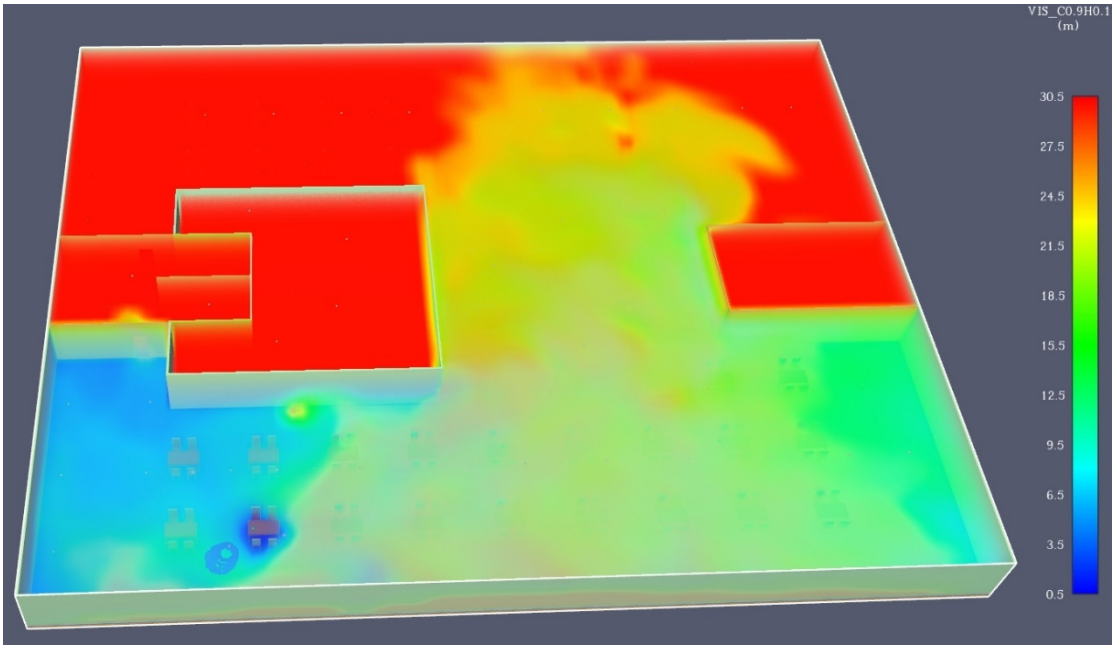


*Figure 92. 3D evolution of visibility at 275 seconds.*

The performance and contribution of the sprinklers can be comprehended through a comparison of the plots of the thermocouple, placed on the table adjacent to the ignition point, from this simulation, presented in Figure 94, against the one without sprinklers in Figure 76. In the simulation with active firefighting means the temperature of the FR plywood never reached its autoignition temperature of 600ºC, which means, that in this case, the sprinklers successfully hindered the development and growth of the fire from the carpet towards other objects.

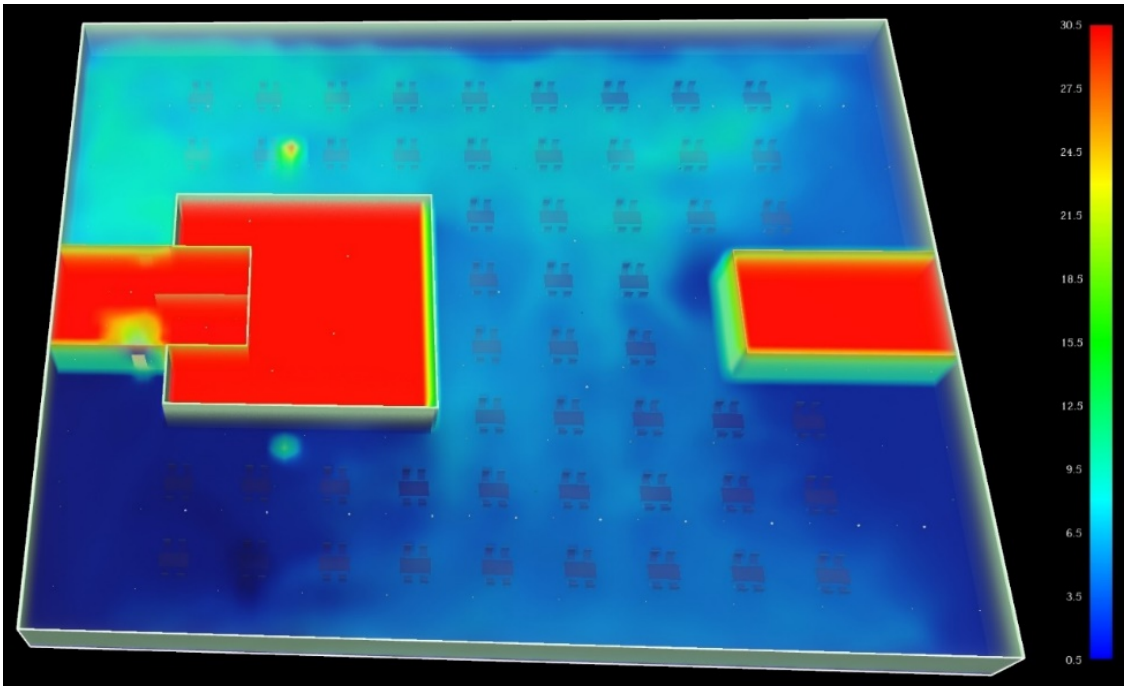


*Figure 93. 3D evolution of visibility at 600 seconds*

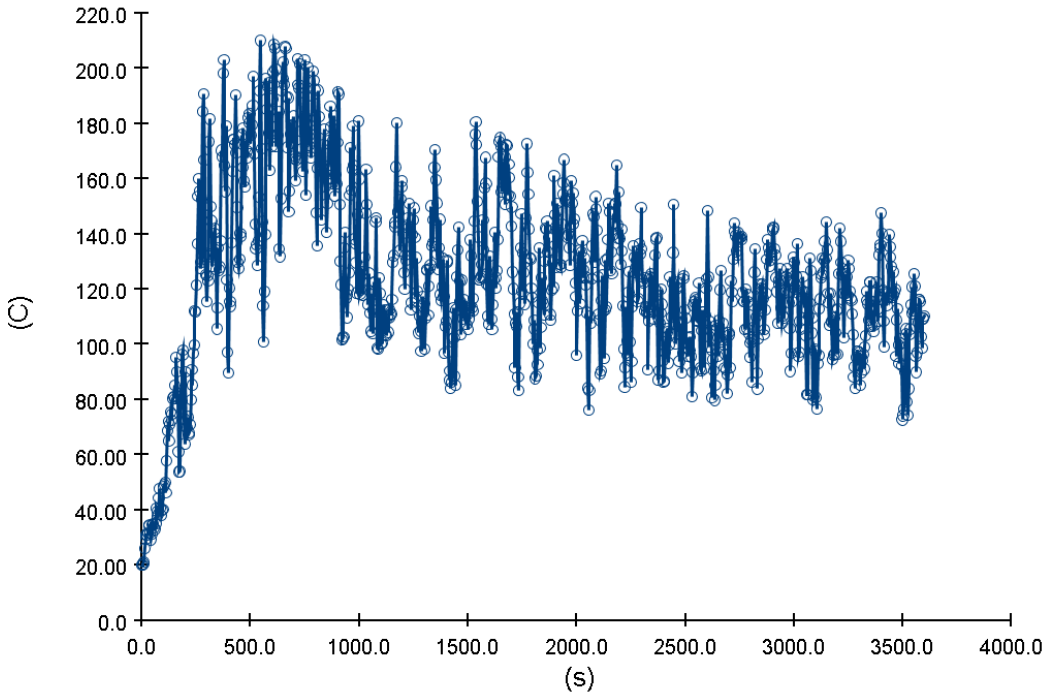


*Figure 94. Plot of thermocouple placed on table adjacent to the fire initiation point (with sprinklers).*

To assess the impact of the fire and the extent of smoke accumulation, devices to measure smoke layer height and visibility were strategically positioned within the cabin and at various points along the corridor. These can be found in the appendix, namely Appendix B4.

Concerning the FED of the scenario, the plot is presented in Figure 95. The FED value never reached a magnitude of 1, therefore, unless an occupants is very close to the fire, no incapacitation/fatalities are expected.

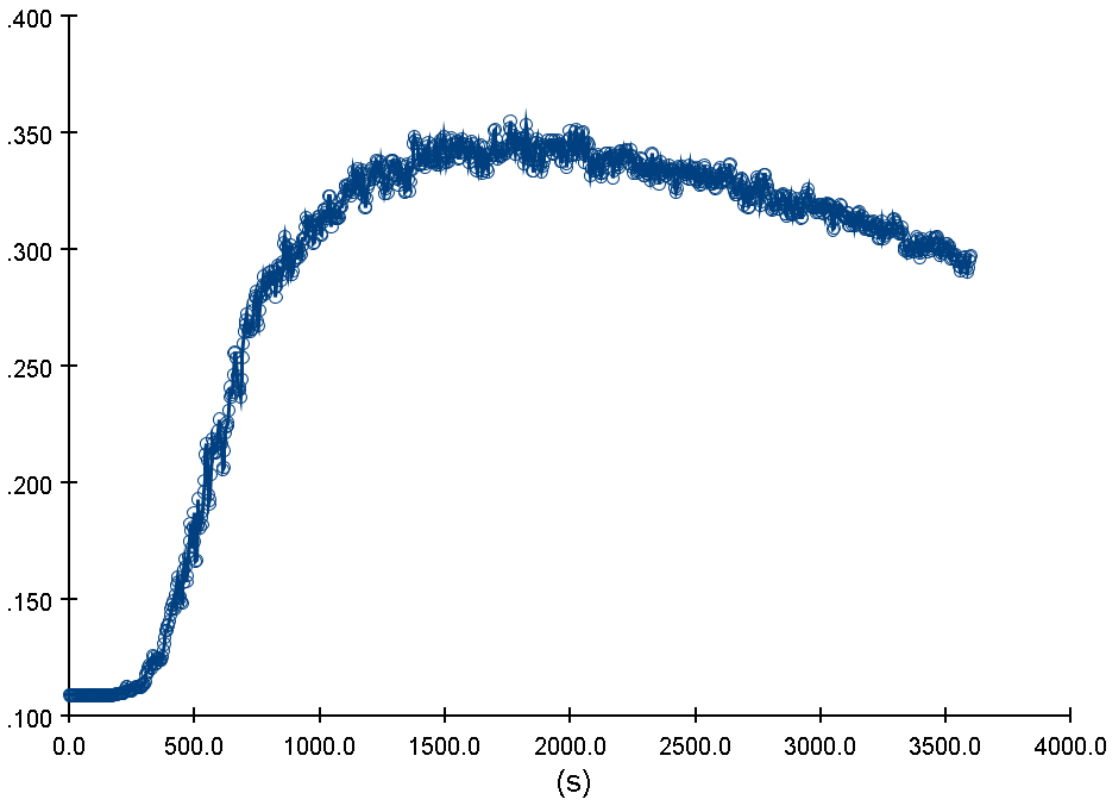


*Figure 95. FED of the large public space fire simulation with active fire-fighting.*

# 9. Engine Room Fire Simulation Case Study

## 9.1. Background

In the cabin and large space compartments a deterministic approach was employed utilising the thermophysical and pyrolysis parameters of real materials. Contrarily, for the engine room the available materials for combustion are paint, and cables. By utilising paint calculators that major providers offer, such as Jotun's "Technical Calculator (Jotun, n.d.), the amount of paint could be easily determined provided that enclosure dimensions are known, therefore, part of the combustible mass that is present could be calculated. On the other hand, explicit knowledge on the amount, location, and type of all cables available is rather laborious and, sometimes, impossible to obtain.

Provided that such information was available, a deterministic approach, as the one used for the cabin and large public space decks, would require precise fire safety and thermophysical data through TGA/DSC experiments. Since the vessel is fictitious while such experimental data is unavailable, a conventional design fire approach was sought.

Furthermore, the paint thickness is that of microns, cables consist of many layers of sheathing, insulators, etc., with circular shapes. In order to obtain useful simulation (output) data, except for the proper fire modelling, the mesh should be able to capture/reflect the geometry accordingly, which would result in an infinitesimal small mesh., which, in turn, would render the simulation obsolete with respect to the computational power and time that would be required for such an endeavour.

## 9.2. State-of-the-Art in Design Fires

In this section the current state of the art concerning shipborne design fires is provided while a case on why this cannot be utilised in a straightforward manner in engine room is made. The material within this section were employed during the construction of the engine room's design fire.

### 9.2.1. Heat Release Rate

The fire plume, the extent and movement of the hot and cold temperature layers are controlled to a great extent by the rate of energy release. A very fitting and common representation of this energy is the heat release rate (HRR) expressed in kW (Drysdale, 2011). Figure 96 presents a typical HRR curve including all stages of fire development, except that the ignition/stage has been merged with the growth.

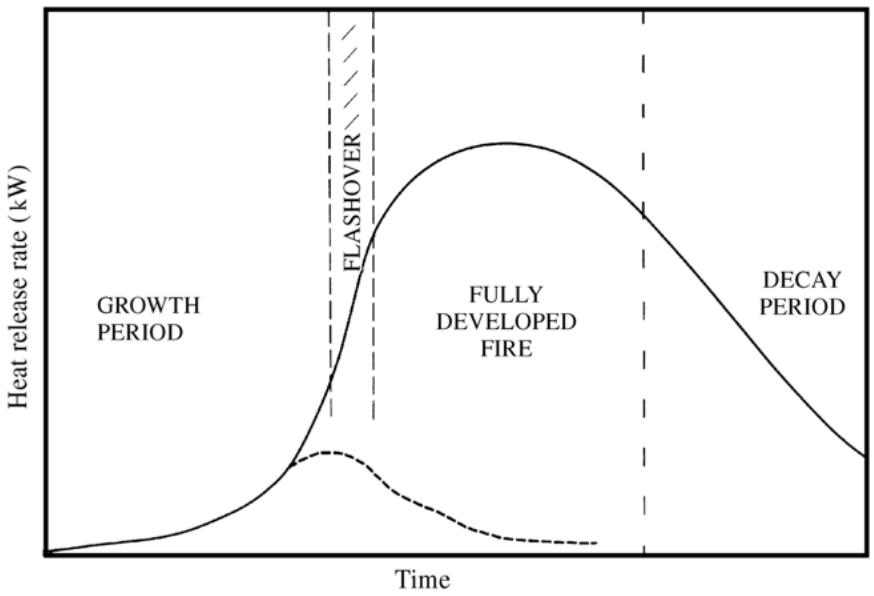


*Figure 96. Heat Release Rate curve. Source:* (Drysdale, 2011)

The mathematical representation of the growth of the HRR of an enclosure fire is, typically, represented by a t-squared ($t^2$) approach. The formulas are as per below (Themelis and Spyrou, 2012, 2010):

$$Q(t) = \begin{cases} \dot{Q}_{ign} \dfrac{t}{t_{ign}}, & 0 \le t \le t_0 (Incipient) \\ a\left(t - t_{ign}\right)^2 + \dot{Q}_{ign}, & t_0 \le t \le t_g (Growth) \\ \dot{Q}_{max}, & t_g \le t \le t_d (FullyDeveloped) \\ Q_{max}\, e^{\frac{t - t_d}{\tau}}, & t > t_d \ (Decay) \end{cases} \quad \text{Eq. 1}$$

where:
$\dot{Q}(t)$ : HRR (kW),
α : growth constant (kW/s$^2$),
τ : decay constant,
$\dot{Q}_{max/peak}$ : maximum HRR,
$t_{ign}$ : time of ignition stage (sec),
$t_d$ : time of decay stage (sec)

The incipient/ignition stage is when the fire begins to develop. At this stage the intensity of the HRR is lesser compared to other stages. Despite that, it is extremely significant for human occupant safety as during the incipient stage smouldering combustion is usually taking place, which produces the majority of the toxic effluents and smoke (Hurley et al., 2016).

Provided that sufficient oxygen exists in the compartment, the fire will grow, involving greater extends of the combustible mass within. Usually, the growth depends on the

available fuel. If there is adequate oxygen in the compartment than the fire is termed as fuel-surface controlled (Drysdale, 2011; Hurley et al., 2016). If not, then the burning is directed by the available oxygen, termed as ventilation-controlled.

The growth stage of a fire is usually considered to be that of a squared function, in the fashion of $Q = \alpha t^2$ (Hurley et al., 2016). It is, also, common to assume that initiation of the growth stage ensues at a HRR value greater than 1,055kW (Karlsson and Quintiere, 2000). A classification of various growth rates along with relevant times to reach the criterion of 1,055kW is presented in Table 17.

*Table 17. Categories of t-squared fires from BS-ISO.*

| Description | Design Fire Scenario | α ($kW/s^2$) | Required time ($t_0$, sec) to reach 1,055kW i |
|---|---|---|---|
| Slow | Floor coverings | 0.00293 | 600 |
| Medium | Shop counters, office furniture | 0.01172 | 300 |
| Fast | Bedding, displays and padded workstation portioning | 0.0469 | 150 |
| Ultrafast | Upholstered furniture and stacked furniture near combustible linings, lightweight furnishings, packing material in rubbish pile, non-fire-retardant plastic foam storage, cardboard of plastic boxes in vertical storage arrangement | 0.1876 | 75 |

Examination of the table reveals that this scheme has been statistically and experimentally (fire tests) derived for residential purposes. Needless to say, that such studies do not exist for ships, hence, ship fire safety engineers commonly use this in lack of a suitable alternative.

Flashover is the phenomenon under which there is a total involvement of the fuel in the fire, also termed as spreadover (Hurley et al., 2016). Usually, following a flashover, a fire is termed as fully developed and that is where the majority of the heat is expected.

Decay follows the flashover/fully developed fire, due to the fact that the majority of combustible mass has already been involved in the fire and the available oxygen is limited due to continuous combustion, where the fire is ventilation-controlled. A common assumption for the initiation of the decay phase is when 70-80% of the combustible mass has been “consumed” (Karlsson and Quintiere, 2000).

### 9.2.1. Burning of Solids and Liquids

The HRR can be expressed as the mass flow rate of the (fuel) vapours, and the effective heat of combustion as follows:

$$HRR = \dot{m}\ \chi\ \Delta Hc \qquad \text{Eq. 2}$$

where:

$\dot{m}$ : mass flow rate of fuel vapours (kg/sec)
X : combustion efficiency
$\Delta H_c$ : heat of combustion of the generated volatiles (kJ/kg).

This equation, although very basic, can be used in the absence of fire data for real objects and materials as a starting point. Furthermore, the mass flow rate of the vapours is usually termed as the burning rate of a fire (Tewarson, 1982).

### 9.2.2. Pool Fires

Through experiments conducted in (Alpert, 2002), the mass flux $\dot{m}''$was considered as more fitting for the burning rate, expressed as (Alpert, 2002; Babrauskas, n.d.; Hall A.R., 1973):

$$\dot{m}'' = \frac{\rho_l\ R\ 10^{-3}}{60} \qquad \text{Eq. 3}$$

where:

$\dot{m}''$ : mass flux of fuel vapours (kg/m$^2$ sec)
$\rho_l$ : is the density of the liquid (kg/m3), and
R : regression rate of burning (mm/min)

Consequently, this expression can be used in Eq.2 to estimate the HRR of a pool fire.

### 9.2.3. Flashover - Ventilation-Controlled

Flashover is commonly expected when the enclosure temperature reaches 500-600$^o$C and requires adequate oxygen for the fire to be fuel-surface controlled. The latter and, in turn, the flashover are ultimately dictated by the openings of the enclosure, termed as the ventilation factor.

The rate of flow of air into an opening, termed as the ventilation factor, is:

$$\dot{m} = 0.5\ A_0\ \sqrt{H_0}, \qquad \text{Eq. 4}$$

where $A_0$ :area of opening, and
$H_0$ : height of the opening.

The maximum amount of fuel that can be burned completely through the ventilation factor is termed as the stoichiometric amount. McCaffrey, through experiments, noted that for most fuels the heat released per unit mass of air is around 3MJ/kg of air (Themelis and Spyrou, 2012, 2010).

Therefore, the stoichiometric HRR is:

$$\dot{Q_{stoich}} = 1{,}500\ A_0\ \sqrt{H_0} \qquad \text{Eq. 5}$$

Other definitions of McCaffrey are as follows:

$$\dot{Q} = 610(h_k A_T A_0 \sqrt{H_0})^{1/2}, \qquad \text{Eq. 6}$$

or

$$\dot{Q} = 620(h_k A_T A_0 \sqrt{H_0})^{1/2} \qquad \text{Eq. 7}$$

where:

$h_k$ : effective heat transfer coefficient (kW/m$^2$K), and
$A_T$ : floor/enclosure area (m$^2$)

Thomas proposed his own formula for flashover occurrence considering that the flashover criterion requires an upper layer temperature of 577ºC:

$$\dot{Q}_{flashover} = 7.8\ A_T + 378 A_0 \sqrt{H_0} \qquad \text{Eq. 8}$$

### 9.2.4. Flashover - Fuel-Surface Controlled

In order to derive the peak HRR of a fuel surface-controlled fire, prior knowledge on the rates of every material present in the geometry must be existing. This means that for every item in an enclosure, fire calorimeter tests are required (Hopkin et al., 2019). Provided that these exist, then an engineer would simply add up all the HRRs, assuming that all fuels reach their peak HRR simultaneously.

### 9.2.5. Decay

After a fully developed fire, the HRR decreases with time. In theory, as in the fuel-surface controlled HRR, the decay of the fire should be determined by analysing fire tests of the items in the enclosure. As the absence of such data is very common, alternatives are employed.

A common metric for the onset of the decay stage is that the 80% of the fire load has been consumed (Staffansson, 2010).

The energy that can be released from a fire is (Staffansson, 2010):

$$E = \int_{t_i}^{t_j} \dot{Q(t)}\, dt \qquad \text{Eq. 9}$$

where $t_i$ and $t_j$ correspond to the initiation and termination times respectively.

The energy that can be released is expressed as:

$$E = 13{,}100\, V\, (0.23 - 0.10)\rho_{air} \qquad \text{Eq. 10}$$

where $\rho_{air}$ : density of the air, and
V : volume of the compartment.

The decay expression of the HRR in can also be expressed as:

$$\dot{Q}(t) = \alpha_{decay}(t_{decay} - t)^2 \qquad \text{Eq. 11}$$

where $\alpha_{decay}$ :exponential decay rate coefficient
$t_{decay}$ :time when decay begins
t :time instance

Additionally, the three distinct stages of the fire in Figure 96 can be expressed in terms of the energy released on each stage. Namely, $E_1$ for the initiation/growth, $E_2$ for the fully developed and $E_3$ for the decay. These are calculated from the integration of the energy formula and are cited hereunder:

$$E_1 = \frac{\alpha(t_g)^3}{3} \qquad \text{Eq. 12}$$

$$E_2 = Q_{peak}(\dot{t_{max}} - t_g) \qquad \text{Eq. 13}$$

$$E_3 = a_d(\frac{{t_d}^3}{3} - \frac{{t_{max}}^3}{3}) \text{ or} \qquad \text{Eq. 14}$$

$$E_3 = \frac{\dot{Q_{peak}}(t_d - t_{max})}{2} \qquad \text{Eq. 15}$$

where $t_{max}$ : time when the fire goes out, and
$Q_{peak}$ : peak HRR.

The decay stage has two expressions in lieu of experimental data. Specifically, the two expressions for E3 are equalled in order to derive the decay coefficient $\alpha_d$.

### 9.2.6. Fire Load (Q)

The combustible mass itself, is often expressed as the Fire Load (Q), a measure of the energy (MJ) that can be released provided that all combustible mass present has ignited (perfect combustion).

The fire load is usually expressed as the Fire Load Density (Q'') which is the total fire load per unit area of the enclosure, measured in ($J/m^2$).

The Fire Load Density formula is:

$$Q = \frac{\sum m_i \times h_i}{A_f}, \quad \text{Eq. 16}$$

where:
$m_i$ :mass of the $i^{th}$ item (kg),
$h_i$ :calorific value of the $i^{th}$ item (kJ/kg), and
$A_f$ : floor/enclosure area ($m^2$).

Depending on the dimensions of an enclosure, fire engineers may use the total enclosure area instead of the floor one. This is usually performed for large enclosures, especially concerning the height, which in turn, influences the position of the smoke layers, which affects the occupants (Hurley et al., 2016).

Moreover, another way to express the Fire Load Density (Q'') is via a representation in terms of the total mass of combustible materials, termed as Fuel Load Density (FLD):

$$FLD = Q\frac{\sum m_i}{A_f} \quad \text{Eq. 17}$$

Consequently, the Fire Load Density can be expressed as (Themelis and Spyrou, 2012, 2010):

$$Q'' = FLD \sum \frac{m_i}{M} h_i \quad \text{Eq. 18}$$

where:

M is the total mass of combustible materials (kg) present in the enclosure/scenario.

### 9.2.7. Limitations Towards Engine Room Simulation

Due to the absence of fire engineering test data, the parameters affecting the shape and magnitude of the HRR are usually treated in a probabilistic manner. Statistical distributions are defined, or assumed, for the fire growth coefficient α, fuel area $A_f$, ventilation factors, so on and so forth, in order to derive sets of HRR curves. This is usually performed to evaluate possible designs, especially regarding goal-based designs.

Prime examples of probabilistic approaches are presented in project FIREPROOF (FIREPROOF consortium, 2010), and the relevant scientific papers emanating from it

(George et al., 2012; Themelis et al., 2011; Themelis and Spyrou, 2012, 2010), as well as via VTT's Probabilistic Fire Simulator through project SURSHIP-FIRE (Hakkarainen et al., 2009; Hostikka et al., n.d.; Hostikka and Keski-Rahkonen, 2003).

These studies share a common characteristic in that their methodologies have been applied to scenarios involving specific applications, usually of residential or industrial nature where extensive past research on the parameters exists, including full size fire tests. Consequently, indicative values, limits, and corresponding distributions derived from available data were relied upon.

Concerning objects that are usually found in ship engine rooms, no studies and/or publicly available experiments, for example within the efforts of EU FP7 research programmes, are available as these only pertain to the maritime or oil and gas industries. It is to be expected as full-scale tests are laborious and rather expensive to conduct (Arvidson et al., n.d.). Therefore, data fitting approaches have been commonly employed due to the lack of dedicated studies or experiments conducted specifically for ship engine rooms. The unique characteristics of each ship, including its layout, machinery, and materials used, coupled with the laborious and costly nature of full-scale tests, have hindered comprehensive research in this domain.

An illustrative example showcasing the reliance on available fire engineering data is the growth rate parameter, denoted as α, presented in Table 17. Despite its derivation from residential settings, fire safety engineers universally adopt these values as no viable alternative exists, apart from utilizing calorimeter data.

### 9.3. Scenarios

Due to the historical contribution of leaked flammable oil creating engine room fires, a relevant scenario was sought. The fire originates from a fuel oil leak from one of the two engines within the MVZ of investigation. Fuel oil leak originated from a hypothetical leak from the common rail, comes into contact with a hotspot on the engine and immediately ignites. The heat from the fire pyrolyzes the engine/room equipment/material which in turn give off flammable vapours that will ignite due to the flaming combustion of the fuel oil.

Figure 97 presents the fictitious general arrangement of engine room decks No.1-3, within MVZ No.5, that were considered in the simulation. Decks number one to three were modelled as the engines compartment spans over these. The red box indicates the aforementioned for ease of reference.

The pool ignites the port engine (v-type), which will successfully ignite the other engine and the generators via radiation, presented in Figure 98.

Contrastly to living spaces, in service spaces inlet fans (HVAC) can be switched off to either control the fire by starvation or control its spread by trying to alter it from a fuel-surface to a ventilation-controlled fire. To that effect, the following scenarios were simulated:

1. No sprinklers,
2. No sprinklers and control logic to switch off inlet fans when a smoke detector activates, and
3. Sprinklers (automatic).

The simulation time for all aforementioned scenarios was set to reflect the duration of the fire until decay ensues,

### 9.4. Engine Room Design Fire Approach

Initially, the concept was to use the pyrolysis approach, but due to regulatory and fire engineering limitations expressed previously this could not be achieved. Instead, the scenario involved the generation of a design fire HRR curve by considering the contribution of only the paint in the engine compartment/enclosure.

To that effect, the equations representing each stage of a design fire along with those describing the total and intermediate stage energy, cited previously within this case study were utilised towards the construction of a HRR curve consisting of an incipient/initiation, flashover, and decay stages, while assumptions were absolutely required.

In terms of the incipient stage, the jet leak manner that the fuel oil would hypothetically adhere to, following a leak from the common rail, which houses fuel oil in a pressure excessive of 1,000 bar, cannot be modelled in FDS.

Therefore, a fuel oil pool representing the amount of fuel oil leak was modelled. In terms of fire development and toxic effluents, this approach does not affect the simulation in any way. Conventional fire representation in FDS is usually via burners, which represent the whole fire load, therefore, the assumption of an oil pool fire via a burner is valid.

The maximum allowable fire load, combustible material, is limited to 45kg/$m^2$ as per (IMO, 2001b). Therefore, this acts as input for the calculation of the available fire load and fuel load distributions (FLD) via eq. 16, 17 and 18. Concerning the rubber seething of the cables in the engine room enclosure, the most common material that those are made out of is rubber. On the other hand, marine paints are largely based on epoxy. A primer and topcoat approach are usually used for ships, while the enclosure dimensions are known and, therefore, the available weight of paint was ascertained as such.

An assessment of the calorific values of these revealed that epoxy has a much higher calorific value than rubber (Hurley et al., 2016), while there is not data concerning the quantities of rubber sheathing within such enclosures. In order to overcome the lack of data necessary for the calculation of mass of the rubber in equation 16, the simplified equation 18 was utilised while the calorific value of the epoxy paint was used. Since the maximum allowable combustible material is limited, such as assumption, in fact, overestimates the FLD and was therefore considered to be valid.

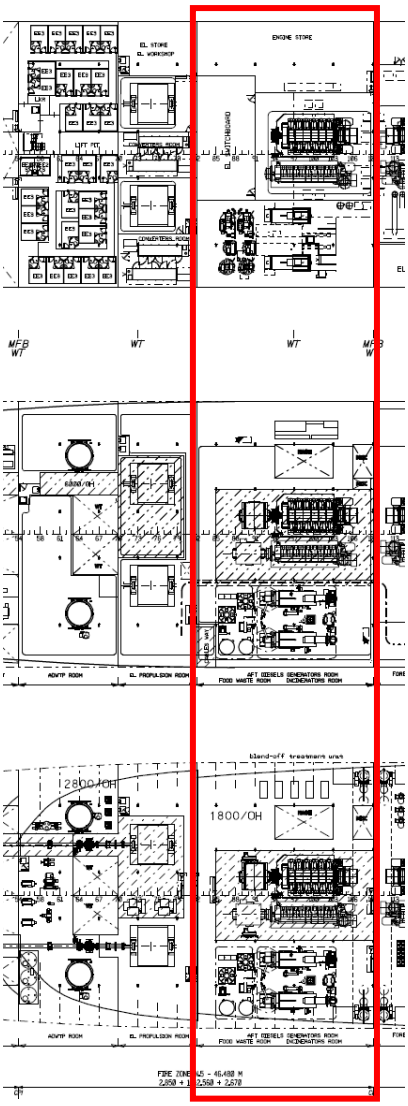

*Figure 97.MVZ No.5 Engine Room Decks 1-3*

The flash-over criterion from equation 8, could then be used to ascertain the necessary fire energy (kW) required for it to occur. Furthermore, the state-of-the-art methodologies utilise probability distributions in order to evaluate ventilation openings and their effects on the fire, but these are not necessary as the geometry of the enclosure is known and these can be calculated explicitly via equation 4. The ventilation-controlled flashover is then derived via equation 5.

Provided that fire test data were available for all fuel packages in the enclosure, the fuel-surface controlled flashover HRR could be potentially calculated and the lowest of the two to be considered as the peak HRR $Q_{peak}$. In absence of such data, the ventilation-controlled HRR was utilised.

The HRR for the fully developed fire was modelled via successful ignition of the paint from different machinery, while successful ignited item's HRR was superpositioned on the previous one, having in mind the spatial arrangement of the engines and generator units (serving as fuel packages). Equation 10 was then employed to calculate the fire energy (kW) resulting from the successful ignition of those. Then, by using the

common formula $Q = at^2$, the time to ignite each item was calculated, which was used to construct the time instances of the ignition of each fuel package.

The fire growth rate (α) for household or other common items is widely known. Engine room machinery are not included in the commonly used databases. For this purpose, an independent fire expert surveyor (with experience in engine room fires) was interviewed. The surveyor was questioned about the fashion of the fire growth rates that are expected from their experience against the ones cited in Table 17.

Reportedly, a growth rate between medium and fast was anticipated. due to the uncertainty pertained, the growth rate was treated probabilistically. Monte Carlo simulations were conducted for each successive item that was ignited, which follows the state-of-the-art procedures cited earlier. Uniform distributions were utilised (Salem, 2016; Themelis and Spyrou, 2012, 2010), having as upper and lower limits the aforementioned growth rates. Out of 1,000 iterations for each item, the 95$^{th}$ percentile was chosen.

Finally, in order to model the decay phase of the engine room design fire, the FLD was utilised along with the fire energy (J) equations.

It must be noted that the decay stage is not necessary for the context of FDS, as extinguishing is not modelled as such, but is of outmost importance with respect to the completeness of the design fire.

#### 9.4.1. Geometry

The top view of the engine room geometry, decks one to three in Figure 52, modelled in Pyrosim is presented in Figure 98. Figure 99 presents a profile view from the starboard. The two engines along with their respective generators are in yellow colour.

Since the fire was modelled via a burner, there was no need to model machinery outside of the room that the engines are contained, while the fire boundaries, namely A-60 since it is a service space, were modelled since prior information had been obtained due to other simulations conducted for the purposes of the risk model. Furthermore, as a deterministic approach was not employed, all surfaces, except for the fire boundaries, were modelled as inert.

The red parallelograms in Figure 117 indicates the location of the oil pool. Furthermore, and mentioned in the methodology of this case study, only the room containing the two engines was considered in the design fire. The red parallelogram in Figure 118 denotes the simulation domain, which was limited from the forwards extents of the decks up to the corridor outside the room with the engines. This decision was taken in order to evaluate the effects of the fire not only in the engines' room but also in the corridor right outside of it, providing tenability data to the MVZ fire risk model in terms of evacuation.

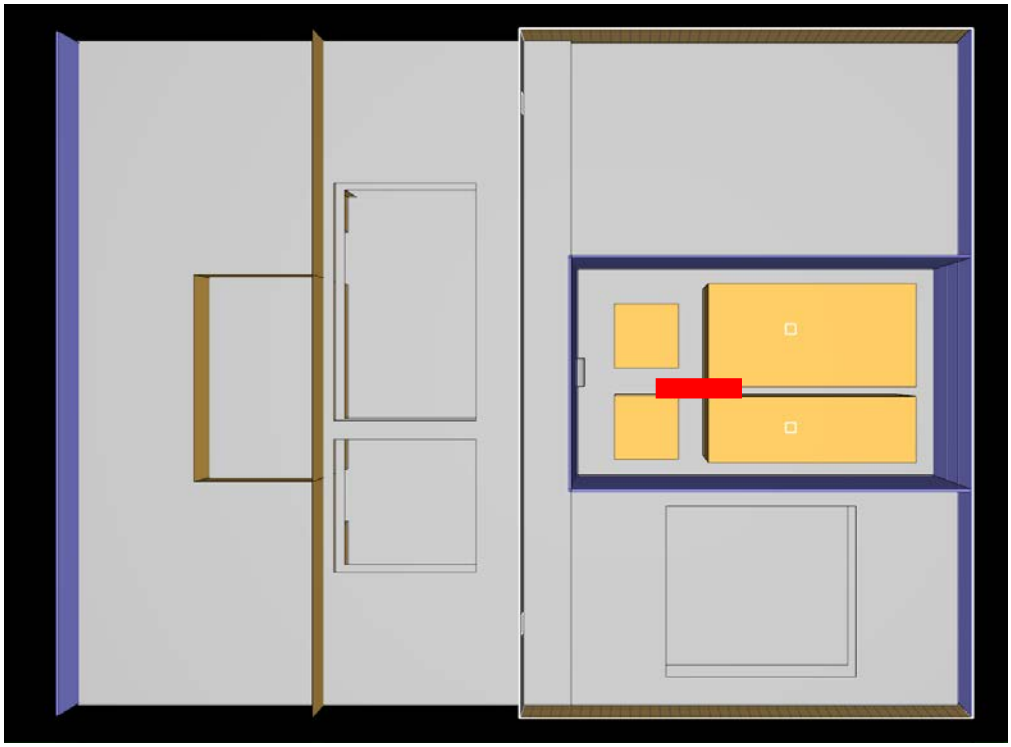

*Figure 98. Top view of engine room in Pyrosim, oil pool indicated by red parallelogram*

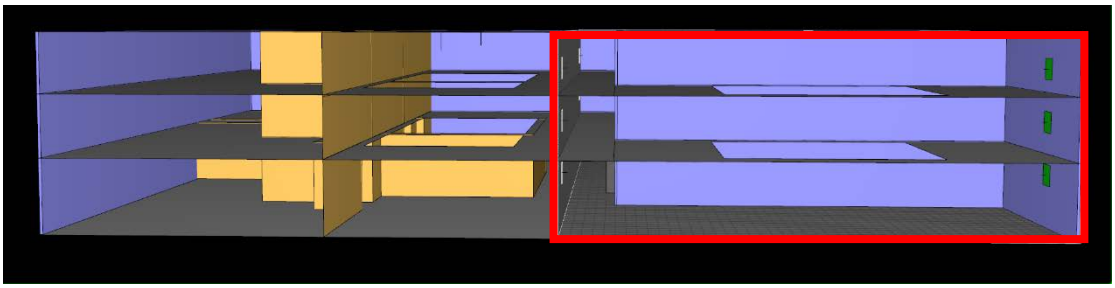

*Figure 99. Starboard profile view of engine room decks No.1-3 in Pyrosim*

### 9.4.2. Ventilation Characteristics

The ventilation characteristics for the both the engines' room and the corridor portion, were identified from SOLAS, being service spaces. Specifically, air charges per hour were identified and pertinent inlet and outlet ventilation outlets were modelled in Pyrosim in way of inlet/outlet vents. Concerning the room containing the engines, the inlet vents were modelled as close to the engine air manifolds, the turbocharger suction ports, as possible as required by engine makers (Wärtsilä, 2007).The HVAC module was not employed as the HVAC plans for the decks, including smoke extraction strategy, were not available.

### 9.4.3. Detection and Firefighting/Suppression Systems

The appropriate quantity and spacing of smoke detectors as well as sprinklers were identified for both rooms of interest. The smoke detectors were installed on both the ceiling and at intermediate heights around the engine openings, keeping in mind that the domain spans over three decks. The same philosophy was utilised towards the sprinklers.

#### 9.4.4. Post-processing devices

Appropriate post-processing devices were allocated throughout the geometry. Specifically, 3D slices for temperature and visibility were placed in the engine compartment, whilst 2D slices were placed on both x and y directions to monitor quantities such as temperatures, visibility, and smoke velocity.

Moreover, since the A-60 boundaries have been modelled thermal radiation devices were placed strategically around, and on the outside, of the engine compartment. This was performed to measure heat fluxes that were assumed to be required for successful ignition of fuel packages.

### 9.5. Design Fire

#### 9.5.1. Leaked Fuel Oil Calculation

The common rail dimensions, its operating principles, and respective pressure were taken from a V-type engine from Wärtsilä (Wärtsilä, 2007), namely the same engine used for the first case of this thesis in Chapter 5.

This information, coupled with the historical leak size and frequency, acted as input for the derivation of the amount of oil that could be leaked. This was realised through DNV's Process Equipment Leak Frequency data (Det Norske Vertias (DNV), n.d.). The most historically frequent leak size for pressure vessels as such, was identified as 1-3mm. For this case study, the average value of 2mm was selected.

The leak flowrate of this size is given by (Det Norske Vertias (DNV), n.d.):

$$Q_L = 2.1 \times 10^{-4} \times d^2 \times \sqrt{(\rho_L P_L)} \qquad \text{Eq. 19}$$

where:

d : leak hole diameter,
$\rho_L$ : density of leaked substance (HFO in this case), and
$P_L$ : pressure of the common rail (1,000 bar)

The leak flow rate resulting from a 2mm hole in the common rail was calculated as 0.83kg/sec.

#### 9.5.2. Oil Pool Thickness and Initiation Stage HRR

An assumption was made that the engine's/engine room's control system requires 10 seconds to realise that a leak is taking place. Furthermore, it was also assumed that the safety system stopped the engine and the fuel pumps which, in turn, stopped the leak. Furthermore, the amount of fuel oil contained within the piping itself that could potentially vent to the ambient, and furtherly increase the fire load of the incipient stage was neglected as no prior information was available.

Within these 10 seconds, 8.3kg of HFO were hypothetically leaked.

The definition of an oil pool requires that it has a maximum thickness of 5mm(Drysdale, 2011; Karlsson and Quintiere, 2000; Quintiere, n.d.). This, combined with the density of HFO as well as the spatial arrangement of the engines enabled for the calculation of the characterises of the oil pool.

The HRR that results from the ignition of the oil pool can be calculated through (Drysdale, 2011):

$$\dot{Q}_c = \chi \, \dot{m}'' A_f \Delta H_c \; (kW) \qquad \text{Eq. 20}$$

where:

$\chi$ : combustion efficiency factor taking into account incomplete combustion,
$\dot{m}''$ : mass loss rate / burning rate (kg/m$^2$sec),
$A_f$ oil pool area (m$^2$), and
$\Delta Hc$ : effective heat of combustion (kJ/kg).

The combustion efficiency for sooty flames is commonly set to 0.7 (DiNenno et al., 2002; Hurley et al., 2016).

The oil pool area and the HoC of the HFO are also commonly available in (DiNenno et al., 2002; Hurley et al., 2016).

The mass loss rate is expressed as (Karlsson and Quintiere, 2000):

$$\dot{m}'' = (\rho_l \, R \, 10^{-3})/60 \qquad \text{Eq. 21}$$

where:

$\rho_l$ : density of HFO, and
R : is a regression rate (mm/min).

By identifying the regression rate for HFO with more than 0.3% water content (Karlsson and Quintiere, 2000), the HRR from the oil pool was found to be 1,865.9kW.

It was ascertained that the resulting heat release rate from the oil pool fire of this case study particularly, exceeds the flashover criterion of 1,055kW (Hurley et al., 2016), which, in theory, implies that established burning shall be achieved. Another assumption that must be stipulated is the fact that we considered that this HRR from the oil was achieved almost instantaneously, specifically 2 seconds. This was chosen to reflect real scenarios where ignition is instant (provided that the fuel comes into contact with a hot spot).

Therefore, to conclude the initiation stage, the oil pool ignition results in the generation of 1,865.9kW of heat within two seconds from the leak/scenario initiation.

### 9.5.3. Fuel Load Density and Energy Released from the Fire

Since the permissible combustible mass is dictated by IMO as 45kg/m$^2$, the neglection of cables, as discussed in the approach adopted section, is only limited to their calorific value $h_i$. The amount of paint, taking into account both the primer and top-coat, for the engine room enclosure was calculated as 786.3kg, whilst the calorific value of epoxy is 30.7 MJ/kg.

From equation 18, the FLD was calculated as 1,381.5 MJ/m$^2$.

The energy (E) released from a fire of this FLD was calculated as 3,303,354 kJ, via utilisation of equation 9.

### 9.5.4. Flashover Criterion and Peak HRR for Ventilation-controlled fire

The flashover criterion was calculated from Thomas's equation: $\dot{Q}_{flashover} = 7.8\,A_T + 378A_0\sqrt{H_0}$ and was found to be $Q_{fo}$=7,434.85kW.

Ventilation openings dimensions, the engines' room door, were explicitly known.

The ventilation-controlled HRR from Thomas equation 8 was calculated as $Q_v$=7,440.51kW.

Hence, $Q_v = Q_{peak}$ = 7,440.51kW.

### 9.5.5. Heat Release Rate of the Fully Developed Fire

Having calculated the oil pool HRR, the equation 22 below, was solved for $\dot{Q}$ (HRR) for each successive fuel package item. Then, by using the common formula Q = at$^2$, the time to ignite each item was calculated.

$$\dot{q}_r'' = \frac{\chi_r \dot{Q}}{4\pi R^2} \qquad \text{Eq. 22}$$

The results of the Monte Carlo Simulations for the calculation of the growth coefficient (α) are presented in Table 18. The successive ignition of the items and their superposition resulted in a few hundred of kW remaining in order to achieve the $Q_{peak}$. Therefore, this was assumed to be from cables.

*Table 18. Results of Monte Carlo Simulations conducted for the fire growth rate of each successive item ignited.*

| Item | α (95$^{th}$ percentile) |
|---|---|
| M/E 1 | 0.044855 |
| M/E 2 | 0.0366098 |
| D/G 1 | 0.0403374 |
| D/G 2 | 0.0390161 |

Table 19 presents the evolution of the HRR by successful ignition of the paint from different machinery. Each successful ignited item's HRR was superpositioned on the previous one. The fire originated on the oil pool, while it spread on the engine on the port side of the domain. Then, via radiation, the alternator of the in-capture engine establishes burning, which, via radiation spreads over to the starboard side engine.

*Table 19. Calculated design fire HRR by superposition of fuel package ignition*

| Time (sec) | HFO | M/E 1 | M/E 2 | D/G 1 | D/G 2 | Cables | Total HRR |
|---|---|---|---|---|---|---|---|
| 0 | 0 | 0 | 0 | 0 | 0 | 0 | 0 |
| 2 | 1865.90 | 0 | 0 | 0 | 0 | 0 | 1865.90 |
| 70.33 | 1865.90 | 209.44 | 0 | 0 | 0 | 0 | 2075.34 |
| 221.60 | 1865.90 | 209.44 | 837.76 | 0 | 0 | 0 | 2913.09 |
| 437.78 | 1865.90 | 209.44 | 837.76 | 1884.96 | 2144.66 | 0 | 6942.71 |
| 440 | 1865.90 | 209.44 | 837.76 | 1884.96 | 2144.66 | 498.29 | 7441.00 |

### 9.5.6. Decay Phase

For the purpose of design fire completeness, the energy equations 9 to 15, were combined in order to derive the maximum time the design fire may burn before decay ensues $t_{max}$, the maximum time the fire may burn $t_{decay}$. The decay time resulting from this design fire was found to be 440seconds, presented in Table 19.

### 9.5.7. Simulation Particulars

Regarding the mesh, a characteristic fire diameter approach was employed to derive appropriate mesh sizes. The characteristic fire diameter D* was found to be 2 meters, whilst a coarse mesh of approximately 0.5m was selected. The mesh was also taken as coarse considering the extent of the simulated geometry.

Each simulation scenario is cited hereunder respectively. The simulation time was not set to reflect the duration of the fire until decay ensues, but for 600 seconds. Furthermore, since the A-60 boundaries have been modelled thermal radiation devices were placed strategically around, and on the outside, of the engine compartment. This was performed to measure heat fluxes that were assumed to be required for successful ignition of fuel packages.

### 9.5.8. Simulations

#### 9.5.8.1. Engine Room Simulation without Active Firefighting

Figure 100 presents the evolution of the HRR curve of this scenario. As dictated, and expected, from the design fire, the HRR follows that of Table 19.

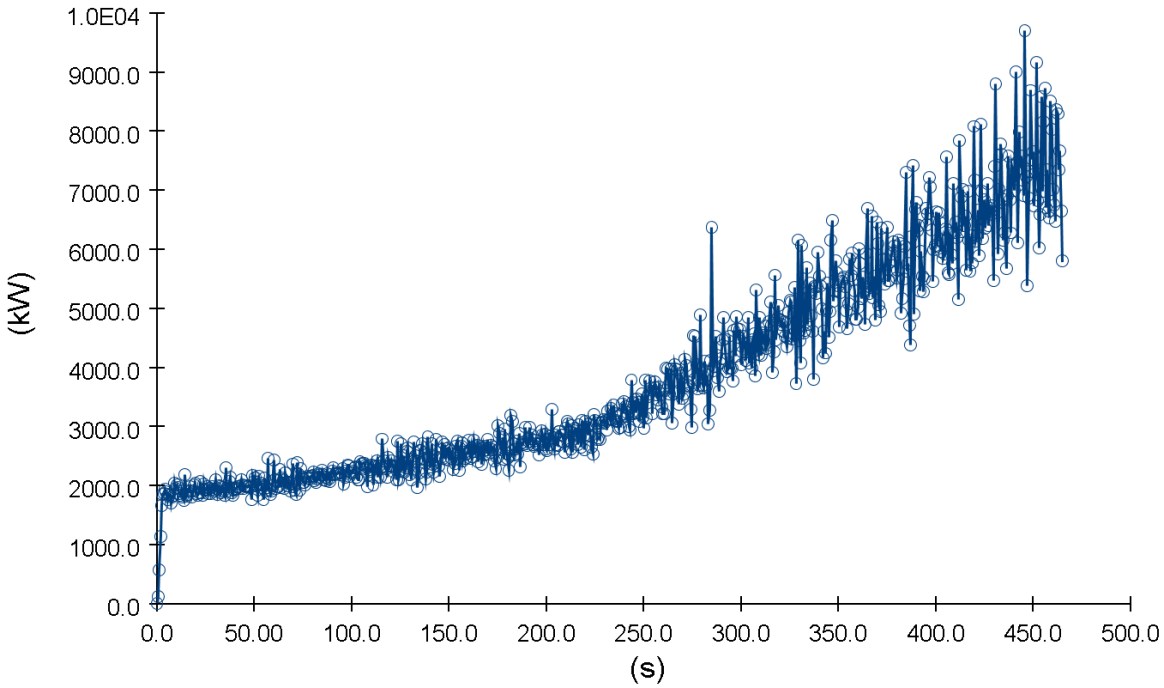


*Figure 100. HRR evolution of E/R simulation with no sprinklers*

The evolution of temperatures via 2D slices is presented in Figure 101. It was noted that at the height of the generators, namely 1.5m, temperatures were in the order of 100-120ºC whereas, whereas at the ceiling in the order of 180ºC. This is attributed to the great height of the enclosure, namely 9.2m, keeping in mind that it spans overs three decks while the engine deck (deck 1) is slightly taller compared to others.

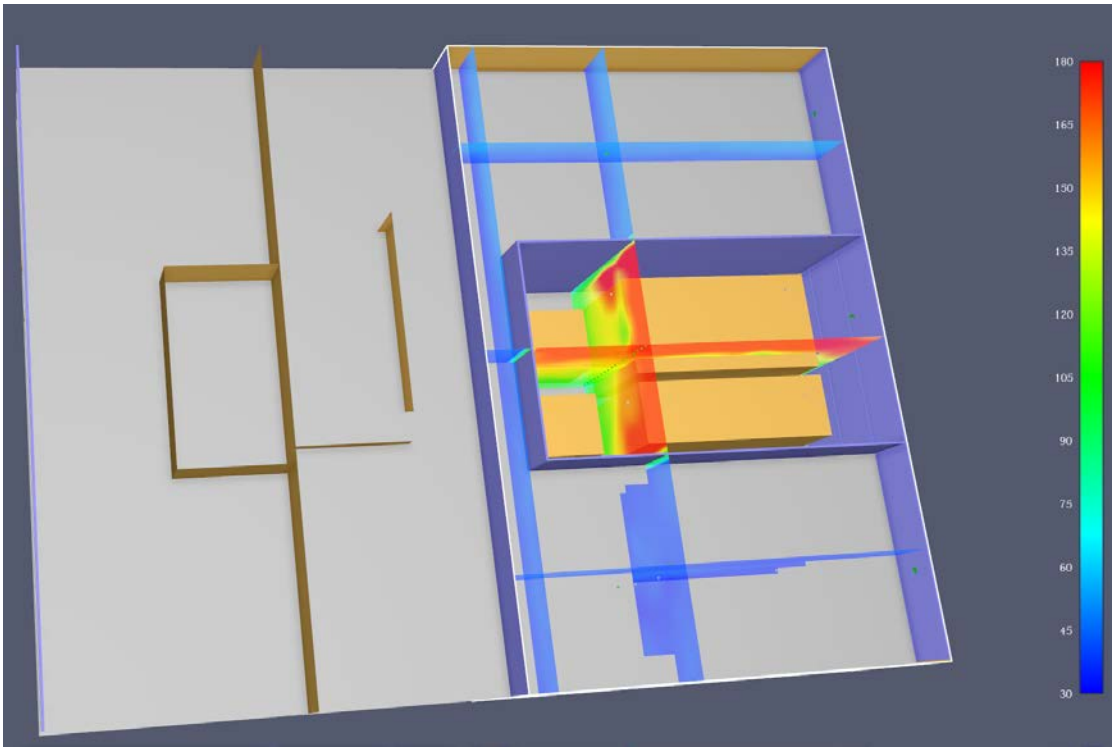


*Figure 101. Temperature slices (2D) at 440 seconds.*

The evolution and transport of smoke to the other parts of the geometry are highlighted through Figure 102, Figure 103 and Figure 104. Figure 102 was captured early in the simulation, namely at 175 seconds, whilst the last two at 325 seconds. At 175sec the smoke from the engine enclosure began spreading to the incinerator area in Deck 1 (located on starboard side), where, through a hole in the same location it escapes on Deck 2 and spreads further halting visibility.

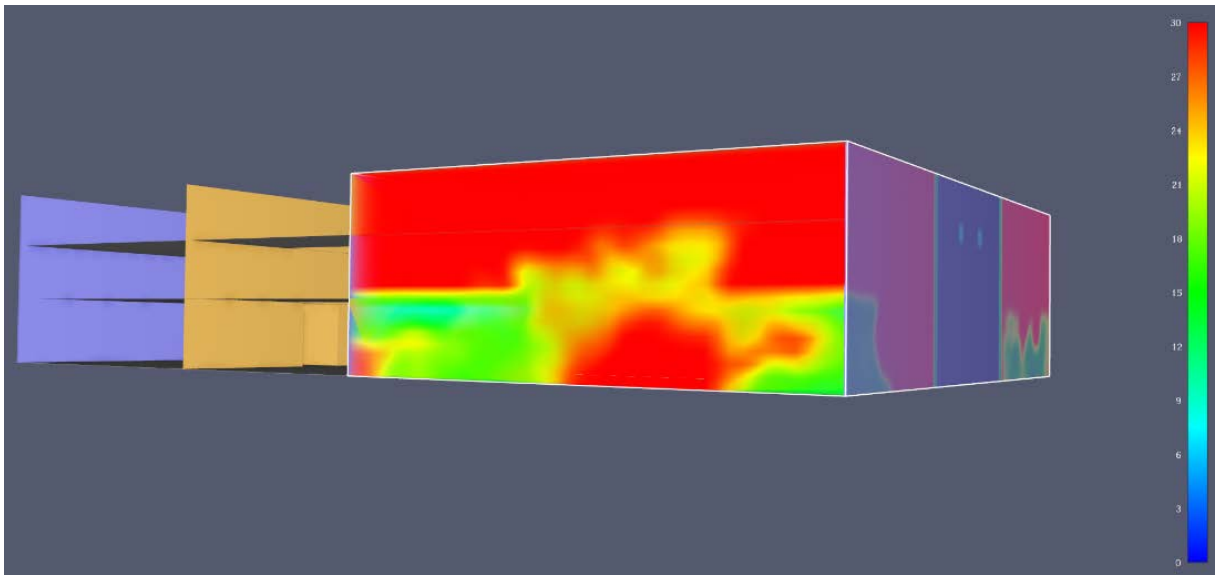


*Figure 102. Visibility and transport of smoke at 175 seconds.*

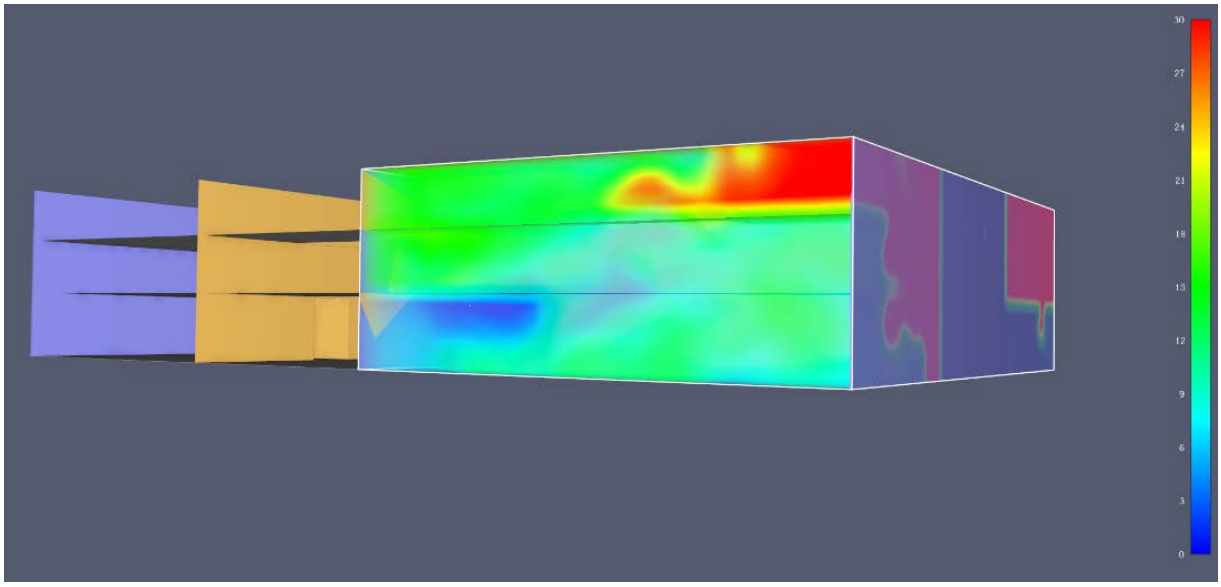


*Figure 103. Visibility and transport of smoke at 325 seconds.*

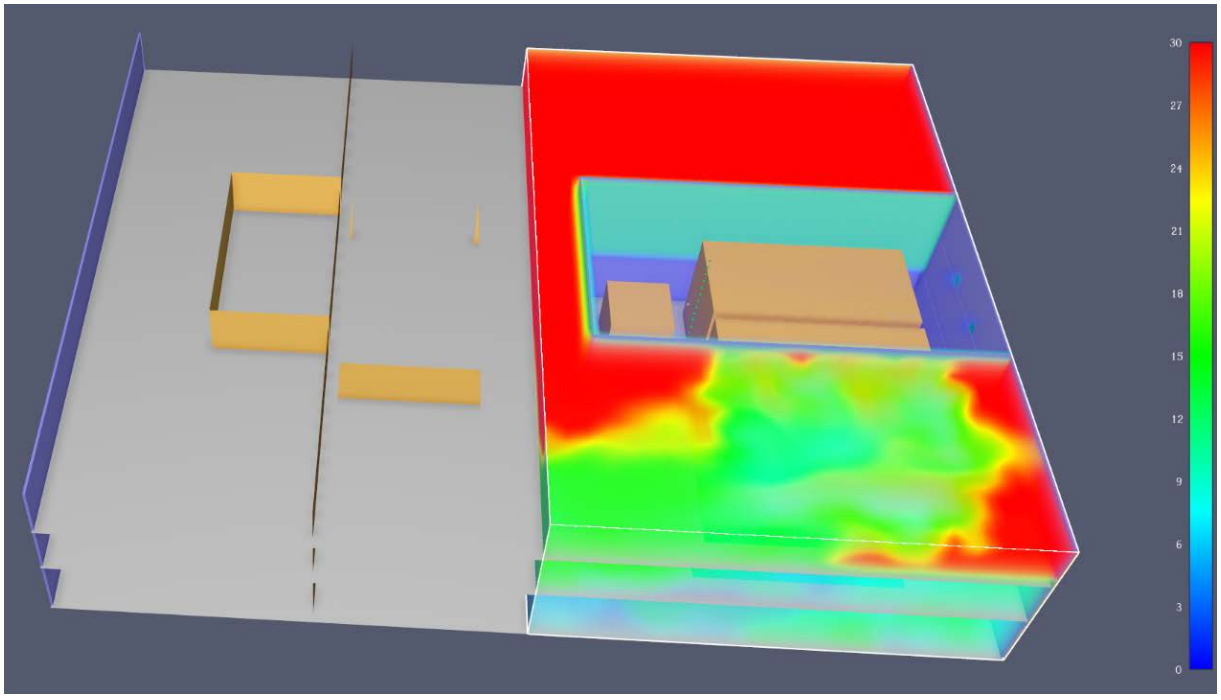


*Figure 104. Top view of visibility and smoke transport at 325 seconds.*

To assess the impact of the fire and the extent of smoke accumulation, devices to measure smoke layer height and visibility were strategically positioned within the cabin and at various points along the corridor. These can be found in the appendix, namely Appendix B5.

The FED emanating from the fire reaches a value over 1 at 400seconds, as presented in Figure 105.

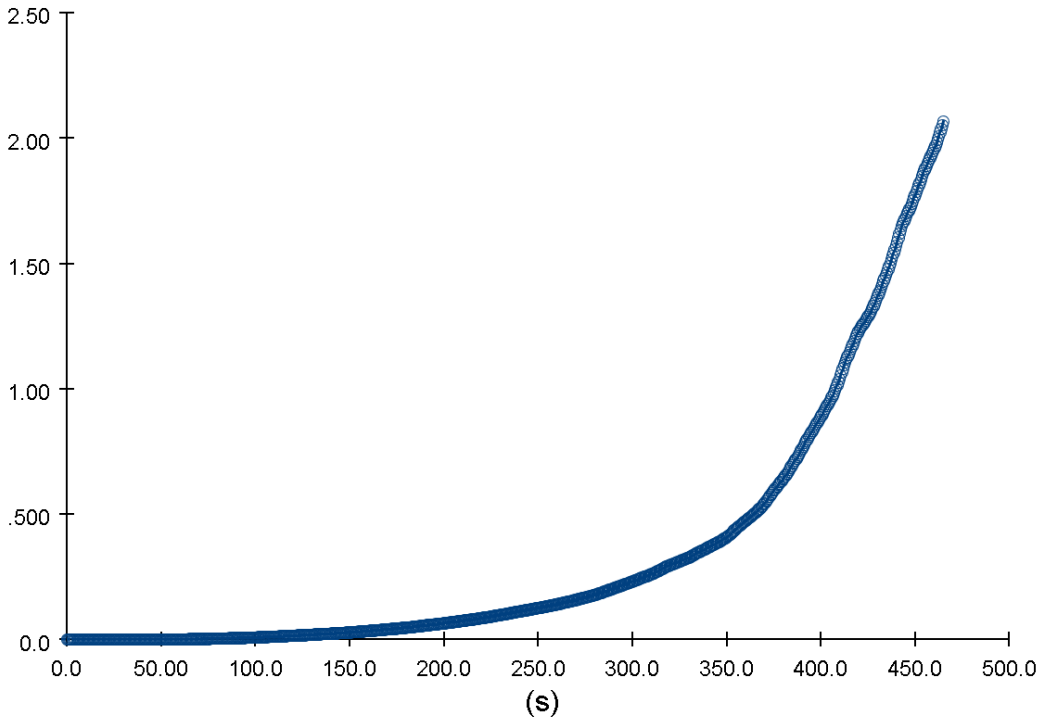


*Figure 105. FED of Engine Enclosure (no sprinklers).*

#### 9.5.8.2. Engine Room Simulation without Active Firefighting, and Smoke Dampers

Figure 106 presents the evolution of the HRR curve of this scenario. The control logic was set to deactivate the engine enclosure inlet fans, to simulate a fire under normal practices where the crew might try to starve the fire.

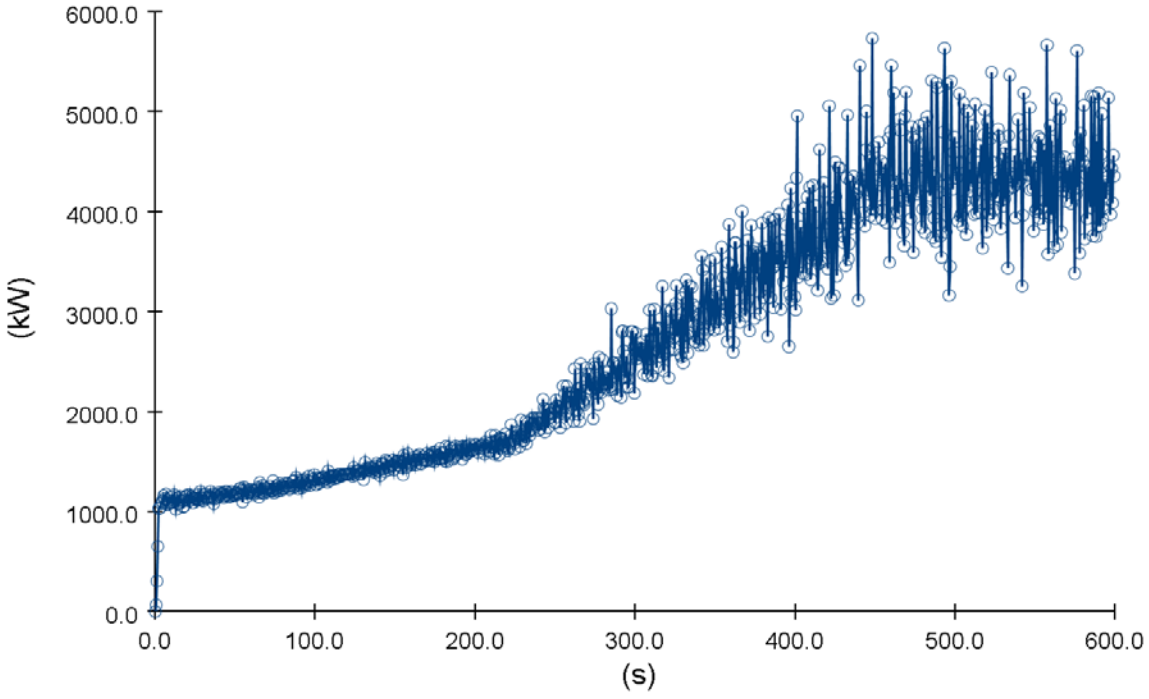


*Figure 106. HRR evolution of E/R simulation with no sprinklers & control logic.*

Interestingly, the operation of the smoke dampers via the control logic, of the inlet fans results in a reduction of the HRR in the magnitude of 2-3 MW, compared against Figure 100.

The effect of the automatic stoppage of the inlet fans is highlighted through a comparison of Figure 107 and Figure 108 against the ones from the scenario with inlet fans working, namely Figure 102 and Figure 103. The engine enclosure has very poor visibility, but the smoke has not escaped out of the enclosure's door and there is no spread to other parts of the geometry.

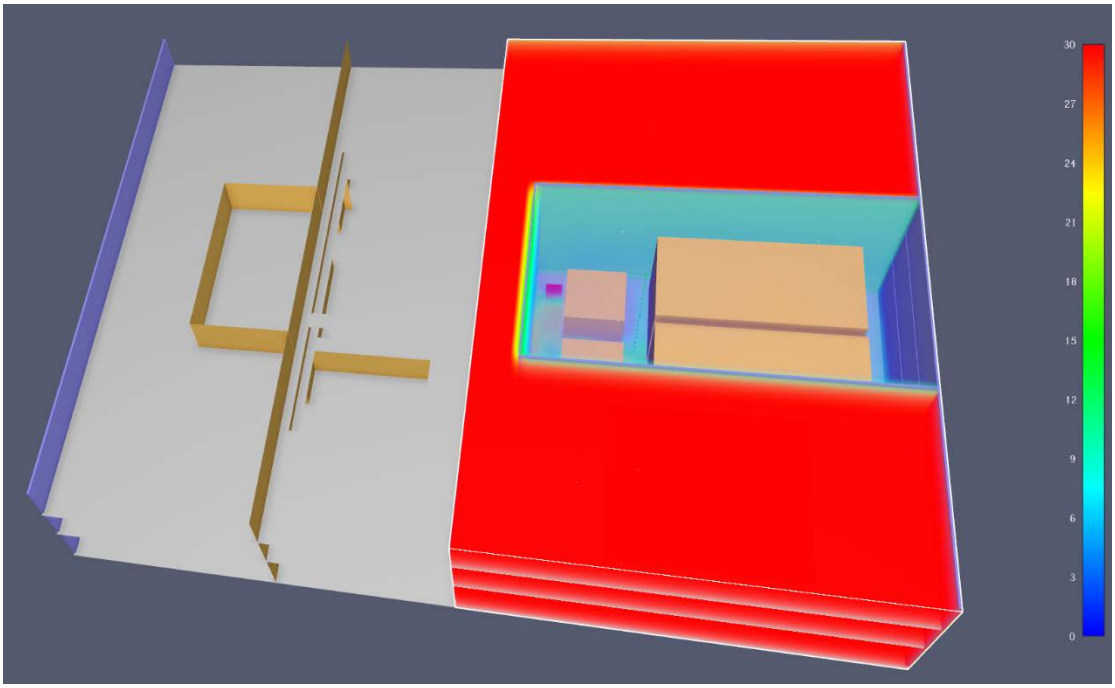


*Figure 107. Visibility and transport of smoke at 175 seconds (with control logic).*

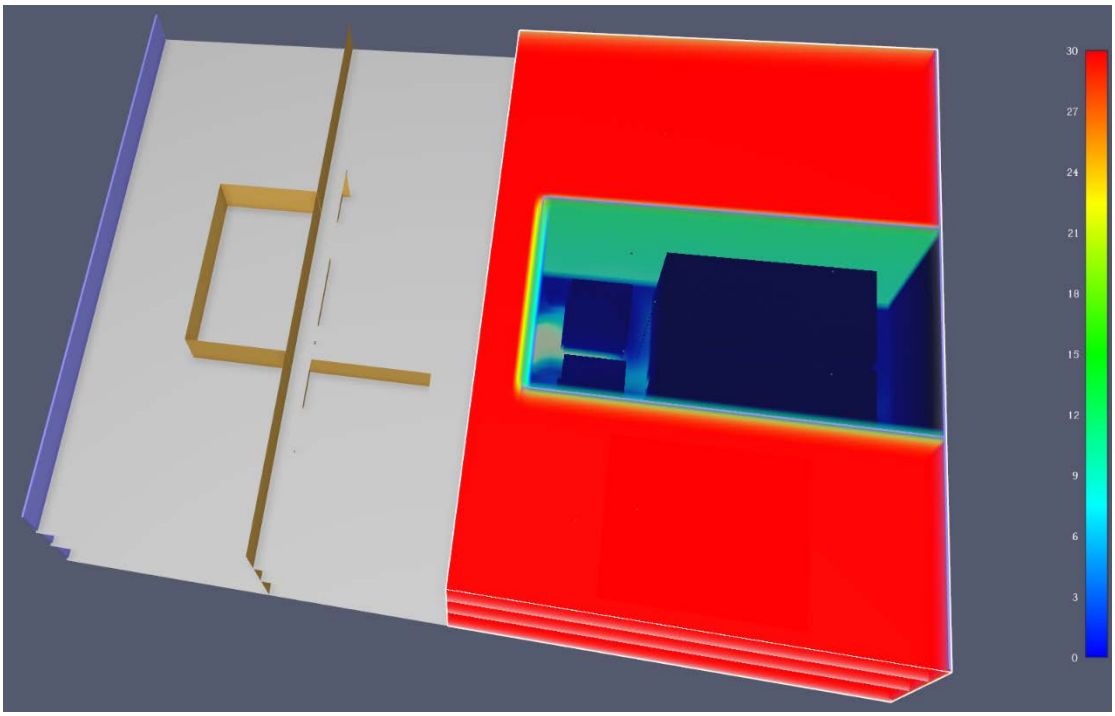


*Figure 108. Visibility and transport of smoke at 325 seconds (with control logic).*

To assess the impact of the fire and the extent of smoke accumulation, devices to measure smoke layer height and visibility were strategically positioned within the cabin and at various points along the corridor. These can be found in the appendix, namely Appendix B6.

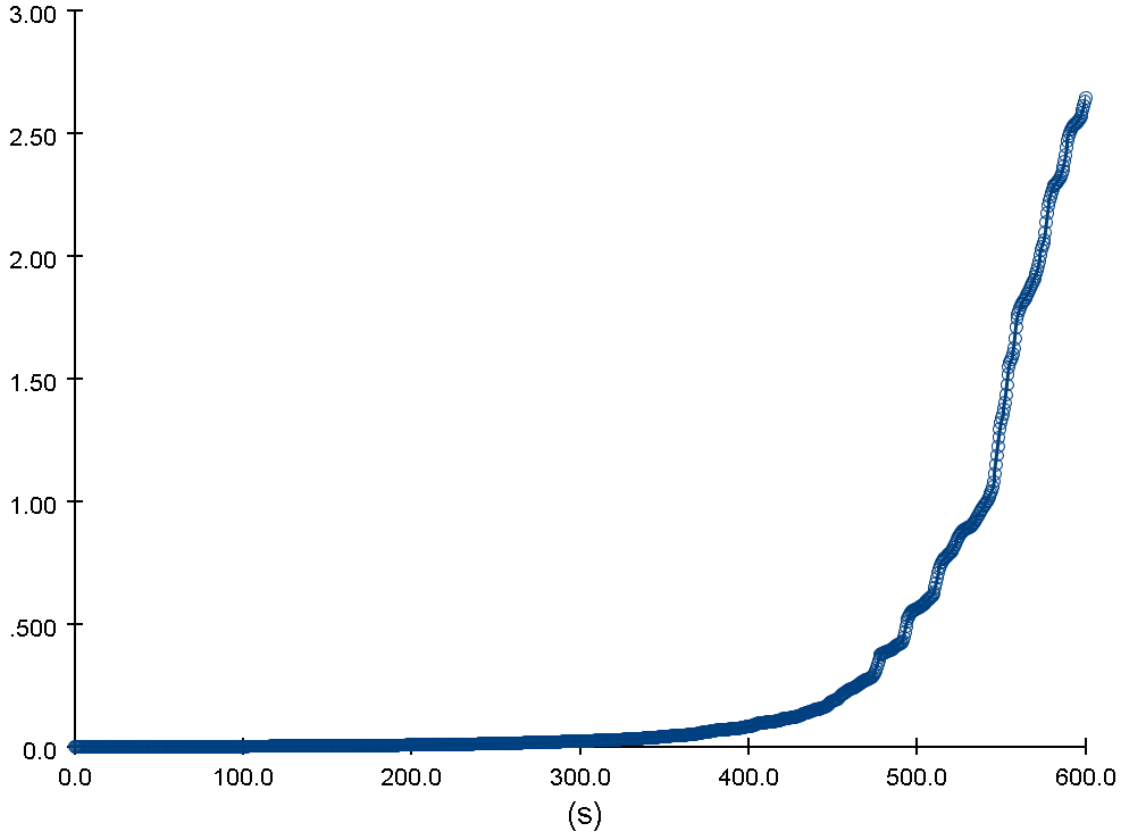


*Figure 109. FED of Engine Enclosure with smoke dampers and no sprinklers.*

To conclude with this scenario, Figure 109 presents the evolution of FED in the engine enclosure. It was ascertained that incapacitation does not occur within the duration of the design fire.

#### 9.5.8.3. Engine Room Simulation with Sprinklers

Interestingly, the effect of sprinklers was not adequate in limiting the HRR of the scenario. The HRR curve of the scenario is presented in Figure 110.

The effect of sprinklers can be highlighted by examining the temperatures in the enclosure and, ultimately, the smoke layer height and the FED.

Figure 111 presents 2D temperature slices at 450seconds. A comparison against Figure 101 revealed that the sprinklers aided in reducing the maximum temperature of the enclosure.

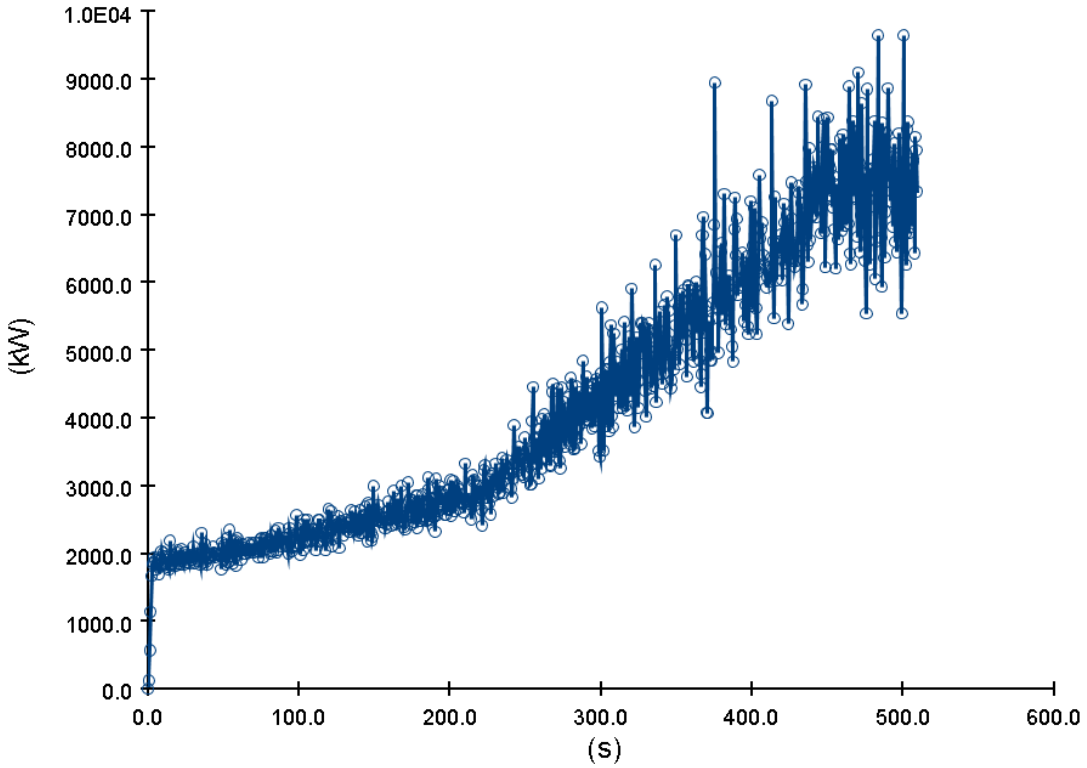


*Figure 110. HRR evolution of E/R simulation with sprinklers.*

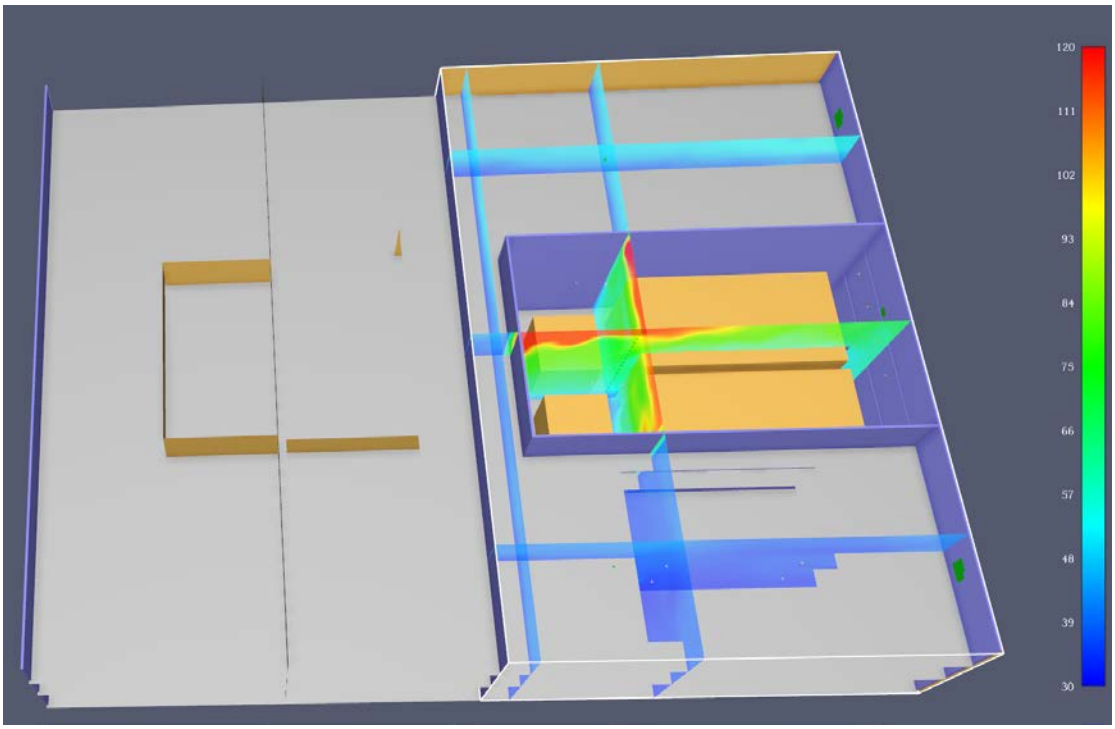


*Figure 111. Temperature Slices at 440 seconds (sprinklers)*

Figure 112 presents the smoke layer height of the engine enclosure, whilst Figure 113 and Figure 114 the upper and lower smoke layer temperatures respectively.

The smoke layer height at the end of the simulation is approximately over 2m whereas in the scenario with no sprinklers it was a little bit below 2m.

With respect to the temperatures of the smoke layers, these were lower than the simulation with no firefighting as presented in Appendix B5.

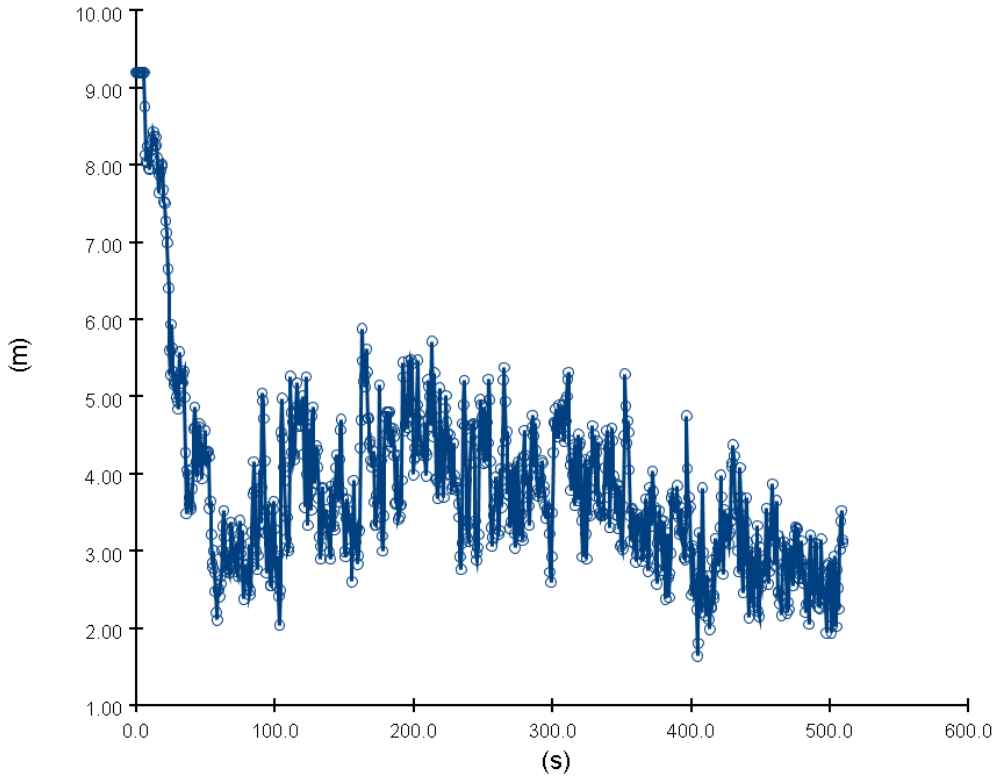


*Figure 112. Smoke Layer Height in Engine Compartment with sprinklers.*

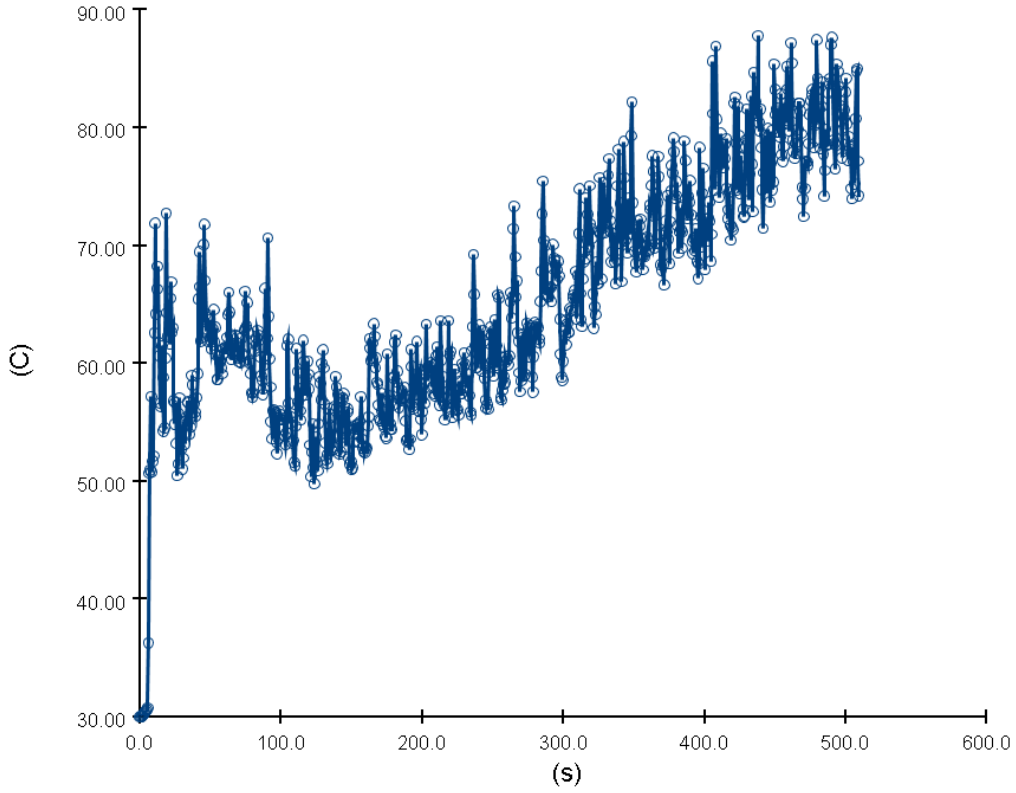


*Figure 113. Upper Smoke Layer Height Temperature (sprinklers).*

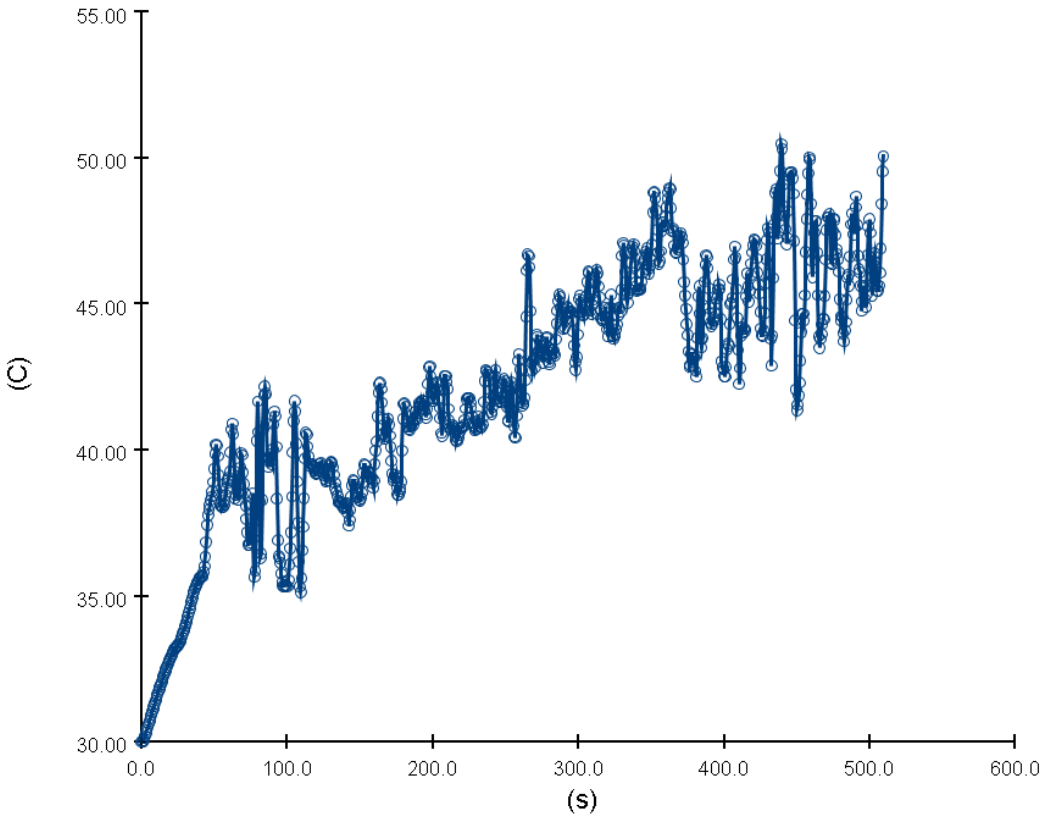


*Figure 114. Lower Smoke Layer Height Temperature (sprinklers).*

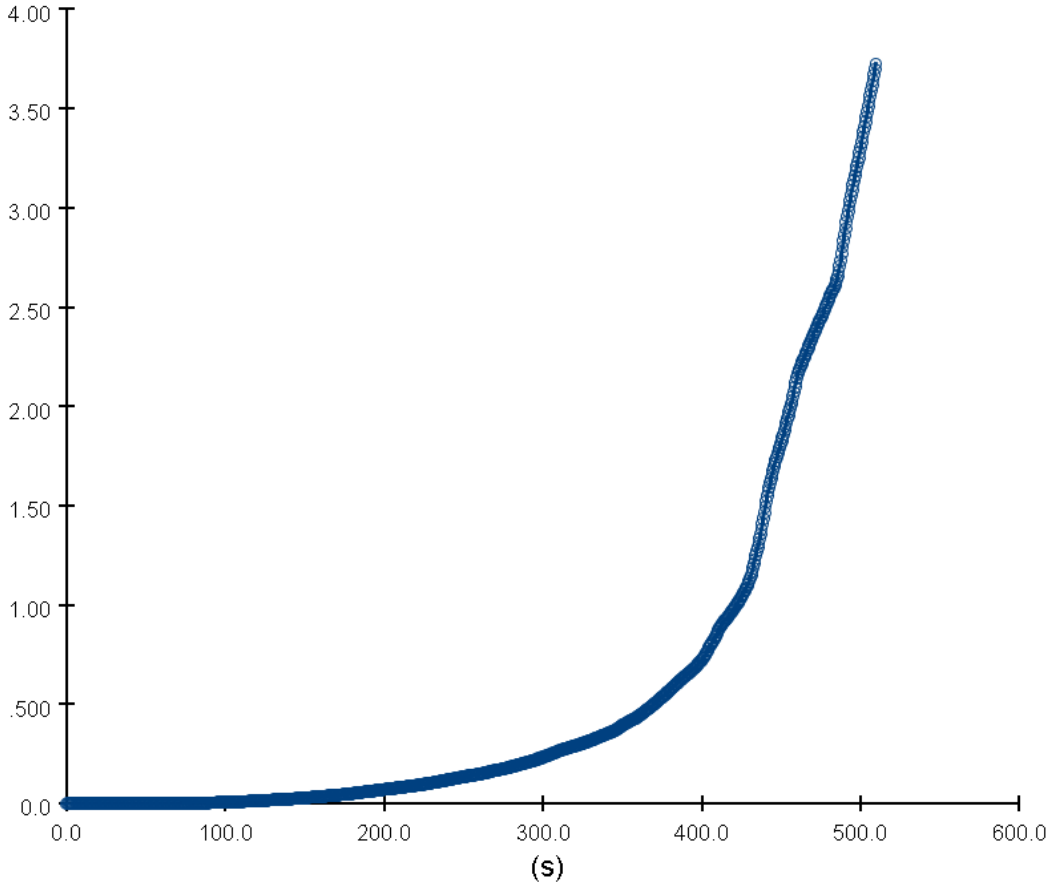


*Figure 115. FED of Engine Enclosure (sprinklers).*

Finally, the engine compartment reaches untenable conditions after 421 seconds, a difference of 20 seconds.

## 10. Discussion

Out of all types of ship accidents, fire appears to be amongst the most prevalent in terms of frequency and consequences, with foundering/grounding being the top contender. On a yearly basis, there are numerous accidents/incidents taking place, while the regulatory stakeholders, IMO, Flag Administrations, etc., have been attempting to avert those. Despite the regulatory efforts, and as per the relevant statistical analysis provided in the literature review chapter, the frequency of these events increased by 10%. Additionally, the frequency is purely dominated by cruise ships that become more and more complex every year, while passenger ships are top candidates in terms of fatalities, which is to be expected considering the amount of passenger ships against luxurious cruise ships. Moreover, as passenger ships are becoming larger over time, both the increased passenger capacity and the complexity of the designs become intricate issues in terms of fire. Hence, for the purposes of this thesis, focus was given only on very large passenger ships due to the great number of passengers and crew.

In terms of the spatial origin of fire across all ship types, engine room fires have been known to be the most prevalent historically, followed by cargo and accommodation spaces respectively. Passenger ships cargo areas, usually, pertain to vehicle decks which are accompanied by relevant fire risks, with electrical faults being the most common. Research endeavours such as project FIRESAFE and EMSA's tenders for Firesafe I and II, heavily investigated vehicle deck fire safety, including provisions for alternative fuelled vehicles almost a decade before these became relevant. Currently, as this thesis was compiled, another research project was ongoing, namely LASHFIRE, which aims to de-risk alternative fuelled vehicles with focus on battery powered vehicles and applicable firefighting strategies, procedures, and equipment. Therefore, considerable research efforts were and still are being undertaken towards passenger ship vehicles decks (RoPax).

Statistically, engine room fires have been caused due to pressurised flammable oil leaks, usually fuel or lubricating oil, which comes into contact with hot surfaces, which are found in many machinery within an engine room, such as combustion engines, boilers, incinerators, etc. These two causes represent two elements of a fire triangle, the fuel, and the heat source respectively. Relevant SOLAS provisions exist for both elements; namely, flammable oil lines shall not be placed adjacent to hot surfaces, and hot surfaces must be kept below 220$^{o}$C. Since the flashpoint of heavy fuels is a little shy over 60$^{o}$C, engine room fires are still taking place. As per (McNay et al., 2019), the current focus of engine room fire safety lies on proximate events immediately prior to ignition taking place, while a plethora of mitigating measures also exists. The hypothesis made in the aforementioned research work, of detection of only proximate-direct events prior to ignition, was evidenced during the first case study, where the fuel oil system of an existing very large passenger ship was investigated and, consequently, it was ascertained that existing fuel oil leak sensors would detect a potential leak after it has been realised. The way forward, was believed to be achieved via a systematic approach, with focus on the left of a fire risk bow-tie, such that systemic and contributing factors are accounted for, apart from the direct which are somewhat looked after. Treating hot surfaces was not deemed as a viable solution

towards averting engine room fires as these hot surfaces are very pertinent to ship and machinery layouts while the condition of the necessary insulation may degrade over time due to improper fitting and degradation after repairs of the machinery. To that end, this thesis focused on averting flammable oil releases in a systemic manner.

With reference to the systemic approach mentioned previously, safety barriers were considered to be a promising way of treating latent causal factors in ship engine rooms. A plethora of industries, such as the process and oil and gas, have successfully employed safety barriers to treat hazards that are very relevant with those noted in a ship's engine room, which essentially acts as a process and propulsion plant. On the other hand, the placement of safety barriers requires a systematic approach, while monitoring of the safety barriers, irrespectively of their nature (active/passive), was deemed absolutely necessary, hence, dynamic barrier management via sensory equipment was considered to be the most promising method.

Although engine room fires are historically more prevalent against other passenger ship areas, these do not always pose the greatest risk in terms of injuries and fatalities to passengers, the number of which greatly exceeding that of the crew. This is attributed due to the fact that passengers are not allowed in service spaces, and to passive firefighting means such as fire boundaries, subdivision of the ship into main vertical zones which used to "isolate" parts of the ship, redundant deluge systems, etc. According to a high-level HAZID conducted via qualitative evaluation of fire accident statistics, and a semi-quantitative HAZID undertaken amongst experts from various stakeholders of the maritime industry, conducted as part of research project SEAMAN – where the author of thesis was part of, such passive means have contributed to keeping the fire contained in the engine room spaces and such fires pose little risk to passengers compared to others. To that end, passenger cabin and large public space decks were ascertained to be very relevant towards fire risk.

Following the principle of main vertical fire zones, a main vertical fire risk model for very large passenger ships was proposed in this thesis, in the manner of a risk contribution tree (bow-tie). Up to the point of the compilation of this thesis no fire risk model had been stipulated as such, with particular focus on a main vertical zone of a very large passenger ship, and investigation on the relevant areas of concern, being the engine room, and passenger cabin and large public space decks.

The methodology of the fire risk model involved operations towards both the preventive and mitigative parts of the risk contribution tree. Concerning the preventive measures, left of the bow-tie, the DBM framework was established, whilst for the mitigating aspect fire simulations were conducted. The starting point was the conduction of a high-level qualitative HAZID on ship fires conducted via the literature review chapter. The spatial origins of fire along with the historical frequencies were used towards the HAZID.

With respect to preventative measures, the left-hand side of a bow-tie diagram, a novel framework for the derivation of safety barriers in large passenger ship engine room was proposed. The framework was demonstrated though a case study, cited in Chapter 5, in which a safety barrier was derived, able to monitor the fuel oil lines from

the service tanks to the main engines, the Release Prevention Barrier. The framework was subdivided accordingly with the operating pressure of the fuels in a such a situation, namely low-pressure and high-pressure technical barrier elements. In order to enable DBM, sensors were utilised to infer/diagnose the status of the technical barrier element. A real very large passenger ship was selected to demonstrate the framework, which already had sensory equipment installed. To that end, the framework allows for the investigation of potential existing sensory systems to be included towards the inference of the barrier status, and provides adequate guidance, including necessary computational means/applications, for utilisation on other engine rooms. Moreover, a commercial-off the-shelf tool was used to analyse the behaviour of the technical barrier element. Recommendations towards the organisational and operational barrier elements were also provided within the framework.

During the dynamic barrier management case study, a plethora of challenges were encountered. The available leak detection technologies cannot be applied on the flammable oil line in a simple manner. The inherent limitation of the hardware-based solutions was verified towards its inability to treat shipborne fuel oil leaks, mainly due to the chaotic environment of the engine room, with a major limitation being the pressure pulses and different origins of vibration. Additionally, software-based solutions require an exhaustive amount of sensors which would exponentially increase the cost considering the complexity of the flammable oil lines on board. The review conducted revealed that a digital twin model of the flammable oil line was imperative towards ascertaining the necessary amount and spatial allocation of sensors, including the decision on appropriate functional requirements of the LDS, which serves as the technical barrier element of the release prevention barrier.

Additionally, since the DBM solution would be destined towards a real ship which has already been sailing, actual data from the flammable oil line would also be used towards the validation and verification of the digital twin. Furthermore, no such data were available, and the available tool for the purpose of this thesis could not utilised towards the creation of a full-scale digital twin. Specialised application like DNV's Open Simulation platform would be appropriate for use in this case (DNV, 2018). Moreover, necessary operations towards the remaining RPB barrier elements, the operational and organisational, were identified but these could not be fully established due to the aforementioned technical limitations of the technical barrier element. To that end, recommendations were made towards the remaining elements in an effort to provide a solid framework towards DBM in large passenger ships engine rooms. As an example, the operational element is imperative to be looked after and accordingly with the leak detection solution employed and its particularities. If a specialised software and respective user are required, these must be taken into account in the operational element jointly. Needless to say, that the same applies for the organisational element, taking into account both the blunt and sharp edge.

Preventative measures were not sought for the purpose of the MVZ fire risk model, except for the framework for the RPB. This decision was taken since the current state of engine room fire safety focuses mainly on immediate contributing factors and mitigation. Additionally, both active and passive fire-fighting systems have already been scrutinised in project FIREPROOF, and other small-scale ship fire research

endeavours. To that end, mitigating safety barriers were taken for granted, such as fire boundaries, deluge systems, dampers, etc. Consequently, the mitigating aspect of the risk contribution tree was focused in quantifying the effects of an engine room fire in the case that the release prevention barrier failed, while taking into account all the mitigating measures prescribed through SOLAS and other relevant regulatory provisions. Nevertheless, the aforementioned quantification included cases when the deluge system fails, in order to quantify the risk pertaining properly, as a worst-case scenario. Moreover, passenger cabin and large public space decks were also considered towards the fire risk quantification following occupancy trends.

Full 3D computational field model simulations were conducted towards the fire risk quantification of the selected spaces (engine room, passenger cabin deck, large public space deck) via FDS/Pyrosim which were cited in three separate case studies. A different very large passenger ship was selected for the purposes of the risk quantification, showcasing the potential and applicability of the MVZ fire risk model proposed in this thesis. This case study vessel was part of Horizon 2020 research project SafePASS, while the cabin and large public space simulations were an integral part of it.

In general, first principle deterministic approaches were favoured over probabilistic methodologies for the construction of the design fires, as the latter is more fitting towards goal-based and/or alternative designs, allowing for the evaluation of fire risk of many possible designs. Furthermore, the utilisation of first-principle engineering in way of deterministic design fires was considered as a novel approach in shipborne fire safety. For both the passenger cabin and large public space deck simulations, the pyrolysis phenomenon was utilised for the first time in the context of ship fire simulations, where there is little to no data in terms of calorimeter tests or full-scale experiments. Challenges were faced, mainly on the selection of appropriate materials within the cabin and large public space simulations, along with relevant fire behaviour, pyrolysis, data. Even if these were identified easily, the usage on full 3D CFD simulation is not straightforward. Nevertheless, the cabin deck simulations were both validated and verified in way of input parameters and results against an examination on real full-scale fire tests of a cabin. Since the materials utilised on the large public space simulations were almost identical to those within the cabin, these simulations were also considered as verified. Unfortunately, the full scale large public space experiments conducted under the FP7 programme were not available to the author of this thesis, so no comparison was possible. In order to furtherly ensure the validity of the large public space simulations, outmost attention was given on the appropriate allocation of the fire load as per (IMO, 2001b), in order to ensure that the heat obtained from the fire would be realistic towards such spaces.

Conversely with the large public space and cabin deck, the majority of the challenges were faced in the engine room case study. Firstly, no such CFD simulations were identified in the literature review. Additionally, as per SOLAS, the majority of the machinery/items inside an engine room are non-combustible, which is in line with the mentality of minimising available fuel. A deterministic approach such as the one utilised for the other simulations was not possible to be employed due to the very small thickness, in the magnitude of a couple millimetres, of combustibles inside the

engine room, namely paint. Another fuel load that posed great challenges were the cabling inside the engine room, the amount of which was largely unknown and very tied with the size of the ship engine room, the machinery within and their allocation spatially. No studies were identified containing information towards the actual composition of the cable sheathing, nor the pertinent thicknesses. Moreover, even if such information/data were available, modelling such items in FDS is quite trivial in terms of the circular shape and the mesh size required to adequately capture the fire phenomena. For example, in order to properly model the paint, a mesh size accordingly with the paint thickness would be required, which coupled with the size of the geometry would lead to an extremely intensive simulation in terms of the time and required hardware, in other words, it is impossible to do so with the current available simulation means.

To that effect, a hybrid approach was employed, combining both deterministic and probabilistic procedures. Ignition of successive fuel packages via radiation was employed in order to construct a design fire. The starting point of the fire was a pressurised oil leak, which was modelled according to the historical leak sizes and pressure magnitude and the assumption that the oil forms a pool, necessary in modelling the fire in FDS. Paint thicknesses were also employed in a realistic manner. The fire stemmed from the oil pool and spread in a successive manner to consecutive fuel packages which represented the machinery within the enclosure. It must be mentioned that in order for this approach to work a substantial assumption was employed in way of the fuel distribution load (FLD). Specifically, the calorific value of the cables was considered to be identical to that of the epoxy paint in way of the FLD. Nevertheless, it is the author's opinion that since these two calorific values are close in magnitude no underestimation of the FLD was undertaken keeping in mind that there must be no more than 45kg of combustible material per square meter of the enclosure. Additionally, since no full-scale experiments were available, the engine room fire simulation approach cannot be effectively validated and verified.

In terms of the fire growth (α), the fire acceleration, the commercial values, presented in Table 17, were employed in a probabilistic manner towards its derivation, in line with the state-of-the-art probabilistic fire safety. No other variables were treated as such since the MVZ fire risk model was showcased in an existing ship and there was no necessity to consider various designs and arrangements as such.

The results of the fire simulations were in way of life-safety performance metrics such as the fire radiation, fractional effective doses of the toxic fire effluents, smoker layer heights and visibility. These can be utilised to assess the tenability of an enclosure.

## 11. Conclusion and Recommendations for Future Work

The research conducted in this thesis aimed at averting engine room fires from taking place while establishing a main vertical zone fire risk model. The main conclusions drawn from the undertaking of the research questions and consequent methodology are discussed hereunder. The current status of engine room fire safety was ascertained to be on the detection of proximate events prior to ignition, while particular focus was given on mitigation measures. This mentality follows the reactivity of the industry towards safety. Meanwhile, fires keep taking place, with a steady total loss trend and a frequency that points towards RoPax vessels, both of which highlight the inadequacy of the rules.

Engine room fires being the usual spatial origin on board usually break out due to the release, leak, of flammable oil which comes into contact with a hot surface, which are abundant in such a geometry. Moreover, treating hot surfaces was not considered to be the way towards a fire free engine room due to the degradation of both the insulation and the engine room as a whole over time. This is also supported by the introduction of voluntary classification notation such as DNV's CAP programme, aimed at monitoring hotspots, amongst other operations. Instead, systemic treatment of the release from pressurised vessels/lines was considered to be the way forward.

To that effect, safety barriers with the use of sensory equipment towards a dynamic barrier management framework were considered to be the solution. Since the examination was systemic, technical, organisational and operational barrier elements were necessary. The technical element, the leak detection system, acts as the backbone, therefore, the investigation was initially focused at this. Leak detection solution were heavily scrutinised towards their suitability, while the framework was demonstrated via a case study on the fuel oil line of a very large cruise ship, by conducting a series of operations towards the safety assessment of the system. It was ascertained that none of the available hardware solutions were suitable for the application at hand, while a software solution with the use of flowmeters, pressure and temperature sensors was deemed as favourable. The limitation of this approach is that a plethora of sensors are necessary, therefore, a digital twin was imperative towards the establishment of the technical barrier element of the release prevention barrier. Moreover, since the technical element, being the backbone of the barrier, could not be fully examined due to lack of data, recommendations were made towards the operational and organisational elements.

The DBM framework examined and presented served as the preventative aspect of the MVZ fire safety risk model proposed in this thesis, specifically on the left-hand side of the bow-tie risk model. With respect to the right-hand side, the mitigating measures, the ones from the provisions, SOLAS and FSS Code, were considered to be adequate. To that effect, full scale 3D CFD simulations were conducted, in three separate case studies on a very large passenger ship, in order to quantify the risk in case an engine room fire broke out. Additionally, simulations were also conducted on other fire-prone decks/geometries since the engine room fires rarely break out of it. Large public spaces and cabin decks were prime candidates following the occupancy trends of such ships, for day and night-time respectively.

First principle fire safety engineering was employed for all simulated scenarios, which has not been performed yet in the context of a ship. Furthermore, such a task was considered paramount despite the limitations posed due to the lack of available fire safety data, contrastingly with building fire safety, as thus far probabilistic methods were employed, with varying degrees of uncertainty. A pyrolysis modelling approach was utilised for the cabin and large public space scenarios, via modelling the pyrolysis phenomenon which usually takes place under a fire. No such approach has ever been employed in a ship. Towards the engine room, and due to the lack of available data and CFD modelling limitations, a hybrid approach was devised, taking into account both deterministic and probabilistic operations in order to construct a design fire.

Finally, for all scenarios/case studies undertaken, simulations were performed having in mind normal firefighting readiness, meaning that firefighting measures were performing as intended, and without, in an effort to capture all scenarios for the risk model. Life safety performance criteria were ascertained for all scenarios and geometries, proofing the validity of the MVZ fire risk model.

Recommendations Towards Future Work

As the notion of a main vertical zone fire risk model is quite novel, the presented research work should not be deemed as complete or sufficient in terms of the fire risks. A plethora of operations could supplement the fire risk model in order to make it whole and widely applied. Amongst others, these recommendations are:

- Systemic expansion, and extension of the DBM framework towards all flammable oil hazards within the engine room, taking into account all the machinery and fuel lines that have the potential to create a loss of containment.

- Digital twin model of the a flammable oil line with a goal of creating a virtual RTTM model that behaves as the original system, where the functional requirements of the RTTM can be stipulated against reality (quantities that can be effectively “measured”, including necessary data science operations)

- Investigation on the potential of the electrical equipment within engine room and respective service spaces to create fires, and extension or derivation, as necessary, of the DMB framework towards those spaces.

- Derivation of DBM tool that takes into consideration all employed barriers in the engine room, as a safety system and station. The facilitation of such would necessitate barrier aggregation strategies and relevant decision support tools and strategies.

- Extension of the consequence analysis into other geometries within the main vertical zone. The first principles approach for the quantitative evaluation of the fire risk could be extended to other fire prone decks, or even all of the decks, as it utilises thermophysical data in order to model the objects and materials present in an enclosure.

- Incorporation of more complex fire models, avoiding the single fuel assumption, aggregation of reactions and effluents.

- Expansion of the fire risk model to the whole passenger ship. Again, this would necessitate appropriate decision support schemes and methods.

- Inclusion of evacuation analyses for the considered fire simulations, or the risk model itself, in order to be able to assess potential loss of life, instead of only obtaining life performance criteria such as the fractional effective dose.

## References


Adegboye, M.A., Fung, W.K., Karnik, A., 2019. Recent advances in pipeline monitoring and oil leakage detection technologies: Principles and approaches. Sensors (Switzerland) 19.

AGCS, 2014. Safety and Shipping Review 2014.

AGCS, 2022. Safety and Shipping Review of 2022.

Aina Eltervåg, Tommy B. Hansen, Elisabeth Lootz, Else Rasmussen, Eigil Sørensen, Bård Johnsen, Jon Erling Heggland, Øyvind Lauridsen, G.E., 2017. Principles for barrier management in the petroleum industry - Barrier Memorandum 2017.

Aizpurua, J.I., Catterson, V.M., n.d. Towards a Methodology for Design of Prognostic Systems 1–14.

Akib, A.B.M., Saad, N. Bin, Asirvadam, V., 2011. Pressure point analysis for early detection system. Proceedings - 2011 IEEE 7th International Colloquium on Signal Processing and Its Applications, CSPA 2011 103–107.

Allianz, 2019. Safety and Shipping Review 2019.

Allianz, 2020. Safety and Shipping Review 2020, AGCS.

Alpert, R.L., 2002. Review of Blinov and Khudiakov's Paper on ' "Certain Laws Governing Diffusive Burning of Liquids" by Hoyt C. Hottel. Journal of Fire Protection Engineering 12, 5–7.

Anantharaman, M., Khan, F., Garaniya, V., Lewarn, B., 2015. Reliability of Fuel OilSystem Components Versus Main Propulsion Engine: An Impact Assessment Study. Safety of Marine Transport 175–180.

Arvidson, M., Axelsson, J., Hertzberg, T., n.d. Large-scale fire tests in a passenger cabin.

Astrup, O.C., Wahlstrøm, A.M., King, T., 2016. A framework addressing major accident risk in the maritime industry. Transactions - Society of Naval Architects and Marine Engineers 123, 251–272.

Azizpour, H., 2016. BBN Model with Quantitative Inputs for Risk Analysis of Uncontrolled Fire in Machinery Space. Norwegian University of Science and Technology.

Azzi, C., 2010. Design for Fire Safety Onboard Passenger Ships.

Baalisampang, T., Abbassi, R., Garaniya, V., Khan, F., Dadashzadeh, M., 2018. Review and analysis of fire and explosion accidents in maritime transportation. Ocean Engineering 158, 350–366.

Babrauskas, V., n.d. Estimating Large Pool Fire Burning Rates.

Baker^, R.R., Baker^, B., Coburn, S., Liu, C., Mcadam, K.G., 2016. The science behind the development and performance of reduced ignition propensity cigarettes. Fire Science Reviews 2016 5:1 5, 1–15.

Besnard, D., Hollnagel, E., 2014. I want to believe: Some myths about the management of industrial safety. Cognition, Technology and Work 16, 13–23.

Bolbot, V., Theotokatos, G., Bujorianu, L.M., Boulougouris, E., Vassalos, D., 2019. Vulnerabilities and safety assurance methods in Cyber-Physical Systems: A comprehensive review. Reliab Eng Syst Saf 182, 179–193.

Breinholt, C., Ehrke, K.-C., Papanikolaou, A., Sames, P.C., Skjong, R., Strang, T., Vassalos, D., Witolla, T., 2012. SAFEDOR – The Implementation of Risk-based Ship Design and Approval. Procedia Soc Behav Sci 48, 753–764.

Butt, N., Johnson, D., Pryce-roberts, N., Vigar, N., 2015. 15 Years of Shipping Accidents : A review for WWF Southampton Solent University 44, 37–63.
Bužančić Primorac, B., Parunov, J., 2016. Review of statistical data on ship accidents. Proceedings of 3rd International Conference on Maritime Technology and Engineering, MARTECH 2016 2, 809–814.
Canedy, B.D., Nobles, C., 2003. Boiler Room Blast Kills 4 Crew Members on Cruise Ship. New York Times.
Carlos Guedes Soares, Andrzej Jasionowski, J.J., Dag McGeorge, Apostolos Papanikolaou, E.P., Pierre C. Sames, Rolf Skjong, Jeppe Skovbakke Juhl, D.V., 2009. Risk-Based Ship Design, Risk-Based Ship Design.
Charchalis, A., Czyż, S., 2011. Analysis of fire hazard and safety requirements of a sea vessel engine rooms. Journal of KONES 18, 49–56.
Cicek, K., Turan, H.H., Topcu, Y.I., Searslan, M.N., 2010. Risk-based preventive maintenance planning using Failure Mode and Effect Analysis (FMEA) for marine engine systems. 2010 2nd International Conference on Engineering System Management and Applications, ICESMA 2010 1–6.
Condition assessment programme (CAP) [WWW Document], n.d. URL https://www.dnv.com/services/condition-assessment-programme-cap--17741 (accessed 3.6.23).
Dawson, L., Muna, A., Wheeler, T., Turner, P., Wyss, G., Gibson, M., 2015. Assessment of the Utility and Efficacy of Hazard Analysis Methods for the Prioritization of Critical Digital Assets for Nuclear Power Cyber Security. In: IAEA-CN-228-12.
Defense, D. of, 1998. MIL-HDBK-338B, Electronic Reliablity Design Handbook, Mil-Hdbk-338B.
Det Norske Veritas, 2000. Engine room fires can be prevented.
Det Norske Vertias (DNV), n.d. Failure Frequency Guidance: Process Equipment Leak Frequency Data for use in QRA.
DiNenno, P.J., Drysdale, Dougal., Beyler, C.L., Walton, W.Douglas., Custer, R.L.P., Hall, J.R., Watts, J.M., National Fire Protection Association., Society of Fire Protection Engineers., 2002. SFPE handbook of fire protection engineering. National Fire Protection Association.
DNV, 2001. Marine risk assessment, Offshore Technology Report.
DNV, 2002. Formal Safety Assessment - Large Passenger Ships. Risk: Collision, Contact, Powered Grounding.
DNV, 2006. Level of safety of ships in the period 1999-2004.
DNV, 2018. Open Simulation Platform [WWW Document]. DNV Research Review.
DNV-GL, 2019. Offshore leak detection.
Dokmo Bjørkås, H., 2016. Developing a risk model for fire in passenger ships.
DRShip Europe, n.d. B-15 Fireproof Cabin Door – DRShip [WWW Document]. URL https://drshipeurope.com/marine-accommodation-products/fireproof-marine-doors/b15-doors/b-15-fireproof-cabin-door (accessed 7.15.22).
Drysdale, Dougal., 2011. An introduction to fire dynamics. Wiley.
Eliopoulou Eleftheria, Papanikolaou Apostolos, M.V., 2016. Statistical analysis of ship accidents and review of safety level. Saf Sci 85, 282–292.
EMSA, n.d. Fire safety in ro-ro passenger ships – FIRESAFE studies [WWW Document]. URL http://www.emsa.europa.eu/firesafe.html (accessed 3.17.21).

Engineering Toolbox, n.d. Emissivity Coefficients of Common Products [WWW Document]. URL https://www.engineeringtoolbox.com/emissivity-coefficients-d_447.html (accessed 7.15.22).
Esther Marshall, 2023. Fire breaks out on cruise ship balcony as thousands of guests forced to evacuate cabins [WWW Document]. Express.co.uk. URL https://www.express.co.uk/travel/articles/1775067/fire-cruise-ship-pacific-adventure (accessed 6.7.23).
Feng, C., Chen, J., Deng, W., 2016. Experimental study of combustion characteristics of the airplane aviation carpet.
Fire, S., Analysis, I., 2014. SHIP FIRE INCIDENT ANALYSIS BALTIC SEA MIRG Baltic Sea Maritime Incident Response Group Project.
FIREPROOF consortium, 2010. Project FIREPROOF - Publishable summary.
Ford, M.C., 2012. A Master's Guide to: Using Fuel Oil On-board ships.
Fornes, L., 2016. Goliat Barrier Status Panel. Operational Barrier Management HFC Forum 27–28.
Geiger, G., 2006. State-of-the-art in leak detection and localization. In: Erdoel Erdgas Kohle. pp. 193–198.
George, M., Angus, G., Nikos, T., Richard, P., Philipp, L., 2012. Fire Risk Modelling. In: 11th International Marine Design Conference.
Germanischer Lloyd, 2009. Project SAFEDOR - Press Release.
Goble, W.M., Siebert, J.F., 2008. Field Failure Data – the Good , the Bad and the Ugly.
Golmohamadi, M., 2015. Pipeline leak detection. MISSOURI UNIVERSITY OF SCIENCE AND TECHNOLOGY.
Grønli, M.G., Várhegyi, G., di Blasi, C., 2002. Thermogravimetric analysis and devolatilization kinetics of wood. Ind Eng Chem Res 41, 4201–4208.
Hakkarainen, T., Hietaniemi, J., Hostikka, S., Karhula, T., Kling, T., Mangs, J., Mikkola, E., Oksanen, T., 2009. Survivability for ships in case of fire Final report of SURSHIP-FIRE project, VTT Tiedotteita - Valtion Teknillinen Tutkimuskeskus.
Hall A.R., 1973. Pool burning: a review [WWW Document]. Oxidation and Combustion Reviews. URL https://www.osti.gov/biblio/5325833 (accessed 11.5.22).
Haugen, S., Almklov, P.G., Nilsen, M., Bye, R.J., 2016. Norwegian national ship risk model. In: Proceedings of 3rd International Conference on Maritime Technology and Engineering, MARTECH 2016. pp. 831–838.
Haugen, Stein; Almklov, Petter Grytten; Nilsen, Marie; Bye, R.J., n.d. NTNU Open: Norwegian national ship risk model [WWW Document]. URL https://ntnuopen.ntnu.no/ntnu-xmlui/handle/11250/2483643 (accessed 4.12.21).
Heinrich, H.W., 1941. Industrial Accident Prevention. A Scientific Approach. Industrial Accident Prevention. A Scientific Approach.
Henrie, M., Carpenter, Philip., Nicholas, R.Edward., 2016. Pipeline Leak Detection Handbook.
Hillston, J., 2003. Model validation and verification. Www.Inf.Ed.Ac.Uk/Teaching/Courses/Ms/Notes/Note 14.
Hopkin, C., Spearpoint, M., Hopkin, D., 2019. A Review of Design Values Adopted for Heat Release Rate Per Unit Area. Fire Technol.
Hostikka, S., Keski-Rahkonen, O., 2003. Probabilistic simulation of fire scenarios. Nuclear Engineering and Design 224, 301–311.
Hostikka, S., Olavi, R.-K., Timo, K., n.d. Probabilistic Fire Simulator ( Pfs ).

Hostikka, Simo., Keski-Rahkonen, O., Korhonen, Timo., (Otamedia), 2003. Probabilistic fire simulator : theory and user's manual for version 1.2. Technical Research Centre of Finland.
Hurley, M.J., Gottuk, D., Hall, J.R., Harada, K., Kuligowski, E., Puchovsky, M., Torero, J., Watts, Jj.M., Wieczorek, C., 2016. SFPE Handbook of Fire Protection Engineering, SFPE Handbook of Fire Protection Engineering, Fifth Edition. Springer New York, New York, NY.
IMO, 1996. MSC.57(67): Adoption of amendments to the international convention for the safety of life at sea.pdf.
IMO, 2000. MSC.98(73) - Adoption of the International Code for Fire Safety Systems.
IMO, 2001a. MSC/Circ. 1002: Guidelines on alternative design and arrangements for fire safety.
IMO, 2001b. Guidelines on a simplified calculation for the total amount of combustible materials per unit area in accommodation and service spaces, MSC/Circ.1003.
IMO, 2007. MSC 83/INF.2: Consolidated text of the Guidelines for Formal Safety Assessment (FSA) for use in the IMO rule-making process (MSC/Circ.1023−MEPC/Circ.392).
IMO, 2010. Resolution MSC.307(88) - International Code for Application of Fire Test Procedures (FTP Code).
IMO, 2013. MSC.1/Circ. 1455: Guidelines for the approval of alternatives and equivalents as provided for in various IMO instruments.
IMO, 2014. Safety of Life At Sea.
IMO, 2015a. FSS CODE: International Code for Fire Safety Systems.
IMO, 2015b. International Code for Fire Safety Systems (FSS Code) -.
IMO, 2016a. IMDG Code : International Maritime Dangerous Goods Code - Vol. 2.
IMO, 2016b. IMDG Code : International Maritime Dangerous Goods Code - Vol. 1.
IMO, 2016c. MSC.1/Circ.1552: Amendments to the guidelines on alternative design and arrangements for fire safety.
IMO, 2018a. MSC-MEPC.2/Circ.12/Rev.2: Revised Guidelines for Formal Safety Assessment (FSA) for Use in the IMO Rule-Making Process.
IMO, 2018b. ISM code : International safety management code with guidelines for its implementation., 2018th ed.
IMO, 2019a. MSC.457(101): Amendments to the International Code for Fire Safety Systems (FSS Code).
IMO, 2019b. MSC.1/Circ.1615: Interim guidelines for minimizing the incidence and consequences of fires in Ro-Ro spaces and special category spaces of new and existing Ro-Ro passenger ships.
IMO, 2020. SOLAS Consolidated Edition 2020.
IMO, 2023. MEPC 80/WP.12 - Report of the Working Group on Reduction of GHG emissions from ships (Secretariat).
IMO, n.d. MSC/Circ. 1023: Guidelines for Formal Safety Assessment (FSA) for use in the IMO Rule-Making Process.
IMO - GISIS Report, 2019. Norman Atlantic Incident [WWW Document]. URL https://gisis.imo.org/Public/MCI/Browse.aspx?Form=Incident&Action=View&IncidentID=9510 (accessed 12.28.14).
IMO - Submitted by Denmark, 2008. MSC 85/17/1 | FSA - Cruise Ships.
Institution, B.S., 2018. BSI Standards Publication Failure modes and effects analysis (FMEA and FMECA).

Ioannou, S., 2019. Case study of fire spread in cruise ship public space. National Technical University of Athens, Athens.
Isermann, R., 2011. Fault diagnosis Applications, Fault-Diagnosis Applications.
Isermann, R., 2012. Fault-Diagnostis Systems -- An Introduction from Fault Detection to Fault Tolerance, Springer.
ISOVER, n.d. Technical Insulations: Information for designers and assembly companies.
Janssens, M., 2005. Polymer Flammability.
Jeong, K., Choi, B., Moon, J., Hyun, D., Lee, J., Kim, I., Kim, G., Kang, S., 2016. Risk assessment on abnormal accidents from human errors during decommissioning of nuclear facilities. Ann Nucl Energy 87, 1–6.
Jonassen, Ø., Sjølie, E., 2016. Barrier management in operation for the rig industry - A joint industry project. Offshore Technology Conference Asia 2016, OTCA 2016 388–395.
Jotun, n.d. Jotun - Technical Calculator [WWW Document]. URL https://paintcalculator.z6.web.core.windows.net/ (accessed 7.20.22).
Karlsson, B., Quintiere, J.G., 2000. Enclosure fire dynamics. CRC Press.
Kecklund, L.J., Edland, A., Wedin, P., Svenson, O., 1996. Case study Safety barrier function analysis in a process industry: A nuclear power application, International Journal of Industrial Ergonomics.
Khaleghi, B., Khamis, A., Karray, F.O., Razavi, S.N., 2013. Multisensor data fusion: A review of the state-of-the-art. Information Fusion 14, 28–44.
Khattak, M.A., Mukhtar, A., Azam Khan, K., 2016. Common Root Causes of Pressure Vessel Failures : A Review Akademia Baru. Journal of Advanced Research in Applied Mechanics 21, 22–37.
Kim, D., n.d. What Is Systems Thinking? In: Introduction to Systems Thinking.
Knutsen, E.K., Manno, G., Vartdal, B.J., 2014. Beyond Condition Monitoring in the Maritime Industry.
Konstantinos Milioulis, 2019. Safety Assessment of an LNG Fuelled Vessel Fuel Feeding System.
Krasny, J.F., Parker, W.J., Babrauskas, V., 2007. Fire Behavior of Upholstered Furniture and Mattresses. Fire Behavior of Upholstered Furniture and Mattresses 1–431.
Kritonas Dionysiou, 2019. 4th Year Analysis of Safety Implications for the Power Plant Auxiliary Systems of Cruise Ships.
KROHNE Group, n.d. PipePatrol Leak Detection | KROHNE Group [WWW Document]. URL https://krohne.com/en/solutions/monitoring-solutions/pipepatrol-pipeline-management/pipepatrol-leak-detection/ (accessed 4.24.20).
Krystosik-Gromadzińska, A., 2016. Engine room fire safety. Scientific Journals of the Maritime University of Szczecin 47, 29–35.
Kujath, M.F., Amyotte, P.R., Khan, F.I., 2010. A conceptual offshore oil and gas process accident model. J Loss Prev Process Ind 23, 323–330.
Lauridsen, O., Lootz, E., Husebo, T., Ersdal, G., 2016. Barrier management and the interaction between technical, operational and organisational barrier elements. In: International Conference and Exhibition on Health, Safety, Security, Environment, and Social Responsibility.
Liu, H., Yue, Z., Chybowski, L., 2023. Study of the Relationship between the Level of Lubricating Oil Contamination with Distillation Fuel and the Risk of Explosion in

the Crankcase of a Marine Trunk Type Engine. Energies 2023, Vol. 16, Page 683 16, 683.
Livkiss, K., Andres, B., Bhargava, A., van Hees, P., 2018. Characterization of stone wool properties for fire safety engineering calculations. J Fire Sci 36, 202–223.
Logistics Technology Support Group, N., (CDNSWC), S.W.C., 2010. Handbook of reliability prediction procedures for mechanical equipment, Carderockdiv, NSWC-92/L01.
MADe, 2019. MADe Prognostics and Health Management.
MADe-PHM Technology, 2018a. MADe Module User manual.
MADe-PHM Technology, 2018b. PHM Module User Manual.
Mariska Buitendijk, 2022. Ship fires not decreasing and still a major cause of total loss [WWW Document]. SWZ Maritime.
Maritime Organization, I., 1996. MSC.61(67) - Adoption of the international code for application of fire test procedures.
Martins, J.C., Seleghim, P., 2010. Assessment of the performance of acoustic and mass balance methods for leak detection in pipelines for transporting liquids. Journal of Fluids Engineering, Transactions of the ASME 132, 0114011–0114018.
Martis, M.S., 2006. Validation of simulation based models: A theoretical outlook. Electronic Journal of Business Research Methods 4, 39–46.
Marvin Rausand, A.H., 2004. System Reliability Theory: Models, Statistical Methods, and Applications, 2nd Edition | Wiley.
McGrattan, K., Hostikka, S., Floyd, J., McDermott, R., Vanella, M., 2022a. Fire Dynamics Simulator User's Guide. Gaithersburg, MD.
McGrattan, K., Hostikka, S., Floyd, J., McDermott, R., Vanella, M., 2022b. Fire Dynamics Simulator Technical Reference Guide Volume 3: Validation. Gaithersburg, MD.
McGrattan, K., McDermott, R., Vanella, M., Hostikka, S., Floyd, J., 2022c. Fire Dynamics Simulator Technical Reference Guide Volume 2: Verification. Gaithersburg, MD.
McGrattan, K.B., Hostikka, S., Floyd, J., McDermott, R., Vanella, M., 2004. Fire dynamics simulator : User's Guide. Gaithersburg, MD.
McNay, J., Puisa, R., Vassalos, D., 2019. Analysis of effectiveness of fire safety in machinery spaces. Fire Saf J 108.
Mikulčić, H., Jin, Q., Stančin, H., Wang, X., Li, S., Tan, H., Duić, N., 2019. Thermogravimetric analysis investigation of polyurethane plastic thermal properties under different atmospheric conditions. Journal of Sustainable Development of Energy, Water and Environment Systems 7, 355–367.
Mohd Ismail, M.I., Dziyauddin, R.A., Salleh, N.A.A., Muhammad-Sukki, F., Bani, N.A., Izhar, M.A.M., Latiff, L.A., 2019. A review of vibration detection methods using accelerometer sensors for water pipeline leakage. IEEE Access 7, 51965–51981.
Moir, K., Niculita, O., Milligan, W., n.d. Prognostics and Health Management in the Oil & Gas Industry-A Step Change.
Moltó, J., Font, R., Conesa, J.A., Martín-Gullón, I., 2006. Thermogravimetric analysis during the decomposition of cotton fabrics in an inert and air environment. J Anal Appl Pyrolysis 76, 124–131.
Morgan Advanced Materials, n.d. Marine & Offshore Fire Divisions: Bulkhead, Deck and Floor Systems.

Murvay, P.S., Silea, I., 2012. A survey on gas leak detection and localization techniques. J Loss Prev Process Ind 25, 966–973.

M/V al-Salam Boccaccio 98, 2006. . RINA.

Navas de Maya, B., Komianos, A., Wood, B., de Wolff, L., Kurt, R.E., Turan, O., 2022. A practical application of the Hierarchical Task Analysis (HTA) and Human Error Assessment and Reduction Technique (HEART) to identify the major errors with mitigating actions taken after fire detection onboard passenger vessels. Ocean Engineering 253.

Network, F.C., n.d. Flowmeter Accuracy Matters [WWW Document]. URL https://www.flowcontrolnetwork.com/instrumentation/flow-measurement/turbine/article/15560770/flowmeter-accuracy-matters (accessed 4.24.20).

Niculita, O., Irving, P., Jennions, I.K., 2012. Use of COTS functional analysis software as an IVHM design tool for detection and isolation of UAV fuel system faults. Proceedings of the Annual Conference of the Prognostics and Health Management Society 2012, PHM 2012 28–45.

Niculita, O., Nwora, O., Skaf, Z., 2017. Towards Design of Prognostics and Health Management Solutions for Maritime Assets. Procedia CIRP 59, 122–132.

Nilsen, O.V., 2005. SAFEDOR: FSA for Cruise Ships: Task 4.1.1 - Hazid Identification.

omega.co.uk, n.d. Emissitivity of Common Materials [WWW Document]. URL https://www.omega.co.uk/literature/transactions/volume1/emissivitya.html#s (accessed 7.15.22).

OptaSense, n.d. Leak Detection [WWW Document]. URL https://www.optasense.com/pipeline-monitoring/leak-detection/ (accessed 4.23.20).

OREDA, P., 2009. OREDA : offshore reliability data handbook, 4th ed.. ed, Offshore reliability data handbook. Høvik, Norway : OREDA Participants : Distributed by Der Norske Veritas, Høvik, Norway.

Ostapkowicz, P., 2016. Leak detection in liquid transmission pipelines using simplified pressure analysis techniques employing a minimum of standard and non-standard measuring devices. Eng Struct 113, 194–205.

Over 280 dead in Chinese ferry disaster - World Socialist Web Site [WWW Document], n.d. URL https://www.wsws.org/en/articles/1999/12/chin-d06.html (accessed 2.13.23).

Panchangam, S.P., Naikan, V.N.A., 2013. Reliability analysis of temperature sensor system. International Journal of Reliability, Quality and Safety Engineering 20.

Papanikolaou, A., Bitha, K., Eliopoulou, E., Ventikos, N.P., 2015. Statistical analysis of ship accidents that occurred in the period 1990–2012 and assessment of safety level of ship types. Maritime Technology and Engineering - Proceedings of MARTECH 2014: 2nd International Conference on Maritime Technology and Engineering 1, 227–233.

Pipe, A., n.d. Mass/Volume Balance Solution Description [WWW Document]. URL https://www.atmosi.com/en/products-services/atmos-pipe/ (accessed 4.24.20).

Pitblado, R., Fisher, M., Nelson, B., Fløtaker, H., Molazemi, K., Stokke, A., 2016. Concepts for dynamic barrier management. J Loss Prev Process Ind 43, 741–746.

Prasad, M.H., Reddy, G.R., Srividya, A., Verma, A.K., 2010. Reliability prediction of control valves through mechanistic models 2, 52–57.

Psarros, G., Skjong, R., Eide, M.S., 2010. Under-reporting of maritime accidents. Accid Anal Prev 42, 619–625.
Quintiere, J.G., n.d. Principles of Fire Behavior, 2nd ed.
Rathnayaka, S., Khan, F., Amyotte, P., 2011a. SHIPP methodology: Predictive accident modeling approach. Part II. Validation with case study. Process Safety and Environmental Protection 89, 75–88.
Rathnayaka, S., Khan, F., Amyotte, P., 2011b. SHIPP methodology: Predictive accident modeling approach. Part I: Methodology and model description. Process Safety and Environmental Protection 89, 151–164.
Reason, J., 2000. Human error: Models and management. Br Med J.
RISE Institute, n.d. RI.SE fire access database (ex-SURSHIP-FIRE db) [WWW Document]. URL https://firedb.extweb.sp.se/ (accessed 3.10.23).
Rising, J.M., Leveson, N.G., 2018. Systems-Theoretic Process Analysis of space launch vehicles. Journal of Space Safety Engineering 5, 153–183.
Rudov-Clark, S., Ryan, A., Stecki, C., Stecki, J., 2009. Automated design and optimisation of sensor sets for Condition-Based Monitoring. Proceedings of Thirteenth Australian International Aerospace Congress.
Rudov-Clark, S.D., Ryan, A.J., Stecki, C.M., Stecki, J.S., n.d. Automated design and optimisation of sensor sets for Condition-Based Monitoring.
SafePASS COnsortium, 2022. SafePASS: Next Generation of Life-Saving Appliances and Systems [WWW Document].
Salem, A.M., 2006. Risk-Based Design for Fire Safety of Ro-Ro / Passenger Ships.
Salem, A.M., 2016. Use of Monte Carlo Simulation to assess uncertainties in fire consequence calculation. Ocean Engineering 117, 411–430.
Sargent, R.G., 2010. Verification and validation of simulation models. Proceedings - Winter Simulation Conference 166–183.
SeaRox - Marine & Offshore Insulation, n.d. SeaRox FB 6000 range.
Shama, A.M., El-Rashid, A., El-Shaib, M., Kotb, D.M., 2018. Review of leakage detection methods for subsea pipeline. Maritime Transportation and Harvesting of Sea Resources 2, 1141–1149.
Ship Stability Research Centre (SSRC), 2007. SAFEDOR - Quantitative Risk Analysis (QRA), D 2.5.2.
Siemens, 2017. Siemens – MADe Demonstration • Use Case Walk Thru.
Sinai, Y., Horvat, A., Staples, C., 2007. SAFEDOR D2.5.5: Human Life Safety-Data, Tools and Modelling.
SINTEF, 2002. Offshore Reliability Data Handbook - 4th Edition. OREDA Participants.
SINTEF Technology, 2009. Offshore Reliability Data Handbook 5th Edition.
Skjong, R., Vanem, E., Oyvind, E., 2005. SAFEFOR D4.5.2: Risk Evaluation Criteria.
Sklet, S., 2006. Safety barriers: Definition, classification, and performance. J Loss Prev Process Ind 19, 494–506.
Sobral, J., Guedes Soares, C., 2019. Assessment of the adequacy of safety barriers to hazards. Saf Sci 114, 40–48.
Sondre Øle, Anne Wahlstrøm, Helle Fløtaker, S.R., 2016. Barrier management in operation for the rig industry - Good practices, Offshore Technology Conference Asia 2016, OTCA 2016.
Souglakos, N., 2022. 4th Year Individual Project: Assessment of the Fire Safety of large passenger vessels. Glasgow.
Staffansson, L., 2010. Selecting design fires. Lund.

Stefanidis, F., Oh, D., Ahmed M.P., M., Sotiralis, P., Zagkliveri, T., Podimatas, V., Annetis, E., Hamann, R., 2020. D6.1 SafePASS Risk Model v1.0. Glasgow.
Sulaman, S.M., Beer, A., Felderer, M., Höst, M., 2019. Comparison of the FMEA and STPA safety analysis methods–a case study. Software Quality Journal 27, 349–387.
Sun, Q.-L., Shi, X.-G., Lin, Y.-L., He, Z., Wang, X., Cheng, C.-G., Liu, J.-H., 2007. Thermogravimetric-Mass Spectrometric Study of the Pyrolysis Behavior of PVC, Journal of China University of Mining & Technology.
Tewarson, A., 1982. Experimental Evaluation of Flammability Parameters of Polymeric Materials*. Flame - Retardant Polymeric Materials 3.
Thames Water, n.d. Understanding water pressure | No water/low pressure | Thames Water [WWW Document]. URL https://www.thameswater.co.uk/help-and-advice/no-water-or-low-pressure/understanding-water-pressure (accessed 4.22.20).
Themelis, N., Niotis, S., Spyrou, K.J., 2011. Managing uncertainty in performance-based fire safety assessments of ships, Sustainable Maritime Transportation and Exploitation of Sea Resources.
Themelis, N., Spyrou, K.J., 2010. An efficient methodology for defining probabilistic design fires. In: 4th International Maritime Conference on Design for Safety.
Themelis, N., Spyrou, K.J., 2012. Probabilistic fire safety assessment of passenger ships. Journal of Ship Research 56, 252–275.
Thomas, P.H., Heselden, A.J.M., 1972. Fully developed fires in single compartments. A cooperative research programme of the Conseil Internationale du Bˆatiment .
Troitzsch, J.H., 2016. Fires, statistics, ignition sources, and passive fire protection measures. J Fire Sci 34, 171–198.
US Department of Defence, 1980. MIL-STD-1629A.
Vrijdag, A., Stapersma, D., van Terwisga, T., 2009. Systematic modelling, verification, calibration and validation of a ship propulsion simulation model. Journal of Marine Engineering and Technology 8, 3–20.
Walton, W.D., Twilley, W.H., 1984. Heat release and mass loss rate measurements for selected materials. Gaithersburg, MD.
Wärtsilä, 2007. Wärtsilä 46 Engine Project Guide.
Whaley, R.S., Nicholas, R.E., Reet, J.D.V., 1992. Tutorial on software based leak detection techniques. PSIG Annual Meeting 1992.
Xiang, Y., Du, J., Smedskjaer, M.M., Mauro, J.C., 2013. Structure and properties of sodium aluminosilicate glasses from molecular dynamics simulations. Journal of Chemical Physics 139.
Yuan, S., Yang, M., Reniers, G., Chen, C., Wu, J., 2022. Safety barriers in the chemical process industries: A state-of-the-art review on their classification, assessment, and management. Saf Sci 148, 105647.
Zalok, E., Hadjisophocleous, G. v., Mehaffey, J.R., 2009. Fire loads in commercial premises. Fire Mater 33, 63–78.
Zhang, A., Liu, Y., Barros, A., Wang, Y., 2018. Prognostic and health management for safety barriers in infrastructures : Opportunities and challenges 1035–1042.
Zhang, M., Liu, X., Chen, Z., Wang, J., Song, W., 2014a. Experimental study of the heat flux effect on combustion characteristics of commonly exterior thermal insulation materials. In: Procedia Engineering. Elsevier Ltd, pp. 578–585.

Zhang, M., Liu, X., Chen, Z., Wang, J., Song, W., 2014b. Experimental study of the heat flux effect on combustion characteristics of commonly exterior thermal insulation materials. In: Procedia Engineering. Elsevier Ltd, pp. 578–585.

## Appendix A

Appendix A1

Details of Low-Pressure RPB

The low-pressure fuel oil system and, therefore, of the low-pressure RPB consists of the following sub-systems and respective components:

1. Feed sub-system components:
   1.1. Valve_1_FD_upper
   1.2. Valve_1_FD_lower
   1.3. Valve_2_FD_upper
   1.4. Valve_2_FD_lower
   1.5. Motor 1 & 2
   1.6. Pump 1 & 2
   1.7. Suction Strainer 1 & 2
   1.8. Pipes 1 & 2 (to link flowrate from pump to PCL_1 & 2 sensors) - Modelling assumption.
   1.9. Connecting flow pipe (to merge the flows and allow exit from subsystem) - Modelling assumption.
   1.10. NRValve_FD_upper (non-return valve)
   1.11. NRValve_FD_lower
   1.12. Control Unit 1 - Modelling assumption.
2. Filtering sub-system components:
   2.1. Valve_1_FLT_upper
   2.2. Valve_1_FLT_lower
   2.3. Valve_2_FLT_upper
   2.4. Valve_2_FLT_lower
   2.5. 3wayValve_1_FLT_upper
   2.6. 3wayValve_2_FLT_upper
   2.7. 3wayValve_1_FLT_lower
   2.8. 3wayValve_2_FLT_lower
   2.9. Filter (manual)
   2.10. Auto back-flushing filter
   2.11. Control Unit 2
   2.12. PDI
   2.13. PDAH_FLT
   2.14. Connecting flow pipe FLT. Modelling assumption
   2.15. Branching flow pipes 1 & 2. Modelling assumption
3. Flowmeter sub-system
   3.1. Valve_1_FLM_Lower
   3.2. Valve_2_FLM_Lower
   3.3. Valve_FLM_Upper
   3.4. Non-return Valve_FLM
   3.5. FL_0421
   3.6. Connecting flow pipe FLM
4. De-aeration Tank

5. Venting Valve
6. Booster Sub-system:
    6.1. Valve_1_B
    6.2. Valve_2_B
    6.3. Valve_3_B
    6.4. NRValve_B
    6.5. Motor No.3
    6.6. Booster Pump (No.3)
    6.7. Heater
    6.8. VICALH (visc. sensor that regulates the heater function)
    6.9. TIALH
    6.10. TIC
    6.11. Control Unit 3
7. Control Unit 4
8. Duplex Filter
    8.1. 3-way valve 1 & 2
    8.2. Duplex filters 1 & 2
    8.3. PDAH_DFLT

Note that the nomenclature used above is also utilised in the model created in MADe, to offer consistency and to avoid confusion.

Appendix A2

The high-pressure fuel oil system and, therefore, of the HPRPB consists of the following components:

1. 3-way valve,
2. Pressure damper,
3. SSV,
4. HP_Pump_1,
5. HP_Pump_2,
6. FCV_1,
7. FCV_2
8. Accumulator_1,
9. Accumulator_2,
10. Injection_Valve_1,
11. Injection_Valve_2,
12. Injection_Valve_3,
13. Injection_Valve_4,
14. TE_101
15. PT_101
16. PT155A
17. PT115A
18. PT105
19. FO Return (only for modelling purposes, otherwise, useless in the context of research)
20. Clean Leak FO Drain (as above)
21. Control Unit (as above)

Note that the nomenclature used above is also utilised in the model created in MADe, to offer consistency and to avoid confusion.

## Appendix A3

To create a component, the user must select the function and respective In and Out flows. The “In” and “Out” flows represent the flow characteristics of the in-capture component. For example, the function of a suction strainer, Figure 116, is to refine the flow of fuel oil by removing solid impurities (contamination). Both in and out flows of the component are fuel oil which is translated into “Mixture Liquid-Solid” and the associated flow characteristics are contamination and static pressure. The negative polarity from Contamination to Static Pressure denotes the effect of the former into the later. In summary, depending on the relationship between in and out flows there can be direct or inversely proportional relationship. Following this approach all components were created in MADe.

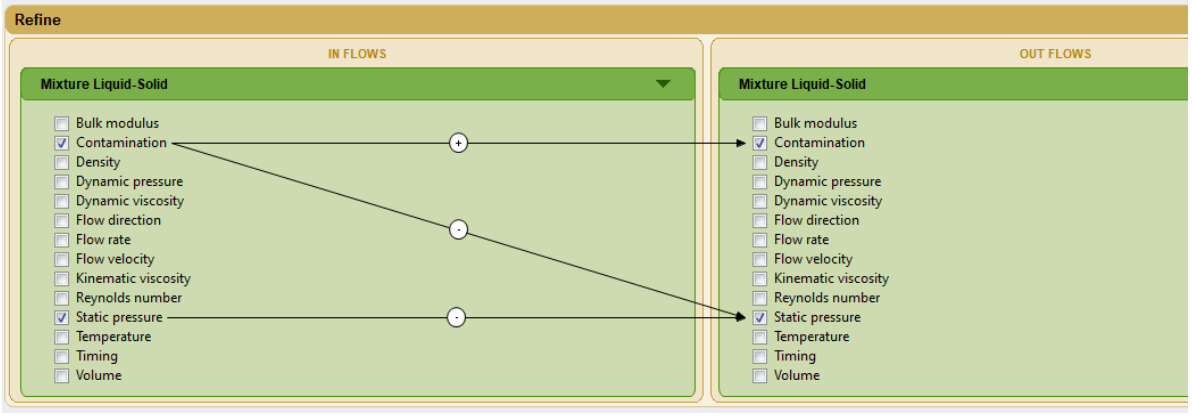


*Figure 116: In flows and out flows of component*

## Appendix A4

Having the sub-systems and components as input the low-pressure fuel oil line FBS can be seen in Figure 34. For consistency, the FBD of the whole system is also shown below, as Figure 117.

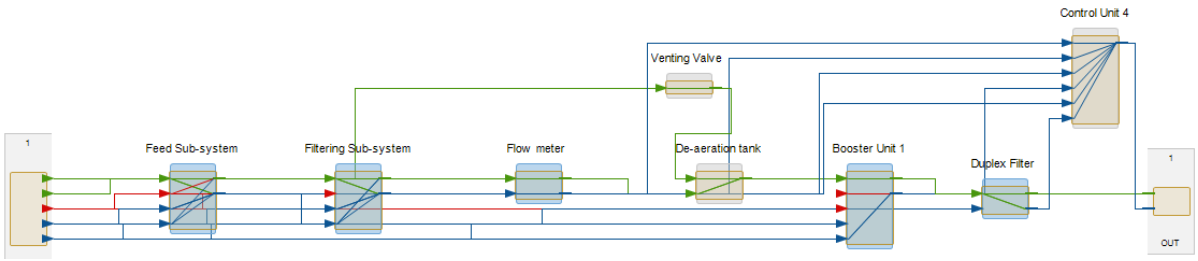


*Figure 117: Functional block diagram of low-pressure FO Line*

Figure 118 represents the Feed sub-system.

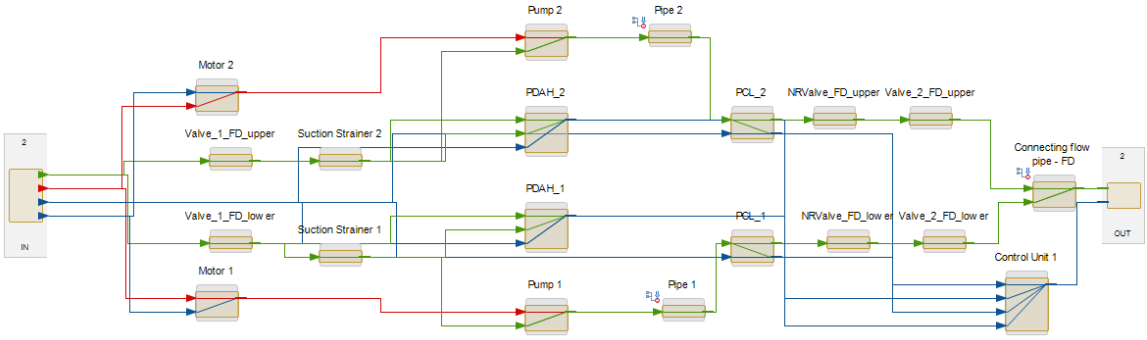


*Figure 118: Feed sub-system FBD*

Figure 119 represents the flowmeter sub-system.

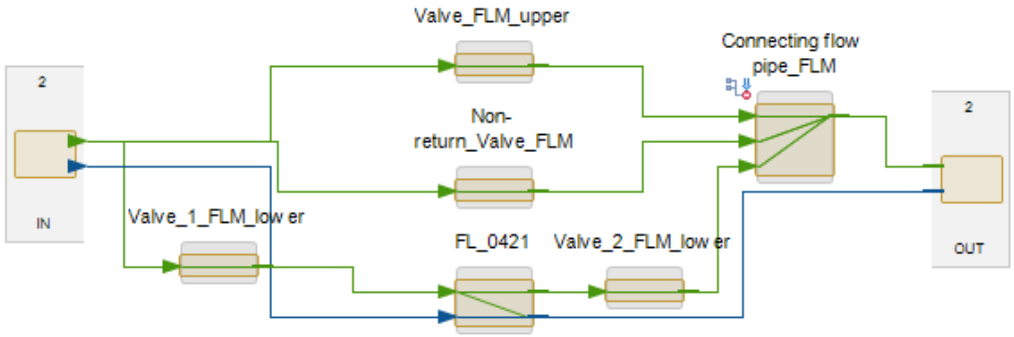


*Figure 119: Flowmeter sub-system FBD*

Figure 120 represents the booster sub-system.

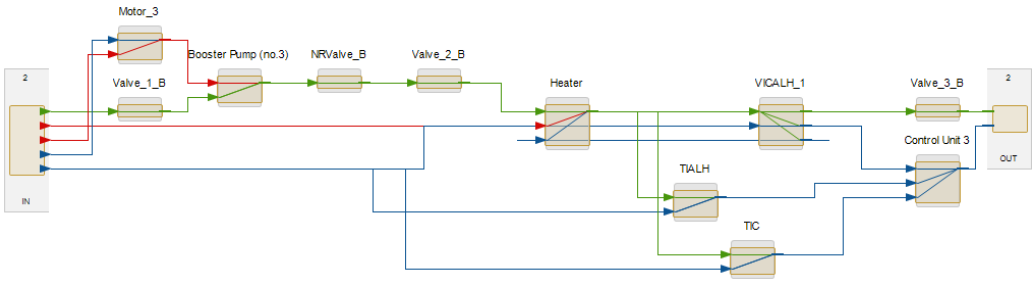


*Figure 120: Booster sub-system FBD*

Figure 121 represents the duplex filter sub-system.

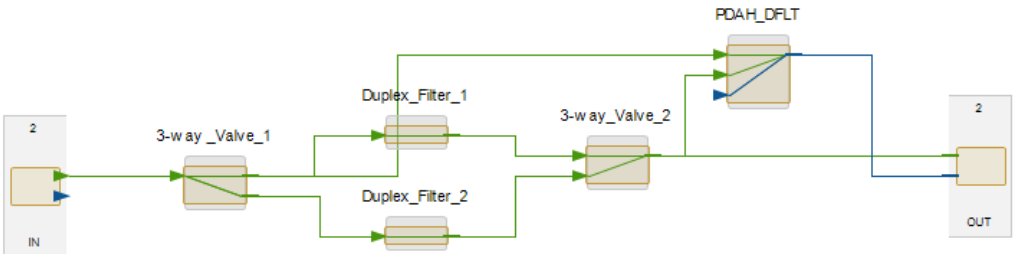


*Figure 121: Duplex Filter sub-system*

The figures above conclude the presentation of the low-pressure technical element of the RPB functional block diagram.

Appendix A5

Table 20 presents all failure modes of each component in the LPRPB per sub-system as identified in the relevant literature.

*Table 20. LPRPB components failure modes.*

| **Sub-system** | **Component** | **Failure Mode** |
|---|---|---|
| Feed Sub-system | Motor | Open Circuit |
| | | Electrical Potential Decreased |
| | | Fractured |
| | | Property Mismatch |
| | Pump | Fractured |
| | | Abraded |
| | Suction Strainer | Blocked |
| | | Loose |
| | Differential Pressure Sensor | Open Circuit |
| | | Electrical Potential Decreased |
| | | Dielectric Strength Decreased |
| | | Property Mismatch |
| | Pressure Sensor (Transducer) | Open Circuit |
| | | Electrical Potential Decreased |
| | | Dielectric Strength Decreased |
| | | Property Mismatch |
| | Valve | Abraded |
| | | Cracked |
| | No-return Valve | Abraded |
| | | Cracked |
| Filtering Sub-system | Valve | Abraded |
| | | Cracked |
| | 3-way Valve | Abraded |
| | | Cracked |
| | Filter | Blocked |
| | | Loose |
| | Auto back-flushing Filter | Blocked |
| | | Open Circuit |
| | | Electrical Potential Decreased |
| | | Open Circuit |

| | | |
|---|---|---|
| | Differential Pressure Sensors | Electrical Potential Decreased |
| | | Dielectric Strength Decreased |
| | | Property Mismatch |
| Flowmeter | Valve | Abraded |
| | | Cracked |
| | No-return Valve | Abraded |
| | | Cracked |
| | Flowmeter Sensor | Open Circuit |
| | | Electrical Potential Decreased |
| | | Dielectric Strength Decreased |
| | | Property Mismatch |
| N/A | De-aeration Tank | Corroded |
| | | Perforated |
| Booster Sub-system | Valve | Abraded |
| | | Cracked |
| | No-return Valve | Abraded |
| | | Cracked |
| | Motor (booster pump) | Open Circuit |
| | | Electrical Potential Decreased |
| | | Fractured |
| | | Property Mismatch |
| | Pump | Fractured |
| Booster Sub-system (Continued) | Valve | Abraded |
| | | Cracked |
| | | Electrical Potential Decreased |
| | | Dielectric Strength Decreased |
| | | Property Mismatch |
| | Heater | Oxidized |
| | | Perforated |
| | | Blocked |

| | | |
|---|---|---|
| N/A | Venting Valve | Abraded |
| | | Cracked |
| Duplex Filter | Filter | Blocked |
| | | Loose |
| | 3-way Valve | Abraded |
| | | Cracked |

Appendix A6

Symbol “i” indicates the time instances that the qualitative simulation was run. A red cell has the value “-1” which implies that the reaction was less, i.e. the pressure dropped. Table 21 presents the complete step response table for the diagnostic what-if simulation for a low pressure failure injection on Valve_1_FD_upper, in relation to the response presented in Figure 37.

*Table 21: Step response table for low pressure failure injection on Valve_1_FD_upper in the LPRPB*

| Component | Flow Property | i | 1 | 2 | 3 | 4 | 5 | 6 | 7 | 8 | 9 | 10 | 11 | 12 | 13 | 14 | 15 | 16 | 17 | 18 | 19 | = |
|---|---|---|---|---|---|---|---|---|---|---|---|---|---|---|---|---|---|---|---|---|---|---|
| 3-way _Valve_1 | Mixture Liquid-Solid Static pressure | | | | | | | | | | | | | | | | | | | | | 0 |
| 3-way _Valve_1 | Mixture Liquid-Solid Static pressure | | | | | | | | | | | | | | | | | | | | | 0 |
| 3-way _Valve_1 | Mixture Liquid-Solid Contamination | | | | | | | | | | | | | | | | | | | | | 0 |
| 3-way _Valve_1 | Mixture Liquid-Solid Contamination | | | | | | | | | | | | | | | | | | | | | 0 |
| 3-way_Valve_2 | Liquid Static pressure | | | | | | | | | | | | | | | | | | | | | 0 |
| 3wayValve_1_FLT_lower | Mixture Liquid-Solid Contamination | | | | | | | | | | | | | | | | | | | | | 0 |
| 3wayValve_1_FLT_lower | Mixture Liquid-Solid Static pressure | | | | | | | | | | | | | -1 | -1 | -1 | -1 | -1 | -1 | -1 | -1 | -1 |
| 3wayValve_1_FLT_upper | Mixture Liquid-Solid Contamination | | | | | | | | | | | | | | | | | | | | | 0 |
| 3wayValve_1_FLT_upper | Mixture Liquid-Solid Static pressure | | | | | | | | | | | | | -1 | -1 | -1 | -1 | -1 | -1 | -1 | -1 | -1 |
| 3wayValve_2_FLT_lower | Mixture Liquid-Solid Contamination | | | | | | | | | | | | | | | | | | | | | 0 |
| 3wayValve_2_FLT_lower | Mixture Liquid-Solid Static pressure | | | | | | | | | | | | | | -1 | -1 | -1 | -1 | -1 | -1 | -1 | -1 |

| | | | | | | | | | | | | | | | | | | | | | |
|---|---|---|---|---|---|---|---|---|---|---|---|---|---|---|---|---|---|---|---|---|---|
| 3wayValve_2_FLT_upper | Mixture Liquid-Solid Static pressure | | | | | | | | | | | | | -1 | -1 | -1 | -1 | -1 | -1 | -1 | -1 |
| 3wayValve_2_FLT_upper | Mixture Liquid-Solid Contamination | | | | | | | | | | | | | | | | | | | | 0 |
| Auto back-flushing filter | Mixture Liquid-Solid Contamination | | | | | | | | | | | | | | | | | | | | 0 |
| Auto back-flushing filter | Mixture Liquid-Solid Static pressure | | | | | | | | | | | | -1 | -1 | -1 | -1 | -1 | -1 | -1 | -1 | -1 |
| Booster Pump (no.3) | Mixture Liquid-Solid Contamination | | | | | | | | | | | | | | | | | | | | 0 |
| Booster Pump (no.3) | Mixture Liquid-Solid Flow rate | | | | | | | | | | | | | | | | | | | | 0 |
| Booster Unit 1 | Discrete Data | | | | | | | | | | | | | | | | | | | | 0 |
| Booster Unit 1 | Mixture Liquid-Solid Contamination | | | | | | | | | | | | | | | | | | | | 0 |
| Booster Unit 1 | Mixture Liquid-Solid Static pressure | | | | | | | | | | | | | | | | | | | | 0 |
| Branching flow pipe 1_FLT | Mixture Liquid-Solid Contamination | | | | | | | | | | | | | | | | | | | | 0 |
| Branching flow pipe 1_FLT | Mixture Liquid-Solid Static pressure | | | | | | | | | | | -1 | -1 | -1 | -1 | -1 | -1 | -1 | -1 | -1 | -1 |
| Branching flow pipe 1_FLT | Mixture Liquid-Solid Static pressure | | | | | | | | | | | -1 | -1 | -1 | -1 | -1 | -1 | -1 | -1 | -1 | -1 |
| Branching flow pipe 1_FLT | Mixture Liquid-Solid Contamination | | | | | | | | | | | | | | | | | | | | 0 |
| Branching flow pipe 2_FLT | Mixture Liquid-Solid Contamination | | | | | | | | | | | | | | | | | | | | 0 |
| Branching flow pipe 2_FLT | Mixture Liquid-Solid Static pressure | | | | | | | | | | | -1 | -1 | -1 | -1 | -1 | -1 | -1 | -1 | -1 | -1 |
| Branching flow pipe 2_FLT | Mixture Liquid-Solid Static pressure | | | | | | | | | | | -1 | -1 | -1 | -1 | -1 | -1 | -1 | -1 | -1 | -1 |
| Branching flow pipe 2_FLT | Mixture Liquid-Solid Contamination | | | | | | | | | | | | | | | | | | | | 0 |
| Connecting flow pipe_FLM | Mixture Liquid-Solid Static pressure | | | | | | | | | | | | | | | | | -1 | -1 | -1 | -1 |

| | | | | | | | | | | | | | | | | | | | | | | |
|---|---|---|---|---|---|---|---|---|---|---|---|---|---|---|---|---|---|---|---|---|---|---|
| Connecting flow pipe_FLM | Mixture Liquid-Solid Contamination | | | | | | | | | | | | | | | | | | | | | 0 |
| Connecting flow pipe - FD | Mixture Liquid-Solid Contamination | | | | | | | | | | | | | | | | | | | | | 0 |
| Connecting flow pipe - FD | Mixture Liquid-Solid Static pressure | | | | | | | | | -1 | -1 | -1 | -1 | -1 | -1 | -1 | -1 | -1 | -1 | -1 | -1 | -1 |
| Connecting flow pipe - FLT | Mixture Liquid-Solid Static pressure | | | | | | | | | | | | | | | -1 | -1 | -1 | -1 | -1 | -1 | -1 |
| Connecting flow pipe - FLT | Mixture Liquid-Solid Contamination | | | | | | | | | | | | | | | | | | | | | 0 |
| Control Unit 1 | Discrete Data | | | | -1 | -1 | -1 | -1 | -1 | -1 | -1 | -1 | -1 | -1 | -1 | -1 | -1 | -1 | -1 | -1 | -1 | -1 |
| Control Unit 2 | Discrete Data | | | | | | | | | | | | | | | -1 | -1 | -1 | -1 | -1 | -1 | -1 |
| Control Unit 3 | Discrete Data | | | | | | | | | | | | | | | | | | | | | 0 |
| Control Unit 4 | Discrete Data | | | | | | -1 | -1 | -1 | -1 | -1 | -1 | -1 | -1 | -1 | -1 | -1 | -1 | -1 | -1 | -1 | -1 |
| De-aeration tank | Mixture Liquid-Solid Contamination | | | | | | | | | | | | | | | | | | | | | 0 |
| De-aeration tank | Mixture Liquid-Solid Static pressure | | | | | | | | | | | | | | | | | | | | -1 | -1 |
| Duplex_Filter_1 | Liquid Static pressure | | | | | | | | | | | | | | | | | | | | | 0 |
| Duplex_Filter_2 | Liquid Static pressure | | | | | | | | | | | | | | | | | | | | | 0 |
| Duplex Filter | Liquid Static pressure | | | | | | | | | | | | | | | | | | | | | 0 |
| Duplex Filter | Discrete Data | | | | | | | | | | | | | | | | | | | | | 0 |
| Feed Sub-system | Discrete Data | | | | | -1 | -1 | -1 | -1 | -1 | -1 | -1 | -1 | -1 | -1 | -1 | -1 | -1 | -1 | -1 | -1 | -1 |
| Feed Sub-system | Mixture Liquid-Solid Static pressure | | | | | | | | | | -1 | -1 | -1 | -1 | -1 | -1 | -1 | -1 | -1 | -1 | -1 | -1 |
| Feed Sub-system | Mixture Liquid-Solid Contamination | | | | | | | | | | | | | | | | | | | | | 0 |
| Filter (manual) | Mixture Liquid-Solid Contamination | | | | | | | | | | | | | | | | | | | | | 0 |
| Filter (manual) | Mixture Liquid-Solid Static pressure | | | | | | | | | | | | | -1 | -1 | -1 | -1 | -1 | -1 | -1 | -1 | -1 |
| Filtering Sub-system | Discrete Data | | | | | | | | | | | | | | | | -1 | -1 | -1 | -1 | -1 | -1 |

| | | | | | | | | | | | | | | | | | | | | | | |
|---|---|---|---|---|---|---|---|---|---|---|---|---|---|---|---|---|---|---|---|---|---|---|
| Filtering Sub-system | Mixture Liquid-Solid Contamination | | | | | | | | | | | | | | | | | | | | | 0 |
| Filtering Sub-system | Mixture Liquid-Solid Static pressure | | | | | | | | | | | | | | | | -1 | -1 | -1 | -1 | -1 | -1 |
| FL_0421 | Mixture Liquid-Solid Contamination | | | | | | | | | | | | | | | | | | | | | 0 |
| FL_0421 | Discrete Data | | | | | | | | | | | | | | | | | | | | | 0 |
| Flow meter | Mixture Liquid-Solid Contamination | | | | | | | | | | | | | | | | | | | | | 0 |
| Flow meter | Discrete Data | | | | | | | | | | | | | | | | | | | | | 0 |
| Flow meter | Mixture Liquid-Solid Static pressure | | | | | | | | | | | | | | | | | | | -1 | -1 | -1 |
| Fuel Oil Feed System | Generic Amplitude | | | | | | | | | | | | | | | | | | | | | 0 |
| Fuel Oil Feed System | Liquid Static pressure | | | | | | | | | | | | | | | | | | | | | 0 |
| Fuel Oil Feed System | Discrete Data | | | | | | | -1 | -1 | -1 | -1 | -1 | -1 | -1 | -1 | -1 | -1 | -1 | -1 | -1 | -1 | -1 |
| Fuel Oil Feed System | Electrical Voltage | | | | | | | | | | | | | | | | | | | | | 0 |
| Fuel Oil Feed System | Generic Data | | | | | | | | | | | | | | | | | | | | | 0 |
| Fuel Oil Feed System | Mixture Gas-Liquid Static pressure | | | | | | | | | | | | | | | | | | | | | 0 |
| Fuel Oil Feed System | Continuous Amplitude | | | | | | | | | | | | | | | | | | | | | 0 |
| Fuel Oil Feed System | Continuous Frequency | | | | | | | | | | | | | | | | | | | | | 0 |
| Fuel Oil Feed System | Mixture Liquid-Solid Static pressure | | | | | | | | | | | | | | | | | | | | | 0 |
| Fuel Oil Feed System | Mixture Liquid-Solid Contamination | | | | | | | | | | | | | | | | | | | | | 0 |
| Heater | Mixture Liquid-Solid Temperature | | | | | | | | | | | | | | | | | | | | | 0 |
| Heater | Mixture Liquid-Solid Static pressure | | | | | | | | | | | | | | | | | | | | | 0 |
| Heater | Mixture Liquid-Solid Contamination | | | | | | | | | | | | | | | | | | | | | 0 |
| Motor_3 | Mechanical - rotational Angular velocity | | | | | | | | | | | | | | | | | | | | | 0 |

| | | | | | | | | | | | | | | | | | | | | | | |
|---|---|---|---|---|---|---|---|---|---|---|---|---|---|---|---|---|---|---|---|---|---|---|
| Motor 1 | Mechanical - rotational Angular velocity | | | | | | | | | | | | | | | | | | | | | 0 |
| Motor 2 | Mechanical - rotational Angular velocity | | | | | | | | | | | | | | | | | | | | | 0 |
| Non-return_Valve_FLM | Mixture Liquid-Solid Static pressure | | | | | | | | | | | | | | | | -1 | -1 | -1 | -1 | -1 | -1 |
| Non-return_Valve_FLM | Mixture Liquid-Solid Contamination | | | | | | | | | | | | | | | | | | | | | 0 |
| NRValve_B | Mixture Liquid-Solid Static pressure | | | | | | | | | | | | | | | | | | | | | 0 |
| NRValve_B | Mixture Liquid-Solid Contamination | | | | | | | | | | | | | | | | | | | | | 0 |
| NRValve_FD_lower | Mixture Liquid-Solid Contamination | | | | | | | | | | | | | | | | | | | | | 0 |
| NRValve_FD_lower | Mixture Liquid-Solid Static pressure | | | | | | | | | | | | | | | | | | | | | 0 |
| NRValve_FD_upper | Mixture Liquid-Solid Contamination | | | | | | | | | | | | | | | | | | | | | 0 |
| NRValve_FD_upper | Mixture Liquid-Solid Static pressure | | | | | | | -1 | -1 | -1 | -1 | -1 | -1 | -1 | -1 | -1 | -1 | -1 | -1 | -1 | -1 | -1 |
| PCL_1 | Mixture Liquid-Solid Contamination | | | | | | | | | | | | | | | | | | | | | 0 |
| PCL_1 | Discrete Data | | | | | | | | | | | | | | | | | | | | | 0 |
| PCL_1 | Mixture Liquid-Solid Static pressure | | | | | | | | | | | | | | | | | | | | | 0 |
| PCL_2 | Mixture Liquid-Solid Static pressure | | | | | | -1 | -1 | -1 | -1 | -1 | -1 | -1 | -1 | -1 | -1 | -1 | -1 | -1 | -1 | -1 | -1 |
| PCL_2 | Discrete Data | | | | | | -1 | -1 | -1 | -1 | -1 | -1 | -1 | -1 | -1 | -1 | -1 | -1 | -1 | -1 | -1 | -1 |
| PDAH_1 | Discrete Data | | | | | | | | | | | | | | | | | | | | | 0 |
| PDAH_2 | Discrete Data | | | -1 | -1 | -1 | -1 | -1 | -1 | -1 | -1 | -1 | -1 | -1 | -1 | -1 | -1 | -1 | -1 | -1 | -1 | -1 |
| PDAH_DFLT | Discrete Data | | | | | | | | | | | | | | | | | | | | | 0 |
| PDAH_FLT | Discrete Data | | | | | | | | | | | | | | -1 | -1 | -1 | -1 | -1 | -1 | -1 | -1 |
| PDI | Discrete Data | | | | | | | | | | | | | | -1 | -1 | -1 | -1 | -1 | -1 | -1 | -1 |

| | | | | | | | | | | | | | | | | | | | | | | |
|---|---|---|---|---|---|---|---|---|---|---|---|---|---|---|---|---|---|---|---|---|---|---|
| Pipe 1 | Mixture Liquid-Solid Static pressure | | | | | | | | | | | | | | | | | | | | | 0 |
| Pipe 1 | Mixture Liquid-Solid Contamination | | | | | | | | | | | | | | | | | | | | | 0 |
| Pipe 2 | Mixture Liquid-Solid Static pressure | | | | | -1 | -1 | -1 | -1 | -1 | -1 | -1 | -1 | -1 | -1 | -1 | -1 | -1 | -1 | -1 | -1 | -1 |
| Pipe 2 | Mixture Liquid-Solid Contamination | | | | | | | | | | | | | | | | | | | | | 0 |
| Pump 1 | Mixture Liquid-Solid Contamination | | | | | | | | | | | | | | | | | | | | | 0 |
| Pump 1 | Mixture Liquid-Solid Flow rate | | | | | | | | | | | | | | | | | | | | | 0 |
| Pump 2 | Mixture Liquid-Solid Contamination | | | | | | | | | | | | | | | | | | | | | 0 |
| Pump 2 | Mixture Liquid-Solid Flow rate | | | | -1 | -1 | -1 | -1 | -1 | -1 | -1 | -1 | -1 | -1 | -1 | -1 | -1 | -1 | -1 | -1 | -1 | -1 |
| Suction Strainer 1 | Mixture Liquid-Solid Contamination | | | | | | | | | | | | | | | | | | | | | 0 |
| Suction Strainer 1 | Mixture Liquid-Solid Static pressure | | | | | | | | | | | | | | | | | | | | | 0 |
| Suction Strainer 2 | Mixture Liquid-Solid Static pressure | | | -1 | -1 | -1 | -1 | -1 | -1 | -1 | -1 | -1 | -1 | -1 | -1 | -1 | -1 | -1 | -1 | -1 | -1 | -1 |
| Suction Strainer 2 | Mixture Liquid-Solid Contamination | | | | | | | | | | | | | | | | | | | | | 0 |
| TIALH | Discrete Data | | | | | | | | | | | | | | | | | | | | | 0 |
| TIC | Discrete Data | | | | | | | | | | | | | | | | | | | | | 0 |
| Valve_1_B | Mixture Liquid-Solid Static pressure | | | | | | | | | | | | | | | | | | | | | 0 |
| Valve_1_B | Mixture Liquid-Solid Contamination | | | | | | | | | | | | | | | | | | | | | 0 |
| Valve_1_FD_lower | Mixture Liquid-Solid Contamination | | | | | | | | | | | | | | | | | | | | | 0 |
| Valve_1_FD_lower | Mixture Liquid-Solid Static pressure | | | | | | | | | | | | | | | | | | | | | 0 |
| Valve_1_FD_upper | Mixture Liquid-Solid Static pressure | | -1 | -1 | -1 | -1 | -1 | -1 | -1 | -1 | -1 | -1 | -1 | -1 | -1 | -1 | -1 | -1 | -1 | -1 | -1 | -1 |

| | | | | | | | | | | | | | | | | | | | | | | |
|---|---|---|---|---|---|---|---|---|---|---|---|---|---|---|---|---|---|---|---|---|---|---|
| Valve_1_FD_upper | Mixture Liquid-Solid Contamination | | | | | | | | | | | | | | | | | | | | | 0 |
| Valve_1_FLM_lower | Mixture Liquid-Solid Contamination | | | | | | | | | | | | | | | | | | | | | 0 |
| Valve_1_FLM_lower | Mixture Liquid-Solid Static pressure | | | | | | | | | | | | | | | | | -1 | -1 | -1 | -1 | -1 |
| Valve_1_FLT_lower | Mixture Liquid-Solid Static pressure | | | | | | | | | | -1 | -1 | -1 | -1 | -1 | -1 | -1 | -1 | -1 | -1 | -1 | -1 |
| Valve_1_FLT_lower | Mixture Liquid-Solid Contamination | | | | | | | | | | | | | | | | | | | | | 0 |
| Valve_1_FLT_upper | Mixture Liquid-Solid Contamination | | | | | | | | | | | | | | | | | | | | | 0 |
| Valve_1_FLT_upper | Mixture Liquid-Solid Static pressure | | | | | | | | | | -1 | -1 | -1 | -1 | -1 | -1 | -1 | -1 | -1 | -1 | -1 | -1 |
| Valve_2_B | Mixture Liquid-Solid Static pressure | | | | | | | | | | | | | | | | | | | | | 0 |
| Valve_2_B | Mixture Liquid-Solid Contamination | | | | | | | | | | | | | | | | | | | | | 0 |
| Valve_2_FD_lower | Mixture Liquid-Solid Contamination | | | | | | | | | | | | | | | | | | | | | 0 |
| Valve_2_FD_lower | Mixture Liquid-Solid Static pressure | | | | | | | | | | | | | | | | | | | | | 0 |
| Valve_2_FD_upper | Mixture Liquid-Solid Static pressure | | | | | | | -1 | -1 | -1 | -1 | -1 | -1 | -1 | -1 | -1 | -1 | -1 | -1 | -1 | -1 | -1 |
| Valve_2_FD_upper | Mixture Liquid-Solid Contamination | | | | | | | | | | | | | | | | | | | | | 0 |
| Valve_2_FLM_lower | Mixture Liquid-Solid Contamination | | | | | | | | | | | | | | | | | | | | | 0 |
| Valve_2_FLM_lower | Mixture Liquid-Solid Static pressure | | | | | | | | | | | | | | | | | | | | | 0 |
| Valve_2_FLT_lower | Mixture Liquid-Solid Static pressure | | | | | | | | | | | | | -1 | -1 | -1 | -1 | -1 | -1 | -1 | -1 | -1 |
| Valve_2_FLT_lower | Mixture Liquid-Solid Contamination | | | | | | | | | | | | | | | | | | | | | 0 |
| Valve_2_FLT_upper | Mixture Liquid-Solid Contamination | | | | | | | | | | | | | | | | | | | | | 0 |

| | | | | | | | | | | | | | | | | | | | | | | | |
|---|---|---|---|---|---|---|---|---|---|---|---|---|---|---|---|---|---|---|---|---|---|---|---|
| Valve_2_FLT_upper | Mixture Liquid-Solid Static pressure | | | | | | | | | | | | | | -1 | -1 | -1 | -1 | -1 | -1 | -1 | -1 |
| Valve_3_B | Mixture Liquid-Solid Static pressure | | | | | | | | | | | | | | | | | | | | | 0 |
| Valve_3_B | Mixture Liquid-Solid Contamination | | | | | | | | | | | | | | | | | | | | | 0 |
| Valve_FLM_upper | Mixture Liquid-Solid Static pressure | | | | | | | | | | | | | | | | | -1 | -1 | -1 | -1 | -1 |
| Valve_FLM_upper | Mixture Liquid-Solid Contamination | | | | | | | | | | | | | | | | | | | | | 0 |
| Venting Valve | Liquid Static pressure | | | | | | | | | | | | | | | | | | | | | 0 |
| VICALH_1 | Mixture Liquid-Solid Static pressure | | | | | | | | | | | | | | | | | | | | | 0 |
| VICALH_1 | Discrete Data | | | | | | | | | | | | | | | | | | | | | 0 |
| VICALH_1 | Generic Data | | | | | | | | | | | | | | | | | | | | | 0 |
| VICALH_1 | Mixture Liquid-Solid Contamination | | | | | | | | | | | | | | | | | | | | | 0 |

Appendix A7

Table 22 presents the detailed table of the FMECA conducted for the low-pressure RPB technical element, along with relevant scoring for the Occurrence, including the corresponding failure rate λ ($10^{-6}$ hrs), Severity, and Detection, including the corresponding risk priority number.

*Table 22: Detailed FMECA Table for LPRPB*

| Sub-system | Component | Failure Mode | Failure End Effect | Detection Method | Occurrence | Severity | Detection | RPN | λ |
|---|---|---|---|---|---|---|---|---|---|
| Feed Sub-system | Motor | Open Circuit | No FO delivered to M/E from that particular "line" (feed line is duplicated for redundancy) | Sensor | 4 | 2 | 2 | 16 | 3.65E-05 |
| | | Electrical Potential Decreased | | | | | | | |
| | | Fractured | | | | | | | |
| | | Property Mismatch | | | | | | | |
| | Pump | Fractured | Ditto | None (visual inspection) | 3 | 2 | 10 | 60 | 7.70E-04 |
| | | Abraded | | | | | | | |
| | Suction Strainer | Blocked | Fuel oil cannot go through the filtering element | Pressure difference sensor | 6 | 10 | 5 | 300 | 1.37E-03 |
| | | Loose | Fuel oil leak | None (visual inspection) | | | | | |
| | Differential Pressure Sensor | Open Circuit | Faulty or no measurement. Filters could clog without any indication of happening, therefore, FO might not be delivered | None (conservative assumption: sensors do not have a self-diagnosing capability, so manual check for | 4 | 2 | 10 | 80 | 6.56E-05 |
| | | Electrical Potential Decreased | | | | | | | |
| | | Dielectric Strength Decreased | | | | | | | |

| | | | | | | | | | |
|---|---|---|---|---|---|---|---|---|---|
| | | Property Mismatch | | confirming operation) | | | | | |
| | Pressure Sensor (Transducer) | Open Circuit | Faulty or no measurement. Filters could clog without any indication of happening, therefore, FO might not be delivered | Ditto | 3 | 2 | 10 | 60 | 8.31E-06 |
| | | Electrical Potential Decreased | | | | | | | |
| | | Dielectric Strength Decreased | | | | | | | |
| | | Property Mismatch | | | | | | | |
| | Valve | Abraded | Fuel oil leak | None (visual inspection) | 3 | 10 | 10 | 300 | 1.78E-05 |
| | | Cracked | | | | | | | |
| | No-return Valve | Abraded | Fuel Oil Leak | None (visual inspection) | 3 | 10 | 10 | 300 | 1.78E-05 |
| | | Cracked | | | | | | | |
| Filtering Sub-system | Valve | Abraded | Fuel oil leak | None (visual inspection) | 3 | 10 | 10 | 300 | 1.78E-05 |
| | | Cracked | | | | | | | |
| | 3-way Valve | Abraded | Fuel oil leak | None (visual inspection) | 3 | 10 | 10 | 300 | 1.78E-05 |
| | | Cracked | | | | | | | |
| | Filter | Blocked | Fuel oil cannot go through the filtering element | Pressure difference sensor | 6 | 10 | 5 | 300 | 1.37E-03 |
| | | Loose | Fuel oil leak | None (visual inspection) | | | | | |
| | Auto back-flushing Filter | Blocked | No or degraded fuel oil output | Pressure difference sensor | 5 | 8 | 2 | 80 | 4.57E-04 |
| | | Open Circuit | | | | | | | |
| | | Electrical Potential Decreased | | | | | | | |
| | | Open Circuit | Faulty or no measurement. Filters | None (conservative | 4 | 2 | 10 | 80 | 6.56E-05 |

| | | | | | | | | | |
|---|---|---|---|---|---|---|---|---|---|
| | Differential Pressure Sensors | Electrical Potential Decreased<br>Dielectric Strength Decreased<br>Property Mismatch | could clog without any indication of happening, therefore, FO might not be delivered | assumption: sensors do not have a self-diagnosing capability, so manual check for confirming operation) | | | | | |
| Flowmeter | Valve | Abraded<br>Cracked | Fuel oil leak | Visual Inspection | 3 | 10 | 10 | 300 | 1.78E-05 |
| | No-return Valve | Abraded<br>Cracked | Fuel Oil Leak | None (visual inspection) | 3 | 10 | 10 | 300 | 1.78E-05 |
| | Flowmeter Sensor | Open Circuit<br>Electrical Potential Decreased<br>Dielectric Strength Decreased<br>Property Mismatch | Faulty or no measurement, fuel oil might be consumed but it will not be, or improperly, logged. | No fuel oil flow readings logged or shown in the ECR | 3 | 6 | 4 | 72 | 8.31E-06 |
| N/A | De-aeration Tank | Corroded<br>Perforated | Less or no fuel reaches the booster unit and, consequently, the engine | Possibly the level alarm sensor | 1 | 7 | 4 | 28 | 6.67E-07 |
| Booster Sub-system | Valve | Abraded<br>Cracked | Fuel oil leak | Visual Inspection | 3 | 10 | 10 | 300 | 1.78E-05 |
| | No-return Valve | Abraded<br>Cracked | Fuel Oil Leak | None (visual inspection) | 3 | 10 | 10 | 300 | 1.78E-05 |
| | | Open Circuit | No fuel delivered to M/E | Sensor | 4 | 8 | 2 | 64 | 3.65E-05 |

| | | | | | | | | | |
|---|---|---|---|---|---|---|---|---|---|
| | Motor (booster pump) | Electrical Potential Decreased | | | | | | | |
| | | Fractured | | | | | | | |
| | | Property Mismatch | | | | | | | |
| | Pump | Fractured | No fuel delivered to M/E | None (visual inspection) | 2 | 8 | 10 | 160 | 8.28E-06 |
| | | Abraded | | | | | | | |
| | Temperature & Viscosity Sensors | Open Circuit | Faulty or no measurement. Viscosity sensor regulates the heat output of the heater, wrong FO viscosity | None (conservative assumption: sensors do not have a self-diagnosing capability, so manual check for confirming operation) | 5 | 10 | 10 | 500 | 1.10E-04 |
| | | Electrical Potential Decreased | | | | | | | |
| | | Dielectric Strength Decreased | | | | | | | |
| | | Property Mismatch | | | | | | | |
| | Heater | Oxidized | Impurities contamination | None (visual inspection) | 2 | 10 | 4 | 80 | 4.27E-06 |
| | | Perforated | FO or steam Leak | | | | | | |
| | | Blocked | No FO delivered to M/E | | | | | | |
| N/A | Venting Valve | Abraded | Fuel oil leak and/or air contaminated FO will be circulated into the M/E | None (visual inspection) | 3 | 10 | 10 | 300 | 1.78E-05 |
| | | Cracked | | | | | | | |
| Duplex Filter | Filter | Blocked | Fuel oil cannot go through the filtering element | Pressure difference sensor | 6 | 10 | 5 | 300 | 1.37E-03 |

| | | | | | | | | | |
|---|---|---|---|---|---|---|---|---|---|
| | | Loose | Fuel oil leak | None (visual inspection) | | | | | |
| | 3-way Valve | Abraded | Fuel oil leak | None (visual inspection) | 3 | 10 | 10 | 300 | 1.78E-05 |

Appendix A8

Table 23 presents the available leak detection sensors in offered in the MADe library.

*Table 23: Available leakage sensor in MADe*

| Item | Sensor |
|---|---|
| 1 | Absolute pressure leak testing |
| 2 | Bubble testing |
| 3 | Electric capacitance sensor |
| 4 | Electric resistance sensor |
| 5 | Electrical conductivity sensor |
| 6 | Electrochemical sensor |
| 7 | Halogen diode leak testing |
| 8 | Hydrogen leak testing |
| 9 | Mass spectrometer leak testing |
| 10 | Mechanical line leak detector |
| 11 | Optical leak detector |
| 12 | Tracer-gas leak testing method |
| 13 | Ultrasonic leak detector |

## Appendix A9

In this appendix, the sensor set solutions for the remaining components are cited below per sub-system (where applicable).

### Filtering Sub-system

The following components were selected for sensor placement:

1. Valves:
    1.1. Valve_1_FLT_upper & lower
    1.2. Valve_2_FLT_upper & lower
    1.3. 3wayValve_1_FLT_upper & lower
2. Filter (manual)

### Flowmeter Sub-system

The following components were selected for sensor placement:

1. Valves:
    1.1. Valve_FLM_upper
    1.2. Valve_1_FLM_lower
    1.3. Valve_2_FLM_lower
    1.4. Non-return_Valve_FLM

### Booster Sub-system

The following components were selected for sensor placement:

1. Valves:
    1.1. Valve_1_B
    1.2. NRValve_B
    1.3. Valve_2_B
    1.4. Valve_3_B

The above conclude the sensor set analysis.

Appendix A10

*Table 24: High-pressure fuel oil system component failure modes*

| Component | Failure Mode | Failure End Effect |
|---|---|---|
| Flow Control Valve | Abraded | Fuel Oil Leak |
| | Cracked | |
| High Pressure Pump (reciprocating) | Fractured | Fuel Oil Leak |
| | Abraded | |
| Accumulator | Perforated/Cracked | Fuel Oil Leak |
| | Corroded | |
| Injection Valve | Clogged Atomizer | Improper injection & consequently combustion |
| | Early/Late Opening | |
| | Ball seat erosion | Leaking injection valve, leads to improper combustion |
| Start & Safety Valve | Abraded | Fuel Oil Leak |
| | Cracked | |
| Pressure (Pulsation) Damper | Inoperable bladder (if bladder type) | Pulsation from accumulator will not be dampened, pipes might rupture, i.e. FO Leak |
| 3-way valve | Abraded | Fuel Oil Leak |
| | Cracked | |
| Pressure Sensors | Open Circuit | Faulty or no measurements at ECU |
| | Electrical Potential Decreased | |
| | Dielectric Strength Decreased | |
| | Property Mismatch | |
| Temperature Sensor | Open Circuit | Faulty or no measurements at ECU |
| | Electrical Potential Decreased | |
| | Dielectric Strength Decreased | |
| | Property Mismatch | |
| No-return Valve | Abraded | Fuel Oil Leak |

Appendix A11

Symbol “i” indicates the time instances that the qualitative simulation was run. A red cell has the value “-1” which implies that the reaction was less, i.e. the pressure dropped. Table 25 presents the complete step response table for the diagnostic what-if simulation for a low pressure failure injection on FCV_01, in relation to the response presented in Figure 48.

*Table 25. Step response table for low pressure failure injection on FCV_1 in the HPRPB*

| Component | Flow Property | i | 1 | 2 | 3 | 4 | 5 | 6 | = |
|---|---|---|---|---|---|---|---|---|---|
| 3-way valve | Liquid Static pressure | | | | | | | -1 | -1 |
| 3-way valve | Liquid Static pressure | | | | | | | -1 | -1 |
| Accumulator_1 | Liquid Static pressure | | | | -1 | -1 | -1 | -1 | -1 |
| Accumulator_1 | Liquid Static pressure | | | | -1 | -1 | -1 | -1 | -1 |
| Accumulator_1 | Liquid Static pressure | | | | -1 | -1 | -1 | -1 | -1 |
| Accumulator_1 | Liquid Static pressure | | | | -1 | -1 | -1 | -1 | -1 |
| Accumulator_1 | Liquid Static pressure | | | | -1 | -1 | -1 | -1 | -1 |
| Accumulator_2 | Liquid Static pressure | | | | | -1 | -1 | -1 | -1 |
| Accumulator_2 | Liquid Static pressure | | | | | -1 | -1 | -1 | -1 |
| Accumulator_2 | Liquid Static pressure | | | | | -1 | -1 | -1 | -1 |
| Clean Leak FO Drain (103) | Liquid Static pressure | | | | -1 | -1 | -1 | -1 | -1 |
| Control Unit | Discrete Data | | | | | | -1 | -1 | -1 |
| FCV_1 | Liquid Static pressure | | -1 | -1 | -1 | -1 | -1 | -1 | -1 |
| FCV_2 | Liquid Static pressure | | | | | | | | 0 |
| FO Return (102) | Liquid Static pressure | | | | | | -1 | -1 | -1 |
| High Pressure Fuel Oil Line | Continuous Amplitude | | | | | | | | 0 |
| High Pressure Fuel Oil Line | Liquid Static pressure | | | | | | | | 0 |
| High Pressure Fuel Oil Line | Liquid Static pressure | | | | | | -1 | -1 | -1 |
| High Pressure Fuel Oil Line | Liquid Flow velocity | | | | | | | -1 | -1 |
| High Pressure Fuel Oil Line | Liquid Temperature | | | | | | | | 0 |
| High Pressure Fuel Oil Line | Continuous Frequency | | | | | | | | 0 |
| High Pressure Fuel Oil Line | Liquid Static pressure | | | | | | | -1 | -1 |
| High Pressure Fuel Oil Line | Liquid Flow velocity | | | | | | -1 | -1 | -1 |
| High Pressure Fuel Oil Line | Liquid Flow velocity | | | | | | -1 | -1 | -1 |

| | | | | | | | | | |
|---|---|---|---|---|---|---|---|---|---|
| High Pressure Fuel Oil Line | Discrete Data | | | | | | | -1 | -1 |
| High Pressure Fuel Oil Line | Liquid Flow velocity | | | | | | | -1 | -1 |
| HP_Pump_1 | Liquid Flow rate | | | -1 | -1 | -1 | -1 | -1 | -1 |
| HP_Pump_1 | Liquid Flow rate | | | -1 | -1 | -1 | -1 | -1 | -1 |
| HP_Pump_2 | Liquid Flow rate | | | | | | | | 0 |
| HP_Pump_2 | Liquid Flow rate | | | | | | | | 0 |
| Injection_Valve_1 | Liquid Flow velocity | | | | | -1 | -1 | -1 | -1 |
| Injection_Valve_1 | Liquid Static pressure | | | | | -1 | -1 | -1 | -1 |
| Injection_Valve_2 | Liquid Static pressure | | | | | -1 | -1 | -1 | -1 |
| Injection_Valve_2 | Liquid Flow velocity | | | | | -1 | -1 | -1 | -1 |
| Injection_Valve_3 | Liquid Flow velocity | | | | | | -1 | -1 | -1 |
| Injection_Valve_3 | Liquid Static pressure | | | | | | -1 | -1 | -1 |
| Injection_Valve_4 | Liquid Static pressure | | | | | | -1 | -1 | -1 |
| Injection_Valve_4 | Liquid Flow velocity | | | | | | -1 | -1 | -1 |
| Non-return Valve | Liquid Static pressure | | | | | -1 | -1 | -1 | -1 |
| Pressure Damper | Liquid Static pressure | | | | | | -1 | -1 | -1 |
| PT101 | Discrete Data | | | | | | | | 0 |
| PT105 | Discrete Data | | | | | | | -1 | -1 |
| PT115A | Discrete Data | | | | | | -1 | -1 | -1 |
| PT155A | Discrete Data | | | | | -1 | -1 | -1 | -1 |
| SSV | Liquid Static pressure | | | | | -1 | -1 | -1 | -1 |
| TE101 | Discrete Data | | | | | | | | 0 |

Appendix A12

Table 26 presents the detailed table of the FMECA conducted for the high-pressure RPB technical element, along with relevant scoring for the Occurrence, including the corresponding failure rate λ ($10^{-6}$ hrs), Severity, and Detection, including the corresponding risk priority number.

*Table 26. Detailed FMECA Table for HPRPB*

| Component | Failure Mode | Failure End Effect | Detection Method | Occurrence | Severity | Detection | RPN | λ |
|---|---|---|---|---|---|---|---|---|
| Flow Control Valve | Abraded | Fuel Oil Leak | Sensors (x2) on valve to check position, not leaks. No detection. | 2 | 10 | 9 | 180 | 1.90E-06 |
| | Cracked | | | | | | | |
| High Pressure Pump (reciprocating) | Fractured | Fuel Oil Leak | None | 2 | 10 | 9 | 180 | 6.1506E-06 |
| | Abraded | | | | | | | |
| Accumulator | Perforated/Cracked | Fuel Oil Leak | The accumulators are connected via piping. The FE and DE accumulators have pressure sensors. | 1 | 9 | 2 | 18 | 8.279E-07 |
| | Corroded | | | | | | | |
| Injection Valve | Clogged Atomizer | Improper injection & consequently combustion | Valve is electronically controlled by ECU, BUT with unknown function "options", no detection | 3 | 7 | 10 | 210 | 4.14E-05 |
| | Early/Late Opening | | | | | | | |
| | Ball seat erosion | Leaking injection valve, leads to improper combustion | | | | | | |
| | Abraded | Fuel Oil Leak | | 2 | 10 | 9 | 180 | 1.90E-06 |

| | | | | | | | | |
|---|---|---|---|---|---|---|---|---|
| Start & Safety Valve | Cracked | | Dedicated UNKNOWN sensor on valve, no detection | | | | | |
| Pressure (Pulsation) Damper | Inoperable bladder (if bladder type) | Pulsation from accumulator will not be dampened, pipes might rupture, i.e. FO Leak | None | 2 | 10 | 10 | 200 | 4.17E-06 |
| 3-way valve | Abraded | Fuel Oil Leak | None | 3 | 10 | 10 | 300 | 1.78E-05 |
| | Cracked | | | | | | | |
| Pressure Sensors | Open Circuit | Faulty or no measurements at ECU | None | 4 | 8 | 9 | 288 | 6.56E-05 |
| | Electrical Potential Decreased | | | | | | | |
| | Dielectric Strength Decreased | | | | | | | |
| | Property Mismatch | | | | | | | |
| Temperature Sensor | Open Circuit | Faulty or no measurements at ECU | None | 5 | 7 | 9 | 315 | 1.10E-04 |
| | Electrical Potential Decreased | | | | | | | |
| | Dielectric Strength Decreased | | | | | | | |
| | Property Mismatch | | | | | | | |
| Control Unit | Open Circuit | Faulty or no measurements at ECU | Control System | 2 | 7 | 4 | 56 | 1.14E-05 |
| | Short Circuit | | | | | | | |
| No-return Valve | Abraded | Fuel Oil Leak | None (visual inspection) | 3 | 10 | 10 | 300 | 1.78E-05 |

## Appendix B

### Appendix B1

Figure 122 presents the smoke layer height at the aft starboard corridor, adjacent to the access way of the MVZ. Initially, the smoke layer height rests at the ceiling, and as the fire grows it falls at around 2.5 meters from the deck, where it fluctuates.

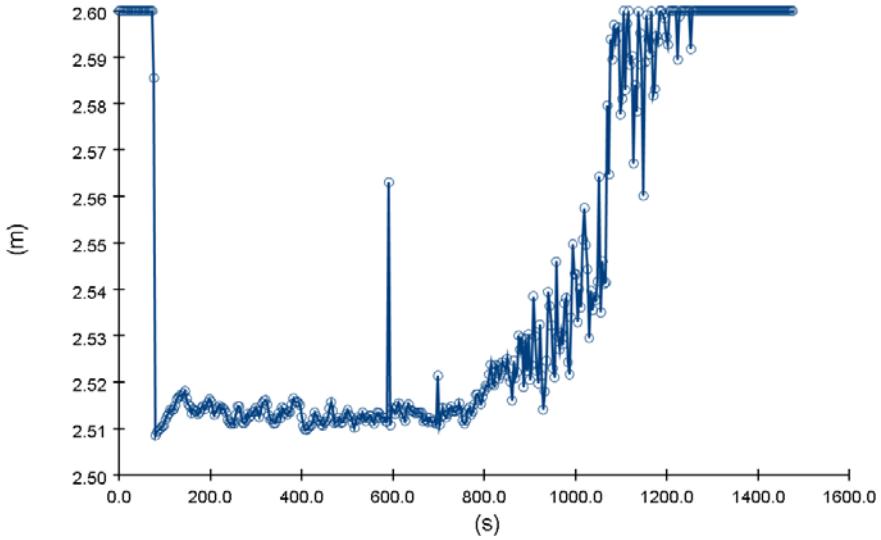


*Figure 122. Smoke layer height at aft starboard corridor*

Figure 123 and Figure 124 present the upper and lower smoke layer height temperatures at the same location, with no considerable difference in temperatures between the two smoke layers.

Figure 125 presents the readings of the visibility device in the aft starboard corridor. Through this figure, the effect of smoke filling on the visibility of the occupants can be appreciated.

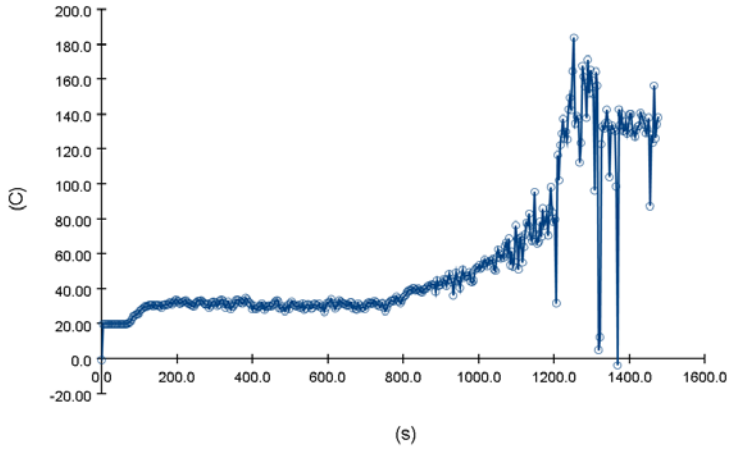


*Figure 123. Upper smoke layer temperature at aft starboard corridor*

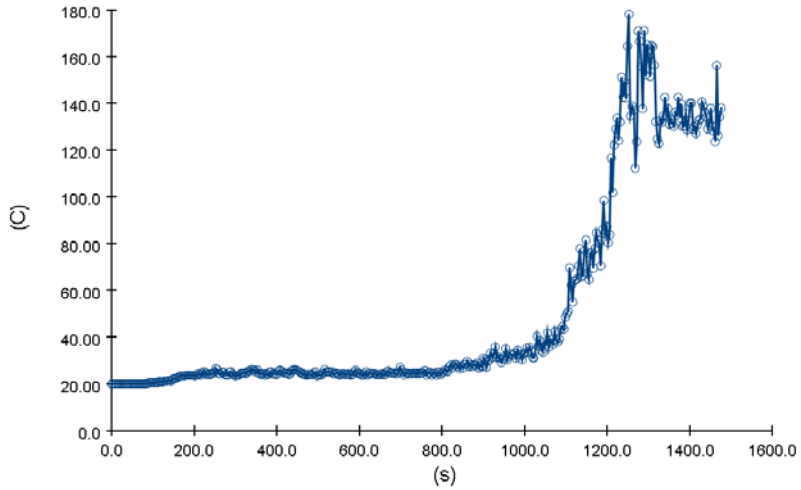


*Figure 124. Lower smoke layer temperature at aft starboard corridor*

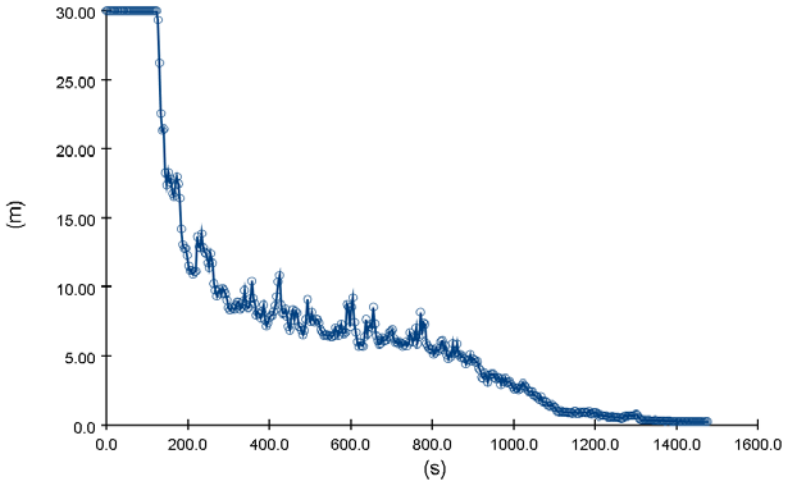


*Figure 125. Visibility at aft starboard corridor*

Appendix B2

Figure 126 presents the smoke layer height at the aft starboard corridor, adjacent to the access way of the MVZ, as in the scenario with no sprinklers. Interestingly enough, the smoke layer height had the same behaviour, approximately 10 cm below the ceiling.

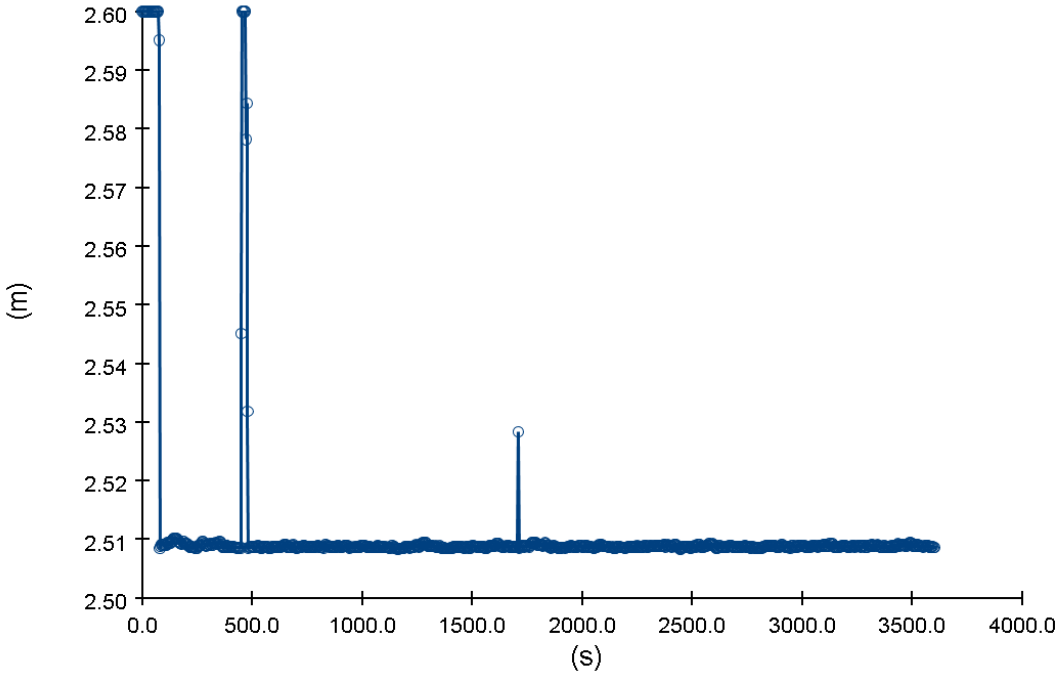


*Figure 126. Smoke layer height at aft starboard corridor.*

Figure 127 and Figure 128 present the temperatures of the lower and upper smoke layers respectively. It was noted that there are no temperatures of increased magnitude, rather both layers have very similar low temperatures (very close to ambient), which was attributed to the effect of the sprinklers.

Figure 129 presents the visibility at the aft starboard corridor. It was noted that the visibility is around 5 meters throughout the simulation, which does not pose any issues in case of a possible evacuation.

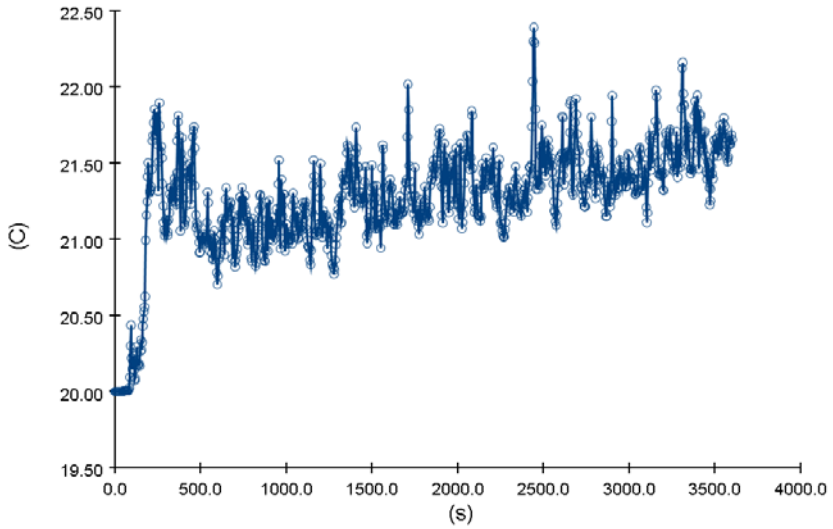


*Figure 127. Lower smoke layer height temperature at aft starboard corridor.*

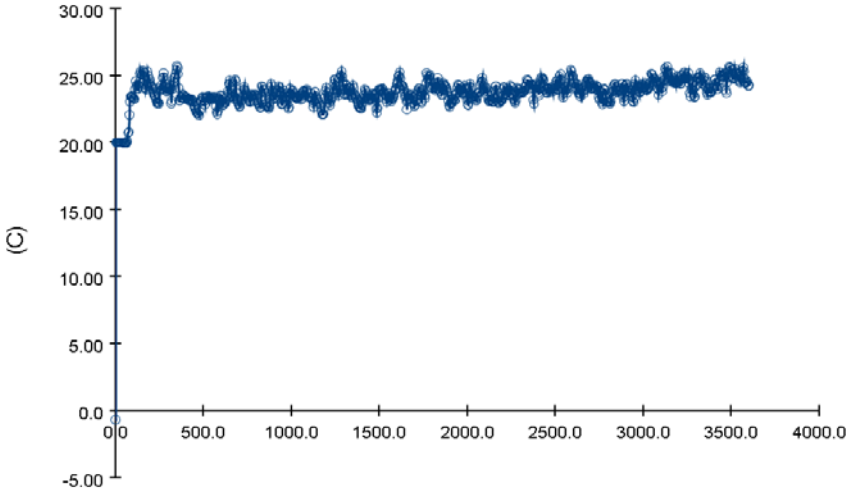


*Figure 128. Upper smoke layer height temperature at aft starboard corridor*

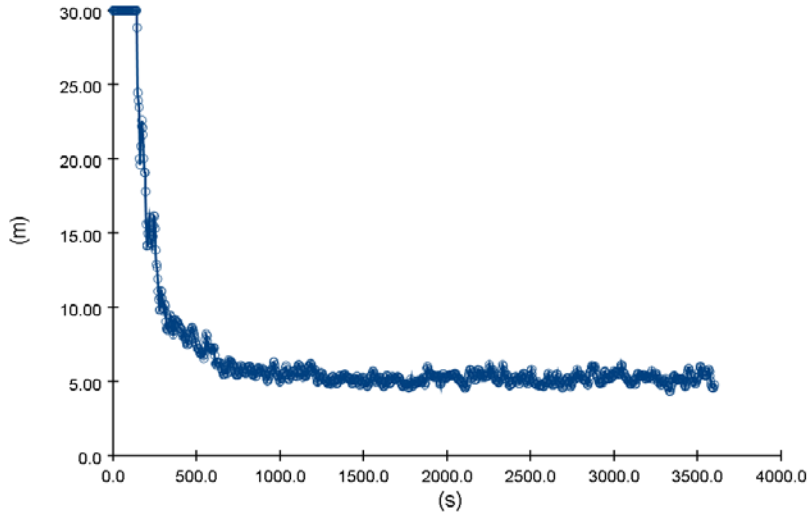


*Figure 129. Visibility at aft starboard corridor*

Appendix B3

Figure 130 presents the smoke layer height at the aft starboard side of the deck. As the fire grows, the smoke layer heights moves towards the floor, it drops, for about 10 centimetres.

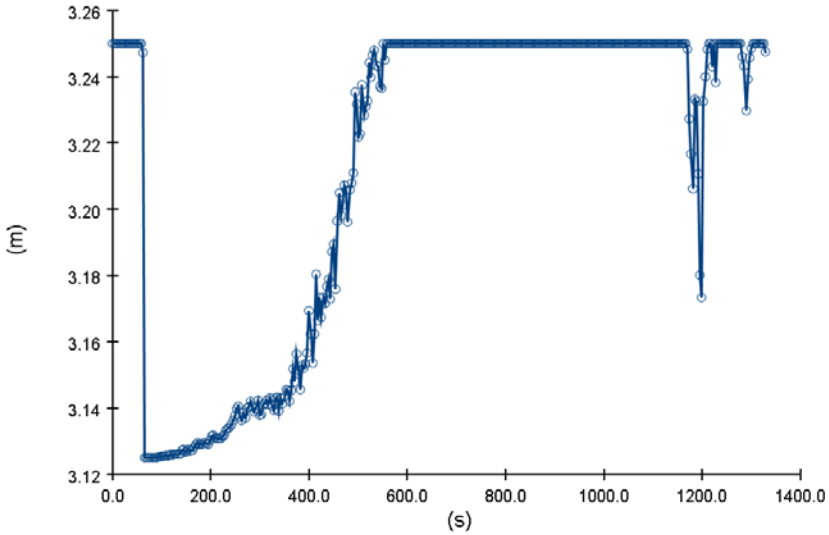


*Figure 130. Smoke Layer Height of the enclosure at aft starboard side*

Figure 131 and Figure 132 present the temperatures of the upper and lower smoke layer heights respectively.

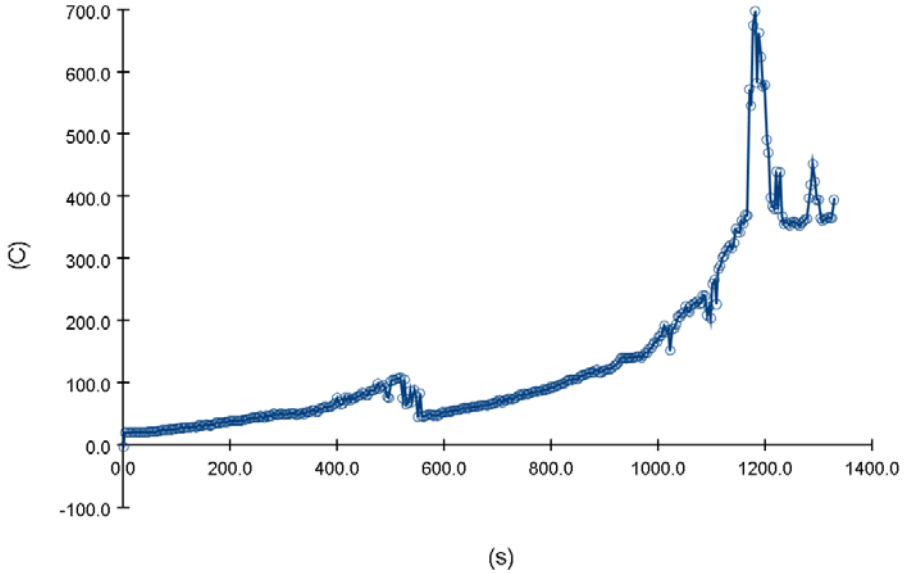


*Figure 131. Upper smoke layer temperature*

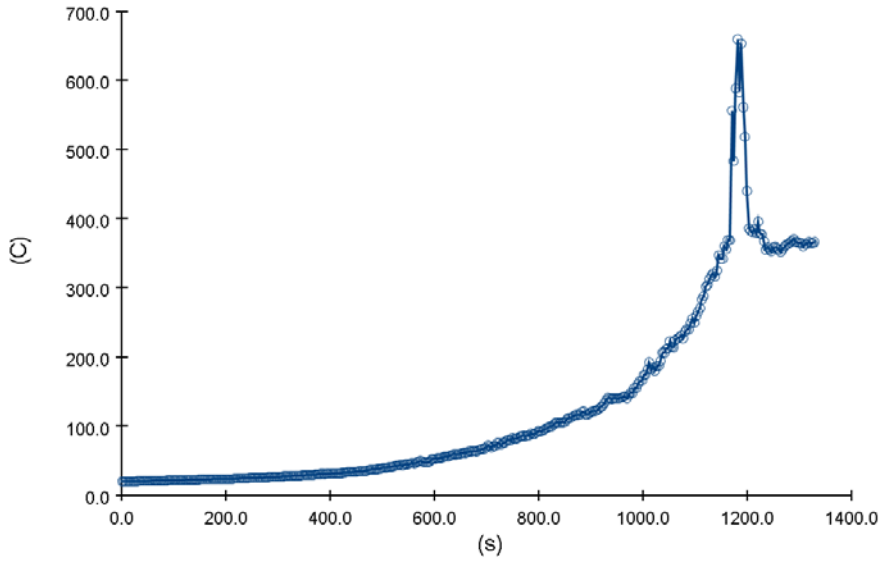


*Figure 132. Lower smoke layer temperature*

Appendix B4

Figure 133 presents the smoke layer height at the aft starboard side of the deck. As the fire grows, the smoke layer height falls for approximately 15 centimetres.

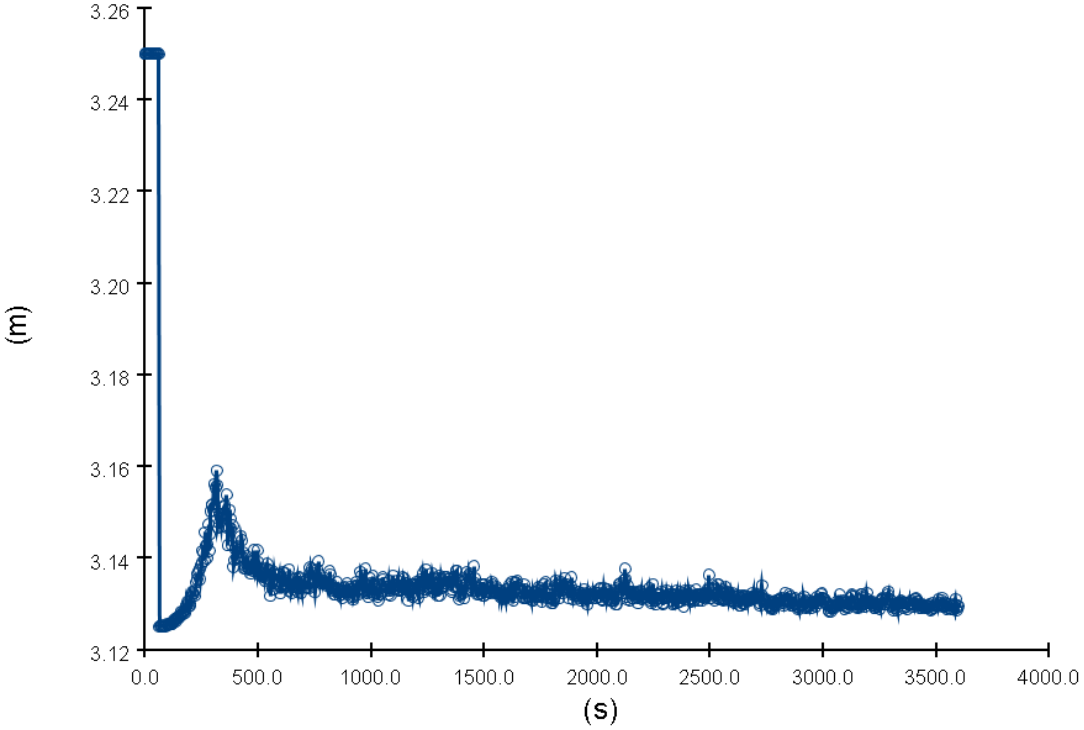


*Figure 133. Smoke layer height of the public space deck with sprinklers*

Figure 134 and Figure 135 present the temperatures of the upper and lower layers respectively. It was ascertained that both layers had considerably lower temperatures than the ones in the worst-case scenario, attributed to the effect of the sprinklers on fire development.

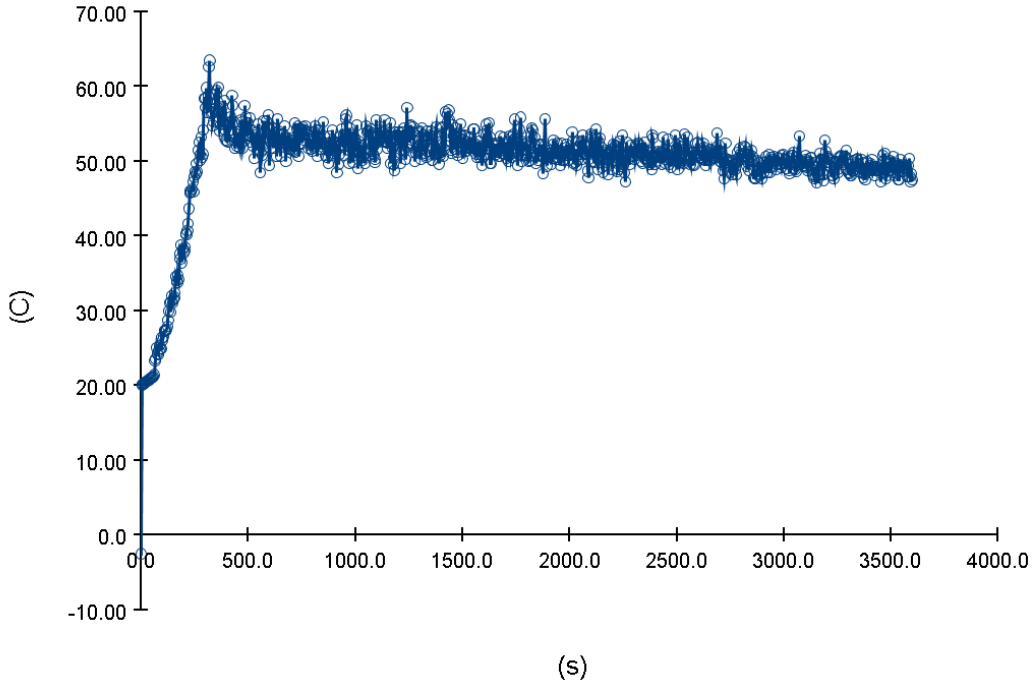


*Figure 134. Upper smoke layer temperature*

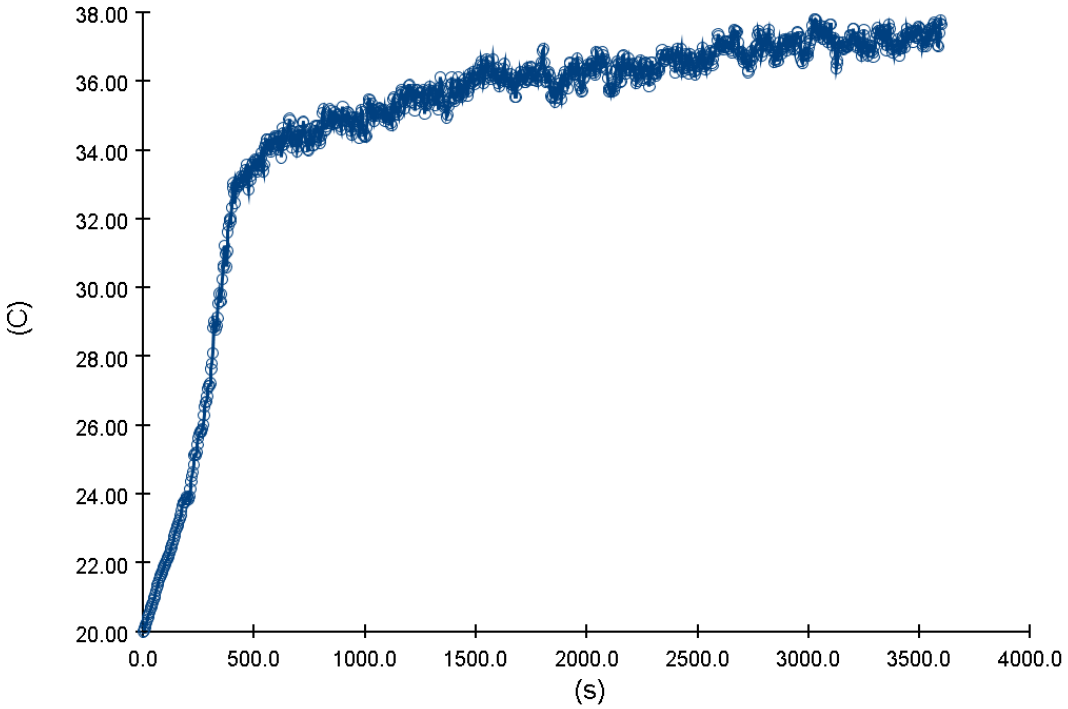


*Figure 135. Lower smoke layer temperature*

Appendix B5

Figure 136 presents the evolution of the smoke layer height in the engine compartment only (9.2m tall), where the smoke layer decreases with time and at the end of the fully developed fire it rests at around 2m.

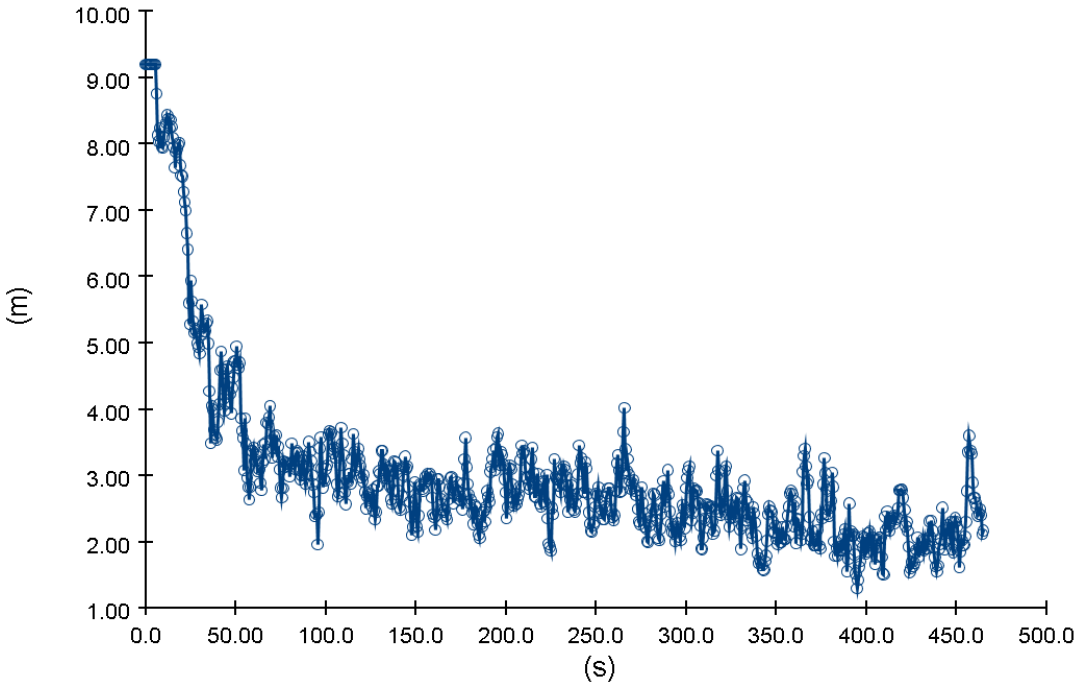


*Figure 136. Smoke Layer Height in Engine Compartment (no sprinklers).*

Figure 137 and Figure 138 present the temperatures on the upper and lower smoke layer height of the enclosure.

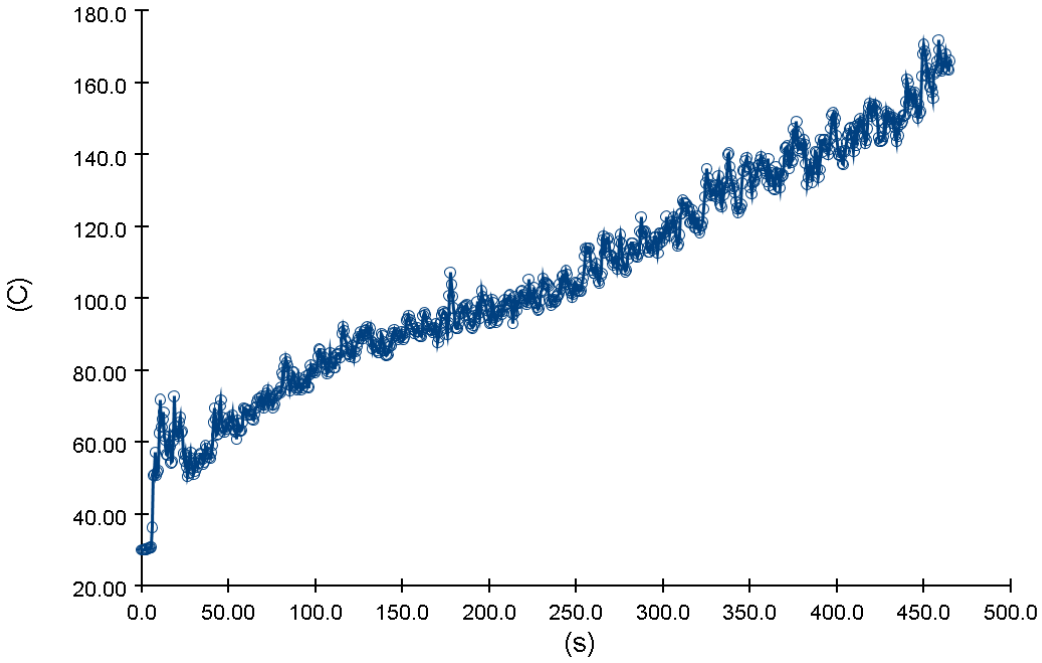


*Figure 137.Upper Smoke Layer Temperature (no sprinklers).*

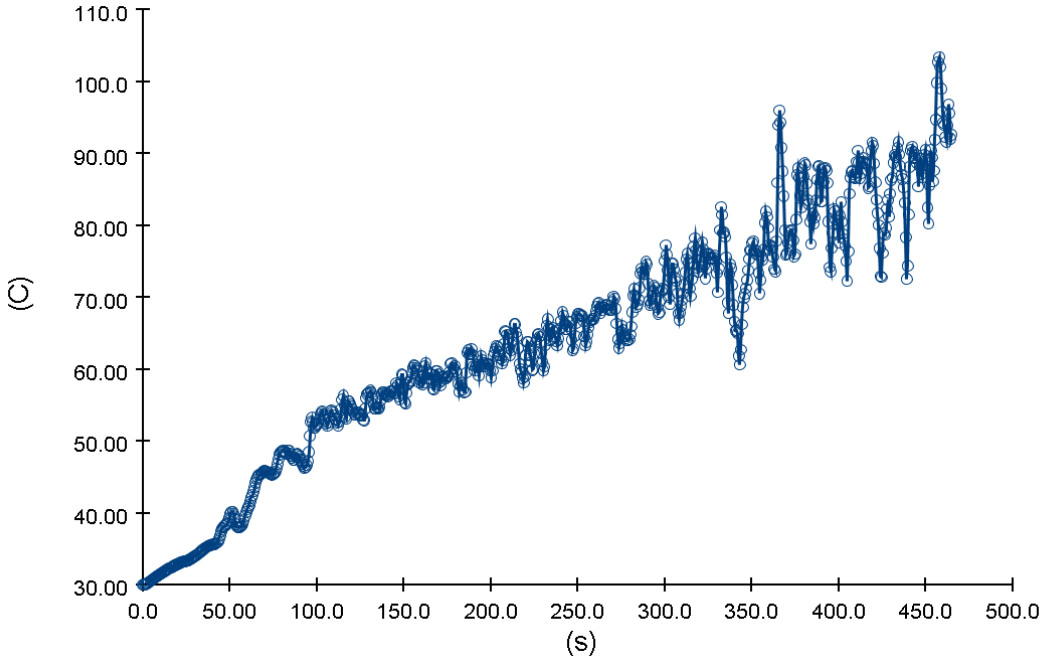


*Figure 138. Lower Smoke Layer Temperature (no sprinklers).*

Figure 139 presents the smoke layer of this scenario. No significant differences between this scenario and the one without control logic were noted. Conversely, the effect of the ventilation was noted through the temperatures of the upper and lower smoke layer heights respectively, presented in Figure 140 and Figure 141. Specifically, the lower layer temperature is less than in the simulation with inlet fans working, from around 100 to 46ºC.

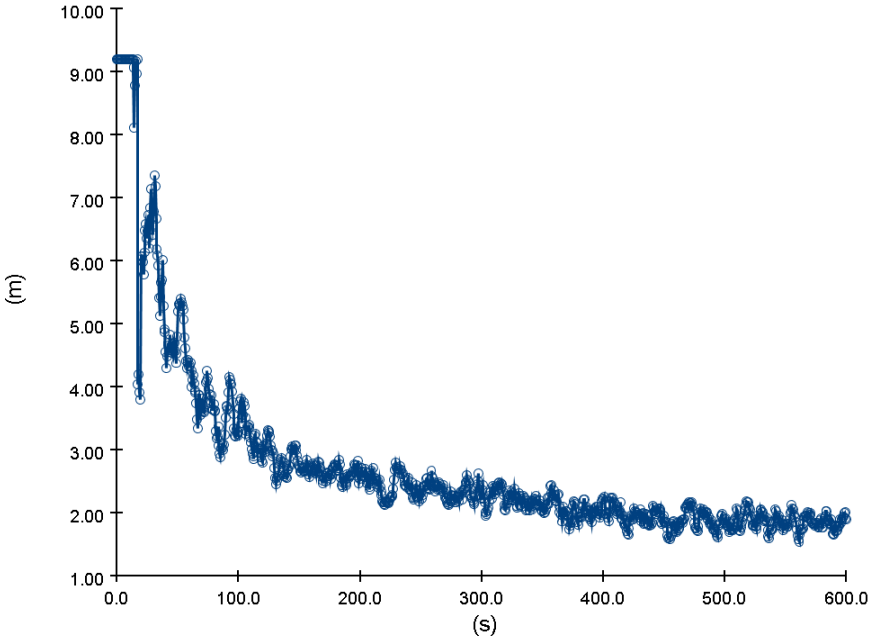


*Figure 139. Smoke Layer Height in Engine Compartment (no sprinklers & control logic).*

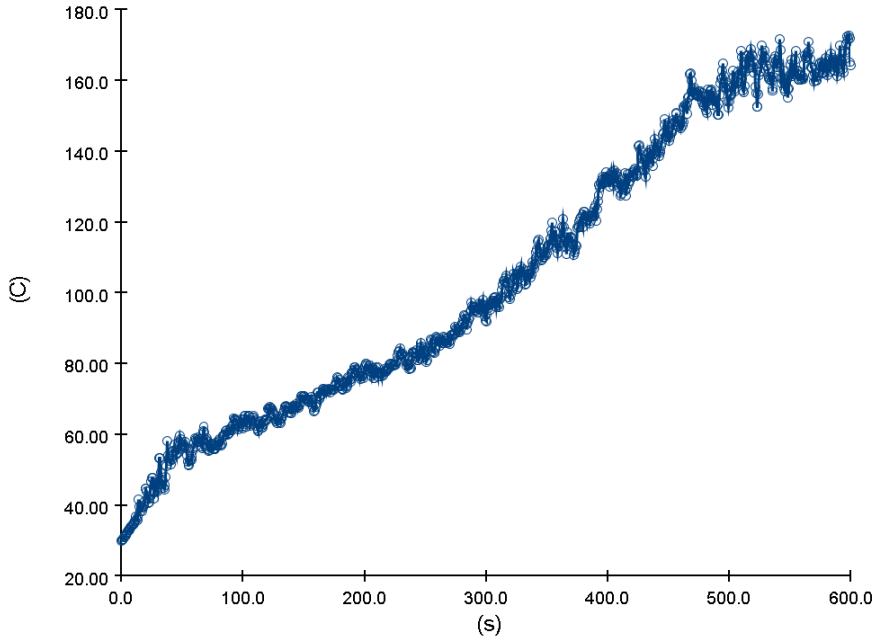


*Figure 140. Upper Smoke Layer Height in Engine Compartment (no sprinklers & control logic).*

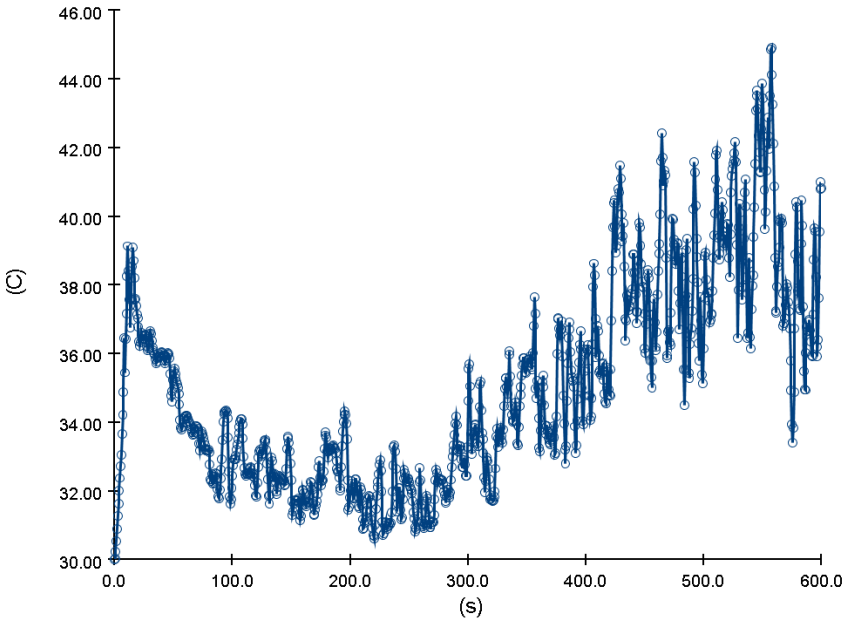


*Figure 141. Lower Smoke Layer Height in Engine Compartment (no sprinklers & control logic).*